The role of PI3K/AKT/mTOR pathway in programmed cell death of Cajal-Retzius cells and their contribution in the maturation of functional and dysfunctional cortical circuits

Nasim Ramezanidoraki

Université Paris Cité

Ecole doctorale Bio Sorbonne Paris Cité, ED 562

UMR_S 1266 Institut de psychiatrie et neurosciences de Paris

UMR_S 1163 Institut des Maladies Génétiques

Equipe Génétique et développement du cortex cérébral

The role of PI3K/ AKT/ mTOR pathway in programmed cell death of Cajal-Retzius cells and their contribution in the maturation of functional and dysfunctional cortical circuits

Soutenue par :

Nasim RAMEZANIDORAKI

Thèse de doctorat de :

Neurobiologie

Présentée et soutenue publiquement le : **01/12/2022**

Composition du jury:

Mme Stephanie BAULAC DR, Sorbonne Université	Rapportrice
M. Carlos CARDOSO DR, Aix-Marseille Université	Rapporteur
M. Heiko LUHMANN Professor, Johannes Gutenberg University Mainz	Examinateur
M. Franck OURY DR, Université Paris Cité	Président du jury
Mme Alessandra PIERANI DR, Université Paris Cité	Examinatrice
M. Pierre BILLUART HDR, Université Paris Cité	Directeur de thèse

Acknowledgement

First and foremost, I would like to express my sincere gratitude to the jury members who have agreed to attend this special occasion. I am grateful for your valuable feedback and honored to have had the opportunity to share these exciting scientific moments with you.

I would like to thank Alessandra Pierani for welcoming me into her laboratory, believing in me, and supporting me in realizing my long-held ambition of doing a PhD.

I would like to express my appreciation to Pierre Billuart, my esteemed advisor, for all the guidance, support, and instruction he provided me throughout my doctoral studies. I'm grateful to you for constantly pushing me to investigate the results from a variety of angles, which greatly shaped my scientific mind.

In addition, I would like to express my gratitude to all of the lab members—past and present—who have assisted and guided me over the course of these years. In particular, I would like to thank Eva, Sofia and Lisa for always being there to help me and explain to me when I felt lost, as well as for the emotional support they have provided for me. I would also like to thank Patrick for all the corrections of my French pronunciation and for enhancing my self-esteem by pointing out my strengths and making me aware of them.

I would like to thank the two students I had the chance to train Margaux and Elise, you made me realize this quote “Alone We Go Faster, Together We Go Further”, I had a great time working with you, and I wish you the best in your respective careers.

I am grateful to all of the individuals with whom I collaborated during my PhD and who assisted me in completing the project, including Mahboubeh Ahmadi, Philippe Bun, Stéphanie Moriceau, Elena Dossi, and Gwenaelle Lepen.

In addition, I would like to express my gratitude to the staff and facilities at the Institute of Psychiatry and Neurosciences of Paris and the Institute Imagine for providing me with wonderful scientific assistance.

Thanks to all my family, in Iran and in France for their assistance and encouragement throughout my education.

A special thanks to my beloved husband Meghdad. Over the past few years, we have endured a great deal of hardship together and have grown stronger. I must admit that none of this would have been possible without you. You have always been the light that showed

me the path and the fire that warmed my heart and encouraged me to keep going. You have shown me how love is entwined with patience and sacrifice. I would like to share with you the joy of obtaining this PhD, we finally succeeded!

ABSTRACT

The role of PI3K/ AKT/ mTOR pathway in programmed cell death of Cajal-Retzius cells and their contribution in the maturation of functional and dysfunctional cortical circuits.

Cajal-Retzius (CR) cells are a class of transient excitatory neurons, generated from different domains located at the edges of the pallium in the embryonic telencephalon, the pallial septum (SE), the pallial-subpallial boundary (PSB), the cortical hem (CH), and the thalamic eminence (ET). SE-CRs, CH and ET contribute to approximately 80% of the total population of CRs in the neocortex, which commonly expresses the DeltaNP73 gene. From these sources, they migrate tangentially to cover the entire surface of the developing cortex. CRs play a key regulatory role in several stages of cortical development such as controlling neuronal migration, layer formation, and cortical areas patterning in the developing telencephalon via the secretion of several proteins such as extracellular matrix glycoprotein Reelin. After fulfilling their roles, CRs largely disappear during the first two postnatal weeks in mice by programmed cell death.

Persistence of CRs during postnatal life has been detected in several pathological conditions related to epilepsy. Still, it is not yet clear whether their persistence is a cause or a consequence of these diseases. In order to study their contribution to these diseases, it is essential to decipher the possible molecular mechanisms involved in their death.

The PI3K/AKT/mTOR pathway is well known to play an important role in several cellular functions related to cell proliferation, growth, metabolism as well as PCD modulation by regulating apoptosis and autophagy. In addition, dysregulation of this pathway has been shown to be one of the main causes of malformations of the cortex during development (MCD) and responsible for epileptic seizures.

Considering the critical role of this pathway in cell survival, the main objective of this PhD project is to explore the role of this pathway in the modulation of PCD in the CRs.

We first focused on the physiological activity of this pathway in CRs derived from DeltaNP73 positive progenitors at two stages: embryonic day 17.5 (E17.5) and post-natal day 1 (P1) before the cell death occurred. We have shown that this pathway is less active in

CRs after birth. In parallel, we separately explored the spatio-temporal activity of the AKT and mTOR pathways, which revealed the presence of a spatial difference in the activity of the two pathways in the rostro-caudal and medio-lateral axes.

Then, using targeted genetic approaches involving positive (PIK3CA) or negative (PTEN or TSC1) regulators of the pathway, we demonstrated that maintaining its activity leads to a significant survival of CRs at a post-natal stage, with a stronger effect in PTEN. This survival is accompanied by a significant increase in the expression and secretion of Reelin by persistent CRs.

A more focused analysis of the PTEN mutant showed that the morphology of persistent cells in the brain of these animals is modified leading to alterations in their intrinsic electrophysiological properties and their responses to injected currents. However, the cortex of mutated animals for PTEN does not show major alterations in the layers of pyramidal neurons but an increase in the activation of their mTOR pathway activity. Behavioral analyzes of locomotor activity, anxiety or working memory do not show any differences compared with controls. Similarly, increased mTOR signaling in the cortex is not associated with hypersensitivity to the development of seizures induced by kainate injection.

Altogether, I showed that the reduction in the activation of the PI3K/AKT/mTOR pathway in CRs primes these cells to cell death probably through inhibiting an anti-apoptotic mechanism, and that the mTOR branch of the pathway contributes less to this survival.

Keywords: Development, cell death program, Cajal-Retzius cells, neuronal survival, PI3K/AKT/mTOR pathway

RÉSUMÉ

Le rôle de la voie PI3K/ AKT/ mTOR dans la mort cellulaire programmée des cellules Cajal-Retzius et leur contribution à la maturation des circuits corticaux fonctionnels et dysfonctionnels.

Les cellules Cajal-Retzius (CR) sont une classe de neurones excitateurs transitoires, générés à partir de différents domaines situés aux bords du pallium dans le télencéphale embryonnaire Environ 80 % de la population totale de CR dans le néocortex expriment précocement le gène DeltaNP73. À partir de ces sources, elles migrent tangentiellement pour couvrir toute la surface du cortex au cours de son développement. Les CR jouent un rôle de régulateur clé dans plusieurs étapes du développement cortical via la sécrétion de plusieurs protéines dont la glycoprotéine de la matrice extracellulaire Reelin : le contrôle de la migration des neurones, la formation de couches et la structuration des zones corticales dans le télencéphale en développement. Au cours des deux premières semaines post-natales chez la souris, les CR sont largement éliminés suivant un programme de mort cellulaire (PCD).

La persistance des CR au cours de la vie postnatale a été détectée dans plusieurs conditions pathologiques liées à l'épilepsie, mais il n'est pas encore clair si leur persistance est une cause ou une conséquence de ces maladies. Pour pouvoir étudier leur contribution dans ces maladies, il est essentiel de déchiffrer les éventuels mécanismes moléculaires impliqués dans leur mort.

La voie PI3K/AKT/mTOR est bien connue pour jouer un rôle important dans plusieurs fonctions cellulaires liées à la prolifération cellulaire, la croissance, le métabolisme ainsi que la modulation de la PCD en régulant l'apoptose et l'autophagie. En outre la dérégulation de cette voie a été démontrée comme l'une des causes principales de malformations du cortex au cours développement (MCD) et également responsable de crises d'épilepsie.

Considérant le rôle critique de cette voie dans la survie cellulaire, l'objectif principal de ce projet doctoral est d'explorer le rôle de cette voie dans la modulation de la PCD dans les CRs.

Nous nous sommes d'abord concentrés sur l'activité physiologique de cette voie dans les CR dérivés des progéniteurs positifs pour DeltaNP73 à deux stades périnataux avant la

survenue de leur mort cellulaire. Nous avons montré que cette voie est moins active dans les CR après la naissance. En parallèle, nous avons exploré séparément l'activité spatio-temporelle des voies AKT et mTOR et cette étude a révélé qu'il existe une différence spatiale dans l'activation des deux voies dans les axes rostro-caudal et médio-latéral.

Ensuite, en utilisant des approches génétiques ciblées portant sur de régulateurs positif (PIK3CA) ou négatifs (PTEN ou TSC1) de la voie, nous avons démontré que le maintien de son activation conduit à une survie plus ou moins importante des CR à un stade post-natal avancé avec un effet plus marqué dans le cas du mutant PTEN. Cette survie est accompagnée par une augmentation significative de l'expression et de la sécrétion de la Reelin dans les CR persistantes.

Une analyse plus focalisée sur le mutant PTEN a montré que la morphologie des cellules persistantes dans le cerveau de ces animaux est modifiée conduisant à des altérations de leurs propriétés electrophysiologiques intrinsèques et de leurs réponses à des courants injectés. Toutefois le cortex des animaux mutés pour PTEN ne présente pas d'altération majeures des couches de neurones pyramidaux mais une augmentation de l'activation de leur voie mTOR. Les analyses comportementales de l'activité locomotrice, de l'anxiété ou encore de la mémoire de travail ne montrent pas de différences avec les contrôles. De même, l'augmentation de la signalisation mTOR dans le cortex n'est pas associée à une hypersensibilité au développement de crises induites par l'injection de kainate.

En conclusion, j'ai montré que la réduction de l'activation de la voie PI3K/AKT/mTOR dans les CR sensibilise ces cellules à la mort cellulaire en inhibant probablement un mécanisme anti-apoptotique, et que la branche mTOR de la voie contribue peu à cette survie.

Mots-clés : Développement, programme de mort cellulaire, cellules de Cajal-Retzius, survie neuronale, voie PI3K/AKT/mTOR

List of Abbreviations

ACSF: artificial cerebral spinal fluid

AHS: Ammond's horn syndrome

AMPA: α-amino-3-hydroxy-5-methyl-4-isoxazolepropionic acid

ANR: Anterior neural ridge

AP: Action potential

AP-5: (2R)-amino-5-phosphonovaleric acid

APAF1: Apoptotic protease activating factor-1

ApoER2: Apolipoprotein E receptor 2

aRG : Apical Radial glia cells

ASK1: Apoptosis signal-regulating kinase 1

AUDp: Primary auditory area

ASD: Autism spectrum disorder

Atg: Autophagy-related proteins

Bad: Bcl-2 associated death promoter

BAK: BCL2 antagonist-killer

BAX: BCL2 associated X protein

BCL-2: B-cell lymphoma 2

BCL-XL: BCL-extra large

BFL-1/A1: Bcl-2 related gene expressed in fetal liver/ protein A1

BH: BCL-2 Homology,

Bid: BH3 interacting-domain death agonist

Bim: Bcl-2-like protein 11

BMPs: Bone morphogenetic proteins

BOK: BCL-2 ovarian killer

bRGs: Basal Radial glia cells

CA1: Cornu Ammonis1

CC: Corpus Callosum

CGE: Caudal ganglionic eminence

CH: Cortical hem

ChP: Choroid plexus

CLC2: Voltage-dependent chlorine channel 2

CNQX: 6-cyano-7-nitroquinoxaline-2,3-dione

CNS: Central nervous system

Couptf1: Chicken ovalbumin upstream promoter transcription factor 1

CP: Cortical plate

CPN: Callosal projection neurons

CREB: cAMP response element-binding

CRs: Cajal-Retzius cells

CSF: Cerebrospinal fluid

CSPG: Chondroitin sulfate proteoglycan

CThPN: Corticothalamic projection neurons

CXCL12: Chemokine (C-X-C motif) ligand 12

CXCR-4: C-X-C chemokine receptor type 4

CytoC: Cytochrome-C

Dab1:

dATP: Deoxyadenosine triphosphate

DED: Death effector domain

DG: Dentate gyrus

DISC: Death inducing signaling complex

DIV: Days in vitro

DNA-PK: DNA-dependent protein kinase

DTA: Diphtheria toxin

DV: Dorso-ventral

E: Embryonic day

EGF: Epidermal growth factor

Emx2: Empty spiracle homeobox 2

ET : Eminentia thalami

FADD: Fas-associated protein with death domain

FasL: Fas ligand

FCD: Focal cortical dysplasia

FGFs: Fibroblast growth factors

FLIP: FLICE inhibitory protein

FOXO1: Forkhead box protein O1

GAP: GTPase Activation Protein

GE: Ganglionic eminences

GFP: green fluorescent protein

GN: Granular neurons

GPCRs: G protein-coupled receptors

GSK3B: Glycogen synthase kinase 3 β

GW: gestation week

HF: hippocampal fissure

Hipp: Hippocampus

Hrk: Hara-kiri

IAPs: Inhibitor of apoptosis proteins

ICAD: Inhibitor of caspase-activated DNAse

ILK: Integrin-linked kinase

INs: Interneurons

ipRGCs: intrinsically photosensitive retinal ganglion cells

IPs: Intermediate progenitors

JIP1: NK-interacting protein 1

JNK: c-Jun N-terminal kinase

KCC2: K+/Cl- co-transporter

kDa: kilodalton

L1: Layer 1

L2: Layer 2

L3: Layer 3

L4: Layer 4

L5: Layer 5

L6: Layer 6

LC3: Microtubule associated protein 1-light chain 3

LGE: Lateral ganglionic eminence

LOT: Lateral olfactory tract

LV: Lateral ventricle

MAP: Mitogen-activated protein

MCDs: Malformation of cortical developments

MCL-1: Myeloid cell leukemia 1

MEG: megalencephaly

MGE: Medial ganglionic eminence

mGluR1: Metabotropic glutamate receptors 1

mGluR2: Metabotropic glutamate receptors 2

MAM: Mitochondria-associated membranes ()

MKK4: Mitogen-Activated Protein Kinase Kinase 4

mLST8: Mammalian lethal sec-13 protein 8

MOMP: Mitochondrial outer membrane permeabilization

MOp: Primary motor area

Ms: Milliseconds

mSIN1or MAPKAP1: Mammalian stress-activated MAPK-interacting protein 1

mTOR: Mammalian target of rapamycin

mTORC1: Mammalian target of rapamycin complex 1

MEA: Multielectrode array

MZ: Marginal zone

NCx: Neocortex

NEDD4: Neural precursor cell expressed developmentally down-regulated protein 4

NEs: Neuroepithelial cells

NKCC1: Na-K-Cl cotransporter 1

NMDA: Ionotropic N-methyl-D-aspartic acid (NMDA)-like glutamate receptors

NSPCs: Neural stem/progenitor cells

OML: Outer molecular layer

oRGs: OuterRadial glia cells

p75NTR: The p75 neurotrophin receptor

Pax6: Paired box gene

PCD: Program of cell death

PDK1: 3-phosphoinositide-dependent protein kinase-1

PH: Pleckstrin homology

PI3,4,5-P3: Phosphatidylinositol-3,4,5-triphosphate

PI3Ks: Phosphatidylinositol-3-kinases

PI-4,5-P2: Phosphatidylinositol-4,4-bisphosphate

PIK3CA: phosphatidylinositol-4,5-bisphosphate 3-kinase, catalytic subunit alpha

Pir: Piriform cortex

PKB: Protein kinase B

PKC β II: Protein kinase C β II

PNs: projection neuron

POA: Preoptic area

PP: Preplate

PSB: Pallial-subpallial boundary

Puma: p53 upregulated modulator of apoptosis

Raptor: Regulatory associated protein of mTOR

RGs: Radial glia cells (RGs)

RHEB: RAS homolog enriched in the brain

Rictor: Rapamycin-insensitive companion of mTOR

S6K: 40S ribosomal S6 kinases

SCPN: Subcerebral projection neurons

SE: pallial septum

Ser: Serine

SGK: Serine/threonine-protein kinase

SHH: Sonic hedgehog protein

SIPL1: Shank-interacting protein-like 1

SLM: Stratum lacunosum moleculare

SMAC: Second mitochondria-derived activator of caspases

SP: Subpallium

SP: Subplate

Sp8: Trans-acting transcription factor 8

SSp: Primary somatosensory area

SST: Somatostatin

SVZ: Subventricular zone

TA: Transactivating

Tbr2 : T-box brain protein 2

TFs: Transcription factors

TNF: The tumor necrosis factor

TRADD: Tumor necrosis factor receptor type 1-associated DEATH domain protein

TRAIL: TNF-related apoptosis-inducing ligand

TTX: Tetradotoxin

VDCC: Voltage-dependent calcium channel

VISp: Primary visual area

VLDLR: Very low density lipoprotein receptor

VP: Ventral pallium

vRGs: Ventricular Radial glia cells

VZ: Ventricular zone

XIAP: X-linked IAP

β gal: β-Galactosidase

Mm: Micro meter

Table of Contents

Table of Figures

INTRODUCTION

1. Overview on the cerebral cortex

Anatomically cerebral cortex can be split into two major parts, allocortex which is evolutionary older, including the hippocampus and the olfactory cortex, and neocortex which is unique to mammals (Klingler, 2017; Luzzati, 2015) . The cerebral cortex is located in the outermost part of the brain which controls sensory perception, motor behaviors and cognitive functions. These functions are relying on a complex architecture of neural networks that begins to be established during both embryonic and early postnatal development. Cell proliferation and cell death are two main selective and conserved evolutionary mechanisms which play a crucial role in sculpting the mature cerebral cortex through refinement of the developing neural circuits (Wong & Marín, 2019) . Studies in the past decades have discovered that disruption in the balance between these two mechanisms have been linked to the etiology of several neurological and psychiatric disorders such as macrocephaly (Buxbaum et al., 2007), microcephaly, autism spectrum disorders (ASD), epilepsy (Enriquez-Barreto & Morales, 2016), intellectual disability and schizophrenia (Parenti et al., 2020; L. Wang et al., 2017).

1.1. Neuronal composition

In the radial dimension, the neocortex is composed of 6 layers. This laminar structure emerges from a dichotomy between two major neuronal subpopulations, spiny excitatory neurons (glutamatergic) and non-spiny inhibitory interneurons (GABAergic), which constitute almost 80% and 20% of the cortical neuronal population, respectively. Glutamatergic neurons are split into two subpopulations: projection (pyramidal) neurons and stellate neurons. The principal cells of the neocortex are pyramidal neurons, and each subtype differs in terms of layer position, morphology, dendritic arborization, and axonal projection targets. Pyramidal neurons are responsible for both axonal projections to the cortex and subcortical structures. stellate neurons are mainly located in layer 4 of primary sensory areas. GABAergic interneurons, show a huge diversity in both morphological and physiological structure and mainly have a local axonal projection within a circuit (Figure 1.B) (Kwan et al., 2012).

1.2. Architecture of the neocortex: layers, areas, and connectivity

Anatomically cerebral cortex is composed of two hemispheres that communicate with each other and allow synchronized processing of sensory, motor, and cognitive information. Each hemisphere is split into two major parts, the allocortex, including the archicortex (hippocampus), the paleocortex (olfactory cortex), and the neocortex (isocortex) (Klingler et al., 2019). From an evolutionary point of view, the neocortex is likely the most recent structure of the brain compared to the allocortex, which is unique to the mammalian brain and has undergone a drastic expansion likely associated with the emergence of multiple complex functions (Kandel, 2013).

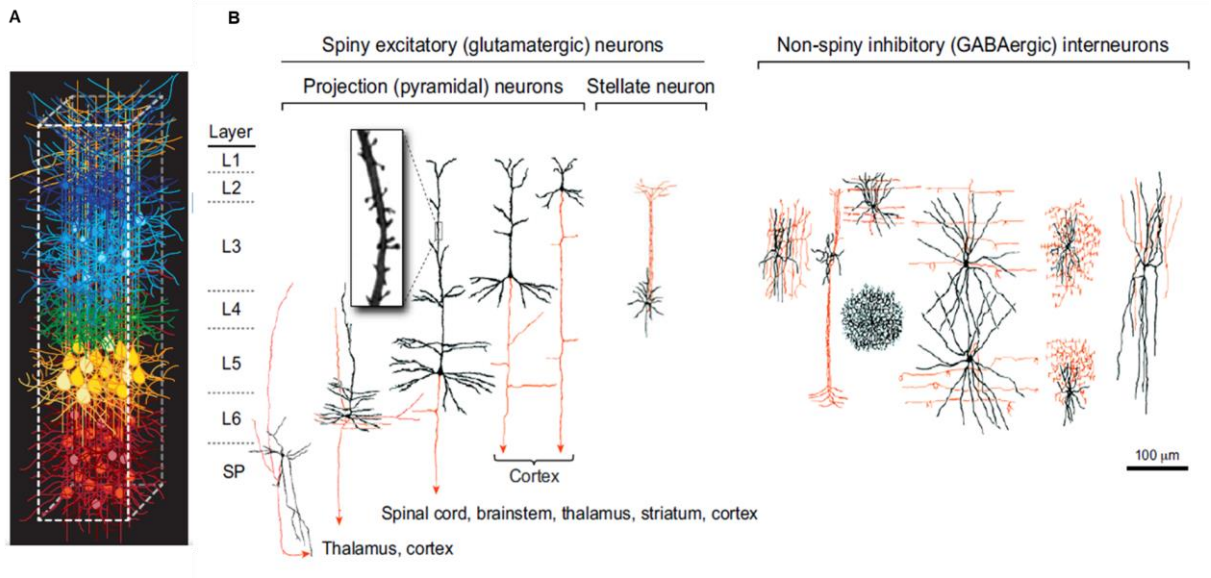

Figure 1| Organization of the neocortex

A. Schematic representation of the cortical organization in six tangential layers and radial columns, each containing pyramidal neurons. The dense apical dendrites of the pyramidal neurons in the underlying layers can be found in Layer 1 (L1), despite the fact that L1 lacks any pyramidal neurons (left panel). (Lodato & Arlotta, 2015) B. Principal types of neuronal cells in the adult cerebral cortex, Glutamatergic spiny excitatory neurons (left panel) and GABAergic non-spiny inhibitory interneurons (right panel). Dendrite (black) and axons (red). Targets of projection neurons toward the cortex and subcortical structures differ significantly depending on subtype and layer. Axons are directed within a local circuit by non-spiny interneurons with a wide range of morphology. Interneurons' subtypes also exhibit laminar preferences, which contributes to the cortical circuitry's layer differences (Kwan et al., 2012). Dendritic spines (inset).

Additional abbreviation: SP, Subplate

1.2.1. Layers

In the radial dimension, the neocortex is distinguished by its organization of neurons into six horizontal layers (Figure 1.A) (Greig et al., 2013a). Starting from the surface or pia there is layer 1 (L1), or molecular layer which has a limited density of neurons, mainly limited to GABAergic interneurons, however, it hosts plenty of dendritic processes and axonal projections of pyramidal neurons from deeper layers and glial cells. During the embryonic and very early post-natal development (The first two weeks) L1 is mainly populated by Cajal-Retzius cells (CRs) known as transient neurons (Harris & Shepherd, 2015; Ibrahim et al., 2020; Tremblay et al., 2016). Deeper are layers 2/3 (L2/L3) historically defined as supragranular layers. These layers contain a large density of projection neurons that project into both collateral and contralateral cortices.

Layer 4 (L4) known as the granule layer, contains projection and spiny stellate (granule) neurons. This layer is the main receiver of the sensory inputs originating from primary thalamic nuclei (Feldmeyer, 2012; Lodato & Arlotta, 2015). Below the upper layers of the neocortex (L2-L4) are the deep or subgranular layers called Layer 5 (L5) and Layer 6 (L6). L5 contains mainly large projection neurons that shape or establish the major part of the subcerebral axonal projections. (Hendrickson & Ward, 1975). L6 is the deepest cortical layer which contains the biggest morphologically and physiologically diverse cell types. Projection neurons in that layer make a great contribution to the cortico-thalamic tract (Briggs, 2010, p. 6; Greig et al., 2013a; Harris & Shepherd, 2015).

1.2.2. Areas

The human cortex is gyrencephalic, it contains many folds (gyri) split by elongated grooves called (sulci). This evolutionary convoluted form is believed to permit the presence of a greater number of neurons inside the limited space of the skull. In the mouse lack of gyri and sulci give the brain a smooth form. There is a pathological condition in humans, called lissencephaly, in which the absence of the grooves in the cerebral cortex, giving the brain a smooth shape similar to that of mice (Kato & Dobyns, 2003). Despite the

discrepancies in the superficial shape, the mammalian neocortex shares a similar structure. The cerebral cortex is tangentially subdivided into separated functional regions, called cortical areas. The areas can be split into primary areas which are surrounded by higher-order areas, including secondary and associative. Cortical areas are defined by their model of connectivity with the thalamus: primary areas receive inputs from thalamic first-order nuclei (Pouchelon et al., 2014). There are three sensory primary areas, called visual area (VISp), somatosensory area (SSp), and auditory area (AUDp). These primaries receive and process sensory information collected at the periphery: the eye (vision), body (somatosensation), and ear (audition) (Figure 2). The fourth primary area is the motor (MOp), which controls the execution of voluntary movements. After processing of the information received by primary areas they will be transmitted to higher order thalamic nuclei and eventually to the secondary area and from here to associative areas which incorporate multimodal inputs coming from various stimuli, demonstrating a cortico-thalamic-cortical loop (Alfano & Studer, 2013; Jabaudon & López Bendito, 2012; O'Leary et al., 2007; Pouchelon et al., 2014).

1.2.3. Connectivity

From a functional point of view, in the cortex, neurons establish horizontal connections within and across cortical areas as well as radial connections within functional columns. Cortical columns refer to groups of neurons from different layers in a vertical cluster within the sensory cortical areas that share a common response to the same type of stimulus (visual, auditory, etc.) (Figure 1.A) (Crowley & Katz, 1999; da Costa & Martin, 2010; Horton & Adams, 2005; Lodato & Arlotta, 2015).

Interestingly, the organization of the neocortex into the laminar and radial plane is not only limited to this level but can also be found at the level of individual pyramidal neurons as building blocks of the neocortex. Pyramidal neurons mainly establish two groups of connection: intracortical which refers to the connection inside the cortex and corticofugal which points to connections projected from the cortex to the other parts of the brain (Figure 2) (Lodato et al., 2015). Neurons located at the superficial level of layers (2, 3, 4) mostly establish intracortical axonal projection. In contrast, neurons localized in the deepest

cortical layers mainly project axons to the subcortical structures such as corticothalamic neurons in L6 which target the thalamus, and neurons in L5 which project to the tectum, hindbrain, and spinal cord (Jabaudon, 2017). The hierarchy construction of the laminar neocortex provides a link between structure and function (Feldmeyer, 2012; Larkum et al., 2018).

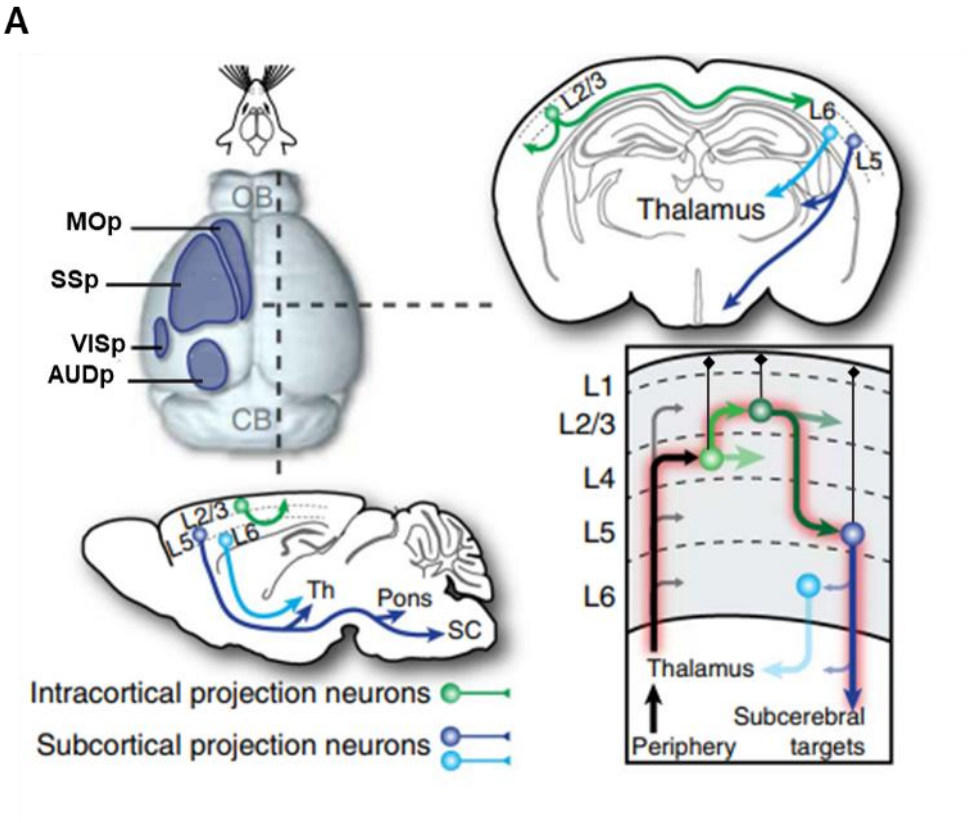

Figure 2| Brain areas, cortical and subcortical connectivity

A. Schematic representation of the distinct primary cortical areas in the mouse brain (left-top panel). Schematic representation of the Intracortical and Corticofugal connections in the cerebral cortex: sagittal plane (left-bottom panel), coronal plane (right-top panel). Intracortical connections are established by neurons in the superficial layers 2-4. Corticofugal connections are made by deep layers neurons 5 and 6. Top-down transmission of information in addition to bottom-up connection (Jabaudon, 2017). Abbreviations: VISp, Visual primary area; SSp, Somatosensory primarya rea; AUDp, Auditory area primary; Mop, Motor primary area.

The classical dogma for the bottom-up cortical information processing implies that the collected sensory input from the periphery will transmit to L4 excitatory neurons through primary thalamic nuclei. From layer 4 excitatory neurons project to upper layers

2 and 3 and from there information will be transmitted to the collateral or contralateral cortex, and the deeper layers (L5 and L6) pyramidal neurons (Bartolini, Ciceri, & Marín, 2013; Harris & Shepherd, 2015). Eventually, received inputs from upper layers by L5 and L6 pyramidal neurons will be transmitted to subcortical regions (Harris & Shepherd, 2015; Jabaudon, 2017).

There is a top-down flow of information in addition to bottom-up connection, which transmits data from the sensory organ to the neocortex (Cauller, 1995; Ibrahim et al., 2020; Rubio-Garrido et al., 2009). Neocortical L1 is the main conduit for top-down information, where axonal input reaches neural networks directly, modulating their connectivity. This modulation is particularly significant because it frequently activates entire columns of the underlying cortex by reaching the apical dendrites of pyramidal neurons situated in several neocortical layers. One model in the somatosensory cortex that underlies conscious behavior and active touch discrimination (Cauller, 1995), as well as the ability to distinguish between internally and externally generated sensory representation (Keller & Mrsic-Flogel, 2018), and predictions, suggest that the integration of top-down and bottom-up information in L1 is essential for active perception.

Numerous studies have been conducted on the cerebral cortex, a sophisticated organ whose function is unknown. It is impossible to comprehend one's organization without considering its sequential development. Since some processes occur after birth, the initial steps begin very early and continue throughout the embryo's life.

2. Development of the cerebral cortex:

The development of the brain is made up of multiple unique processes that are strictly regulated, and defects in any of those processes can have a detrimental effect on the growth of this sophisticated structure (Figure 3). Accordingly, I will briefly discuss some of the major processes that contribute to the maturation of the mouse brain in this chapter. These processes include the formation of the central nervous system (CNS), patterning of the primordia of important brain regions, proliferation of neuroepithelial cells, differentiation and migration of immature neurons, and removal of non-specific connections and excess or abnormal neurons through program cell death (PCD).

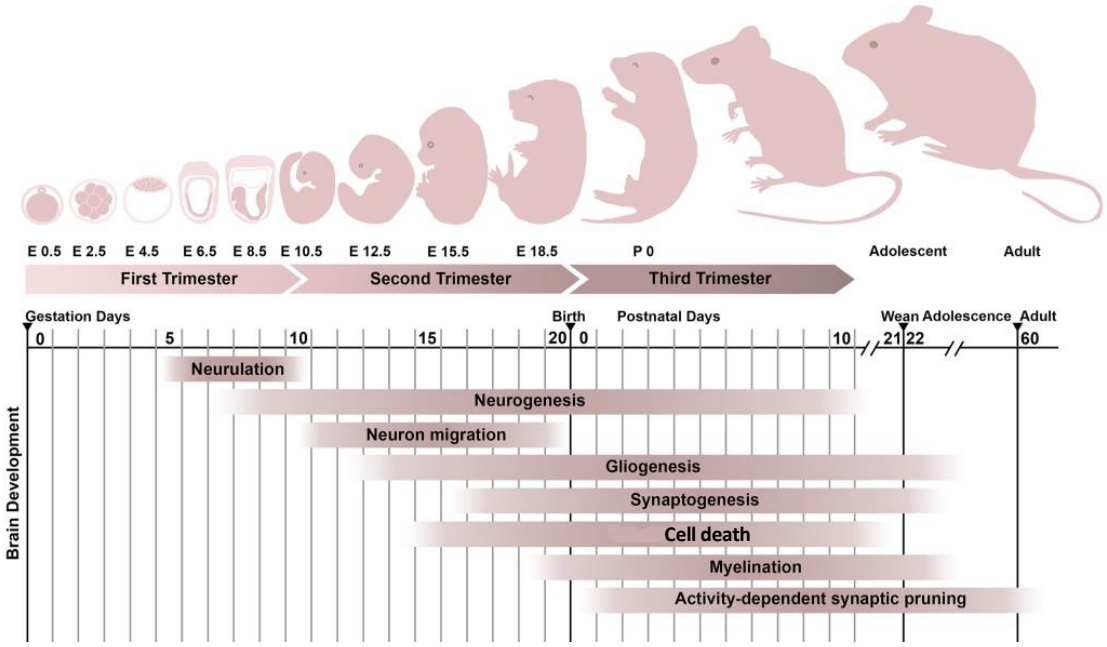

Figure 3 | Mouse brain development timeline

Schematic representation of major events occurring during embryonic (E) and postnatal (P) mice brain development. The shaded horizontal bars indicate the approximate timing of neurobiological processes (Wen et al., 2022).

2.1. General overview on telencephalic development

The zygote goes through multiple rounds of cell division and migration after fecundation to eventually form the three germ layers known as the ectoderm, mesoderm, and endoderm. During neurulation, the ectoderm in mice begins to thicken and differentiate into the neural plate around the embryonic day 7.5 embryonic day (E 7.5) (Figure 4). After that, the neural plate will bend dorsally, bringing its two ends together, forming the neural tube at E8.5 in mice. The neural tube differentiates into the three primary vesicles known as the forebrain, midbrain, and hindbrain shortly after closure into the antero-posterior (AP) axis. The forebrain eventually separates into secondary vesicles such as the telencephalon. Pallium (also known as the cerebral cortex) is produced by the dorsal part of the telencephalon, while subpallium, which primarily produce the basal ganglia and migratory neurons, is produced by the ventral part (Kandel, 2013; Puelles & Rubenstein, 2003).

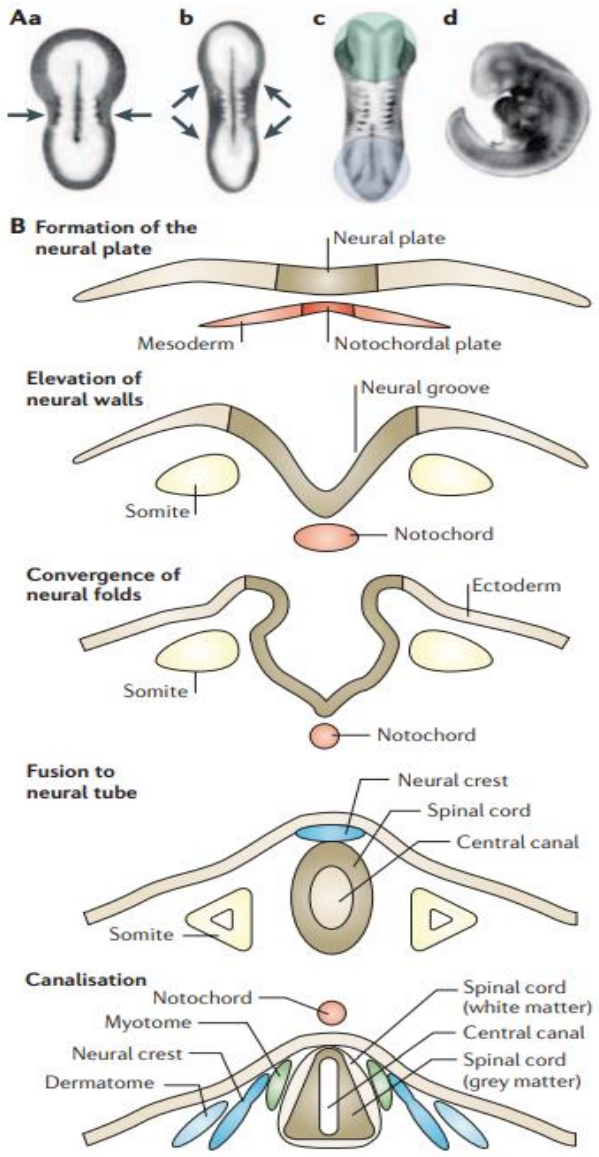

Figure 4 | Neural tube closure in the developing mouse brain

A. Four different phases of primary neurulation during neural tube closure. Aa–c are dorsal views, whereas panel Ad is a lateral view. B. Stages of neural tube closure in a coronal view (Blom et al., 2006).

Cortical patterning is initiated very early by E10 through the patterning of the neural tube along the AP and dorso-ventral (DV) axis, which is mediated via secreted gradients of morphogens and signaling molecules produced by organizing centers in the developing brain. Morphogens are essential for defining distinct subdomains, such as cortical areas, as well as distinct regions of the CNS (Figure 5) (dorsal versus ventral),

which is being done through regulation of the expression of transcription factors (TFs), necessary for neuronal differentiation and glial cell identity (Fukuchi-Shimogori & Grove, 2003; Greig et al., 2013a; Rallu et al., 2002). There are three organizing centers in the telencephalon: the anterior neural ridge (ANR) which rostro-medially secretes Fibroblast growth factors (FGFs) (Fgf8 and Fgf17), (Bachler & Neubüser, 2001; Crossley & Martin, 1995), cortical hem (CH) which caudo-medially secretes Wnts and Bone morphogenetic proteins (BMPs), and anti-hem also called the ventral pallium (VP) which laterally secretes Wnt antagonists and Epidermal growth factor (EGF) are organizing centers secreting morphogens in the dorsal telencephalon (Figure 5)(Assimacopoulos et al., 2003). Sonic hedgehog protein (SHH) is most abundant in the ventral part of the telencephalon, where is more involve in the development of ganglionic eminences (GE) and generation of interneurons (Hoch et al., 2009). Choroid plexus (ChP) secrets all different types of morphogens in to the Cerebrospinal fluid (CSF) which fills the lateral ventricles (LVs) (Greig et al., 2013a). Particularly, four main TFs whose expression is reciprocal in pairs have been identified. Empty spiracle homeobox 2 (Emx2) and paired box gene 6 (Pax6) are expressed in a caudo-medial and rostro-lateral gradients, respectively (Gulisano et al., 1996; Walther & Gruss, 1991). Chicken ovalbumin upstream promoter transcription factor 1 (Couptf1) and trans-acting transcription factor 8 (Sp8) are expressed in a caudo-lateral and rostro-medial gradients, respectively (Borello et al., 2014; Q. Liu et al., 2000). Each postmitotic neuron can acquire a distinct area identity based on the level of TFs expression defined by these complementary gradients, which define coordinates. The motor identity is specifically determined by the expression of Pax6 and Sp8 in the rostral direction, while the specification of sensory areas is driven by the presence of Emx2 and Couptf1 in the caudal direction. In fact, numerous studies

have demonstrated that altering the expression of one of these factors can reorganize cortical regions. For instance, in the cortex, both the conditional ablation of Couptf1 and the haploinsufficiency of Emx2 result in an expansion of motor areas at the expense of sensory areas. On the other hand, the ablation of Pax6 has the opposite effect, resulting in a reduction in the size of motor areas and an increase in the size of sensory areas (Bishop et al., 2002; Greig et al., 2013b; Ohshima et al., 2004).

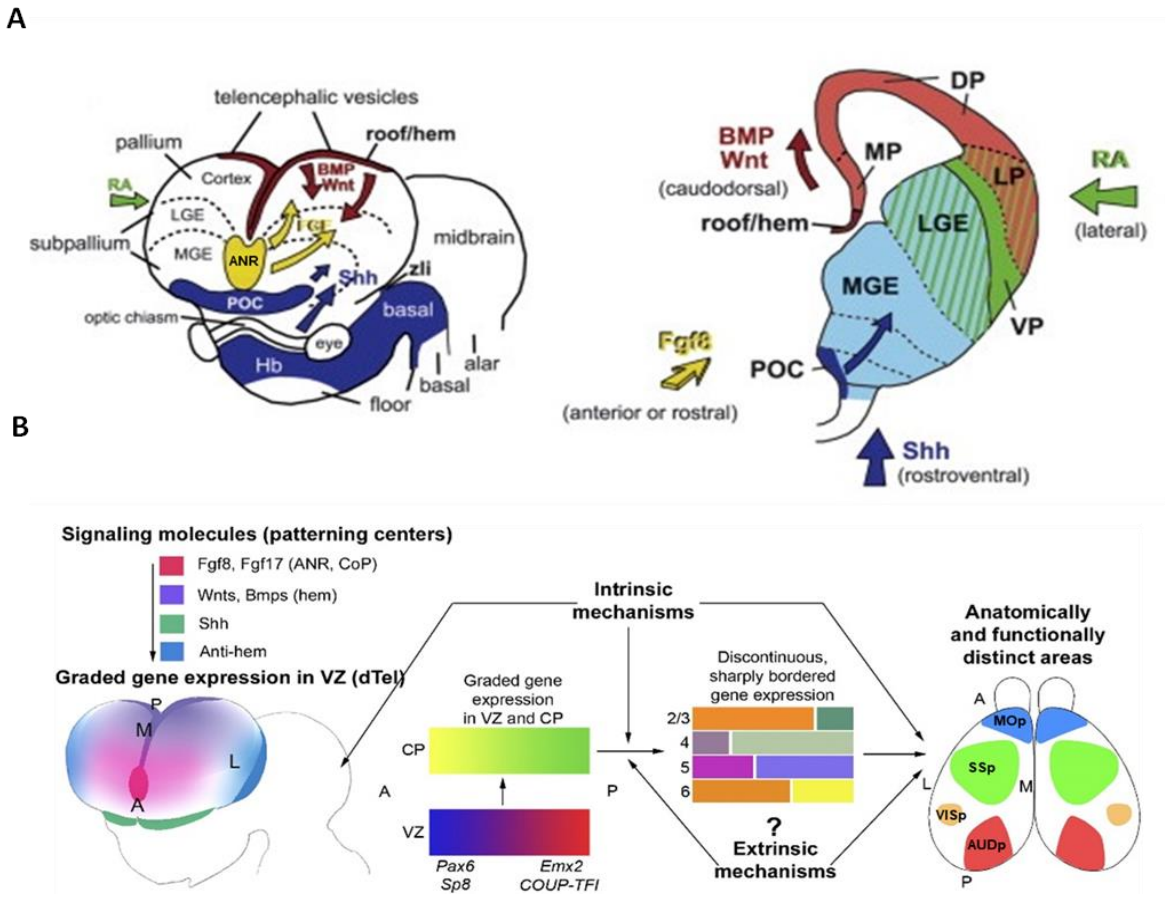

Figure 5 | signaling molecules and TFs involved in pallial patterning

A. Schematic illustrations of the signaling pathways and proteins involved in pallial patterning in the mouse brain (left) and frontal telencephalic hemisection (right). This included dorso-caudal signals of BMP and Wnt proteins from the roof plate and/or the cortical hem, rostral signals of FGF8 from the ANR and, ventral signals of Shh from the precordal plate (initially) and the basal forebrain (later). Adopted from (Medina & Abellán, 2009) . B. Schematic representation of the gradient of main organizing centers involve in the patterning of the pallium. The differential expression of TFs, which, together with extrinsic signals, contributes to the establishment of cortical area identity, is regulated by the gradient of morphogens. Adopted from (O'Leary et al., 2007).

Abbreviations: CP, cortical plate; MZ, marginal zone; VZ, ventricular zone; DP, dorsal pallium; VP, Ventral pallium ; LP, lateral pallium ; MGE, medial ganglionic eminence; CGE, caudal ganglionic eminence; LGE , lateral ganglionic eminence; ANR, anterior neural ridge

2.2. Generation and migration of cortical neurons

In the central nervous system, neurons are produced by neural stem cells, which this process is called neurogenesis. This is followed by, neuronal migration, dendritic and axonal growth, and synaptogenesis.

The pallium, also known as the cerebral cortex, is formed by the dorsal telencephalon, and the ventral telencephalon transforms into the subpallium, which further produces GE and migrating neurons (Kandel, 2013; Puelles & Rubenstein, 2003). Undifferentiated neuroepithelial cells (NEs) construct the pallium telencephalic wall in mice at E10.5 (Rubenstein & Beachy, 1998). At this time, some of these progenitors begin to differentiate into bipolar radial glia cells (RGs) and establish the primary germinal zone known as the ventricular zone (VZ). Since these cells are located in the apical VZ, they are referred to as apical RGs (aRGs), ventricular RGs, or vRGs. These cells are typically found in the developing brains of all mammalian species (Figure 6) (Paridaen & Huttner, 2014).

aRGs span the thickness of the cortex by a short apical process that touches the ventricular surface (apical) of the developing cortex, and a longer basal process that touches the other superficial surface, the cortex' basal surface (pial surface) (Greig et al., 2013a; Rakic, 1971). At E11.5, RGs in the VZ undergo symmetric division to significantly increase the pool of aRGs progenitors and to generate additional progenitor classes, including intermediate progenitors (IPs) and outer RG basal RGs (bRGs, or outer RGs, oRGs, which collectively form the subventricular zone (SVZ). Unlike aRGs, bRGs do not have an apical process and remain attached to the pial surface via their basal process. bRGs are especially prevalent in humans (Hansen et al., 2010; Paridaen & Huttner, 2014).

IPs have a multipolar morphology and eventually divide either proliferatively to produce two progenitors or differently to produce two neurons. It has been demonstrated that microcephaly may result from mutations in the EOMES gene, which is responsible for encoding Eomesodermin, also known as T-box brain protein 2 (Tbr2) proteins. The fact that Eomesodermin/Tbr2 is highly expressed in IPs and plays an important role in their differentiation into other neurons lends credence to the significance of IPs in regulating neocortex size (Englund et al., 2005). The earliest-born neurons migrate away from the ventricular surface to segregate from progenitors and form the preplate (PP), which is

composed of the earliest-born neurons and differentiated from Neural stem/progenitor cells (NSPCs) in the VZ. At the same time, a/bRGs begin to produce projection neurons, which establish PP (Angevine & Sidman, 1961; Greig et al., 2013a).

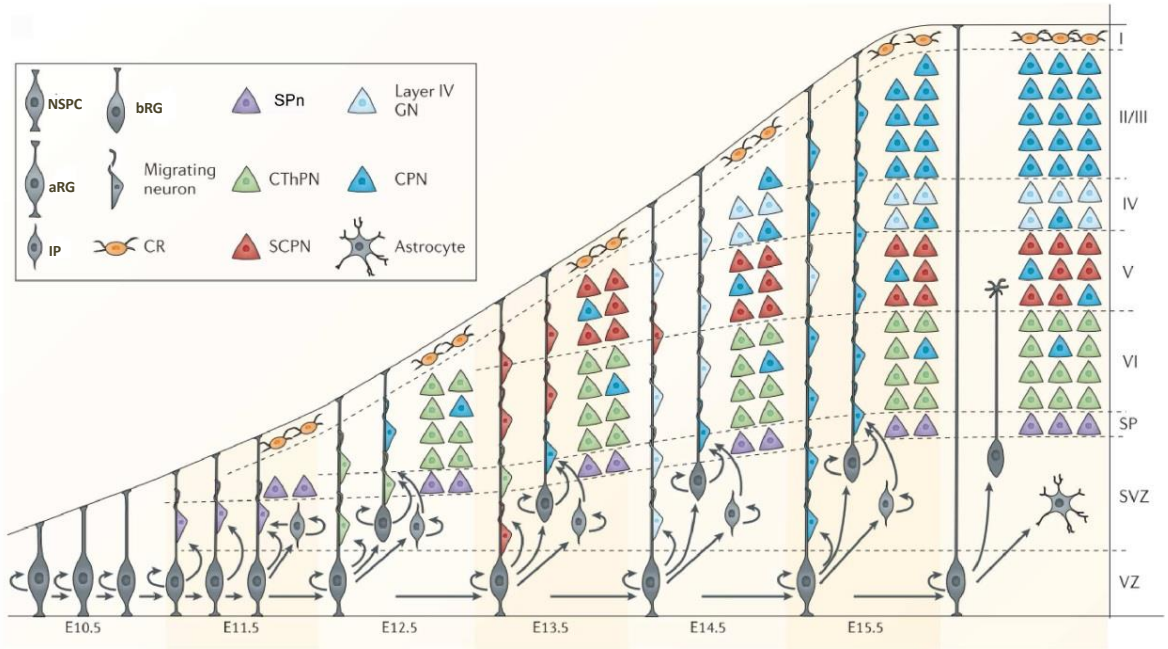

Figure 6 | Corticogenesis during mice brain development

Schematic representation of the generation and migration of pyramidal neurons. NSPC produce aRGs, which multiply to expand the pool of progenitors and generate IPs, bRGs, and neurons. Before becoming neurons, IPs and bRGs undergo limited proliferation. Excitatory projection neurons of various subtypes are produced and colonize the cortical plate in an "inside out," manner, the earliest-born neurons in the deep cortical layers and the later-born neurons in the upper cortical layers (Greig et al., 2013).
Abbreviations: CThPN, corticothalamic projection neurons; CPN, callosal projection neurons; GN, granular neurons; SCPN, subcerebral projection neurons.

As neurogenesis progresses, projection neurons settle into the PP to establish the newly formed cortical plate (CP). The CP divides the PP into the subplate (SP), which will comprise a portion of layer 6, and the marginal zone (MZ), which will shape the entire neocortex L1. The neocortex's CP will eventually become L2 to 6. (Kwan et al., 2012; Marin-Padilla, 1978; Noctor et al., 2001; Sakayori et al., 2013).

As neurogenesis proceeds and the thickness of cortex and distance to travel increase, neurons undergo a radial migration that can be broken down into four steps. Newly

generated neurons at the VZ migrate radially into the SVZ during the first phase. In phase 2, new neurons lack polarization and they do not seem attached to the guiding extension of the radial glia cells, they move slowly in an RG-independent manner and extend and retract multiple processes into all direction. Neurons move into the locomotion mode during phase 3, they stretch an extension towards the basal dendrite of the adjacent RGs to use them as a scaffold to cross the CP through RGs and reach their final position. In Phase 4, they detach from the RGs and perform a terminal somatic translocation to conclude their migration (Kanatani et al., 2005; Noctor et al., 2004).

Excitatory projection neurons of various subtypes are produced and colonize the cortical plate at various time points: SP neurons start to invade the cortex at around E11.5, shortly after that at E12.5 and E13.5, corticothalamic projection neurons (CThPN) and subcerebral projection neurons (SCPN) are produced, respectively (Figure 6). By the E12.5, also some callosal projection neurons (CPN) are born, and those CPN that are born simultaneously with CThPN and SCPN also migrate to deeper layers, but the majority of CPN born between E14.5 and E16.5 migrate to superficial cortical layers. Around E14.5, granular neurons (GN) of L4 are born.

As neurogenesis proceeds, migration of newly-born neurons happens in an inside-first, outside-last manner leading to formation of the neocortex in an 'inside-out' fashion, meaning that early-born neurons in and the neocortex is formed in an 'inside-out' fashion, in which early-born neurons populate and form the deep layers (L6 first and then L 5), whereas later-born neurons migrate past them to progressively populate the superficial neocortical layers (L4, then L2/3) (Greig et al., 2013a; Kwan et al., 2012; Noctor et al., 2001). After neurogenesis is complete, neural progenitor cells shift to a gliogenic mode, to makes glia cells (oligodendrocytes and astrocytes) (Fiacco & McCarthy, 2006).

Unlike excitatory projection neurons generated from progenitors at the VZ of the dorsal pallium, cortical interneurons (INs) originate from progenitors in the subpallium (Figure 7). Several germinal zones had been discovered, which give rise to a variety of neuronal subtypes: NPs and INs the medial ganglionic eminence (MGE), and caudal ganglionic

eminence (CGE), which these two give rise to the majority of inhibitory neurons (60% and 30% respectively), the lateral ganglionic eminence (LGE), and the preoptic area (POA) (Anderson et al., 2001; Flames et al., 2007; Q. Xu et al., 2004).

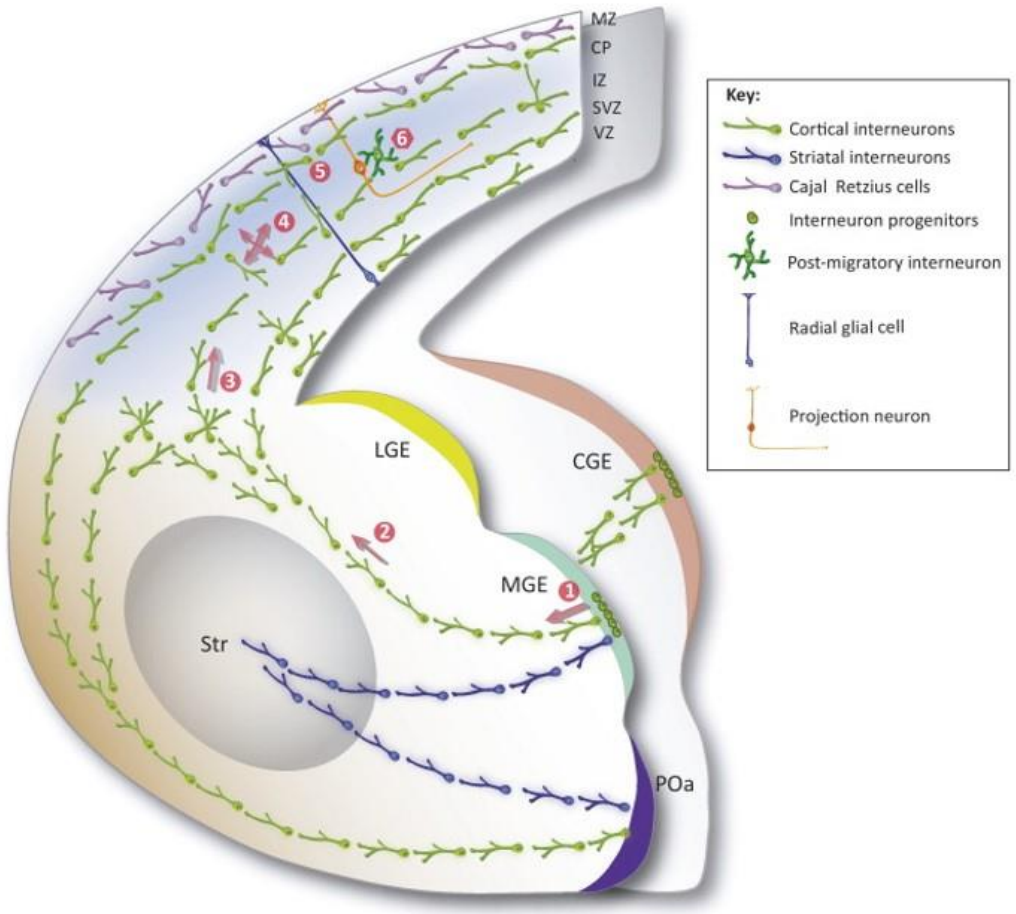

Figure 7 | Migration patterns of interneuron in the developing telencephalon

Schematic representation of the migration of subpallium-derived cortical interneurons at E15 in the rostral and caudal hemisection of the mouse telencephalon. Interneurons that originate in the preoptic area (POA), the caudal ganglionic eminence (CGE), or the medial ganglionic eminence (MGE) exit the proliferative zones and begin their migration toward the developing neocortex and striatum (orange). Interneurons in the cortex travel tangentially into the cortex after passing through the developing striatum and crossing the corticosubpallial boundary. The marginal zone (MZ), the subplate (SP), and the intermediate zone (IZ)/subventricular zone (SVZ) migratory streams are the primary pathways through which cortical interneurons travel to the neocortex. The net directionality of movement is indicated by arrows.(Guo & Anton, 2014).

After arriving at the cortex, INs migrate tangentially in streams above the MZ and below the SVZ and the CP to reach their position in these cortical regions before shifting to the radial migration to invade the CP and reach their ultimate location (Chu and Anderson, 2015). Two waves of INs migration to the cortex have been identified: first at the E12 in mice to join the PP and second later between E13 and E15 to join the CP (Lopez-Bendito et al., 2004; Nadarajah and Parnavelas,2002). It has been shown that INs still continue their migration during post-natal stages depending on synaptic activity. (From Marco Garcia et al., 2011). Besides INs, another population of excitatory neurons, the CRs, has been shown that joins the newly formed cortex at the MZ through tangential migration. (Bielle et al., 2005; Takiguchi-Hayashi et al., 2004; Yoshida et al., 2006)

2.2.1. Cajal Retzius cells at the center of cortical development

2.2.1.1. Discovery of CR cells

Through the use of Golgi staining, Santiago Ramon y Cajal reported for the first time in 1891 the existence of a type of horizontal cell with an ovoid soma and extremely long extensions that were only found on the superficial surface of the cortex of various mammals (cat, rabbit, rat, and dog) (Figure 8) (Ramon y Cajal, 1890). Two years later, in 1893 Gustaf Retzius described a type of bipolar cell with multiple extensions and a cell body that is perpendicular to the surface of the cortex in L1 (Figure 8) (Retzius, 1893). This type of bipolar cell was similar to what Cajal had reported. Comparison of the cells observed by two histologists in the MZ/L1 revealed that the cells in the human brains are quite distinct from those observed in other species, suggesting that the type of species and their developmental stages can significantly affect those cells. At the end of the 19th century, it was decided to give them the name Cajal-Retzius, which their nucleus and extension are located in the L1(Camacho et al., 2014; Martínez-Cerdeño & Noctor, 2014). CRs got more attention only after the recognition of the gene in charge of the reeler phenotype. Falconer first described the reeler mice mutant in 1951. This mutant has a number of behavioral defects that suggest the involvement of the cerebral

cortex and cerebellum, such as jerky gait, ataxia, and tremors (Figure 9) (Falconer, 1951). Further histological examination of the reeler brain reveals that there is a defect in the proper migration of projection neurons that causes abnormal lamination of the cortex, cerebellum, and hippocampus, resulting in the absence of the CP and the subsequent separation of the PP from the SP and MZ (Ogawa et al., 1995).

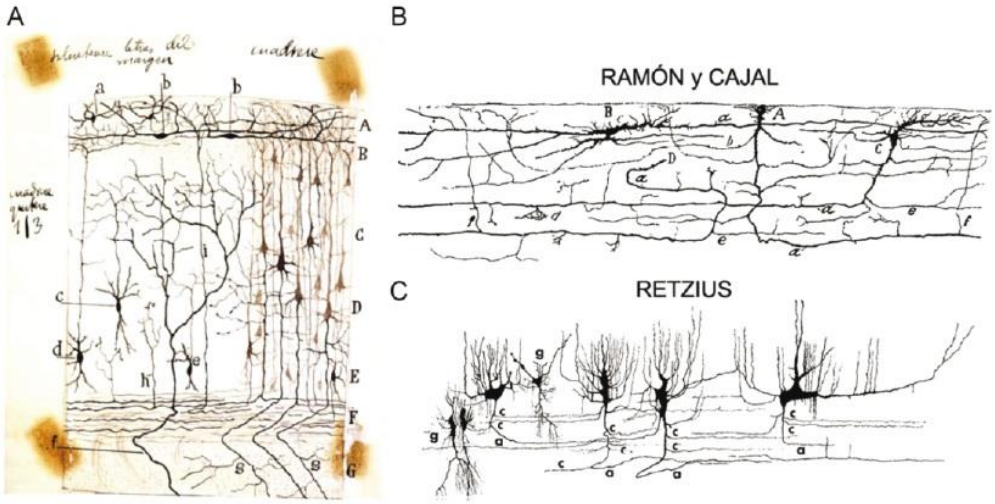

Figure 8 | Discovery of Cajal-Retzius cells

Drawings of layer I (L1) cells obtained through the Golgi impregnation method. A. compilation of cells discovered in the cortex of various small mammal (rabbit, mouse) specimens between 1890 and 1891.It is possible to observe the horizontal, bipolar, and area-restricted cells that Cajal described in the ZM, which are located in region A. (B and C). Represented L1 cells from the motor cortex of a child who was two years old by Ramon y Cajal (B) of a human fetus with 26 weeks old by Retzius .The cells that Retzius first described are depicted in these observation drawings, with their multidirectional extensions and perpendicular soma at the surface (Ramon y Cajal, 1890; Retzius, 1893).

Several month after *Reln*, which encodes reelin protein, has been identified as the gene responsible for the reeler phenotype (D'Arcangelo et al., 1995a). Further study discovered the different sources of reelin in the developing nervous system such as the neocortex, olfactory bulbs, and striatum. According to D'Arcangelo et al, CRs as a transient population of excitatory neurons are the only source of Reelin in the developing cortex (D'Arcangelo et al., 1995a; Del Río et al., 1997; Kirischuk et al., 2014; Marín-Padilla, 1998; Meyer, 2010)

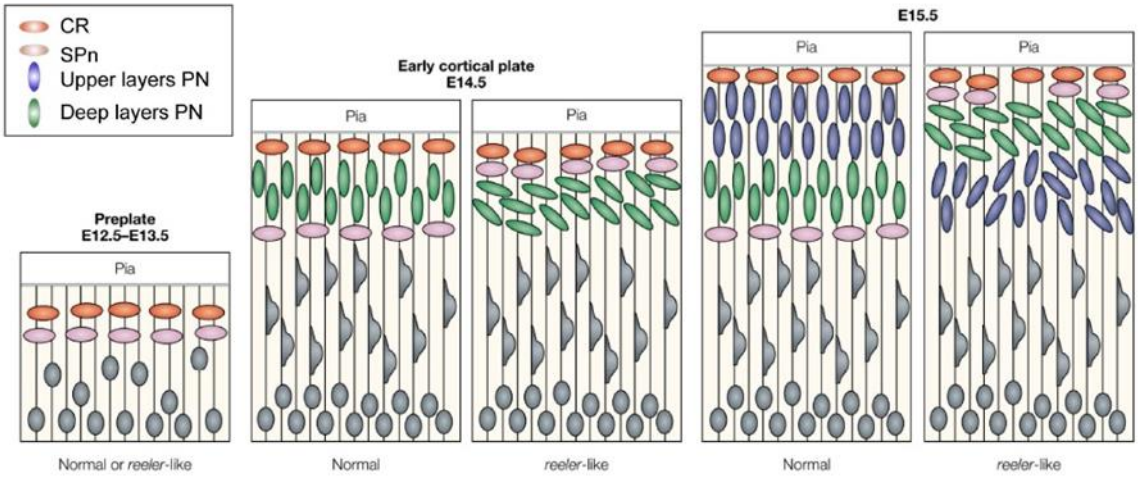

Figure 9. Early cortical development in the reeler mice mutant

At E13.5 the reeler phenotype is not obvious, further at E14.5, when cells need to migrate along radial glial (RG) fibres as migratory distances and the complexity of the environment increase. The early projection neuron (PNs) which make the cortical plate (CP) (green), divides the prelate (PP) into two parts. While the PP is not divided into two parts in the reeler CP, which is packed with cells that are oriented obliquely. In a normal situation, an inside-to-outside gradient is created around E15.5 when the second cohort of PNs (blue) migrates past the normal CP and settles superficially. Whereas the second cohort settles in the deep layers of the CP in reeler mutants, creating a gradient from the outside to the inside. (Tissir & Goffinet, 2003).

2.2.1.2. Developmental origins and migration of CR cells

In the embryonic telencephalon, CRs are among the very first generated transient heterogeneous population of glutamatergic neurons lining the neocortex between E 9.5 to E12.5 in mice (Hevner et al., 2003; Radnikow et al., 2002a; Zecevic & Rakic, 2001). CRs are generated at 4 distinct territories at the edges of the pallium and express pallial markers (Hevner et al., 2003). According to their origin they are divided into 4 subpopulations: the pallial septum (SE), the pallial-subpallial boundary (PSB), the cortical hem (CH), and the eminentia thalami (ET) (Figure 10). CH, SE and PSB account for the majority of cortical CRs. (Ruiz-Reig et al., 2017; Tissir et al., 2009). Despite being known as glutamatergic neurons, CRs tangentially migrate to the surface of the cortex to help forming the PP. Shortly after the development of CP and the separation of the

PP from the SP and MZ, CRs are located in the MZ (Tissir & Goffinet, 2003). CRs depend on their site of origin preferentially populate distinct cortical territories: SE-CRs are located in the rostro-medial, PSB mainly in the rostro-lateral cortex, CH in the medio-caudal, and ET the entorhinal and piriform cortex laterally (Figure 10) (Barber & Pierani, 2016; Bielle et al., 2005a; Griveau et al., 2010; Meyer, 2010; Tissir et al., 2009). In addition to their cortical location, CH-CRs can be found in the hippocampus, specifically at the stratum lacunosum moleculare (SLM) and outer molecular structure of the dentate gyrus (OML).

An extra neocortical source of CRs was first discovered by (Takiguchi-Hayashi et al., 2004). They used the IG17 transgenic line, in which the promoter of the metabotropic glutamate receptor two (mGluR2) controls the green fluorescent protein (GFP) expression. In addition, they demonstrated that cells that express *Reln*, p73, and Calretinin and are positive for GFP are found in the MZ of these animals. In addition, they demonstrate that at E12.5 β-Galactosidase (β gal) positive cells reached the MZ by tangentially migrating in a caudo-medial gradient by ex-utero electroporation of LacZ in mice at the caudo-medial border of the pallium, where CH-CRs are located. At E16.5, the cortex's entire surface is eventually covered in β gal positive cells that are also positive for GFP (Takiguchi-Hayashi et al., 2004). Further studies, has shown that SE-CRs and CH-CRs both express *Reln* and p73, while PSB-CRs express *Reln* and calretinin but not P73, indicating that distinct subtypes of CRs have distinct molecular properties (Griveau et al., 2010). Furthermore, it was demonstrated that SE-CRs begin their migration earlier, travel faster, and migrate more linearly than other populations (Barber et al., 2015). It is clear that CRs are not a uniform population due to their various origins, molecular variations, and distinct distributions.

Using the expression of a Cre recombinase as a genetic tool under the various gene promoters associated with distinct subpopulations of CRs made it possible to trace this neuronal population permanently, for instance: $DNp73^{cre/+,}$ which enables the genetic tracing of CRs originating from the SE, CH, and ET domains (Tissir et al., 2009), $Dbx1^{cre/+}$,

which can target SE and PSB (Griveau et al., 2010), and *Wnt3a*$^{cre/+,}$ which only targets CH (Yoshida et al., 2006) .

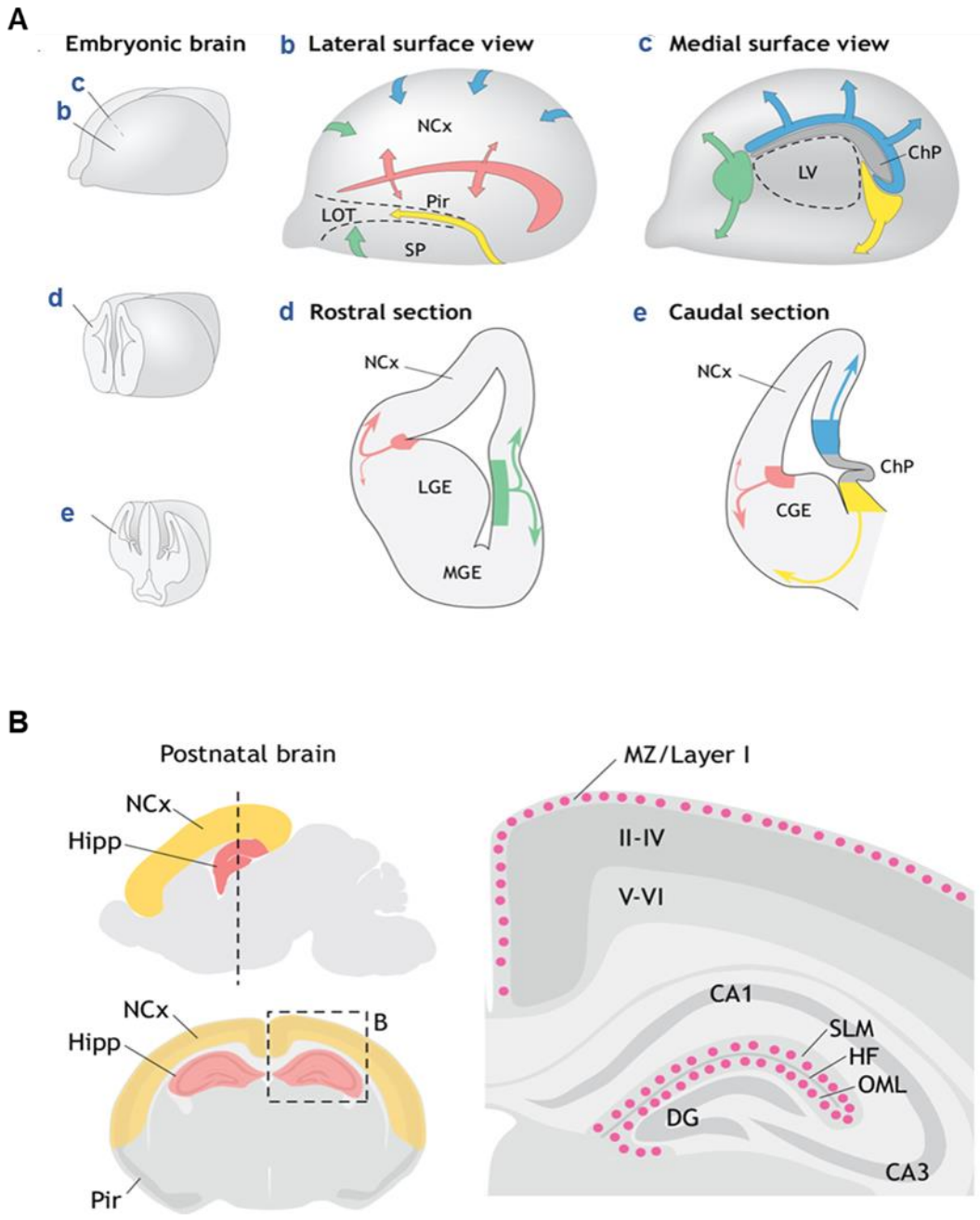

Figure 10. CRs in mice brain

A. Three-dimensional images of the developing brain, the surface views in c and b, as well as the sections in d and e, indicating the migratory streams (arrows) of CRs from the pallial septum (SE) (green), the pallial-subpallial boundary (PSB) (red), the cortical hem (CH) (blue) and the eminentia thalami (ET). (yellow). **B.** Postnatal mouse brain slices, shown in sagittal (upper panel) and coronal (lower panel) views, demonstrating the locations of CRs in the neocortex, hippocampus, and piriform cortex. Abbreviations: CGE, caudal ganglionic eminence; ChP, choroid plexus; LGE, lateral ganglionic eminence; LOT, lateral olfactory tract; MGE, medial ganglionic eminence; NCx, neocortex; Pir, piriform cortex; SP, subpallium.

DG, dentate gyrus; HF, hippocampal fissure; Hipp, hippocampus; NCx, neocortex; OML, outer molecular layer; Pir, piriform cortex; SLM, stratum lacunosum moleculare (Causeret et al., 2021).

2.2.1.3. Functions of CRs

CRs are well-known for their role in the correct migration of projection neurons and cortical lamination through the secretion of Reelin, and various functions in the establishment of the cortex have been associated them (Frotscher et al., 2001). Reelin is a 388 kilodalton (kDa) glycoprotein that phosphorylates the Dab1 adapter by binding to its receptors, apolipoprotein E receptor 2 (ApoER2) and very low density lipoprotein receptor (VLDLR) (Boyle et al., 2011; D'Arcangelo et al., 1995b). Several signaling pathways that control radial migration and dendrite formation in neurons are controlled by phosphorylated Dab1.

As was previously mentioned, the reeler mutant's abnormal cortical lamination is caused by incorrect radial migration and the "inside-out" positioning of projection neurons, as well as problem with the PP's separation into MZ and SP (Figure 9) (Ogawa et al., 1995; Tissir & Goffinet, 2003). Human disorders such as lissencephaly, schizophrenia, bipolar disorder, and autism have been linked to *RELN* mutations (Fatemi et al., 2001; Impagnatiello et al., 1998).

Numerous studies have been carried out to eliminate various subsets of CRs by expressing the fragment A of the diphtheria toxin (DTA), DTA interfere with production of proteins and causes cell death, under the control of various CRs promoters like deltap73, Wnt3a, and Dbx1 in order to investigate the role that CRs play in the development of cortical structures (Griveau et al., 2010; Tissir et al., 2009; Yoshida et al., 2006).

Bielle et al. in 2005 by using Nes^{Cre}; $Dbx1^{DTA}$ lineage eliminated S-CRs and PSB-CRS. Further Fadel Tissir in 2009 was able to eliminate up to 75% of CRs using the *delta* $Np73^{Cre}$; $Wnt3a^{Cre}$ lines, and in both cases there was no evidence of defect in the cortical lamination, regardless of the number of depleted CRs. This suggests that the remaining CRs can make up for the loss of *Reln* or that the cortex contains other sources of *Reln* that can compensate for the lack of CRs (Bielle et al., 2005a; Tissir et al., 2009; Yoshida et al., 2006).

Several works done in our laboratory have highlighted the critical roles of CRs in cortical arealization in the developing telencephalon, CRs are produced at the signaling centers and express several morphogens important for correct cortical arealization. Fgf8, BMP/Wnt, and Egf/anti-Wnt are expressed by SE, CH and PSB CRs, respectively (Alfano & Studer, 2013).

To investigate the role of CRs in the regionalization of the cortex, Amélie Griveau demonstrated in 2010, that ablation of SE-CRs results in a reduction in the proliferation of cortical progenitors in the rostro-medial part of the cortex, where SE-CRs tend to populate. In addition, they showed that upon ablation of SE-CRs, the CH- and PSB-CRs, the other two primary sources of CRs, begin to redistribute to populate the empty cortical region associated with the absence of SE-CRs. The expression of TFs like Pax6, Emx2, and Sp8, which are necessary for correct early regionalization of the cortex, is altered due to this redistribution. As a result, at P8, the mutants' primary motor area has expanded at the expense of their primary somatosensory area (Figure 11) (Griveau et al., 2010). As a direct consequence, the redistribution of CRs causes a reorganization of a number of higher order areas, including a reduce in the size of the secondary visual area (V2) and auditive area (A2), while the size of the secondary somatosensory (S2) and parietal associative (PtA) areas increase (Figure 11) (Barber et al., 2015).

Furthermore, it has been demonstrated that the long-distance secretion of CR-produced morphogens and growth factors (FGFs, BMPs, and Wnts) influences the proliferation and differentiation of neighboring progenitor cells (Griveau et al., 2010). Therefore, CRs function as real mobile signaling centers that are essential for the patterning of the developing cortex by signaling to cortical progenitors. These studies indicate that distinct CR populations have distinct characteristics and functions during embryogenesis.

In addition, CRs play an important role in the regulation of interneurons migration. The ablation of CH-CRs via the $Emx1^{Cre}$; $Wnt3a^{DTA}$ mutant leads to an early tangential migration of interneurons and followed by an anticipated radial migration into the CP. This phenotype is linked to the decrease in the amount of the chemokine (C-X-C motif) ligand 12 (CXCL12) chemokine, which binds to the C-X-C chemokine receptor type 4 (CXCR-4) in interneurons and regulates this type of migration (Caronia-Brown & Grove, 2011).

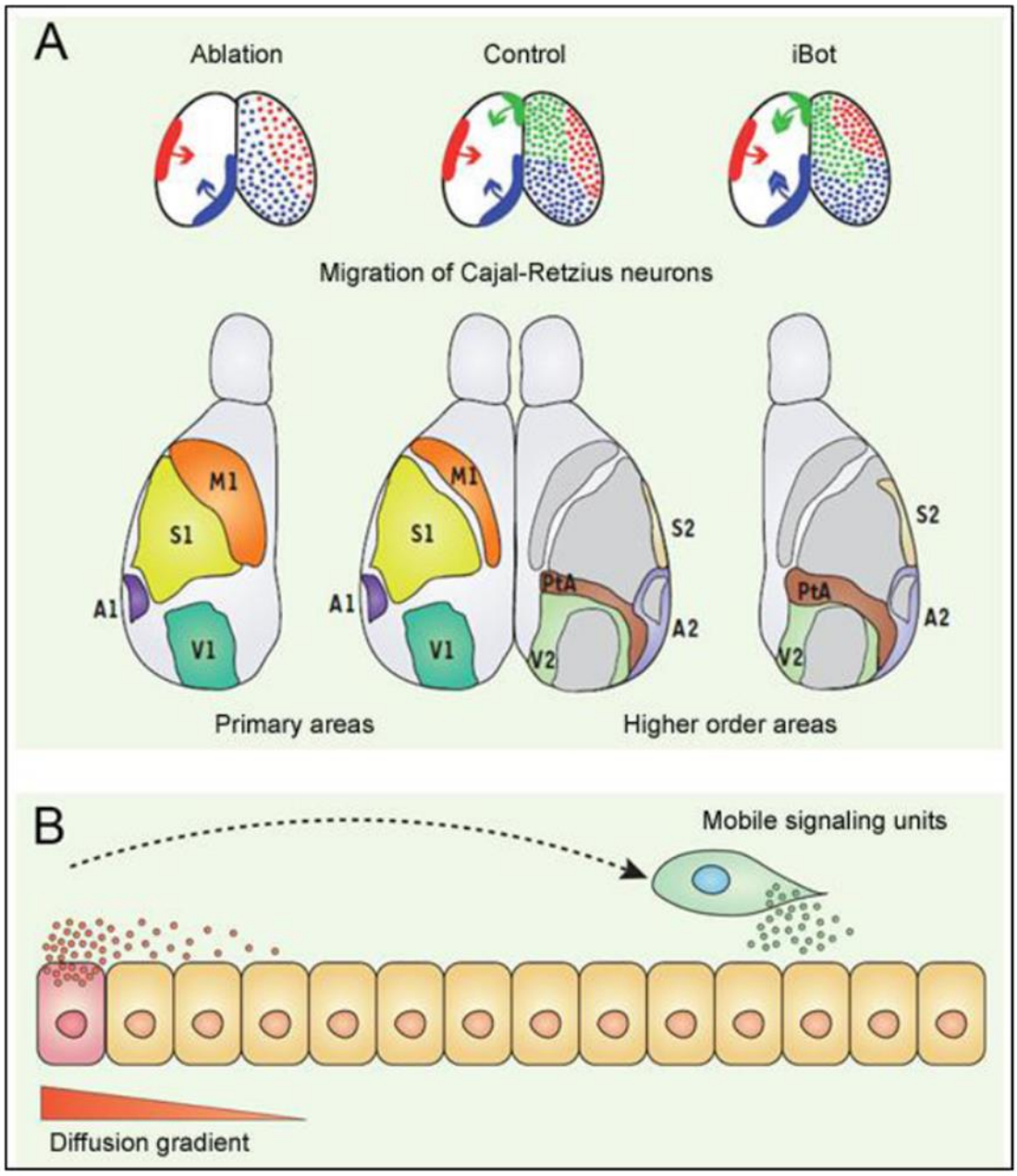

Figure 11. CRs regulate the size and position of cortical areas

A. Ablation of S-CRs (in green) drive to a redistribution of pallial-subpallial boundary (PSB) (red), the cortical hem (CH) (blue) CRs, determining a shift in primary areas, whereas inactivating Vamp1-3 PSB-CRs and CH-CRs in the iBot model leads to a redistribution of these subtypes and a shift in higher order areas. B. By secreting a variety of long-distance factors necessary for correct cortical regionalization, CRs serve as mobile signaling units. Adapted from (Causeret & Pierani, 2016).

Abbreviations: V2, visual area; A2, secondary auditory area; S2, secondary somatosensory area; PtA, parietal associative areas

2.2.1.4. Morphological and electrophysiological properties of Cajal Retzius cells

2.2.1.4.1. Morphology of CRs

Anstotz et al. specifically examined the morphology of neocortical CRs in mice, in 2014, by injecting CR cells with biocytin between P7 and P11. The morphological criteria separated the CRs into two groups: typical and atypical (Anstötz et al., 2014). This classification was very similar to the one Radnikow et al. proposed to distinguish CRs in rat brain between P5 and P11 (Radnikow et al., 2002a).

Typical morphology: Approximately 80% of them are referred to as typical CRs. Their predominant feature is their bipolar shape. They have an ovoid cell body, which is located deep within L1. Their main dendritic branch is located at one of the soma's poles, parallel to the pial surface and it is divided into collaterals not longer than 100 micrometers (µm), perpendicular to the surface. Normally, the axonal processes are spread horizontally in the opposite pole of the soma. The main axon can spread up to 1.7 mm. (Figure 12). All of the extensions have a high density of buttons synapses, which suggests a high connectivity of these neurons (Anstötz et al., 2014; Radnikow et al., 2002b).

Atypical morphology: These type of CRs (20%) are much more diverse than typical CRs and lack their bipolar morphology. Although their dendritic and axonal extensions may not be at opposite poles, their cell bodies are located in the L1 like typical cells. They can extend vertically toward the surface of the pial and spread throughout the entire thickness of L1 (Figure.12).

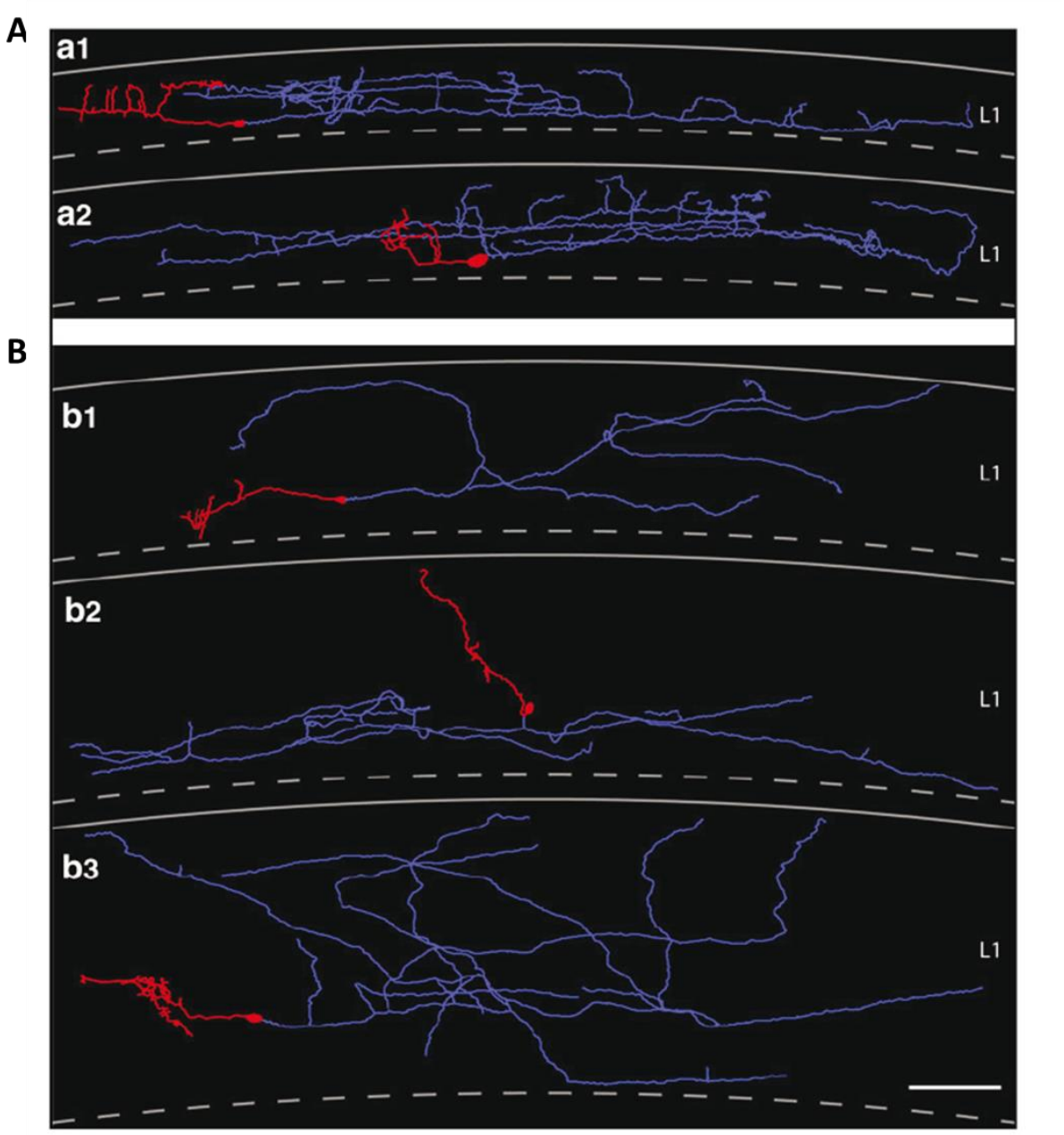

Figure 12. Morphological properties of CRs

Schematic representation of biocytin reconstructed CRs between P7 and P11. **A.** (a1, a2) Two examples of CRs with a typical morphology characterized by their bipolar shape and restricted spreading. **B.** (b1-3) Three examples of CRs with unusual morphology consisting of extensive spreading and long axonal extensions. Dendrites in red and axons in blue. (Anstötz et al., 2014).

Their synaptic content is similar to that of typical CRs (Anstötz et al., 2014; Radnikow et al., 2002b). At P4 and P11, at the level of the axonal and dendritic terminals, growth cones can be seen in both typical and atypical CRs forms. The majority of dendric spines are filopodia-shaped (Anstötz et al., 2014). After P5 the length of the axon' decreases as the number of collateral axons reaches its highest point. Additionally, the number of dendritic ramifications begins at a very low level at P1, rises to its highest level at P3, and then gradually declines over the following two weeks. These findings suggest that CRs retract after the first five days of life, when they acquire their most complex morphology (J et al., 2014). There is no apparent difference in morphology between different subpopulation of CRs, as reported **(Sava et al., 2010).**

2.2.1.4.2. Electrophysiological properties of CRs

CRs maintain a profile of immature neurons during the first few weeks after birth . They have a depolarized resting potential that ranges from -40 to -50 mV, a high membrane resistance of 1-5 G, a low action potential trigger point of -35 mV, which is 14 milliseconds (ms) long and have a low frequency (Anstötz et al., 2014; Sava et al., 2010).

In comparison, interneurons which are located within L1 during the second postnatal week, have a hyperpolarized resting potential of -70 mV, a membrane resistance of 0.5 G, and an action potentials trigger point of -40 mV which last 2.5ms at high frequency (Figure 13) (J et al., 2014). Neither hippocampal CRs nor the various subsets of neocortical CRs (CH-, SH-, or PSB) have been found to differ in any electrophysiological properties (Anstötz et al., 2014; Sava et al., 2010) .

In CRs, GABAergic synapses are mainly located on the soma as well as the proximal dendrite region , whereas the remaining part of the dendrites is covered by non-GABAergic synapses (Anstötz et al., 2014; Radnikow et al., 2002b). Due to the expression of The Na-K-Cl cotransporter 1 (NKCC1) in CRs, similar to all the immature neurons, GABA has a depolarization effect (Achilles et al., 2007). Indeed, a high chlorine

concentration in the intracellular environment is necessary for the depolarizing response to GABA. The cotransporter NKCC1, which is expressed by neurons during embryonic development, keeps this internal concentration high. As a co-transporter, NKCC1 facilitates the simultaneous entry of two Cl- ions as well as a Na+ and K+ ion. After birth, most of neurons transform this GABA's depolarizing activity into hyperpolarizing action.

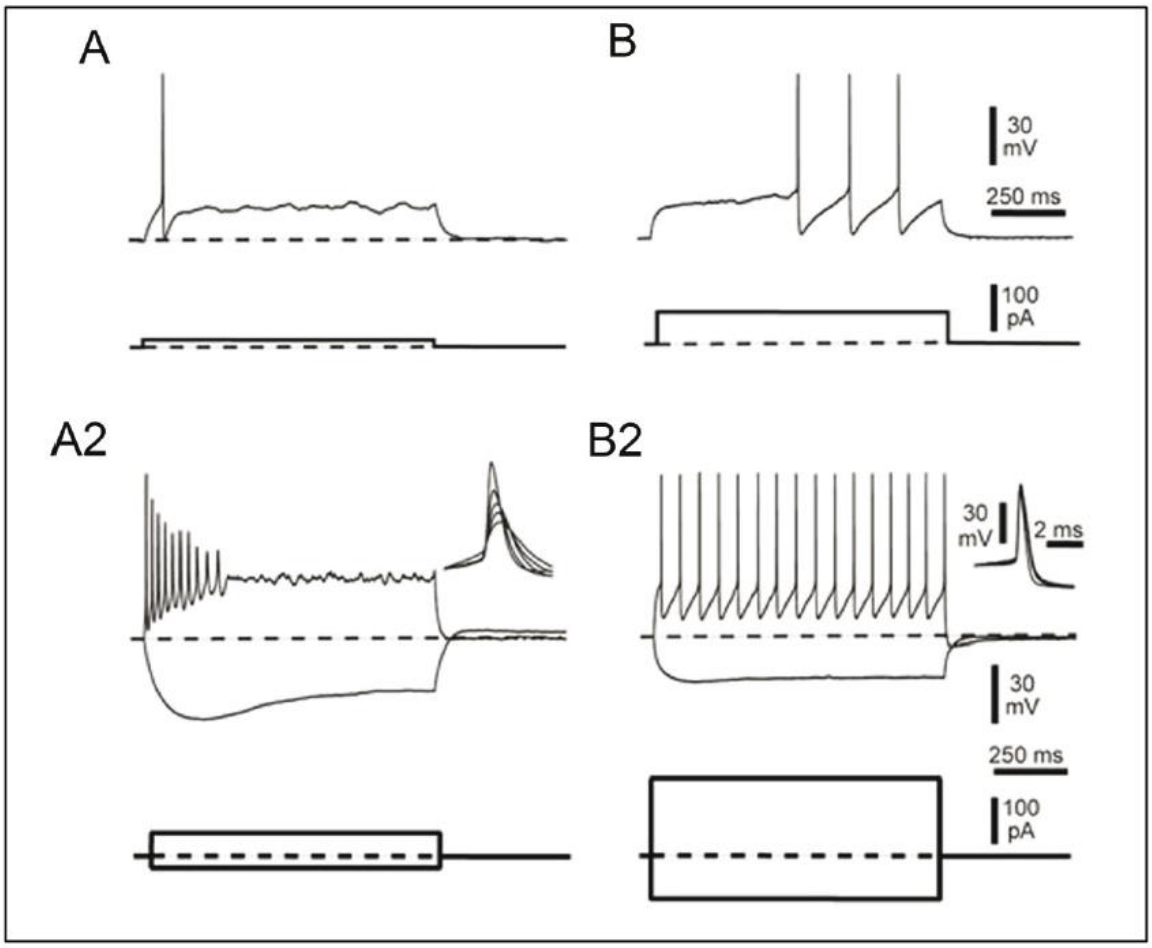

Figure 13. CR and interneuron electrophysiological profiles in L1between P7 and P11

voltage responses to modification of membrane potentials during a 1-second stimulation caused by depolarizing and hyperpolarizing currents pulses in CRs (A-A2) and an interneuron (B-B2). **A.** voltage response to weak hyperpolarizing and depolarizing current from CRs. They trigger only one action potential (AP) at the start of the stimulation. **B.** same stimulation response from interneurons. They can generate several APs following the stimulation, **A2.** Firing patterns in response to more intense depolarizing and hyperpolarizing currents from CRs. They generate different consecutive APs which decrease in amplitude**. B2.** same stimulation response from interneurons. They generate APs of the same amplitude throughout the duration of the stimulation (Anstötz et al., 2014).

A decrease in the expression of NKCC1 and a strong expression of the co-transporter K+/Cl- co-transporter (KCC2) are observed in mice during the first week after birth, which extrude Cl- together with a Na+ ion resulting in low concentration of Cl- inside the cells. This results in low chlorine's intracellular concentration. Following the fixation of its ligand, the opening of the GABAA receptor will allow the chlorine to enter via an osmotic gradient, resulting in neuron hyperpolarization (Figure 14) (Ben-Ari, 2002). The exception to the GABA switch is the CRs, which, according to Menville, continue to be depolarized by GABA until at least P13 in the rat. Indeed CRs do not express KCC2 at P11, whereas interneurons and pyramidal neurons express this co-transporter strongly at this stage (J.-M. Mienville, 1998; Pozas et al., 2008, p. 2). The presence of functional synapses on these neurons has been confirmed by the detection of spontaneous postsynaptic currents in CRs using calcium imaging (Schwartz et al. 1998) and patch clamp in cell attach configuration. Bicuculine, a GABAA receptor antagonist, completely eliminates GABAergic currents (Cosgrove & Maccaferri, 2012; Kilb & Luhmann, 2001).

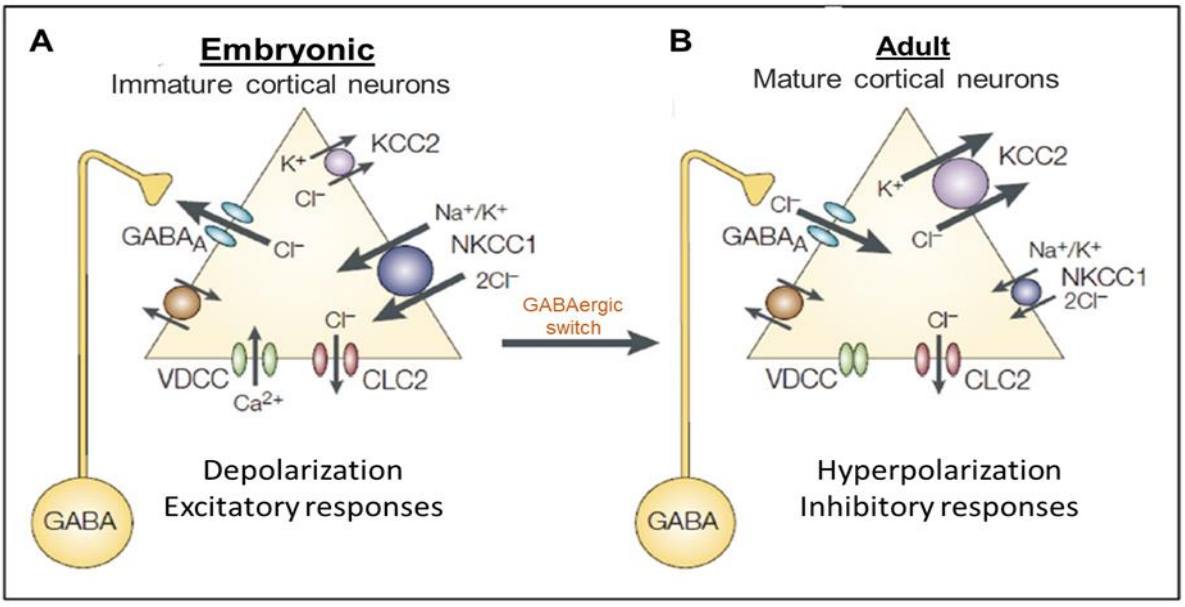

Figure 14. NKCC1 and KCC2 serve as two main regulators of GABA receptors.

A. Immature neurons with a high chlorine intracellular concentration exhibit predominant the Na-K-Cl cotransporter 1 (NKCC1) expression. Chlorine escapes when GABAA receptors are activated. B) The K+/Cl- co-transporter (KCC2) expression is predominated in mature neurons with a low intracellular chlorine content. When GABAA receptors are triggered, chlorine enters the system. Adopted from **(Ben-Ari, 2002).**

Abbreviations: CLC2, Chlorine channel 2; VDCC, voltage-dependent calcium channel.

Regarding the non-GABAergic synapses, the presence of ionotropic N-methyl-D-aspartic acid (NMDA)-like glutamate receptors in rats' CRs has been reported (J. M. Mienville & Pesold, 1999) whereas the α-amino-3-hydroxy-5-methyl-4-isoxazolepropionic acid (AMPA) or kainate receptors are absent on the surface of CRs. Radnikow and colleagues demonstrated the existence of weak currents which are completely eliminated by the application of AP-5, an NMDA receptor antagonist (Radnikow et al., 2002b). CRs also express the metabotropic glutamate receptors 1 (mGluR1) and mGluR2 glutamate receptors but they do not appear functional (Anstötz et al., 2014; Cosgrove & Maccaferri, 2012).. In addition, CRs contain 5-HT3 receptors, and serotonergic projections have been observed on CRs from E15 in mice (Janušonis et al., 2004).

Although CRs express a large number of membrane receptors for various neurotransmitters, only a small number have been found to be functional, probably because their expression varies greatly from species to species and over time. Despite these challenges, the current difficulty is defining the networks into which these CRs are integrated.

2.2.1.5. Integration of CRs into immature cortical circuits

It has not yet been fully clarified how CRs are embedded in brain circuits (Figure 15). The zona incerta's thalamic interneurons have been suggested as potential CRs inputs. In fact, the application of an anterograde tracer demonstrates that these interneurons send their long-distance terminals into L1 (Lin et al., 1991). Stimulation of SP neurons in mice using either electrical stimulation or local injection of GABA pressure produces a very rapid postsynaptic response in CRs (approximately 4 milliseconds after electrical stimulation of SP), indicating that there is a monosynaptic connection between SPs and CRs. Gabazine completely blocks this response, indicating that the SP interneurons are involved in these connections (Myakhar et al., 2011). In addition, an increase in spontaneous postsynaptic currents in CRs was induced by stimulation of Martinotti cells, interneurons positive for somatostatin (SST), which have deep-layer cell bodies and project to L1. This suggests that there is a connection between these two types of cells (Cosgrove & Maccaferri, 2012). Finally, putative synaptic contacts between L1interneurons and CRs have been observed

through light microscopy, indicating that these GABAergic cells may serve as CRs' presynaptic partners (Anstötz et al., 2014). The outputs of neocortical CRs are still largely unknown. Although an experimental demonstration in mice is still lacking, electron microscopy on biocytin-filled CRs in rats has formally demonstrated that CR axons form synapses with dendritic tufts of pyramidal neurons (Figure 15) (Anstötz et al., 2014; Derer & Derer, 1990; Radnikow et al., 2002b) .

In the hippocampus circuits, both interneurons in the oriens lacunosum moleculare (OLM) and neuroglial forms provide local GABAergic inputs to CRs in the SLM (Quattrocolo and Maccaferri 2013). Regarding the output of hippocampal CRs, expression of the photoactivable protein channelrhodopsin in these neurons allowed for the detection of a response in SLM interneurons and CA1 pyramidal neurons, suggesting that CRs play a role in the plasticity of these regions (Figure 15) (Quattrocolo & Maccaferri, 2014).

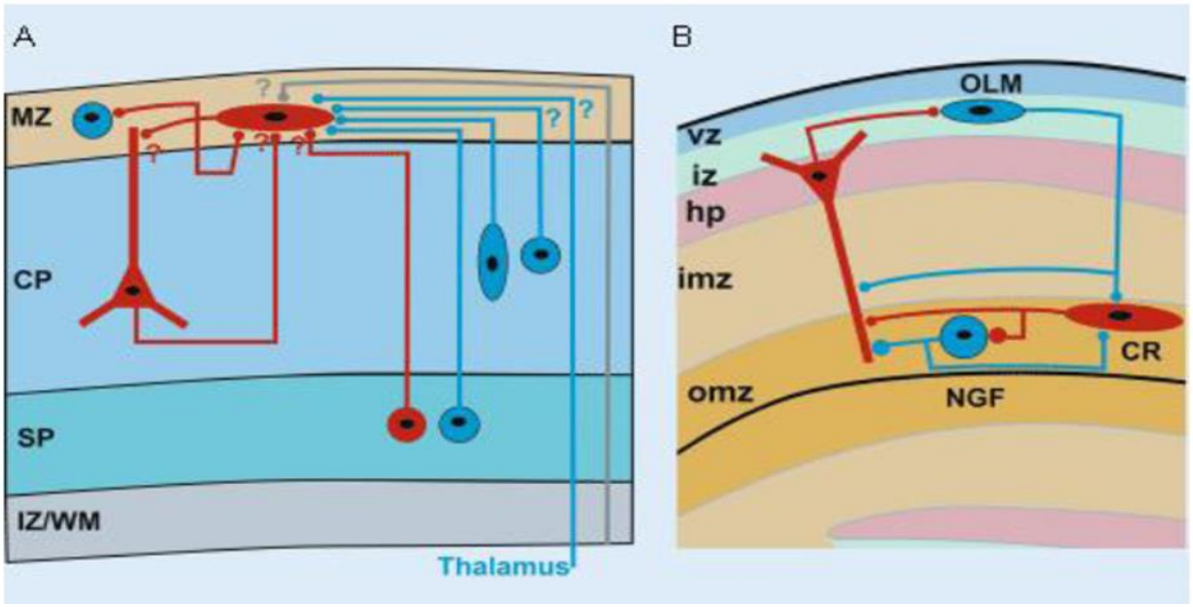

Figure 15. circuits with embedded Cajal-Retzius neurons:

A. Subplate (SP) neurons, Martinotti cells (ovoidal cell bodies) in the CP, and neurons from the thalamic zona incerta provide GABAergic inputs to CRs in the cortex (blue). It is possible for other localized interneurons in the CP to synapse with CRs (represented by a "?"). Glutamatergic inputs may originate from SP neurons or CP pyramidal neurons, but their precise location has not yet been determined. Additionally, raphe or locus cereleus (gray line) could provide serotoninergic or adrenergic inputs to CRs. Synapses between CRs, L1interneurons, and CP pyramidal neurons are thought to exist. **B** In the hippocampus, neuroglial forms (NGF) and oriens lacunosum moleculare (OLM) interneurons provide GABAergic inputs to CRs. NGF interneurons and pyramidal neurons vz form synapses with CRs (Kilb & Frotscher, 2016).

2.2.1.6. Disappearance of CR cells

Morphological studies and permanent labeling in mice have formally and quantitatively demonstrated that CRs die within two weeks after birth through PCD rather than migration, transformation, or dilution in an expanding cortex. The molecular mechanisms by which CRs are eliminated have just started to be identified (Blanquie, Liebmann, et al., 2017; Chowdhury et al., 2010; Ledonne et al., 2016).

Del Rio et al. in 1997, monitored CRs in an in vitro explant of the hippocampus and somatosensory cortex between P0 and P1 on different days in vitro (DIV). They revealed while hippocampal CRs are still present by the last day of analysis (DIV 31), cortical CRs vanish between DIV 5 and 7. In addition, they showed that hippocampal CRs were reduced by four times when co-cultured with entorhinal cortex explants, indicating that the entorhinal cortex may be producing a toxic signal for these neurons (Del Río et al., 1997) .

Neocortical explants were treated with tetradotoxin (TTX) to block sodium voltage channels, which led to a six-fold increase in the number of CRs at DIV 10. The explants were treated with NMDA or AMPA/Kainate receptor antagonists, (2R)-amino-5-phosphonovaleric acid (AP-5), 6-cyano-7-nitroquinoxaline-2,3-dione (CNQX), respectively to ascertain the type of synapse involved. Similar cell survival results to the TTX experiment were observed when CNQX, but not AP-5, was introduced, indicating that AMPA/kainate receptors are the cause of CR elimination (Del Río et al., 1997). Because these channels have not yet been discovered on the membranes of CRs, the outcomes were unexpected (Blanquie, Liebmann, et al., 2017; Cosgrove & Maccaferri, 2012; Kilb & Luhmann, 2001).

CRs from P0/P1 dissociated brains have recently been cultured. The number of CRs at DIV9 increased when TTX was added. Muscimol, a GABAA agonist, also decreased the number of CRs in organotypic cultures at DIV 11. Because GABA is excitatory on CRs due to the high intracellular Chlorine concentration maintained by NKCC1, the authors used bumetanide to block the cotransporter, and they observed an increase in the number of CRs at DIV 19, which eventually decreased. Similar outcomes were observed when the pro-apoptotic factor p75 neurotrophin receptor (p75NTR), whose expression is increased by GABA-induced depolarization on CRs, was inhibited (Blanquie et al. 2017). This study highlights the toxic effect of depolarizing GABA on these neurons and supports the significance of neuronal

activity in CRs PCD. Also mention the kir1.3 model where hyperpolarization of CRs increase CR number in L1.

From the hand, it has been already shown that CH-CRs and SE-CRs express the transcription factor amino-terminal truncated protein, called deltaNp73, which has been shown to be important for their survival. The transcription factor p73 is a member of the p53 family of tumor suppressor proteins, and p53 is well-known for its pro-apoptotic function (Fang et al., 1999; Yoon et al., 2015, p. 73). The nervous system has higher levels of p73 expression (Killick et al., 2011).

In 2000, Pozniak et al. demonstrated that a p73 isoform that lacks the DNA-binding domain necessary for its pro-apoptotic function is specifically expressed in sympathetic ganglion neurons. (Pozniak et al., 2000). It has been called DeltaNp73. The entire p73 form is referred to as transactivating (TA) p73.

According to Simoes-Wust et al., in 2005, this factor is capable of forming a dimer with the TAp73 transcript, which prevents the transcription of pro-apoptotic genes (Simões-Wüst et al., 2005).

In line with that, it has been demonstrated that complete elimination of the deltaNp73 by using deltaNp73cre/cre mutants, causes early death of CRs at E12.5. Therefore, deltaNp73 is essential for CH and SH-CR survival up to P0, when its expression begins to decrease (Tissir et al., 2009). This TF probably protects CRs throughout development, but its downregulation after birth makes these neurons more susceptible to harmful signals, whether intrinsic or external. Work from our laboratory has described an additional player involved in CRs disappearance (Ledonne et al., 2016), through experiment on the pro-apoptotic factor BCL2 associated X protein (Bax). This pro-apoptotic protein regulates apoptosis in a variety of contexts, including the CNS (Buss et al., 2006; Southwell et al., 2012) . Ledonne et al. demonstrated that only SE-CRs die in a Bax-dependent manner by specifically inactivating Bax in SE/CH- (Np73cre) or CH-CRs (Wnt3acre), as a 5-fold increase in CR density was observed exclusively using the deltaNp73cre line at P24 (Figure 16). Interestingly, they demonstrated that, despite the maturation of the cortical circuits in which they are embedded, these rescued CRs maintain the properties of immature neurons and remain active in the network (Ledonne et al., 2016).

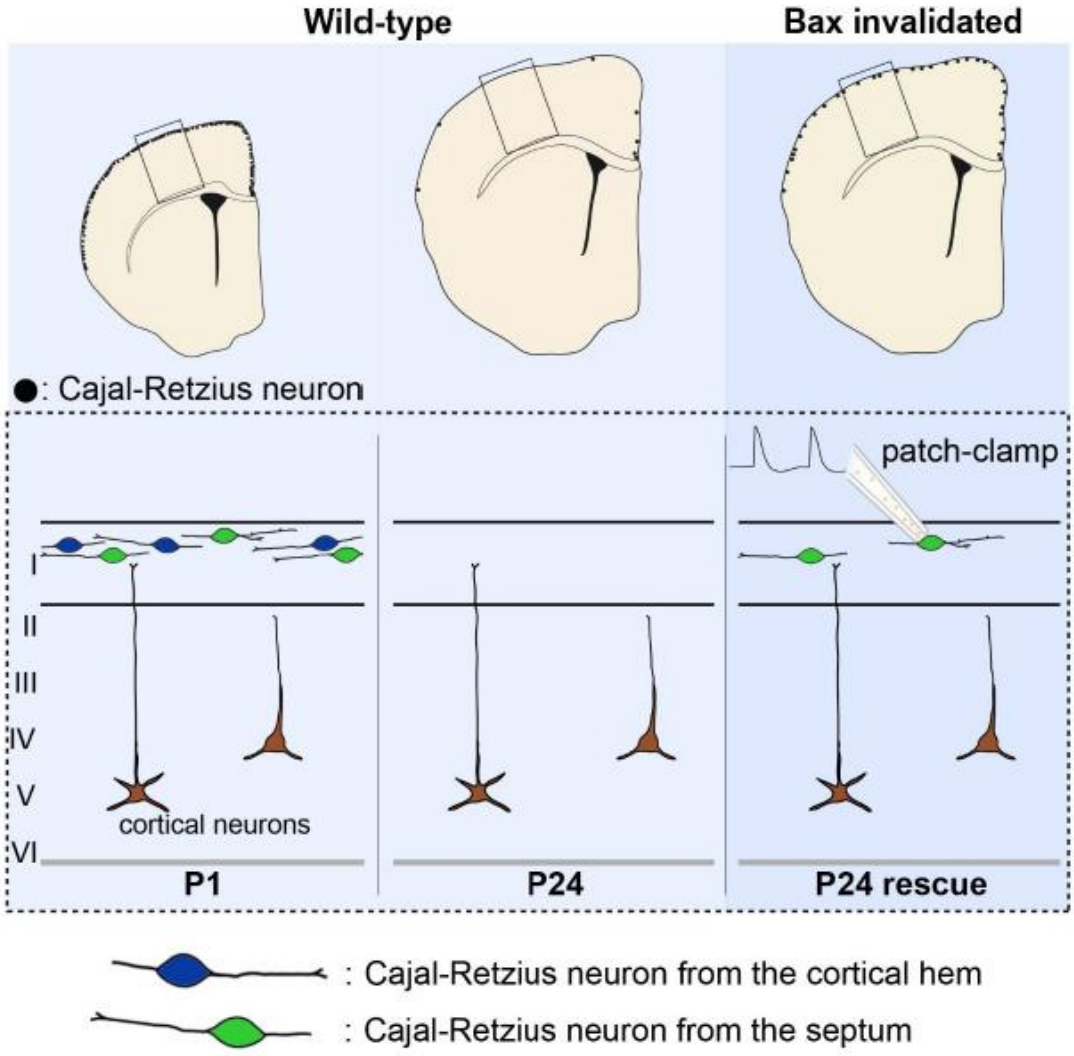

Figure 16 | Model of Bax inactivation in CRs

At P24, CRs had undergone a massive death event, with virtually no cells remaining. SE-CRs, but not CH-CRs, escaped to cell death and remained in L1at P24 thanks to the inactivation of the pro-apoptotic factor Bax. Persistent CRs kept the properties of immature cells (Ledonne et al., 2016).

Despite their common morphology CRs subpopulation are not a uniform population from different aspects, for instance their molecular signature, their preference for populating different territories of developing cortex and also the dynamic of their disappearance differs temporally and spatially. Notably, it has been reported that some CRs in mice's hippocampus survive to adulthood, whereas none are found in the neocortex at this stage (Louvi et al., 2007).

There are three distinct localizations of CRs: between OML and SLM along the hippocampal fissure (HF); in the dentate gyrus' pial surface and L1 of the subiculum, with the HF having the highest density. However, a decrease in cell number was observed between P8 and P60, though to different degrees in various hippocampal regions: 98% in the L1 of the subiculum, 85% in the HF, and 80% in the dentate gyrus' pial surface (Chowdhury et al. 2010; Ma et al. 2014)..

Since hippocampal CRs are derived from the CH, this study demonstrates the significance of the environment for the survival of CRs of the same lineage (Bielle et al. 2005). However, the specific survival factors of hippocampal CRs have not yet been determined.

2.2.1.7. Persistence of Cajal Retzius cells in pathologies

Anomalies in the organization of L1involving neurons with characteristics resembling those of CRs were discovered through histological analysis of surgical resections or postmortem brains from patients with defects in their cortical development.

Eriksson. et al, have looked at 12 polymicrogyria patients between the ages of 21 and 10 years old. Polymicrogyria is a neuronal migration disorder (NMD)-related cortical malformation characterized by an excessive number of abnormally small cortical gyria and disorganized layering (Oegema et al., 2020). After gestation week (GW) 30, a greater number of Reelin+/Calretinin+ cells were found in the L1of patients than in control tissue. These neurons were more likely to be found in the distorted areas. The authors suggest that these cells may be CRs based on their location and expression of markers (Figure 17) (Eriksson et al., 2001).

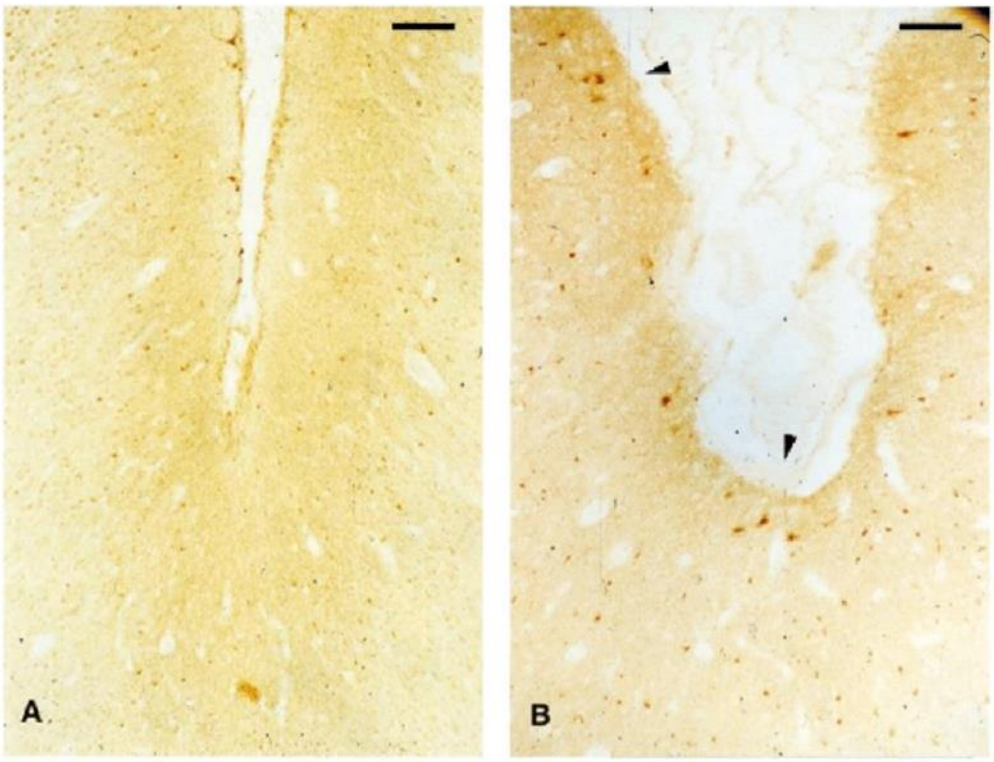

Figure 17 | Persistence of CRs like cell in polymicrogyria

A. An age-matched control's brain section shows presence of few neurons in a sulcus positive for reelin. **B.** Section from the brain of a patient (1 day) diagnosed polymicrogyria shows an increased number of reelin+ cells in a sulcus close to the polymicrogyric zone, as shown by the arrows. Adopted from (Eriksson et al., 2001) .

The spectrum of focal developmental malformations known as focal cortical dysplasia (FCD) is characterized by a disruption of the normal cytoarchitecture of the cerebral cortex and is strongly linked to medically intractable epilepsy (Crino, 2015). Whereas type II FCD is characterized by the presence of dysmorphic/cytomegalic neurons with or without balloon cells, type I FCD is characterized by a dyslamination and disrupted organization of tissue architecture (Crino, 2015; Najm et al., 2018). According to Garbelli et al., in 2001, persistence of Calretinin positive, GABA negative neurons was found in 32 of 33 patients with type II FCD but not in any patients with type I FCD. This suggests that CR survival might be a sign of the former type of FCD (Garbelli et al., 2001).

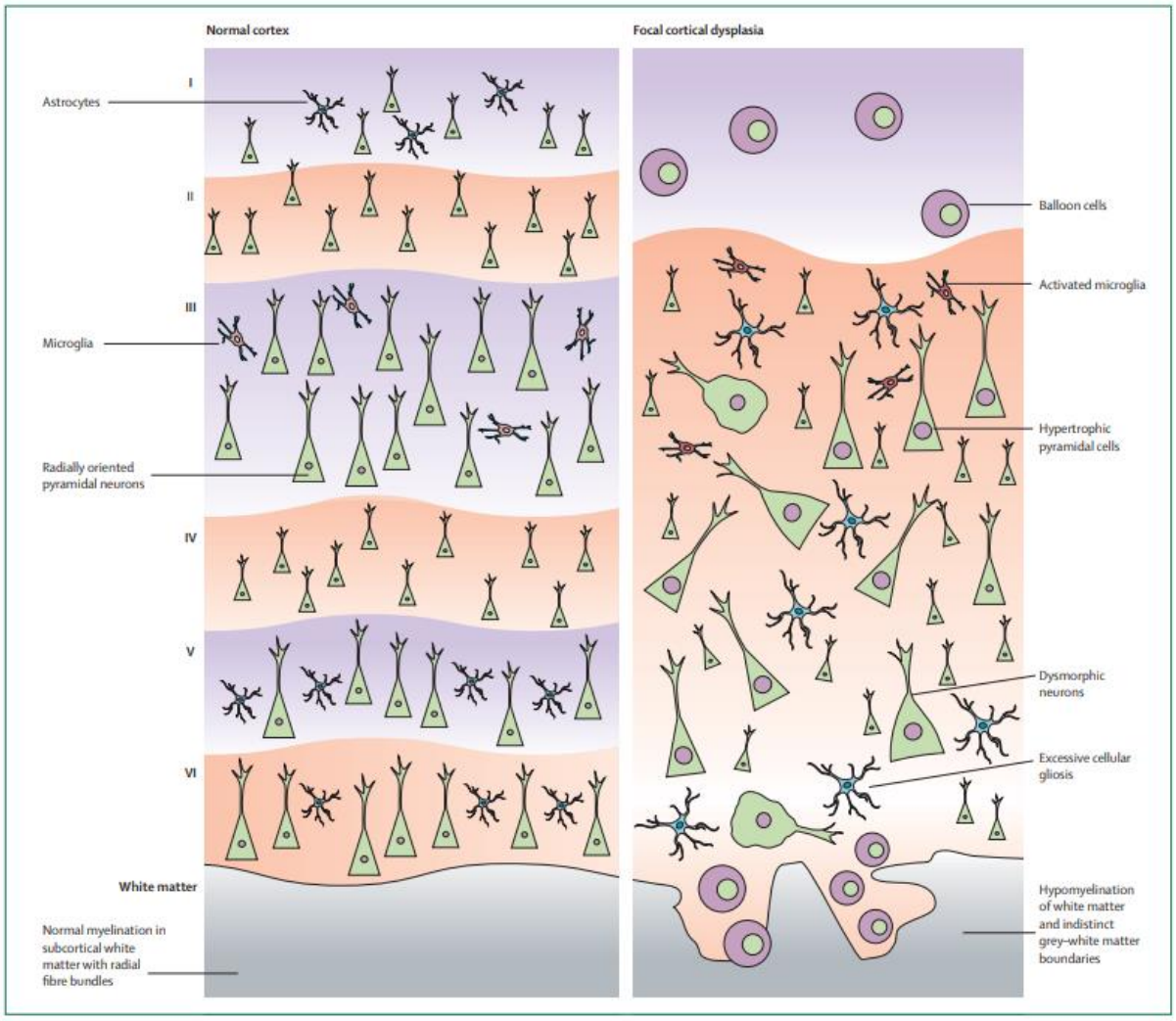

Figure 18. Cytoarchitectural of the cortex in focal cortical dysplasia type IIB

The left panel demonstrate a healthy six-layered cortex. The cytoarchitectural abnormalities found in type FCD II are depicted in the right panel: L1 is defined but widened and contains "balloon cells". The remaining layers are poorly defined and have more active glial cells and dysmorphic neurons. White matter is hypomyelinated and lacks a definite border with the deep layers. In addition, Balloon cells may also be detected in this area (Sisodiya et al., 2009).

In another study, Blumcke et al. discovered that 27 patients with Ammond's horn syndrome (AHS) had an increase in the number of CRs not only in the neocortex but also in the SLM of the hippocampus. (Blümcke et al., 2013).

AHS is associated with pharmaco-resistant temporal lobe epilepsies (TLE) and is characterized by the loss of pyramidal neurons in 3 hippocampus subfields, cornus Ammonis1 (CA1), CA3, and CA4 (Figure 19). This loss is compensated for by an invasion of ectopic glial cells, making the tissue difficult to cut and defining it as sclerotic (Blümcke et

al., 2002, 2013). Interestingly, in another study a decrease in RELN positive neurons was observed in the hippocampus of 22 TLE patients (Haas et al., 2002). In addition, the reeler mouse also exhibits a susceptibility to seizure (Patrylo et al., 2006), indicating that RELN levels probably play a significant role in the onset of epilepsy.

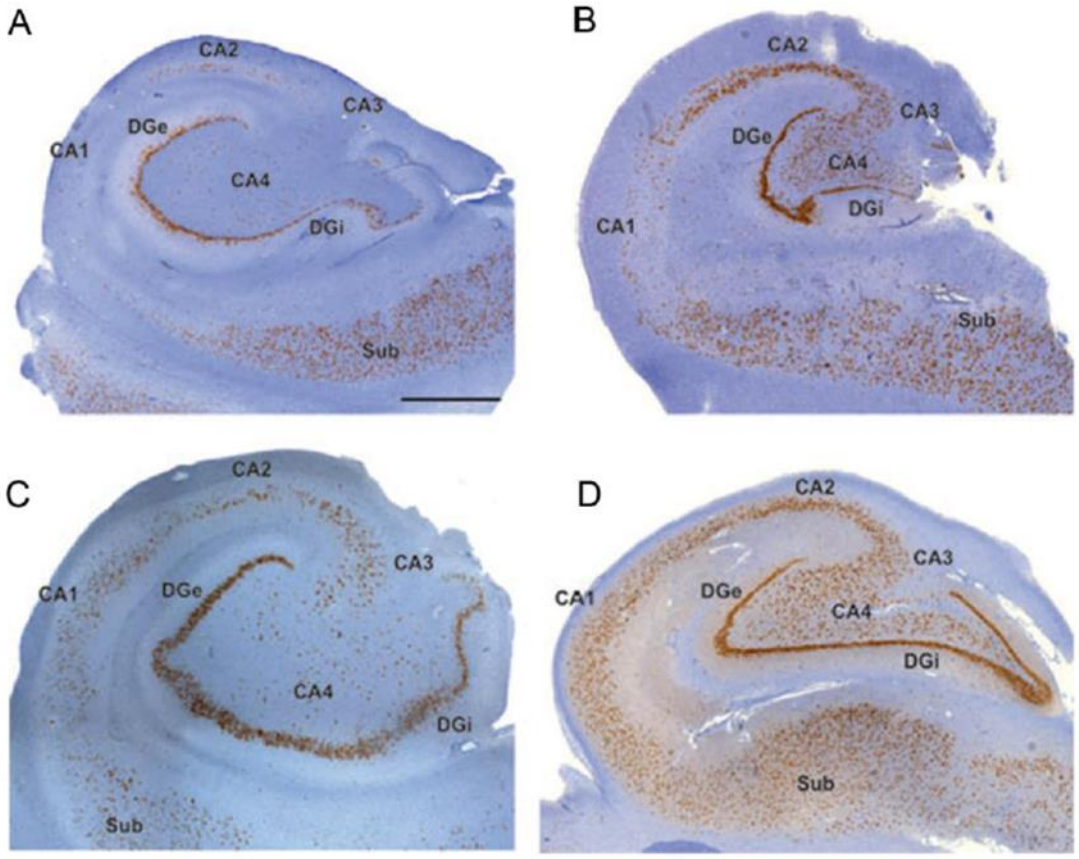

Figure 19 | Different hippocampal sclerosis cases

Different hippocampal sclerosis cases. Resections from human patients' hippocampi immunolabeled with the neuronal marker NeuN (brown) and counter-labeled with hematoxylin (purple). The symptoms of hippocampal sclerosis include **A.** a predominant loss of neurons in the CA1 and CA4 of hippocampal regions, **B.** loss of neurons confined to the CA1 region, **C.** absence of neurons in the CA4 region. **D.** A healthy subject's hippocampus. The dentate gyrus is affected in all three cases almost equally (Blümcke et al., 2002).

Although the cited studies suggest a connection between malformation of cortical developments (MCDs) associated with epilepsy and CR survival, it is unclear whether this abnormal persistence is the cause or just a result of the various diseases. However, it raises

the question of whether the proper maturation of cortical and hippocampal circuits is affected by the loss of CRs.

Further investigation from our lab on SE persisted CRs mediated by inactivation of BAX revealed that the presence of electrically active subsets of CRs can lead to an excitation/inhibition imbalance in upper layer pyramidal neurons due to an increase in dendrite complexity and spine density (Riva et al., 2019). As a result of this, the animals may be more likely to develop seizures (Riva et al., in revision).

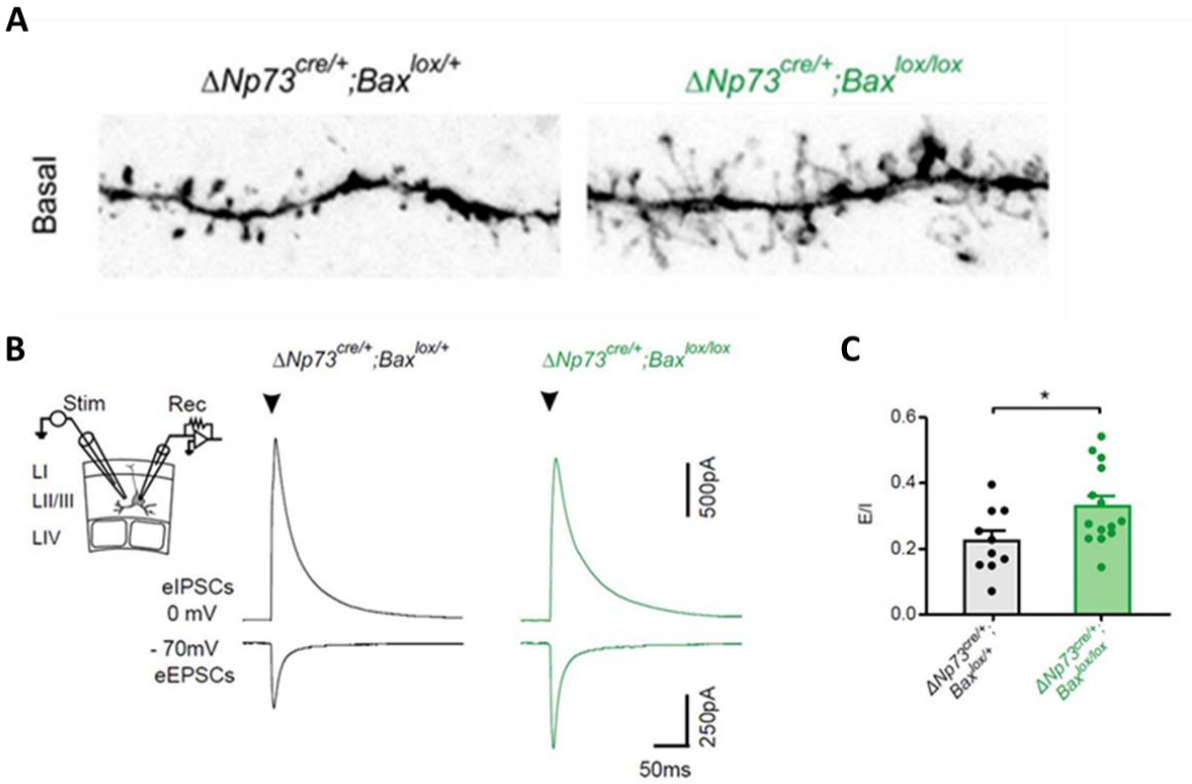

Figure 20 | Spine density and recorded evoked synaptic activity in L2/3 pyramidal neurons in the CRs Bax modele

A. Images showing spines in basal dendritic segments of controls Bax $^{lox/+}$ (left) and mutant Bax $^{lox/lox}$ (right). **B.** voltage-clamp recorded at −70 mV and 0 mV from L2/3 pyramidal neurons between p24-26. **C.** E/I ratio plot calculated from eEPSCs and eIPSCs (Riva et al., 2019).

2.3. Programmed cell death

Despite the high metabolic expense of creating new cells, the brain only contains a small fraction of the neurons formed throughout embryonic development. At postnatal stages, some neuronal subpopulations are reduced, while others are completely

eliminated (Causeret et al., 2018a; Wong & Marín, 2019; Y. Yamaguchi & Miura, 2015). PCD eradicates extra cells from the nervous system at two distinct developmental junctures: during embryonic development, at the level of progenitors and newborn neurons, and after birth, as neurons mature and become integrated into neural circuits. The earliest neural PCD in mice has been observed in the anterior distal epiblast, which is thought to be the neural plate, at E6.5 (Yeo & Gautier, 2004). After this time, the lateral edges of the hindbrain, which are necessary for the lamina terminalis, optic invagination, and closure of the neural tube, experience cell loss. The pallium, the progenitor cells for pyramidal cells, CRs, and SP neurons, has been shown to be the site of cell death beginning as early as E10.5. On the contrary, progenitor cells in the subpallium, which gives rise to cortical GABAergic interneurons, appear to experience cell death less frequently (Causeret et al., 2021; Mihalas & Hevner, 2018).

Studies on mutant mice lacking key pro-apoptotic proteins have demonstrated that embryonic cell death is essential for determining the development of the cerebral cortex. For instance, mouse embryos which are not able to activate executioner Caspases 3 and 7 due to lack of apoptotic protease activating factor-1(Apaf-1) or Caspase 9 manifest a significant expansion of the proliferative zones in the developing cortex (Cecconi et al., 1998; D'Amelio et al., 2010). In cortical progenitor cells, PCD is not caused by the anti-apoptotic protein Bcl-XL or the pro-apoptotic factor Bax, which suggests that neurons and progenitor cells follow at least partially distinct apoptotic pathways (Nakamura et al., 2016; Roth et al., 2000; White et al., 1998). Cell cycle checkpoint is probably connected to cortical progenitor PCD, as it ensures the accuracy of DNA replication, repair, and division. Perhaps progenitor cell death is triggered by changes in mitotic progression, particularly mitotic delay, or defeat of cell cycle checkpoints (J.-F. Chen et al., 2014; Pilaz et al., 2016). Programed cell death is also influenced by progenitor cell interactions with the local microenvironment, in addition to intrinsic factors. During brain development, for instance, alterations in notch or ephrin signaling increase progenitor cell death, pointing to a possible feedback mechanism by which newborn neurons could regulate the number of progenitor cells (Dhumale et al., 2018; Park et al., 2013; X. Yang et al., 2004).

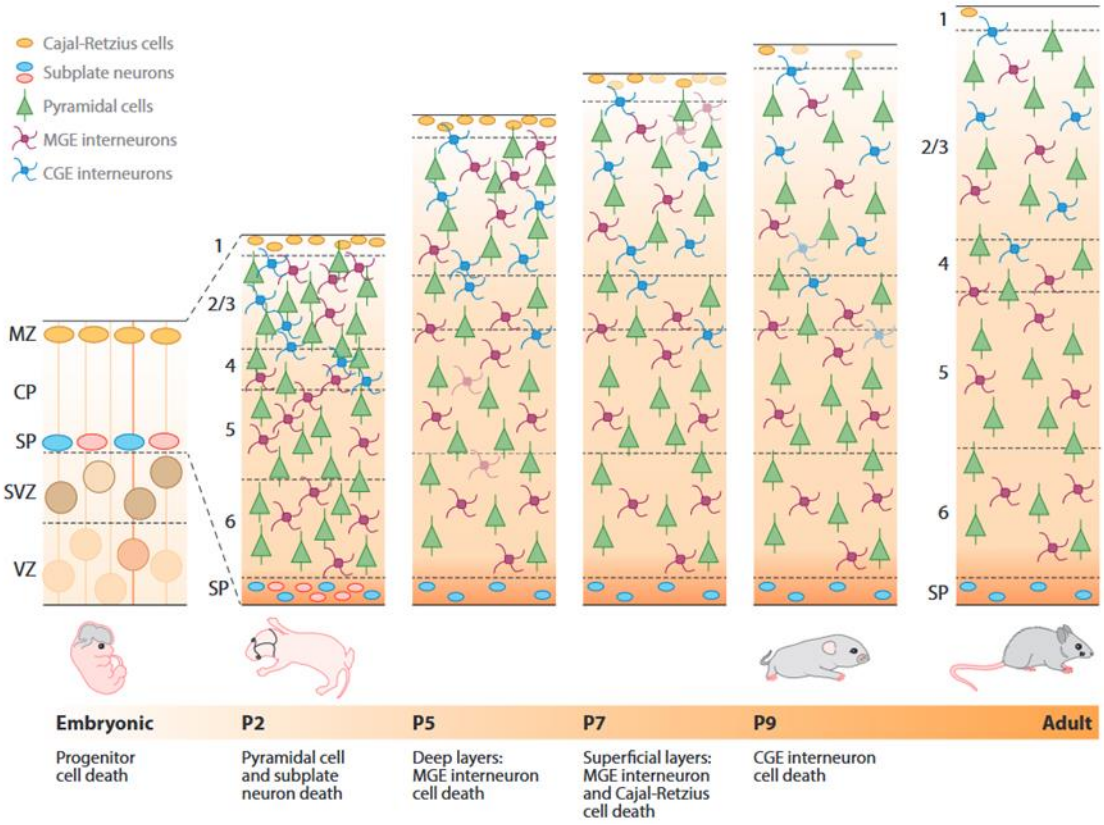

Figure 21 | Timeline of post-natal programed cell death in the mouse developing cortex

During embryonic development, PCD is abundant in progenitor cells of the ventricular zone (VZ) and subventricular zone (SVZ). Starting from postnatal day 2 (P2), pyramidal cells and subplate neurons (SP) undergo PCD. At P5, infragranular medial ganglionic eminence (MGE) interneurons, at P7 supragranular MGE interneurons and Cajal-Retzius CRs cells, and at P9 caudal ganglionic eminence (CGE) interneuron are the next to die (Wong & Marín, 2019).

Additional abbreviations: CP, Cortical plate; MZ, Marginal zone; SP, Subplate

According to a temporal sequence that is only beginning to be understood, the most significant change in the number of cortical cells occurs in mice between the first and second postnatal weeks (Figure 21) (Causeret et al., 2018a, 2021; Verney et al., 2000; Wong & Marín, 2019; Y. Yamaguchi & Miura, 2015). The fact that the formation and growth of neural networks coincide with the cerebral cortex's most active period of PCD may not come as a surprise. The first two weeks of postnatal development in rodents' cerebral cortex are characterized by the formation of mature activity patterns and the modification of embryonic connections and structures (Blanquie, Liebmann, et al., 2017; Blanquie, Yang, et al., 2017; Butt et al., 2017), and the establishment of mature patterns

of activity (Allene & Cossart, 2010; Khazipov & Luhmann, 2006; Luhmann & Khazipov, 2018) Nevertheless, it is now known that different populations of cortical cells are being unevenly affected by PCD: in some cases it leads to the complete eradication of entire populations of transitory cells, but in others, it widely refines the final number of particular neuronal populations (Causeret et al., 2018a, 2021).

2.3.1. The role of programmed cell death in the cortical development

Given the metabolic cost associated with the CNS's excessive production of neurons and glial cells, maintaining a complex, cell-specific PCD mechanism must have significant evolutionary benefits. From a traditional perspective, the primary function of PCD is to eliminate abnormal, misdirected, or potentially hazardous cells prior to the formation of brain circuits. The cerebral cortex, for instance, has neurons with minor types of aneuploidy, an aberrant number of chromosomes in a cell, but extreme aneuploid cells are highly uncommon (Ohashi et al., 2015; Peterson et al., 2012; A. H. Yang et al., 2003). In line with that, it has been demonstrated by Peterson et al. that mice with reduced PCD have significantly more severe forms of aneuploidy in the cerebral cortex (Peterson et al., 2012). Aneuploidy may make cells less suitable for resource competition, which could make it more difficult for the growing cerebral cortex to form connections (Ohashi et al., 2015; J. Zhu et al., 2018).

A certain degree of coordination between the various developmental programs is necessary for the development of tissues and organs with the proper number of cells. Since the initial production of the inputs and outputs is chronologically separated, one notable example of such coordination is the management of cell counts via quantitatively matching cells with reciprocal connections, also known as systems matching. For instance, the number of neurons in the substantia nigra and striatum, two brain regions that are inseparably linked, are highly dependent on one another

(Granholm et al., 2000; Oo et al., 2003). Recent investigations show that this may be directly related to the unique functional properties of each cortical area. In the cerebral cortex, the fraction of cell death is likely determined locally for each area and even for each layer (Blanquie, Yang, et al., 2017).

Controlling programmed cell death is a crucial strategy for precisely shaping the cytoarchitecture of various cortical areas, as evidenced by the fact that interneuron survival is highly dependent on the activity of pyramidal cells (Wong et al., 2018). Regardless of the size of the cerebral cortex, PCD may have developed as a method for altering the ratios of excitatory and inhibitory neurons in the cerebral cortex and maybe other brain regions. This would make it simpler for us to comprehend why species with very different cortical sizes still have roughly the same number of interneurons to pyramidal cells (DeFelipe et al., 2002)

Minor neuropathological and morphological changes are seen in genetically engineered mice with altered pro-apoptotic gene expression, especially in some genetic backgrounds. mice with the anti-apoptotic gene B-cell lymphoma 2 (Bcl-2) overexpressed in neurons or mice with the Caspase 3 and Bax mutations exhibit rather normal brain morphology. However, closer inspection reveals that these mice are deficient in complex functions like learning, suggesting that PCD does play a significant part in the development of brain circuits (Krahe et al., 2015; Leonard et al., 2002).

From the other hand, organization of the developing brain depends on specialized signaling hubs, also known as organizers, which generate molecules in charge of cell specification and regional identity. The distribution of the signals released from brain organizers depends on their position, size, and form, all of which are essential for their proper operation (Kirischuk et al., 2014) Numerous studies have demonstrated that PCD plays a crucial role in controlling the size of brain organizers. Apoptosis, for instance, regulates the size of the anterior neural ridge, which serves as an organizing center essential for the patterning of the telencephalon by producing Fgf8 (Houart et al., 1998) In addition, in the developing telencephalon, CR cells produce several morphogens that regulate progenitor proliferation, neuronal differentiation, and cell migration (Borello &

Pierani, 2010). These cells serve as temporary signaling units, Fgf8, BMP/Wnt, and Egf/anti-Wnt are expressed by SE, CH and PSB CRs, respectively (Alfano & Studer, 2013; Griveau et al., 2010). This theory proposes that CR cells undergo PCD to eliminate developmental signals that are no longer required. This idea is supported by the fact that various neurodevelopmental diseases, including polymicrogyria,, have been connected to the persistence of CR like cells in the adult cortex (Eriksson et al., 2001).

The elimination of neurons that serve as temporary placeholder cells may also be significant in the process of programmed cell death. While waiting for the arrival of input from other neuronal populations, placeholder cells temporarily synaptically link with other neurons (Chao et al., 2009). This function is carried out during the maturation of the cerebral cortex by SP neurons as well as CR cells. SP neurons, in particular, help pyramidal cells migrate by forming temporary connections with them during embryonic development, which is thought to make it easier for them to invade the CP (Ohtaka-Maruyama et al., 2018). Additionally, thalamocortical axons briefly interact with SP neurons before entering the cortical plate to innervate their intended targets (Ghosh et al., 1990; Ohtaka-Maruyama et al., 2018).

When pyramidal cells reach their final location within the CP and thalamocortical axons reach L4, the placeholder function of SP cells becomes obsolete. This may explain why at least some of these neurons experience PCD (Price et al., 1997). Additionally, CR cells serve as temporary resting places for entorhinal axons that project into the hippocampus (Supèr et al., 1998). Del Río et al., in 1997, showed that entorhinal axons make temporary synapses with CR cells in the embryo before moving on to their intended targets, in contrast to the adult hippocampus where they make synapses with the distal dendrites of pyramidal neurons. in addition, they showed that ablation of CR cell during embryonic stage alters the layer specificity of entorhinal axons, suggesting that presence of CRs is necessary for normal development of entorhinal projections into the hippocampal area (Del Río et al., 1997).

Cell death also influences normal neuronal spacing. In the retina, intrinsically photosensitive retinal ganglion cells (ipRGCs) undergo Bax-dependent and proximity-

mediated cell death. During this process, ipRGCs that are close to one another are more likely to undergo apoptosis. In Bax mutants, disruption of PCD alters these cells' ipRGC spacing and connection (S.-K. Chen et al., 2013). In addition, it has been hypothesized that the removal of CRs cells from L1 of the expanding cortex provides more room for the expansion of the terminal dendrites of pyramidal cells (Causeret et al., 2018a).

2.3.2. Apoptosis

Apoptosis is known as the most common form of PCD in the developing nervous system. Apoptosis was first defined by Kerr et al as a type of cell death characterized by intact plasma membranes in its early phase, chromatin condensation, DNA fragmentation, cell shrinkage or fragmentation, and the formation of small vesicles (Kerr et al., 1972). At least two major signaling mechanisms that lead to apoptosis are the intrinsic and the extrinsic pathways, which can be activated via receiving the Extrinsic death ligands or intrinsic signals like DNA damage, survival factor deprivation, ER stress, abnormal ion flux, or reactive oxygen overproduction (Green, 2019). In both cases, transmitted signals result in the activation of an evolutionary conserved family of cysteine proteases, called caspases, which work in a proteolytic cascade to break down and eliminate the dying cell (Degterev & Yuan, 2008).

2.3.2.1. Extrinsic apoptosis pathway

The extrinsic pathway begins outside the cell when circumstances in the extracellular environment necessitate its death, which mainly goes through death receptors. Receptor-mediated mechanisms can be triggered when the death ligands bind to the death receptor such as the tumor necrosis factor (TNF) ligand to TNF receptors, the homotrimeric protein Fas Ligand (FasL) to the Fas receptors, and the TNF-related apoptosis-inducing ligand (TRAIL) to TRAIL receptors (Bradley, 2008; Wajant, 2003). The recruitment of adaptor proteins like Fas-associated protein with death domain (FADD) and the tumor necrosis factor receptor type 1-associated DEATH domain protein

(TRADD) is facilitated when death ligands are ligated to death receptors. Caspase 8, an essential mediator of the extrinsic pathway that ultimately leads to cell apoptosis, is one of the many downstream factors that these adaptor proteins encourage to recruit. The most extensively described death receptors are Fas and the TNF receptor 1 (TNFR1) (Muntané, 2011).

2.3.2.1.1. Fas ligand pathway

As a ligand for Fas, the homotrimeric protein FasL causes its receptor to oligomerize upon binding (Figure 22). This is connected to the clustering of the death domains and the binding of the cofactor FADD. After ligation, the death effector domain (DED), domain of the FADD protein interacts with a similar motif in pro-caspase 8. Fas, FADD, and pro-Caspase 8/10 are collectively known as the death inducing signaling complex (DISC). FADD is prevented from functioning as a co-factor through interaction with the regulator FLICE inhibitory protein (FLIP). After being recruited by FADD, pro-caspase 8's self-cleavage-driven its activation and Caspase 3 and 7 are then activated by active Caspase 8, causing the cell to undergo apoptosis (Caulfield & Lathem, 2014; Volpe et al., 2016).

Caspase 3 can be activated via Caspase 8 through two pathways. In the first pathway, the COOH-terminal portion of B-cell lymphoma 2 (BCL-2) interacting protein (BID), which is cleaved by Caspase 8, translocates to the mitochondria where it mediates cytochrome-C (CytoC) release. Together with deoxyadenosine triphosphate (dATP) and pro-caspase 9, the released CytoC binds to apoptotic protease activating factor-1(APAF1) and activates Caspase 9, which then it mediates the activation of Caspase 3 by cleaving the pro caspase3. In Addition, Caspase 8 has the ability to directly cleave pro-caspase3 to activate Caspase 3. Shortly after, inhibitor of caspase-activated DNAse (ICAD), a DNA fragmentation factor, is cleaved by caspase 3 into a heterodimeric consisting of CAD and cleaved ICAD. CAD oligomerizes with DNase activity as a result of the separation of cleaved ICAD from CAD. The active CAD oligomer is responsible for internucleosomal

DNA fragmentation, an apoptotic marker that indicates chromatin condensation (Caulfield & Lathem, 2014; Griffith et al., 1995; McIlwain et al., 2013; Volpe et al., 2016).

2.3.2.2. Intrinsic apoptotic pathway

Different stresses, such as endoplasmic reticulum stress, growth factor deprivation, or DNA damage, as well as developmental cues, can lead to initiation of the intrinsic apoptotic pathway. The BCL-2 family of proteins, which has more than a dozen members, regulates the intrinsic apoptotic pathway, commonly referred to as the mitochondrial. Each family member is divided into pro-survival or pro-death categories based on how it functions. By having up to four BCL-2 Homology (BH) domains, they are all connected to one another. BCL-2 itself, BCL-extra large (BCL-XL), Bcl-W (Bcl-2L2), myeloid cell leukemia 1 (MCL1), and Bcl-2 related gene expressed in fetal liver/ protein A1 (BFL-1/A1) are among the members that help survival (Czabotar et al., 2014). There are two more subgroups of pro-apoptotic members: the "effector" proteins, such as BAX, BCL2 antagonist-killer (BAK), and BCL-2 ovarian killer (BOK), as well as the "BH3-only proteins," such as Bcl-2-like protein 11 (Bim), p53 upregulated modulator of apoptosis (Puma), NOXA, Bcl-2 associated death promoter (Bad), BH3 interacting-domain death agonist (Bid), BIK, BMF, and harakiri (Hrk), that start the pathway (Matsuura et al., 2016). Despite their distinct functions, the pro-survival proteins and the BAX/BAK/BOK molecules share very similar structural features. There are four conserved BH domains (BH1-4) in the anti-apoptotic Bcl-2 family. Bcl-2's BH1 and BH2 domains are required for dimerization with pro-apoptotic proteins, while the BH3 domain is present in all members and is required for interaction between pro- and anti-apoptotic proteins. Anti-apoptotic activity is linked to the amino-terminal BH4 domain, but pro-apoptotic molecules also contain it (Elmore, 2007; E. F. Lee et al., 2008, 2019; Willis et al., 2007). In contrast, the BH3-only proteins are largely fundamentally unstructured and only contain the BH3 domain (Happo et al., 2012).The sequence of events that lead to initiation of cell death through this pathway is relatively well-known (H.-C. Chen et al., 2015; Llambi & Green, 2011) . In response to cellular stress, the BH3-only proteins are

either "activated" by post-translational modifications, or their transcription is upregulated (Figure 22). The BH3-only proteins then bind the pro-survival proteins, displacing the pre-bound proteins and activating BAX/BAK.

Upon activation, BAX and BAK oligomerize and lead to Mitochondrial outer membrane permeabilization (MOMP) by forming pore-like structures in the outer mitochondrial membrane, this results in the release pro-apoptotic proteins such as: second mitochondria-derived activator of caspases (SMAC) and CytoC into the cytoplasm from the mitochondrial intermembrane space. SMAC frees caspases from inhibitor of apoptosis proteins (IAPs) (Bai et al., 2014; Vucic et al., 2002). Besides, CytoC binds to adaptor protein APAF-1, which leads to forming the caspase-activating apoptosome platform with CytoC and the cofactor dATP (P. Li et al., 1997). Apoptosome platform allows inactive caspase 3/7/9 zymogens to become active proteases. This ultimately causes the cell to die as a result of the cleavage of essential cellular substrates (Matsuura et al., 2016; McIlwain et al., 2013).

Caspase activation during apoptosis is a tightly controlled process, according to biochemical investigations, mice lacking Caspase 3, Caspase 9, or APAF1 exhibit remarkably similar phenotypes, which include brain enlargement caused by a decrease in apoptosis during brain development (Cecconi et al., 1998; D'Amelio et al., 2010; Hakem et al., 1998; Kuida et al., 1998). Both caspase 3 and caspase 9-null mice die rapidly after birth (Kuida et al., 1998). Moreover, there is evidence suggesting a connection between human neural tube closure abnormalities and mutations in the apoptosis-related genes caspase 3, caspase 9, and APAF 1 (X. Zhou et al., 2018), suggesting that all these three play crucial roles in controlling neuronal apoptosis.

As mentioned above, apoptosis occurs in response to different stimuli or deprivation in survival signals such as neurotrophic factors, which are necessary for the survival of neurons.

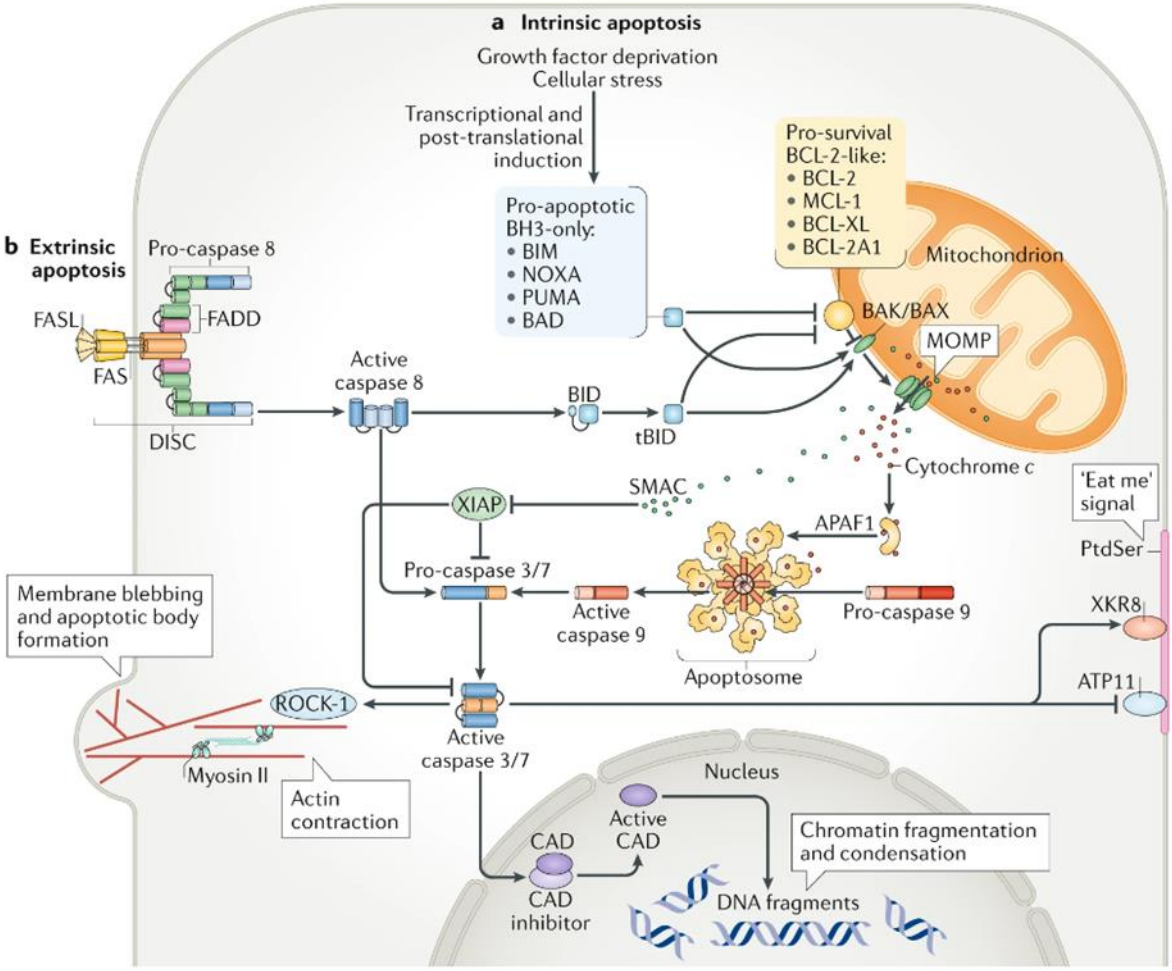

Figure 22. The extrinsic and extrinsic apoptosis pathways

a. Schematic representation of intrinsic apoptotic pathway. Cellular stresses results in the transcriptional and/or post-translational induction of BH3-only proteins, which promote apoptosis. The essential apoptosis effectors, BAK and BAX, are released when the BH3-only proteins bind and deactivate pro-survival BCL-2 proteins, causing mitochondrial outer membrane permeabilization (MOMP). As a result, apoptogenic components such cytochrome c (Cyto-C) and second mitochondrial activator of caspases (SMAC) are released. This leads to the formation of apoptosome by Cyto-C by attaching to apoptotic peptidase activating factor 1 (APAF1). Eventually, apoptosome activates the initiator caspase 9, which in turn proteolytically activates the effector caspases 3 and 7. On the hand, the activity of the caspase inhibitor X-linked IAP (XIAP) is inhibited by SMAC. **b.** Death receptor activation, such as FAS activation by FAS ligand (FASL) on neighboring cells, initiates the extrinsic pathway. The adaptor protein FAS associated via death domain (FADD) facilitates the recruitment of pro-caspase 8 to the intracellular death receptor region, resulting in the formation of the death-inducing signaling complex (DISC), which initiates caspase 8 activation. Through direct proteolytic activation of effector caspases 3 and 7 or indirect proteolytic activation of the BH3-only protein BID into tBID, active caspase 8 initiates cell death. The later one, activates the intrinsic apoptotic pathway (Bedoui et al., 2020).

2.3.2.3. The PI3K/AKT/mTOR pathway

Neuronal survival has been shown to be dependent on the growth factor signaling molecules Phosphatidylinositol-3-kinases (PI3Ks) and mitogen-activated protein (MAP) kinase (Pettmann & Henderson, 1998). Recent research suggests that Protein kinase B (PKB), also known as Akt, one of PI 3-kinase's downstream targets, is primarily responsible for the protective effects (Chong et al., 2005; Luo et al., 2003; G. Song et al., 2005). Besides that, it has been shown that PI3K is an essential regulator of neuronal function. It plays critical roles in the formation of synapse and dendritic spines, necessary for the manifestation of functional connection as well as persistent forms of synaptic plasticity that support learning and memory, by transducing signals to the Akt/mTOR pathway from cell surface receptors (Cuesto et al., 2011; Hoeffer & Klann, 2010; Izzo et al., 2002; Jaworski et al., 2005; Sui et al., 2008). Therefore, it should come as no surprise that a growing body of research identifies dysregulated PI3K activity and subsequent signaling as a major cause of mental disorders and a potential therapeutic target (Jansen et al., 2015a; Kalkman, 2006; Karam et al., 2010; Waite & Eickholt, 2010).

2.3.2.3.1. PI3K

This survival cascade is typically activated when growth factors bind to their corresponding receptors to activate intracellular programs that support proliferation and survival. In vertebrates, PI3K enzymatic activity is mediated by eight distinct catalytic subunits, which then according to their structure, function, and regulatory (inhibitory) subunits are divided into three classes (I, II, III) (Gross & Bassell, 2014; Huang et al., 2022).

Class I PI3Ks, which primarily function as lipid kinases, are heterodimers composed of one catalytic and one regulatory subunit. This class can be divided into two subclasses: IA and IB according to their mode of activation. The class IA isoforms are formed from several catalytic subunits such as p110α (encoded by phosphatidylinositol-4,5-bisphosphate 3-kinase, catalytic subunit alpha (PIK3CA) gene), p110β (PIK3CB), and p110δ (PIK3CD) which are associated with any one of the regulatory

subunits including: p50α, p55α, p85α, p85β and p55γ (Jean & Kiger, 2014; Thorpe et al., 2015; Yudushkin, 2019). Class IA PI3Ks can be activated by receptor tyrosine kinases (RTKs) (Gyori et al., 2017). On the other hand, subclass IB, is composed of one catalytic subunit p110γ (PIK3CG) and the p101 regulatory subunit, can be activated through G protein-coupled receptors (GPCRs) (Fruman et al., 1998; Porta et al., 2014; Vadas et al., 2011; Vanhaesebroeck et al., 2010) There are three distinct subtypes of Class II PI3Ks (PI3K-C2, PI3K-C2, and PI3K-C2). Class III PI3Ks have two subunits, Vps34 and Vps15, and they can be involved in the lysosomal autophagy and phagocytosis pathways (Huang et al., 2022).

Recently, class I PI3Ks got more attention as they frequently comes out as the root cause of several diseases including cancer (L. Zhao & Vogt, 2008), and defect in cortical development (Gross & Bassell, 2014).

Autophosphorylation of tyrosine residues occurs when growth factor RTKs are activated. After that, one of the two SH2 domains in the adaptor subunit directly binds to phosphotyrosine consensus residues of growth factor receptors or adaptors to bring PI3K to the membrane. The catalytic subunit is allosterically activated as a result of this. The second messenger, phosphatidylinositol-3,4,5-triphosphate (PI3,4,5-P3), is produced within a few seconds after PI3K activation from the substrate, phosphatidylinositol-4,4-bisphosphate (PI-4,5-P2). The pleckstrin homology (PH) domain-containing signaling proteins Akt and 3-phosphoinositide-dependent protein kinase-1 (PDK1) are recruited to the membrane by PI3,4,5-P3. Individually, Akt controls a number of cell processes that are necessary for cell survival and the progression of the cell cycle (Fresno Vara et al., 2004; Gross & Bassell, 2014; Huang et al., 2022).

2.3.2.3.2. AKT

Serine/threonine kinase AKT is a crucial PI3K downstream signal. There are three types of AKT: AKT1, AKT2 and AKT3, which are encoded by *PKBα*, *PKBβ* and *PKBγ*, respectively (Y. Xie et al., 2019). Additional research demonstrated that different subtypes of AKT express in a tissue-specific manner for instance: AKT1 is expressed in a

variety of tissues (W. S. Chen et al., 2001), AKT2 is only expressed in insulin-sensitive tissues (Cho, Mu, et al., 2001), the expression of AKT3 is limited in to the brain and testis (Alcantara et al., 2017; Lopes et al., 2019). The distinct tissue expression patterns of the various AKT subtypes point to their critical involvement in the regulation of physiological processes in various tissues or organs.

Three-dimensional structures of the three AKT subtypes are remarkably similar, with an average of 85 % amino acid sequence homology. In contrast, they were made up of three distinct functional domains. Regulation of protein-protein and protein-lipid interactions is carried out by the N-terminus PH domain, and the phosphorylation of Thr308 in this domain is necessary for AKT activation as well. The regulatory region of the C-terminal AKT domain contains Ser473, which is required for complete AKT activation (Du & Tsichlis, 2005; Woodgett, 2005). Several different type of hormones, such as insulin and growth factors, control activation of AKT [26]. As previously indicated, the PI3K regulatory subunit binds to the appropriate receptors or receptor-binding proteins on the cell membrane, activating its catalytic component, which subsequently catalyzes the synthesis of PIP3 and attracts AKT to the cell membrane (Du & Tsichlis, 2005; Tokunaga et al., 2008). Thr308 in the catalytic region of AKT kinase is phosphorylated by PDK1(Dangelmaier et al., 2014),while at Ser473 located in the regulatory region is phosphorylated PDK2 (Chan & Tsichlis, 2001). A number of potential PDK2 kinases have been identified recently, such as, mammalian target of rapamycin (mTORC2), DNA-dependent protein kinase (DNA-PK), integrin-linked kinase (ILK), and protein kinase C β (PKC β II) (Carnero et al., 2008; Du & Tsichlis, 2005). By further phosphorylating the glycogen synthase kinase 3 β (GSK-3β), FoxOs, Bad, Caspase 9, nuclear transcription factor-kappa B (NF-kappa B), mTOR, and p21 proteins, activated AKT mediates regulation of variety of cellular process including the, proliferation, cell growth, cell cycle, cell survival (Huang et al., 2022).

Akt is an anti-apoptotic factor that prevents cell death signaling from happening either directly or indirectly (Shaw & Cantley, 2006). It has been demonstrated that Akt directly interfering with cell death pathways by phosphorylating key apoptosis-regulatory proteins and shifts the ratio of pro- and anti-apoptotic proteins toward the

inhibition of cell death. One procedure in that Akt interferes with apoptosis signaling is by phosphorylating proapoptotic proteins, which reduces their activity.

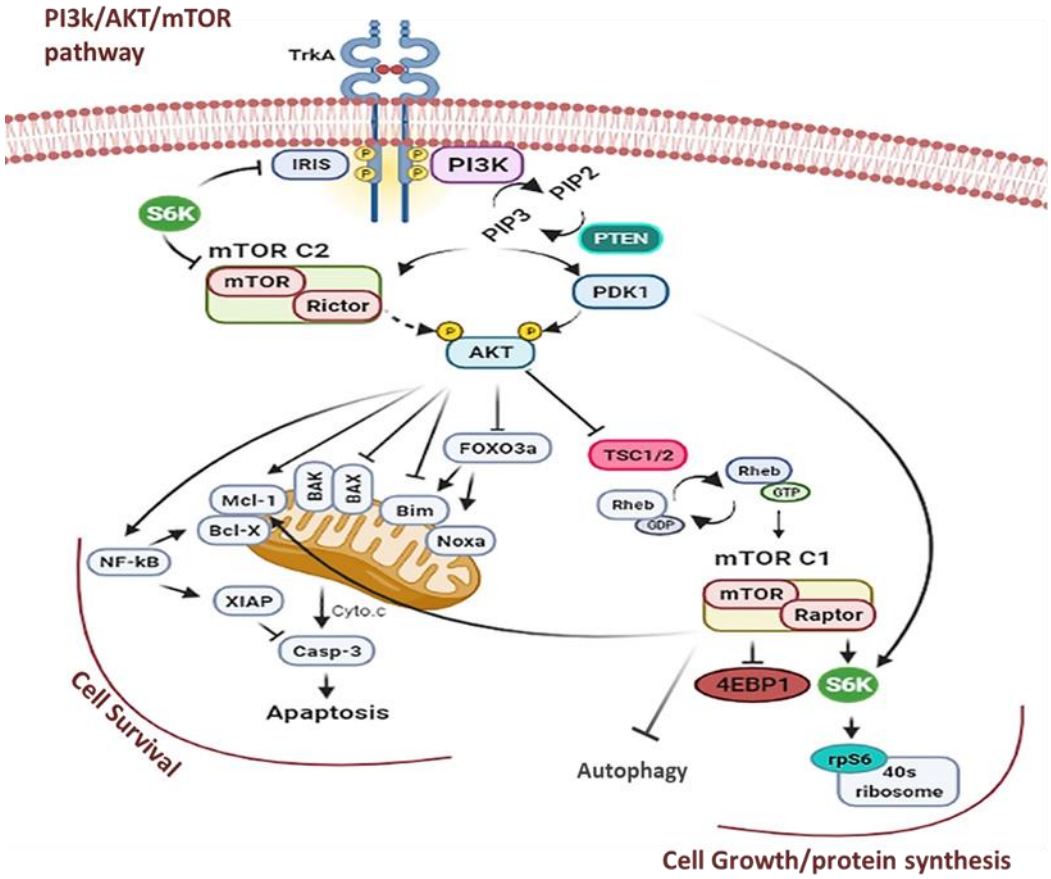

Figure 23 | Schematic representation of the PI3K/AKT/mTOR signaling pathway

This survival cascade is typically activated when growth factor receptors are ligated by their corresponding growth factors to activate intracellular programs that support proliferation and survival.

In line with that, it has been discovered that the serine (Ser)184 residue of Bax is phosphorylated in an Akt-dependent manner (H. Yamaguchi & Wang, 2001), resulting in a conformational change that prevents Bax from being activated (Gardai et al., 2004). Bim, another member of the Bcl-2 family, is also phosphorylated at its Ser 87 residue, just like Bax (Qi et al., 2006). Phosphorylation of Bax and Bim diminishes pro-apoptotic activity. Additionally, phosphorylation of Bim by Akt speeds up its degradation by the proteasome, preventing apoptosis from occurring.

Through the same mechanism Akt also inhibits Bad, Omi/high temperature requirement protein A2 (HtrA2) known as a mitochondrial protease, and Caspase 9 (Parcellier et al., 2008).

In addition to phosphorylating important signal transduction molecules, which directly interfere with cell death signaling pathways, Akt has also been observed to indirectly interfere with cell death programs by phosphorylating TFs. Some of the well-known transcription factors involve in tumor suppressing are p53 and p73 which are crucial for controlling the cell cycle and the initiation of apoptosis. AKT modulates the activity of p53 and p73 mainly through, Mouse double minute 2 homolog (MDM2), which significantly controls p53 and p73 activity via different approaches. AKT- mediated phosphorylation of MDM2's Ser 183 is a key step involved in protein stability and MDM2 nuclear translocation to control activity of p53 and p73, which the later one has higher level of expression in the nervous system (Chibaya et al., 2021; Killick et al., 2011). MDM2 decrease p53 transcriptional activity via forming a complex with p53 protein (Stad et al., 2000), it also suppresses p53 activities by facilitating p53 nuclear export (Boyd et al., 2000), and by acting as a E3 ubiquitin ligase to targets p53 for 26S proteasomal degradation (Honda et al., 1997). In addition, MDM2 inhibit p73 transactivation without promoting p73 degradation. By competing with p73 for binding to the p300/CBP N terminus which facilitate gene expression, MDM2 disrupted p73's interaction with p300/CBP. (Bálint et al., 1999; Zeng et al., 1999).

It has been demonstrated that deltaNp73 which serves as anti-apoptotic isoform of p73 and plays a critical role in CRs survival, is degraded in a c-Jun-dependent manner upon genotoxic stress through proteasome-dependent mechanism (Dulloo et al., 2010). Akt can inhibits can the c-Jun N-terminal kinase (JNK) activation that is induced by stress and cytokines through antagonizing and the formation of the NK-interacting protein 1 (JIP1)-JNK module as well as the activities of upstream kinases Apoptosis signal-regulating kinase 1 (ASK1), Mitogen-Activated Protein Kinase Kinase 4 (MKK4) , MKK7(H.-F. Zhao et al., 2015). Besides, Forkhead transcription factors such as Forkhead box protein O1 (FOXO1), FOXO3a, FOXO4, and FOXO6 as well as the transcription factors NF-

kB and cAMP response element-binding (CREB) protein are all affected (Fulda, 2012). Inhibitors of Apoptosis (IAPs) proteins, Bcl-XL, and Bcl-2, are just a few examples of the many anti-apoptotic NF-KB target genes that can be transactivated as a result of Akt-mediated activation of the transcription factor NF-KB (Ozes et al., 1999; Romashkova & Makarov, 1999). However, when forkhead TFs become phosphorylated by AKT, their transcriptional activity is stopped by cytosolic sequestration. In turn, this leads to a decrease in the production of proapoptotic proteins, such as Bim, Noxa, tumor necrosis factor (TNF)-related apoptosis-inducing ligand (TRAIL), and FAS ligand, which are known to be controlled by forkhead transcription factors (Van Der Heide et al., 2004). Additionally, forkhead transcription factors modulate the levels of ROS by regulating the transcription of antioxidant enzymes (de Keizer et al., 2011).

2.3.2.3.3. mTOR

Another member of the PI3k pathway is the mTOR protein, which acts as a serine-threonine kinase. mTOR is a component of the mTORC1 and mTORC2 complexes (Saxton & Sabatini, 2017). The serine/threonine kinase activity of mTOR regulates cell growth, autophagy, and the actin cytoskeleton in response to growth factor stimulation or the availability of nutrients, energy, or oxygen. These two complexes have distinct structures and functions.

The fact that mTORC1 contains the regulatory associated protein of mTOR (Raptor), and mTORC2 contains the rapamycin-insensitive companion of mTOR (Rictor), may explain why mTORC1 is sensitive to rapamycin treatment while mTORC2 is not. Both complexes have the mammalian lethal sec-13 protein 8 (mLST8), while the Mammalian stress-activated MAPK-interacting protein 1 (mSIN1or MAPKAP1) is just present in mTORC2 (Na et al., 2017; Zhang et al., 2017). mTORC1 can be controlled by the tuberous sclerosis complex (TSC). TSC is a heterotrimer that includes TBC1D7, TSC1, and TSC2. Simultaneously, TSC also serves as a GTPase Activation Protein (GAP) that has the potential to inactivate the small GTP enzyme RAS homolog enriched in the brain (RHEB). AKT-mediated phosphorylation of TSC2 leads to dissociation of the TSC1/2 complex,

which abolishes its GAP activity toward RHEB and consequently activates the mTOR signal (Zou et al., 2020).

Upon activation, by generating two different kinase complexes, mTORC1 and mTORC2, mTOR promotes the phosphorylation of hundreds of substrates either directly or indirectly by activating downstream kinases such as 40S ribosomal S6 kinases (S6K) S6K, AKT, PKC, and Serine/threonine-protein kinase (SGK) (X. Xie et al., 2018, p. 168).

mTORC1 mediates its role in autophagy, protein, lipid, and nucleotide synthesis upon activation via its downstream targets S6K and eukaryotic translation initiation factor 4E (eIF4E)-binding protein 1 (4E-BP1)(Zou et al., 2020). Another example is, autophagy-related protein autophagy-related proteins -1 (Atg-1), which acts as a node in several distinct signaling pathways that control autophagy in vivo. One of Atg-1's upstream signals is mTORC1, and activating the mTOR signal can prevent Atg-1 from inducing autophagy (C. H. Jung et al., 2010; Noda, 2017, p. 1). mTORC2, which phosphorylates Akt Ser 473 to promote cell survival and migration (Baffi et al., 2021), is frequently over activated in cancer cells (Huang et al., 2022).

As mentioned above mTOR pathway is involved in the control of autophagy also known as macroautophagy. Autophagy is a lysosome-mediated process of cellular self-elimination in which damaged organelles, aged proteins, misfolded proteins, or cytoplasmic cargo is transported to lysosomes for bulk degradation in double- or multi-membrane vesicles (autophagosomes) (de Duve, 2005; Noguchi et al., 2020; Settembre et al., 2013). In order to maintain homeostasis, autophagy occurs at a low basal level in cells under normal conditions (Settembre et al., 2013). Autophagic cell death, on the other hand, will take place under unfavorable circumstances like infection, oxidative stress, or a lack of nutrients. The emergence of a double-membrane sequestering compartment is the most noticeable characteristic of autophagy. This temporary organelle encloses a portion of the cytoplasm and develops into an autophagosome, which unites with the lysosome later to allow the cargo to be degraded (Y.-K. Lee & Lee, 2016). A group of Atg genes control autophagy process, for instance: Atg8 (LC3, microtubule associated protein 1-light chain 3) which under specific cleavage and

lipidation it turns to LC3-II. further, LC3-II is brought to the membrane of the autophagosome. Important biomarkers of autophagy include elevated levels of LC3-II proteins and autophagosomes containing LC3-II (Green et al., 2011; Y.-K. Lee & Lee, 2016; Noguchi et al., 2020). Although autophagy helps cells to maintain homeostasis under difficult circumstances as well as fight off apoptosis, excessive autophagy can also kill cells in some cases (Elmore, 2007). This pathway which is characterized by the accumulation of autophagosomes in cells, known as is a type II programmed cell death (Galluzzi et al., 2018; Green, 2019).

2.3.2.3.4. PTEN

Phosphatase and Tensin Homolog (PTEN) is a phosphatase encoded by *PTEN* gene on Chromosome 10 (Shi et al., 2012) .It has been initially identified as a tumor suppressor capable of preventing the conversion of PIP3 to PIP2 by dephosphorylating the 3-position of the inositol ring in PIP3, which in turn inhibits the PI3K signaling (Kreis et al., 2014). Additional studies revealed that PTEN plays a variety of roles in the CNS during the various stages of brain development and in adulthood, besides its tumor suppressor function. In neurons, PTEN is expressed at high levels (Lachyankar et al., 2000). PTEN protein has four structural domains: A PI(4,5)P2 (PIP2) binding domain, a C2 tensin-type part which binds to phospholipids, a catalytic tensin-type phosphatase domain, , and a PDZ-binding domain (J. O. Lee et al., 1999). Expression and function of PTEN is tightly control at different steps: including transcriptional, translational, and posttranslational (Bermúdez Brito et al., 2015). However, posttranslational changes such as: phosphorylation, ubiquitination, and acetylation (Bermúdez Brito et al., 2015; M. S. Song et al., 2011), as well as protein-protein interactions may be the most important means by which PTEN is regulated (Shi et al., 2012). Phosphorylation of the PTEN' C-terminal domain controls PTEN membrane recruitment as well as its lipid phosphatase activity (Rahdar et al., 2009).

PTEN's C-terminal domain, more specifically the amino acids Ser362, Thr366, and Ser370 (Al-Khouri et al., 2005; D. Xu et al., 2010, p. 3), as well as the cluster that includes Ser380, Thr382, Thr383, and Ser385 (Torres & Pulido, 2001), are where the majority of the phosphorylation takes place. The phosphorylation of the aforementioned sites is primarily

mediated by Casein kinase 2 (CK2), and GSK3b (Al-Khouri et al., 2005; Torres & Pulido, 2001). PTEN activity, stability, and localization are negatively impacted by phosphorylation events. In another study it has been shown that ubiquitination of PTEN by neural precursor cell expressed developmentally down-regulated protein 4 (NEDD4), known as E3 ubiquitin-protein ligase, facilitated PTEN nuclear import (Trotman et al., 2007). In addition, protein-protein interactions such as binding of shank-interacting protein-like 1 (SIPL1) to PTEN can inhibits its lipid phosphatase activity (He et al., 2010). Interaction of PTEN with deltaNP73 is another example of this type of regulation, it has been shown that deltaNP73 through direct interaction and block PTEN and inhibits its activity (Vella et al., 2009a). In line with that it, an increase in phosphorylation of AKT has been observed upon overexpression of deltaNP73 suggesting successful inhibition of PTEN activity through this protein (Vella et al., 2009a).

It has been revealed, that PTEN can be found in distinct intracellular location for instance between the cytosol and plasma membrane, in the nucleus, where it is thought to contribute to the genome's stability as well as in cytoplasmic organelles like the endoplasmic reticulum, mitochondria, and mitochondria-associated membranes (MAM). More evidence also suggests that PTEN can be found in extracellularly as well (Figure 24) (Bermúdez Brito et al., 2015).

It has been revealed that PTEN localization in mitochondria, increases upon apoptotic stimuli (Y. Zhu et al., 2006; Zu et al., 2011). It was discover by co-immunoprecipitation that PTEN interacts with BAX, which this protein-protein interaction has been linked to regulating PTEN's recruitment to the outer mitochondrial membrane, at least in the early stages of apoptosis (Y. Zhu et al., 2006; Zu et al., 2011). But, as yet, specific mechanistic insight into a proposed PTEN connection has not been achieved.

Growing number of evidence has revealed that PTEN has several distinct roles in control of cell death independent from PI3K pathway. For instance: it can directly and indirectly regulate activity of p53. Directly via antagonizes the p53-MDM2 interaction and also promoting p300/CBP-mediated acetylation of p53 for stabilizing the protein (Ito et al., 2001, p. 2; Nakanishi et al., 2014). Indirectly through downregulation of PI3K which eventually leads to lack of MDM2 phosphorylation by AKT as well as decrease in expression of MDM2 (Chibaya et al., 2021).

It has been demonstrated that p73α and PTEN proteins can directly bind to one another after DNA damage and form a p73/PTEN complex in the nucleus. Formation of this complex has been associated with the induction of PUMA/Bax. This mechanism initiates apoptosis independently from p53 (Lehman et al., 2011). Besides that, PTEN is a crucial mediator of mitochondria-dependent apoptosis. Dephosphorylates NKAP which leads to suppression of NF-κB (Chatterjee et al., 2019; Vasudevan et al., 2004).

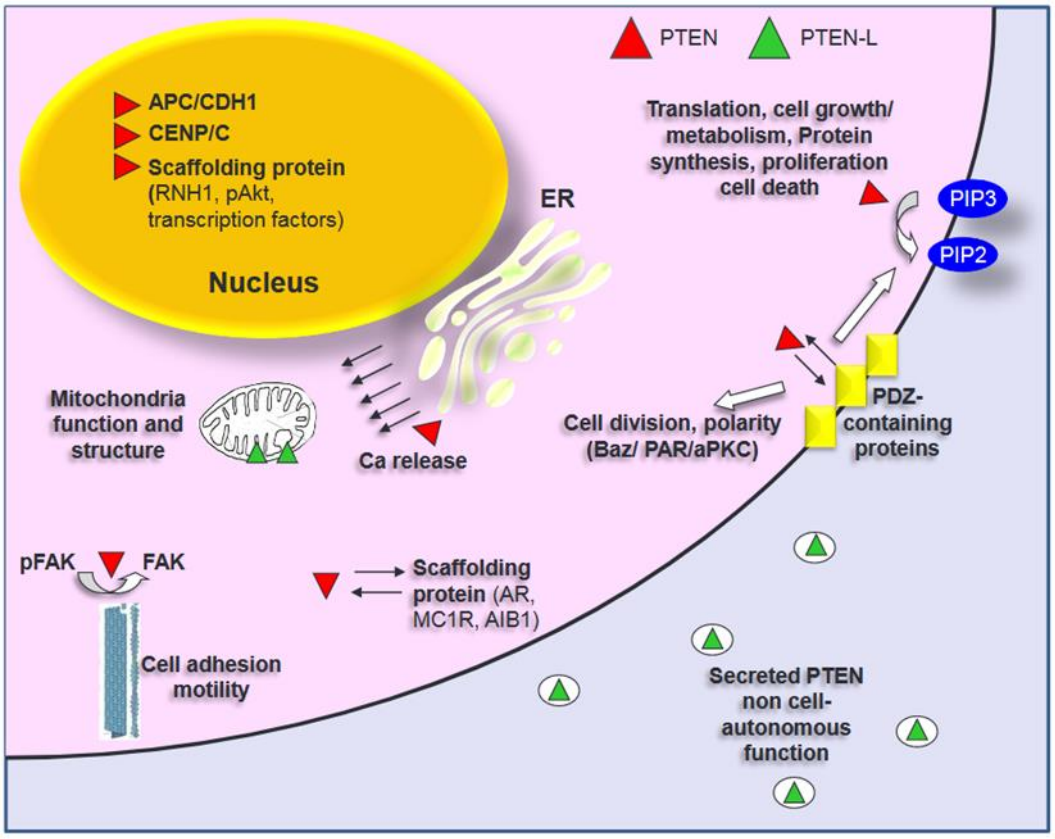

Figure 24 | PTEN multifunctions linked to different cellular localization

PTEN has been shown to reside in the nucleus, where it is thought to contribute to the genome's stability, and between the plasma membrane and the cytosol, as previously mentioned. More evidence suggests that PTEN is also present in extracellular and cytoplasmic organelles like the ER, and mitochondria (Bermúdez Brito et al., 2015).

2.3.2.3.5. Dysregulation of this pathway as a main player in malformation of cortical development

Brain development is made up of multiple unique processes that are tightly regulated, such as: proliferation of neuroepithelial cells, differentiation and migration of immature neurons, establishment of proper synapse and dendritic spines necessary for manifestation of functional connection, and finally removal of excess or abnormal neurons through PCD. Defects in any of those process due to genetic and/or environmental risks can lead to a spectrum of neurological diseases and disabilities. It has been already proven that the PI3K/AKT/mTOR signaling cascade plays critical roles in each and every steps of brain development mentioned above. Therefore, it should not come as a surprise that dysfunction of this node has been identified as the root cause of several neurodevelopmental and neuropsychiatric conditions such as autism spectrum disorders, epileptogenic brain malformations, FCD, and a range of growing brain abnormalities (Moloney et al., 2021; D'Gama et al., 2015; Crino, 2015; Jansen et al., 2015a; Striano & Zara, 2012).

Megalencephaly (big brain) syndromes are most likely genetically mosaic diseases resulting from an increase in the PI3K/Akt3/mTOR pathway activity, due to a variety of Somatic gain of function mutations (Moloney et al., 2021; J. K. Kim et al., 2019; D'Gama et al., 2017; Crino, 2015; Jansen et al., 2015a; D'Gama et al., 2015; Striano & Zara, 2012).

AKT3, PIK3R2(p85 regulatory subunit of PI3K), and PIK3CA (p110α catalytic subunit of PI3K) germline and somatic point mutations have recently been identified in the megalencephaly-related condition. In addition, AKT3, PIK3CA (p110α), and mTOR somatic gain of function point mutations have also been detected in hemimegalencephaly (HME), a rare neurological condition in which one side of the brain, or one half of the brain, is abnormally larger than the other (Sidira et al., 2021; Moloney et al., 2021; J. K. Kim et al., 2019; D'Gama et al., 2017, 2015; Jansen et al., 2015a; Striano & Zara, 2012; Crino, 2015). Typically, HME results in medically severe paediatric epilepsy that needs to be surgically resected (Flores-Sarnat et al., 2003). A variety of brain developmental anomalies, including microcephaly and agenesis of the corpus callosum (ACC), have been linked to deletions of chromosome at 1q42-q44 in the human genome, containing the AKT3 gene (Boland et al., 2007; D. Wang et al., 2013, p. 44). A wide range of brain disorders, including megalencephaly

and HME, exhibit post-zygotic somatic activation of AKT3 (Lopes et al., 2019; Alcantara et al., 2017; Jansen et al., 2015a). The role of Akt3 in controlling brain size has been confirmed in by using mouse models, showing that AK3 inhibition causes brain shrinkage and also impairment of spatial cognition and hippocampal CA1 long long-term potentiation (T. Zhang et al., 2019; Tschopp et al., 2005; Easton et al., 2005), while the brain size and corpus callosum thickness increase when Akt3 is activated (Tokuda et al., 2011). Mice lacking only one of the Akt1 or Akt2 isoforms, in contrast to those lacking the Akt3 isoform, have a diabetes-like syndrome and smaller sizes for multiple organs, respectively (Cho, Mu, et al., 2001; Cho, Thorvaldsen, et al., 2001). Deletion of Key PI3K-Akt-mTOR pathway members Pten, Pdk1, Tsc1/2, mTOR, and Raptor either conventionally or conditionally are all associated with manifestation of microcephaly in mice (Lim et al., 2017; Huber et al., 2015; Costa-Mattioli & Monteggia, 2013; J. Zhou & Parada, 2012). In the developing forebrain, the disruption of mTOR led to aberrant cell cycle progression of NPCs thereby disruption in the progenitor self-renewal process (Ka et al., 2014). Brain lesions, epilepsy, cognitive impairment, and autism are all linked to loss of function mutations in the tuberous sclerosis complex TSC1 or TSC2 genes that result in dysregulated mTOR activity (Lim et al., 2017; European Chromosome 16 Tuberous Sclerosis Consortium, 1993, p. 16).

Loss of Pten has been identified as a risk factor for glioma, macrocephaly, and autism spectrum disorder (ASD), particularly because it increases the activity of the AKT-mTOR pathway (Koboldt et al., 2021; Fraser et al., 2004; L. Li et al., 2002). More recently presence of several PTEN pathogenic variants has been associated with manifestation of polymicrogyria (Shao et al., 2020). Cowden and Bannayan-Riley-Ruvalcaba syndromes, also known as PTEN hamartoma tumor syndrome, are caused by loss of function mutations in the PTEN that result in dysregulated AKT activity. These syndromes are associated with megalencephaly (MEG), cognitive impairment, autism, and epilepsy (Koboldt et al., 2021; Satterstrom et al., 2020; Pilarski et al., 2013; Arch et al., 1997).

Multiple roles in brain development and its maintenance have been identified through conditional elimination of Pten. For instance, Pten disruption in premature neurons caused hypertrophy without affecting NPC proliferation (Fraser et al., 2004), whereas Pten deletion in NPCs elevated its proliferation and self-renewal in vitro and in vivo (Groszer et al., 2001).

It has been recently shown that Pten loss results in inappropriate excitatory excitatory synapse function (Tariq et al., 2022; Skelton et al., 2019). Pten haploinsufficiency (Pten +/-) leads to in a dynamic trajectory of brain overgrowth and altered neural cell scaling, with an increase in the beta-catenin signaling, which known as a risk gene for microcephaly and ASD (J. Chen et al., 2010).

There are many similarities between the neuropathological phenotypes of the TSC, PTEN mutation syndromes, and HMEG, including dysmorphic neurons, cytomegaly, cortical dyslamination, as well as The majority of childhood intractable localization-related epilepsy is caused by FCD (Moloney et al., 2021; Hauptman & Mathern, 2012; Flores-Sarnat, 2002; Huttenlocher & Wollmann, 1991).

3. Objective of the study

In the embryonic telencephalon, CRs are among the very first transient neurons generated in the neocortex which are well-known for their significant roles in the correct migration of projection neurons, cortical lamination by secreting of Reelin, as well as development of cortical structures through the expression of several different morphogens. After fulfilling their roles, CRs largely disappear during the first two postnatal weeks in mice by programmed cell death.

Defects in the elimination of CRs have been associated with some pathological condition associated with epilepsy (Blümcke et al., 2013; Eriksson et al., 2001; Garbelli et al., 2001).

Although the cited studies suggest a connection between the malformation of cortical developments associated with epilepsy and CR survival, it is unclear whether this abnormal persistence is the cause or just a result of the various diseases. However, it raises the question of whether the proper maturation of cortical and hippocampal circuits is affected by the persistence of CRs. Identifying and changing the potential mechanisms involved in the regulation of CRs cell death, as well as looking into the effects of their persistence, can help us answer this question.

Indeed, we have seen in the introduction that a recent study from our lab through conditional inactivation of Bax, one of the pro-apoptotic proteins involved in the intrinsic mitochondrial pathway, showed that not all CRs subtypes die in a Bax-dependent manner. Suggesting the contribution of other cell death mechanisms involved in the elimination of CRs or even the existence of crosstalk between different mechanisms of cell death which can compensate for the loss of other connected pathways (s) (Fricker et al., 2018; Y. Yamaguchi & Miura, 2015). contrast to the multiple cell death mechanisms that work in concert to cause a neuron to die There are just a few systems known to be involved in cell survival that is restricted. In line with that an expanding body of research points to the PI3K/AKT/mTOR pathway as the major participant in providing cells survival signals and ultimately preventing cell death. Intestinally it has been shown that deltaNp73, which is known to be essential for Hem and septum CR survival up to P0, play an important role in the control of this pathway through inhibition of PTEN expression (Vella et al., 2009). PTEN has been known as one of the potent tumor suppressor genes as it serves as the main

negative regulator of the PI3K/AKT/mTOR pathway. However, the existence of this pathway and its function in CRs remain unknown.

The primary goal of my PhD project was to investigate how the PI3K/AKT/mTOR pathway impacts programmed cell death in CR cells and eventually how CR cell persistence contributes to the formation of cortical circuits. To determine that my PhD project included three main objectives to:

- Investigate the physiological activity of the PI3K/AKT/mTOR in CRs.
- Determine whether this pathway is involved in the modulation of CRs programmed cell death.
- Examine the impact of CR persistence on cortical development.

To investigate the role of PI3K/AKT/mTOR pathway in PCD of CRs, we concentrated this project on SE-CRs, CH and ET that contribute to approximately 80% of the total population of CRs in the neocortex, which commonly expresses the DeltaNP73 gene. I first evaluated the physiological activity of this pathway in a spatiotemporal manner to cover the heterogeneity of CRs population together with their death timeline. Then, in order to maintain the activity of this pathway inside CRs, I generated 3 different mouse models by using genetic approaches to target positive (PIK3CA) and negative regulators of the pathway (PTEN and TSC1). Targeting different members of the PI3K/AKT/mTOR pathway gave us the advantage to precisely and piece by piece investigate the role of this large pathway in the PCD of CRs. To investigate the role of CRs persistence in the maturation of functional and dysfunctional cortical circuits and to evaluate the current hypothesis regarding the persistence of CRs as a cause or consequence of some neurological condition mentioned above, we conducted various experiments with different approaches, primarily focusing on PTEN mutants.

We first evaluated the general behavior of PTEN mutants. In addition, we investigate their susceptibility to developing seizures via kainate injection. Additionally, we used patch clamp to examine the CRs' intrinsic properties together with multielectrode array (MEA) to record the field potential of neighboring neurons.

Altogether the result from this PhD project provided an overview of the role of this pathway in the modulation of programmed cell death in CRs and the consequence of the

persistence of CRs through maintaining the activity of PI3K/AKT/mTOR pathway in the system. This work will lead to the publication of one paper already in preparation (Ramezanidoraki et al., manuscript in preparation).

RESULTS

Short description :

The result from the current PhD project will lead to the publication of one paper titled "Activation of the PI3K/ AKT/ mTOR pathway in Cajal-Retzius cells leads to their survival and increases Reelin secretion in the cortex", already in preparation. In this article, the role of this pathway in the modulation of programmed cell death in CRs and the consequence of the persistence of CRs through maintaining the activity of the PI3K/AKT/mTOR pathway in the system have been investigated from three different aspects mentioned below. Techniques and collaborators are mentioned for each section.

- Investigation of the physiological activity of the PI3K/AKT/mTOR in CRs.
    - Generation of animals and preparation of samples were done by **Nasim RAMEZANIDORAKI.**
    - Histological analysis (immunofluorescence staining, image acquisition, quantification, and statistical analysis) done by **Nasim RAMEZANIDORAKI** and Margaux Le.
- Study the role of this pathway in modulation of CRs programmed cell death.
    - Generation of models and preparation of samples was done by **Nasim RAMEZANIDORAKI.**
    - Histological analysis (immunofluorescence staining, image acquisition, and quantification and statistical analysis): was done by **Nasim RAMEZANIDORAKI**, and the writing of macro for 3D analysis of CRs was done by Philippe Bun.
- Study the impact of CR persistence on CRs function, cortical development, and behavior.
    - Generation of PTEN animals was done by **Nasim RAMEZANIDORAKI.**
    - General behavior test: Performing of tests done by **Nasim RAMEZANIDORAKI** and Sabrina JAZA, analysis of the results done by Pierre Billuart and Danae Rolland.
    - kainate injection: Performing of the experiment and the statistical analysis for PTEN were done by **Nasim RAMEZANIDORAKI** and production of the result

was done by Margaux Le. For PI3K the experiment and analysis of the result were done by Stéphanie Moriceau.

- Multielectrode array (MEA): Acquisition was done by **Nasim RAMEZANIDORAKI**, and analysis of results was done by Elena Dossi.
- Patch clamp recording: Performing of experiment and analysis of results was done by Mahboubeh Ahmadi.

- Writing the current article manuscript
  - Introduction, results, and discussion done by Pierre Billuart.
  - Figures, figure legends, Material and Methods, Supplemental Tables done by **Nasim RAMEZANIDORAKI.**

Activation of the PI3K/ AKT/ mTOR pathway in Cajal-Retzius cells leads to their survival and increases Reelin secretion in the cortex.

Nasim Ramezanidoraki[1,2,5], Margaux Le[1,2,5], Mahboubeh Ahmadi[1,5], Stéphanie Moriceau[3], Dossi Elena[4], Danae Rolland[1], Philippe Bun[1], Lepen Gwenaelle[1,5], Mario Pende[3], Guillaume Canaud[3], Nadia Bahi-Buisson[1,2], Nathalie Rouach[4], Rebecca Piskorowski[1,5], Alessandra Pierani[1,2,5], Pierre Billuart §[1,2,5]

[1-] Institut National de la Santé et de la Recherche Médicale (INSERM) U1266**,** Institute of Psychiatry and Neuroscience of Paris (IPNP), Université de Paris Cité, Paris, France**.**

[2-]Institut Imagine, Université de Paris Cité, 75015 Paris, France

[3-]Institut National de la Santé et de la Recherche Médicale (INSERM) U1151, Institut Necker Enfants-Malades (INEM), Université Paris Cité, Paris, France.

[4-]Center for Interdisciplinary Research in Biology (CIRB), College de France, CNRS, INSERM, Labex Memolife, Université PSL, Paris, France

[5-] GHU Paris Psychiatrie et Neurosciences, France

§Correspondence should be addressed to: pierre.billuart@inserm.fr;

Running Title: Post-natal survival of Cajal-Retzius cells after activation of the PI3K/ AKT/ mTOR pathway increases reelin secretion.

Keywords: Development, Cajal-Retzius cells, neuronal survival, PI3K/AKT/mTOR pathway

ABSTRACT

Cajal-Retzius cells (CRs) are a class of transient neurons in the mammalian cortex which play a critical role in cortical development. CRs undergo almost complete elimination in the first two post-natal weeks in rodents and the persistence of CRs during postnatal life has been detected in pathological conditions related to epilepsy. However, it is unclear whether their persistence is a cause or consequence of these diseases. Deciphering the possible molecular mechanisms which are involved in CRs death we investigate the PI3K/ AKT/ mTOR pathway as it plays a critical role in cell survival. We first show that this pathway is less active in CRs after birth before massive cell death. In parallel, we explored the spatio-temporal activation of both AKT and mTOR pathways and revealed area-specific differences in both rostro-caudal and medio-lateral axes. Next, using genetic approaches to maintain active the pathway in CR, we found that the removal of either PTEN or TSC1, two negative regulators of the pathway led to differential CR survivals with a stronger effect in PTEN. Persistent cells in this latter mutant are still active, express, and secrete higher levels of reelin leading to non-cell autonomous activation of the mTOR pathway in the cerebral cortex without altering mice behavior. Altogether we show that the decrease of PI3K/AKT/mTOR activity in CRs primes these cells to death by possibly repressing a survival pathway, the mTORC1 branch contributing less to the phenotype.

Introduction

Cajal-Retzius cells (CRs) are transient excitatory pioneer neurons that migrate tangentially at the surface of the cortex during development (Causeret et al. 2021). They came in multiple flavors depending on their origins. At least four sources at the border of the pallium have been characterized: the cortical hem, the pallial septum, the ventral pallium, and the thalamic eminences (Bielle et al. 2005; Ruiz-Reig et al. 2016). Besides their well-known function in cortical layering through the secretion of Reelin (Reln), they also control multiple steps of cortical development from neuronal proliferation to dendritogenesis but also functional area formation (Causeret et al. 2021). In rodents, CRs are almost eliminated in the two first postnatal weeks according to a neuronal cell-death program which remains to be explored. Our previous studies have shown that Bax-mediated apoptosis is responsible for the elimination of a fraction of CRs, especially the one derived from the septum (Ledonne et al. 2016). In addition, this cell-death mechanism is dependent on neuronal activity since blocking their excitatory inputs from inhibitory neurons (Blanquie et al. 2016) or hyperpolarizing the CRs (Riva et al. 2019) led to their partial survival.

Cell death and survival are two janus faced components of cell life and inactivation of cell survival will lead to the same outcome. Amongst the most well-known pathway involved in cell survival is the PI3K/AKT/mTOR one, which activation inhibits apoptosis potentially leading to human cancer when overactivated in proliferating cells (Yao and Cooper 1995). Class I PI3K catalytic subunits transduce the signal from either receptor tyrosine kinase (RTKs) or G protein-coupled receptors (GPCRs) to AKT which in turn phosphorylates numerous regulators to activate the mTORC1 complex. This pathway is negatively controlled at different levels by various proteins such as PTEN (Phosphatase and Tensin Homolog), which reduces PIP3 levels, or by the TSC1/2 complex (Tuberous Sclerosis Complex), which acts as the GTPase Activating Proteins to inhibit the GTPase Rheb, the main activator of mTORC1 (Bockaert and Marin 2015). Besides its phosphatase activity on PIP3 at the plasma membrane, PTEN functions also in different compartments such as the nucleus, the endoplasmic reticulum, and the mitochondria where it regulates transcription, calcium release from the ER and structure respectively (Bermúdez Brito 2015).

During brain development, activation of the pathway secondary to mutations in its components is responsible for various cortical malformations from hemimegalencephaly to focal cortical dysplasia associated with intractable pediatric epilepsy (Jansen et al. 2015). The severity of the phenotype correlates with the occurrence of the somatic mutation: the earlier, the worse the phenotype (D'Gama et al. 2017).

In the mouse brain, conditional activation of the pathway leads to different outcomes depending on whether eliminated in proliferating cells or neurons (Clipperton-Allen and Page 2020). Deletion of Pten in neural progenitors enhances cell proliferation (Groszer et al. 2001) whereas it causes hypertrophy in early post-mitotic neurons without altering specification and radial migration in principal neurons of the neocortex (Kazdoba et al. 2012). The pathway is also essential for synapse and dendritic development (Jaworski 2005) and participates in synaptic plasticity (Sanna et al. 2002). Pten removal in hippocampal granule cells led to focal seizures or generalized seizures depending on the mosaicism degree (LaSarge et al. 2021).

During postnatal cortical development, active pyramidal neurons inhibit PTEN expression in interneurons and protect from cell death (Wong et al. 2018). Here, we investigated the role of the PI3K/AKT/mTOR pathway in the cell death of CRs derived from the deltaNp73 lineage, which includes 80% of all CRs in the neocortex. We showed that this pathway is physiologically inhibited at post-natal stage in CRs before they start to die through apoptosis. We then sustained its activation using mouse genetics to prevent CRs from death. Both gain and loss-of-function approaches of PI3K or PTEN respectively led to CRs survival whereas the activation of the mTOR pathway by TSC1 removal had little effect on cell numbers. As expected for the activation of this pathway the morphology and the intrinsic properties of the survival CRs are altered but still, they are active and secrete more Reelin in an overall preserved cortex. This Reln increase led to a non-cell autonomous activation of the mTOR pathway underneath pyramidal neurons without altering the neuronal network activity in the S1 Barrel cortex nor increasing the sensitivity of the mice to kainate-induced epilepsy. In this context, activation of the PI3K/AKT pathway in CRs protects them from apoptosis but their persistence is not associated with epilepsy nor alteration in some general behavior tests.

Results

Spatiotemporal regulation of the PI3K/AKT/mTOR pathway activity in deltaNp73-CRs

deltaNp73-CRs constitute approximately 80% of total population of CRs in the neocortex, namely Septum-CRs and Hem-CRs (Tissir et al. 2009). It has been shown that deltaNp73-CRs undergo Bax-mediated apoptosis in the two first postnatal weeks. However, the trigger of such apoptosis or the mechanisms regulating the death of other CR populations are still unknown (Ledonne et al. 2016). PI3K/AKT/mTOR pathway is one of the major cell survival signaling cascade involved in the regulation of mitochondria-mediated apoptosis and it is also known to induce cellular senescence in non-replicative cells (Fulda 2012). To decipher whether activity of this pathway might regulate the death of deltaNp73-derived CRs *in vivo*, we first looked at the physiological activity of the PI3K/AKT/mTOR pathway at prenatal and postnatal stages. We used the *deltaNp73*$^{cre/+}$ line (Griveau et al. 2010; Tissir et al. 2009) to label CRs via the conditional expression of tdTomato (tdT) as a Cre recombinase reporter (Rosa26^{mT}). Brain sections were analyzed along both rostro-caudal **(Fig. 1A)** and medio-lateral **(Fig. S1)** axes at two different stages, embryonic stage E17.5 (E17.5) and postnatal day 1 (P1) before the beginning of massive cell death**.** The activity of the pathway was monitored by double immunofluorescence staining for pAKT (Ser473) and pS6(Ser240/244), two well-known biomarkers of the pathway **(Fig. 1B)**.

Quantification of the total number of tdT positive cells in the marginal zone along the rostro-medial axe showed a 40 % reduction in the level 1 (Sup Table 1.1) corresponding to either altered migration more rostrally or precocious cell-death in this level of the neocortex whereas no change was observed in levels 2 and 3 (**Fig. 1C**). As expected from the expansion of the cortex size between E17.5 and P1 stages, CRs densities along rostral-caudal axis were significantly reduced by 20 to 40% according to the level (**Fig.1D, S1B and S1C**) (Sup Table1.2).

Next, to monitor the activity of the pathway**,** two related markers pATK and pS6 were used to distinguish between the activity of the PI3K/AKT and/or mTOR pathway respectively (**Fig.1B and 1E**). The proportion of tdT cells negative for activity (pink bar in Fig. 1E) or

positive for one or the other marker (gray and green bars in Fig. 1E) or positive for both (dark orange bar Fig. 1E) were quantified.

Rostro-caudal analysis of the brain at E17.5 showed that 60 to 70% of total tdT cells are positive for one or the two markers (Fig.1E) with no difference between levels. At P1 stage there were overall a 40 -50% reduction in the activities of the pathway in all different brain levels in comparison to E17.5 stage (cells negative for any activity, Sup Table 1.3), more specifically the proportion of CRs positive for two markers (cells positive for both markers, Sup Table 1.3) **(Fig. 1E)**. None of the single labeled cells, pAKT or pS6 alone, showed a significant difference between the two stages along the rostro-caudal axis (cells positive for only one marker, Sup Table 1.3).

In contrast, medio-lateral analysis of the brain sections at E17.5 showed a spatial difference in the activities of PDK1 or mTORC2 (pAKT) and S6 kinases (pS6) in CRs (Fig. S1 left panels). CRs positive only for p-AKT were more present in the medial part of the neocortex (pAKT vs tdT, Table 1.4) whereas CRs positive only for pS6 show a mirror pattern with an enrichment more laterally in all three brain levels (pS6 vs tdT, Table 1.4). Cells positive for both markers show differential pattern according to brain levels. In levels 1 and 3, they show mirror distributions with less in lateral and medial regions respectively (Fig. S1A and S1C left panels) (pS6&pAKT vs tdT, Table 1.4) whereas, in level 2, they follow more or less the tdT positive CRs distribution (Fig. S1B left panel). With the expansion of the cortex size, beside the reduced activation of the pathway (Fig. 1E), the different patterns of phosphorylation observed at E17.5 tend to flatten at P1 but overall, they present the same pattern of distributions with less statistical differences compared to tdT positive cells **(Fig. S1A, B, C right panels)** (Table 1.5).

All together the PI3K/AKT/mTOR pathway activity in deltaNp73-CRs presents with differential activation of AKT and mTOR pathways along the medio-lateral axe and a reduction in overall activity from prenatal to postnatal stages. This spatiotemporal control of the pathway activity is compatible with the hypothesis that down-regulation of a pathway involved in cell survival may contribute to CRs death later on during the 2 first postnatal weeks.

Constitutive activation of PI3K/AKT/mTOR pathway activity in deltaNp73-CRs leads to cell survival

The perinatal period is a developmental critical time window for neurons since a lot of them are partially or almost eliminated (Causeret, Coppola, and Pierani 2018). To test if the observed reduction in PI3K/AKT/mTOR pathway activity during this period is responsible for cell death in deltaNp73-CRs, we explored the consequences of maintaining the pathway permanently active in these cells. To do so we used a conditional mouse model R26StopFloxp110* to constitutively express an activated version of the catalytic subunit of PI3K, the PIK3CA in CRs (Srinivasan et al. 2009). Upon CRE recombinase mediated deletion of the STOP cassette, the mutated p110alpha protein is expressed together with tdT reporter in deltaNp73 derived CRs (deltaNp73>P110*). Mutant mouse model was first validated by monitoring the pathway activity at P1 stage using pAKT and pS6 markers in the cortex (**Fig. S2 A top panels**). Quantification of the tdT cells showed an increase in the proportion of double-positive cells for the two markers by 3 to 4 times compared to controls at the 3 levels (**Fig. S2 C**) (CR positive for both markers, Control versus PIK3CA, Sup Table 2.3). None of the proportions for single labelling showed a significant difference between the two stages suggesting that strong AKT activation also leads to activation of mTOR. Thus, this genetic model allows to activate and maintain the activity of the pathway in CRs at a time when it should be physiologically downregulated.

Next, we determined whether the activation of the PI3K could interfere with embryonic development of CRs since deltaNp73 is expressed from E11.5 in post-mitotic cells. We found that cortex size (**Fig. S2A)** and tdT positive CRs densities (**Fig. S2B)** (Sup Table 2.1) do not differ between p110* and controls at P1 stage in the rostro-caudal levels (Control versus PIK3CA, Table 2.2). Therefore, in this context, any difference in cell number after 2 weeks could only be attributed to cell persistence. At P24 stage (**Fig 2A**), the CR densities was reduced from approximately 15 000 (**Fig S2B)** (Sup Table 1.2) to 400 cells/mm^3 (**Fig 2C)** (Sup Table 3.1) in controls as previously reported (Ledonne et al. 2016). In contrast the p110* expressing animals (**Fig 2A**) showed a density of 1 150 cells/mm^3 (**Fig 2C)** (Sup Table 3.1) suggesting a significant increase of 3 to 4 times compared to controls at the same age in all three brain levels (**Fig 2D)** (Control vs PIK3CA Sup Table 4.1). Since we observed some

specific activation pattern of the pathway at E17.5 along the medio-lateral axis (**Fig S1**), we investigated the distribution of the deltaNp73 derived CRs in different cortical areas at P24 (**Fig 2E**). As expected from a gain-of-function experiment with strong pathway activation, almost all areas showed a significant increase of the CR densities with different increases according to the area (**Fig 2F and G**)(**Fig S3**)(Control vs PIK3CA, Sup Table 3.2).

Conditional inactivation of TSC1 or PTEN, two negative regulators of the PI3K/AKT/mTOR pathway, result in specific patterns of CR survival

Results from the expression of the p110* clearly demonstrate the postnatal survival capacity of the pathway in NP73 derived CRs. However, since p110* is expressed in all CRs, we may lose the specificity of the pathway activation according to brain regions or cortical areas as previously observed in E17.5 embryos. We, then turned to a loss-of-function approach to activate the pathway only in places where it is controlled and used the conditional inactivation (cKO) of either *Tsc1* or *Pten*, which encodes for two well-known negative regulators of the PI3K/AKT/mTOR pathway. Beside mTOR pathway, these molecules, especially PTEN are at the crossway of multiple other pathways (Bermúdez Brito 2015) and we tested their respective contribution to the NP73 derived CR survival by comparing both phenotypes. At P1 tdT CRs in these 2 models have different levels of activation according to the neocortex levels (**Fig S2 A and S2 C**). Loss of TSC1 function increased the proportions of cells positive for pS6 in level 3 but not in levels 1 and 2 suggesting that mTOR pathway is more activated in the caudal parts of the cerebral cortex. Regarding the Pten model, only level 3 showed a large increase in the proportion of double positive CRs whereas the proportion of pAKT single labeled CRs was unexpectedly decreased in level 1(**Fig S2 C)** (Control and PTEN, Sup Table 2.3).

Next we determined the consequences of the activation on the development of deltaNp73 derived CRs in both Tsc1 and Pten models. At P1stage, whereas inactivation of Tsc1 did not alter the cortex size (**Fig S2A**) nor the densities of tdT positive cells in the marginal zone of the cortex (**Fig S2B**) (Sup Table 2.2), PTEN removal reduces overall their densities (**Fig S2B)** (Sup Table 2.2) without affecting the brain size (**Fig S2A)**. Thus, the

embryonic development of the deltaNp73 derived CR is not altered in *Tsc1* but lightly in *Pten* cKO.

Next, we quantified the CRs densities at P24 in Tsc1 and Pten cKOs (**Fig. 2C**). At this stage, the pathway was still activated in both models as reveled by the pS6 staining increase in tdT CRs (**Fig 2A**). Loss of *Tsc1* function increased almost 2 times the number of tdT positive CRs in all the brain levels (control versus Tsc1, Sup Tables 3.1 and 4.1) whereas loss of *Pten* increased it by 3 to 6 times depending on the brain levels similarly to p110* model (**Fig 2E** and **2D**) (control versus Pten, Sup Tables 3.1 and 4.1). Looking at in more details the brain areas in each level (**Fig 2E** and **2D**), Pten cKO had a stronger phenotype than Tsc1 since the densities were higher and affected more brain areas compared to Tsc1 cKOs (Tsc1 versus Pten, Sup Table 3.1). From the three levels comparison (**Fig 2B**), both cKOs altered the medial cortical regions of the cortex, namely the prefrontal cortex (ACA), retrosplenial-motor (RSP-MO) and retrosplenial (RSP), characterized by the highest densities of deltaNp73 derived CR in the cortex (**Fig. S3 B, Fig. 2F and Fig S3D**) (Sup Table 3.2). The areas of the intermediate section (level 2) are also more sensitive to the loss of either molecule compared to rostro (level 1) and caudal (level 3) sections (**Fig. 2F/G and Fig. S3 B/C and S3D/E**). These differences in cell densities at P24 in level 2 sections does not correlate with the differences in pathway activation observed at P1 in level 3.

Beside these commonalities, Pten cKOs present with significant increases in more lateral brain areas (**Fig. 2F/G and Fig. S3 B/C and S3D/E**)(Sup Table 3.2). When normalized to respective controls, the fold changes vary according to the areas especially in levels 1 and 2 which shows an increase along the medio-lateral axes (**Fig. 2G and Fig. S3 C and S3E**) (Sup Tables 4.1 and 4.2). This suggest that lateral CRs are more sensitive than the medial one to the loss of Pten, indicating that the endogenous pathway is more inhibited in the lateral cortex. This hypothesis is strongly supported by the differential pattern of pAKT staining observed at P1 especially in level 2 (**Fig S1**)(Sup Table 1.5). Finally, there is no specific brain area where the Tsc1 cKO presents with an increase in CR density but not Pten cKO.

All together NP73 derived cells are differently sensitive to the loss of TSC1 or PTEN function depending on the rostro-caudal axis with a stronger effect in the level 2 and also on the medio-lateral axe with higher numbers of survival CRs in the medial cortex whatever

levels. Finally, NP73 derived cells are more sensitive to Pten cKOs than Tsc1 suggesting that activation of the mTOR pathway contributes little to the survival phenotype observed after either Pi3K activation or PTEN loss of function.

Pten inactivation in CRs alters their morphology and their intrinsic firing properties.

Beside the increases in the CRs number after the activation of the PI3K/AKT pathway, the *Pten* model clearly presents with some obvious morphological alterations in the size and the number of CRs dendrites and/or axons at P24 (**Fig. 2A, 3A and 3B**)(Sup Table 5). These morphological changes resulting from polarity defects and neurite outgrowth have been already reported for other *Pten* conditional models where the AKT pathway has been activated (Kwon et al. 2001, 2006). Surprisingly, this phenotype in dendrites and/or axon was less penetrant after p110* expression than after *Pten* loss-of-function (**Fig. 2A**), which suggest partial compensation by endogenous PTEN in the P110* model or PIP3 independent mechanism of dendritic elongation and branching in CRs regulated by PTEN. In addition, very littles alterations of CR morphology were observed at P1 stage in Pten model (**Fig. S2**A) suggesting that the dendritic phenotype was acquired during the two first weeks and progressed with age as previously reported (Kwon et al. 2001).

We next asked whether the surviving CRs in *Pten* model at P24 were still active neurons. We prepared coronal slices of mutant and control animals and performed whole-cell current clamp recordings of tdT positive cells in the somatosensory barrel S1cortex. All recorded cells were filled with biocytin and post-hoc imaging was performed to analyze cellular morphology (Fig 3A). We found that at P24, CR cells in control animals were extremely difficult to locate, and the soma too small and membranes too fragile to achieve usable electrophysiological recordings. Therefore, we recorded control cells at P10 before they die to allow comparison to the Pten model (Ledonne et al. 2016) .

We found that Pten model CR cells had numerous intrinsic properties and physiological features consistent with active neurons (Fig 3D-F). They had more depolarized resting membrane potentials than control (Fig 3D1; Sup Table 6), higher input resistance (Fig 3D2; Sup Table 6) and higher membrane capacitance (Fig 3D3; Sup Table 6). To examine the

action potential firing properties of CR cells in control and Pten mice, cells were held at -75 mV and depolarizing current steps were injected to induce action potential firing (Fig 3C). From these experiments, Pten CR cells fired significantly more action potentials per current step for current steps larger than 80 pA (Fig 3E1, Sup Table 6) and had larger action potential amplitudes (Fig 3E2, Sup Table 6). Additionally, the AP threshold was significantly reduced (Fig 3F1, Sup Table 6), as well as the AP Halfwidth (Fig 3F2, Sup Table 6) and lastly, the AP latency was longer for Pten CR cells than control (Fig 3F3, Sup Table 6). These results for Pten CR cells at P24 are consistent with surviving cell being larger, electrically active, and capable of repetitive firing compared to control CRs but overall they kept their intrinsic CRs characteristics.

Increases in Reelin expression and secretion does not alter cortical layering in Pten mutants but lead to mTOR activation in the cortex

CR are characterized by expression of the Reln and we tested whether persistent CRs in our models keep to express this marker at P24. We noticed that they not only express it but with an increase in signal intensity (**Fig 2A**). Quantification of Reelin intensities in *Pten* mutant CRs, which present the most extreme phenotypes showed a significant increase of expression compared to controls (**Fig 3C**)(Sup Table 5). Secreted Reelin appears as diffuse signal bands in both cortex and hippocampus (**Fig 4A**). In Pten mutant brains at P1 stage, the Reelin signal intensity was clearly increased around the tdT positive CRs compared to controls showing that Pten mutant CRs not only express more but also secrete more Reelin which diffuse in cortex and in hippocampus. This increase in Reelin secretion did not have any impact on the general cortical organization of the *Pten* mutant brain since they presented with similar thickness of the cortical layers in the S1 barrel field at P24 stage (**Fig 4B**).

Reelin has been shown to activate mTOR pathway in surrounded cells though binding to its receptor, phosphorylation of dab and the activation of PIK3/AKT/mTOR/S6 kinase to regulate dendritic growth of targeted cells (Jossin and Goffinet 2007). Since there was more secreted Reelin in *Pten* mutant brains, we used pS6 staining to monitor the S6kinase activity downstream of mTOR. Brains from *Pten* mutants clearly present with a large increase of pS6

staining in the cortex and the hippocampus compared to control (**Fig. 4A**). Therefore, the increased number of CRs together with the increase of Reelin secretion is responsible for a non-cell autonomous activation of the mTOR pathway in surrounded cells from cortex and hippocampus.

Overall post-natal activation of mTOR in cortex and hippocampus does not induce epilepsy in Pten or PIK3CA CR specific mutants.

Somatic mutations in the PIK3/AKT/mTOR pathway leading to its activation in pyramidal neurons are responsible for various brain malformations and epilepsy depending on the mutation occurrence during brain development (Jansen et al. 2015). In our model with the deltaNp73-Cre driven inactivation, the non-cell autonomous pathway activation due to more secreted reelin was relatively late in the brain development and no massive brain alterations are observed. However, it was still possible that this wide activation leads to an increased sensitivity of the neuronal circuit to epilepsy. To test this hypothesis, we first investigated at adult stages (P75) whether the deletion of PTEN altered neuronal network activity patterns in S1 cortex, a region where the CR densities above and the secreted Reelin were largely increased in the *Pten* model. For this aim, we recorded population activity spontaneously generated in pro-bursting ACSF (Mg^{2+}-free with 6 mM KCl (0Mg6K ACSF) in S1 cortical slices from control and Pten mutant mice by using the multi-electrode array (MEA) technique (**Fig. 4D).** We found that S1 slices from both control and mutant mice mostly display bursting activity (n = 12 out of 14 control slices (85.7%) and n = 13 out of 15 mutant slices (87 %); **Fig. 4E-F**), while only a minority of the slices develops seizures (n = 2 slices for both genotypes) in 0Mg6K ACSF (Sup Table 7). In addition, bursts recorded in control and mutant mice displayed similar frequency and duration (**Fig 4G**) (Sup Table7). These results thus indicate that Pten deletion in CR cells does not affect neuronal network activity in S1 cortex.

We, then used an in-vivo approach to induce seizures by injecting kainate in adult mice and test the sensitivity to the epileptogenic drug. General behavioral characterization of the Pten mutants animals did not display any clinical manifestations using SHIRPA protocol (Rogers et al. 2001) up to 80 days old when they started to manifest cutaneous alterations

(see behavioral section in the material and methods part). More specific tests such as the open-field and the Y maze were also performed to monitor locomotor activity and anxiety or working memory, respectively (**Fig S4 A, B and C**)(Sup Table 8). In agreement with previous phenotypic characterization of Reelin-overexpressing mice, no significant difference was found whatever gender and genotype in all tests (Teixeira et al. 2011). Finally, we injected half of the previously analyzed mice with kainate (15 mg/kg IP) and monitor for 120 minutes the latency, occurrence, and duration of the crisis (**Fig S4 D**). Since the Pten model presents overall with larger variability in several readouts, we also used the P110* one to activate the AKT/mTOR pathway and compared the two approaches for their sensitivity to kainate injection. No significant differences were observed in Pten model (Sup Table 8). However, we noticed a gender difference between the two approaches since the P100* and control littermate females were more sensitive than males whatever genotype (**Fig S4 D bottom left histogram pink and grey**). Although all animals from the p110* and control cohort presented with the same occurrence number of crisis (**Fig S4 D bottom right histogram pink and grey**), the P110* females have longer duration in crises compared to their littermate (**Fig S4 D bottom middle histogram pink and grey**), suggesting they were freeze, immobile during the few occurring crisis (Sup Table 8).

Altogether, the increased number of CRs following the activation of the PI3K/AKT/mTOR pathway did not alter the behavior nor increase the brain sensitivity to epilepsy.

Discussion

The PI3K/AKT/mTOR pathway is one of the major cell survivals signaling cascades involved in the regulation of mitochondria-mediated apoptosis and has been shown amongst others to control interneuron cell death (Wong et al. 2018). Here we focused our study on a particular type of excitatory neuron, the CRs which populate the surface of the cortex during embryogenesis and die postnatally after orchestrating cortical development. We previously showed that Bax-mediated apoptosis and neuronal activity are involved in their death (Ledonne et al. 2016; Riva et al. 2019). By investigating the PI3K/AKT/mTOR activity around postnatal stages, just before massive cell death occurs in deltaNp73 derived CRs, we found that it is decreased suggesting its participation in the control of CRs cell death as well (Fig 1E). Beside this temporal regulation of its activity, we also highlighted a differential spatial activation of PDK1 and S6K along the medio-lateral axes in 3 rostro-caudal levels. Overall, AKT and mTOR activities are higher in the medial/dorsal and lateral cortex respectively at E17.5 and P1 suggesting they are differentially regulated in the marginal zone above the future cortical areas (Fig. S1). We then sustained in vivo the activation of the pathway in these cells using mouse genetics and found that a fraction of them survived at P24 (Fig 2) in the cortex up to 110 days (data not shown) whereas they should be almost eliminated by days 15. By conditionally targeting Pten and Tsc1 in deltaNp73 derived CRs, we found that AKT activation contributes most to the survival CRs phenotype compared to mTOR (Fig. 2A). In addition, the CRs increase in the Pten model was higher in the lateral cortex than in the medio-dorsal (Fig. 2G), which correlates with the lower AKT pathway activation described at E17.5 and P1 stages (Fig S1). Altogether, the PI3K/AKT pathway is more inhibited in the lateral cortex compared to medio-lateral which may confer to the lateral CRs more sensibility to cell death. The various timing of CR elimination along the medio-lateral axe may influence the development of future brain areas as well. Since the secondary somatosensory auditory cortex presents with a 10-fold increase in CR at P24 in the Pten model (Fig 2G), it would be interesting in the future to challenge the animal behavioral response to various tests involving auditory stimulation (ie: pre-pulse inhibition or fear conditioning test).

During this study, we had also the opportunity to test and compare two models of activation through either the expression of an activated PI3KCA mutant protein (p110*) or the deletion of PTEN. Both approaches should increase the PIP3 levels to activate AKT through PDK1 and one would have expected a phenocopy between the 2 mutants and even a stronger phenotype for the P110* which has been shown to strongly activate AKT (Venot et al. 2018). Although the number of persistent CRs is similar between the two mutants (Fig 2A and 2C), the Pten one clearly presents with a large increase in dendrite and/or axonal extensions which is rarely seen in the p110* model. One hypothesis would be the compensation of PIP3 overproduction in P110* mutant CR by endogenous PTEN, but one would expect to also have such compensation effect for cell survival and fewer CRs in P110* compared to Pten. Alternatively, PTEN may have also PIP3 independent functions (Bermúdez Brito 2015). Axodendritic outgrowth requires some reorganization of the actin/microtubule cytoskeleton and, besides the known regulation of F-actin dynamics by phosphoinositides through Rho GTPases, PTEN regulates directly the stability of the microtubules through their detyrosination (Kath et al. 2018). Apart from these morphological differences in CR projections, both mutants CRs present with an increase in the soma size together with an increase in pS6 staining. These two phenotypes are also observed in the Tsc1 mutant CRs (Fig2A) and are linked to the mTORC1 activation and the increase in protein synthesis (Bockaert and Marin 2015).

Surprisingly, whereas loss of Tsc1 in the cortex has been shown to increase the basal dendrite arborization of pyramidal neurons, a phenotype reversible upon rapamycin treatment during a critical period (Cox et al. 2018), only bipolar CRs were observed in Tsc1 cKO (Fig2A). This suggests that activation of the mTORC1 pathway alone is not sufficient in CRs to alter the neuronal polarity and/or the axodendritic outgrowth but it is probably necessary since these morphological changes required an increase in protein synthesis (Jaworski 2005).

Altogether, these results strongly suggest PTEN regulates the growth of CRs extensions by both AKT-dependent and independent pathways.

Our results together with the well-known effects of AKT activation on cell survival (Brunet, Datta, and Greenberg 2001) strongly suggest that apoptosis is inhibited in our Pten

model, which leads to an increase of CRs densities in the postnatal cortex. In theory, PTEN and Bax inactivation should have similar secondary phenotypes linked to CR persistence. They have similar increases in cell densities, about 5 times. However, the Bax model presents with an increase of dendrites and dendritic spine in upper pyramidal neurons which lead to an alteration of the Excitatory to Inhibitory balance and hyperexcitability together with an increase in sensitivity to kainate induced epilepsy. Although we did not investigate the morphological changes of these pyramidal cells in the Pten model, neuronal network activity is unaffected in the S1 barrel cortex and Pten animals do not present sensitivity to epilepsy. The mechanism by which rescued CRs in bax model induces morphological and functional changes in pyramidal neurons remains unresolved. Reelin has been shown to counteract the inhibitory effects of CSPG on dendritic growth in the MZ by activating the AKT pathway in pyramidal neurons (Zluhan et al. 2020).

Therefore, one hypothesis to explain the discrepancies between Bax and Pten models would be the different levels of Reelin secretion. However, we found in our study that the Reelin secretion is increased in the Pten model together with an increase of pS6 staining in the cortex, suggesting the PI3K/AKT/mTOR pathway is activated in pyramidal cells after reelin binding to its receptor. Thus, this hypothesis is unlikely but we need to compare it with Reelin secretion in the Bax model to conclude. Alternatively, Pten inactivation also leads to morphological changes in CRs which are not observed in the Bax model. These changes alter the intrinsic properties of CRs which also respond with larger depolarization to the current application (Garcia-Junco-Clemente and Golshani 2014). Differences in the intrinsic properties and in neuronal activity may explain the different outcomes between the Bax and Pten models similar to the Kir2.1 model in which induced hyperpolarization of CRs increased the CR densities without altering the morphology nor the excitability of underneath pyramidals neurons (Riva et al. 2019).

Finally, the large increase in pS6 staining, a biomarker of mTOR activity seen in the cortex (Fig 4A) is not associated with any change in neuronal network activity (Fig 4D-G) nor sensitivity to kainate-induced epilepsy, a result that contrasts with the abundant literature on focal cortical dysplasia (FCD) associated with mTOR pathway activation (Meng et al. 2013). One current hypothesis for this discrepancy would be the extent of the mTOR

activation in the cortex. Overall activation of the pathway in many cells during neuronal network maturation would lead to compensation and an adaption to the hyperexcitability.

In conclusion, we have identified the PIK3/AKT pathway as a key player in the survival of deltaNp73 derived CRs, which is downregulated soon after birth priming these cells to death after exposition to other stressors (ie.: excitotoxicity, ROS production, DNA damages). Future investigations will determine whether other sources of CRs share the same protective pathway as deltaNp73 derived CRs and which neuronal growth factors control the pathway.

Material and Methods

Animals

deltaANp73^{CreIRESGFP}(deltaNp73^{Cre})(Tissir et al., 2009)*, Ai9 line (Strain#* 007905) *ROSA26$^{loxP\text{-}stop\text{-}loxP\text{-}Tomato}$(R26^{mT})* (Madisen et al., 2010) transgenic mice were kept in a C57BL/6J background. *R26StopFlp110**mice (Strain# 012343) was a gift from Dr. Guillaume Canaud (University Paris Cité). *Pten^{loxP}* mice (Suzuki et al., 2001) and *TSC1^{loxP}* mice (Kwiatkowski, 2002a) were provided by Dr. Mario Pende (University Paris Cité*).* Animals were genotyped by PCR using specific primers (Table in Sup material and methods).

Histology		Behavior	
Control	Mutant	Control	Mutant
deltaNp73$^{Cre/+}$> R26$^{mT/+}$	*deltaNp73$^{Cre/+}$*> R26$^{mT/+}$;Pten$^{lox/lox}$	*deltaNp73$^{+/+}$*> Pten$^{lox/lox}$ *deltaNp73$^{Cre/+}$*> R26$^{mT/+}$	*deltaNp73$^{Cre/+}$*> Pten$^{lox/lox}$
deltaNp73$^{Cre/+}$> R26$^{mT/+}$	*deltaNp73$^{Cre/+}$*> R26$^{mT/+}$;Tsc1$^{-/lox}$	-	-
deltaNp73$^{Cre/+}$> R26$^{mT/+}$	*deltaNp73$^{Cre/+}$*> R26p110*$^{lox/mT}$	*deltaNp73$^{Cre/+}$*>R26$^{+/+}$ *deltaNp73$^{+/+}$*>R26p110*$^{lox/+}$ *deltaNp73$^{+/+}$*> R26$^{+/+}$	*deltaNp73$^{Cre/+}$*>R26 p110*$^{lox/+}$

Patch-cell recording		Multi-electrode array	
Control	Mutant	Control	Mutant
deltaNp73$^{Cre/+}$> R26$^{mT/+}$	*deltaNp73*$^{Cre/+}$> R26$^{mT/+}$;Pten$^{lox/lox}$	*deltaNp73*$^{+/+}$> Pten$^{lox/lox}$ *deltaNp73*$^{Cre/+}$> R26$^{mT/+}$	*deltaNp73*$^{Cre/+}$> Pten$^{lox/lox}$

All animals were handled in strict accordance with good animal practice as defined by the national animal welfare bodies, and all animal experiments were approved by the Veterinary Services of Paris (authorization number: C75-14-03) and by the Animal Experimentation Ethical Committee (CEEA #034) (reference: 20-074).

Tissue preparation and immunohistochemistry

Staging of animals was done, considering midday of vaginal plug as embryonic day 0.5 (E0.5) for the embryonic stage and the birth date as postnatal day 0 (P0) in the postnatal stage. Brain collection and fixation of both embryos and P1 animals were performed as previously described (Bielle et al., 2005b). For juvenile mice (P24 days after birth) brain sections, animals were anesthetized by intraperitoneal administration of a mixture of sedative (Xylazine 10mg/kg) and anesthetic (Ketamine 180mg/kg) substances and were intracardially perfused by 4% paraformaldehyde (PFA) in PBS 1X (v/w), pH 7.4 and post-fixed 2h in 4% PFA at 4°C. Brains were rinsed in PBS for 1 h and placed in 30% sucrose in PBS 1X (v/w) overnight for cryoprotection, then embedded in O.C.T. compound (Sakura). Embedded tissues were sectioned on a cryostat with a 20 µm thickness for embryonic and P1 stage and 50 µm for P24 brains. Three sections from rostral, intermediate, and caudal brain levels were chosen from controls and mutants. Immunostaining on embryonic and P1 sections was performed as previously described (Bielle et al., 2005b). P24 brain sections were washed first in PBS 1X and then in 0.2% triton+ PBS1X before immunostaining. After sections were permeabilized

in PGT (PBS1X 0.25% triton 0.2% Gelatin) for 1h and then incubated with primary antibodies diluted in PGT at 4°C for overnight. The second day, after washing sections were incubated first in PGT for 10 min and then were incubated in a secondary antibody diluted in PGT at room temperature for 1 hour. Double immunostaining of two rabbit antibodies was done using Zenon kit (Zenon Alexa Fluor 488 Rabbit IgG Labeling Kit, Z25302, Invitrogen by Thermo Fisher Scientific). Primary antibodies used for immunohistochemistry were: goat anti-reelin antibody (R and D Systems AF3820, 1:500), rabbit anti-phospho-AKT Serine 473 antibody (Cell signaling Technology 4060, 1:200), rabbit anti-phospho-S6 antibody (Ser 240/244 Cell signaling Technology 5364, 1:1000), rat anti-ctip2 antibody (Abcam ab18465, 1:250), rabbit anti-cux1,2 antibody (Santa Cruz sc-13024, 1:250). Secondary antibodies used against primary antibodies were: donkey anti-rabbit Alexa-488 (711-545-152, Jackson ImmunoResearch Laboratories,1:500), donkey anti-goat Alexa-488 (A-11055, Molecular Probes, 1:500), donkey anti-goat Cy5 (705-175-147, Jackson ImmunoResearch Laboratories, 1:250), donkey anti-rat Alexa-Cy5 (712-175-153, Jackson ImmunoResearch Laboratories, 1:250). DAPI (D1306, ThermoFisher Scientific, 1:1000) was used for nuclear staining. Sections were mounted using Vectashield (H-1000, Vector Labs).

Image acquisition and analysis

Immunofluorescence images were acquired using a confocal Leica SP8 microscope (Leica Microsystems, Mannheim, Germany), except for quantification of CRs at P24 that immunofluorescence images were acquired using a slide scanner Nanozoomer 2.0 (Hamamatsu) with a 20x objective.

At embryonic and P1 stages images were acquired using a 40X oil immersion objective, pinhole size “airy 2” and in order to acquire 20 µm thickness of section 4 z-stacks of 5 µm was defined.

illustrated Images with bigger magnification in the Figure 2 and S2 were acquired with a 40X and 3 digital zoom and 9 to 10 z-stacks of 2 to µm was defined.

illustrated Images including Biocytin filled CRs in the Figure 3 were acquired using a 63X oil immersion objective. 20 to 60 z-stacks of 2 µm was defined depending of the thickness of sections and size of the neurons.

tdTOMATO+ neurons, were counted and analyzed for their position using the ImageJ software. Three sections from each biological replicate at embryonic, P1 and P24 stages were analyzed corresponding to three different brain levels.

At embryonic and P1 stages 500 µm in the length (Medial to lateral cortex) and 100 µm depth from the surface of cortex was straightening and the X and Y position of each cell were recorded. At P24 sections were stained for CUX1/2, CTIPI2 to be able to define the brain areas. Then 150 µm depths from the surface of cortex was straightened and position of cells were recorded.

For each section, the density of CRs (tdTOMATO + CRs/mm3) was calculated taking into account the thickness of the section and the length of the neocortex and areas at p24 and the depth from the surface of the cortex.

Neuronal soma size measurement

To extract the cell volume, we consider the entire z-stack to extract Regions of Interests (ROIs) using the machine learning-based WEKA tool implemented on Fiji/ImageJ2 (Arganda-Carreras et al., 2017). Beforehand, we trained a WEKA classifier on fluorescent series of Td-tomato-loaded cells set with the following features: Gaussian blur, Derivatives, Structure, Minimum, Maximum and Median. Classification was performed using the FastRandom Forest algorithm. Upon extraction of 3D ROIs, we recorded the volume using the 3D ROI manager tool developed by Ollion and colleagues (Ollion et al., 2013).

Patch-Cell recording

Slice preparation: Coronal slices were prepared from *Pten* transgenic animals between P20 and P24. At these ages, animals were anaesthetized with ketamine (100 mg/kg), xylazine (7 mg/kg) and isoflurane, and perfused transcardially with a sucrose-based cutting solution containing the following (in mM): Sucrose 110, KCl 2.5, NaH2PO4 1.25, NaHCO3 30, HEPES 20, glucose 25, thiourea 2, Na-ascorbate 5, Na-Pyruvate 3, CaCl2 0.5, MgCl2 10. Coronal slices were prepared from control animals at P10, as CR cells were non-viable for electrophysiological recording after this age. At P10, animals did not undergo cardiac

perfusion. For both *PTEN* and controls, brains were rapidly removed and placed upright cut into 300 µm thick coronal slices (Leica Biosystems Vibratomes, VT1200S, Germany) in the cutting solution at 4 °C. Slices were transferred to an immersed-type chamber and maintained in artificial cerebral spinal fluid (ACSF) containing the following (in mM): NaCl 125, KCl 2.5, NaH2PO4 1.25, NaHCO3 26, glucose 10, Na-pyruvate 2, CaCl2 2, MgCl2 1. Slices were incubated at 32 °C for approximately 10 minutes then maintained at room temperature for at least 45 minutes. Prior to recording, slices were transferred to a recording chamber perfused with ACSF at 3 ml/min at 30 °C.

Electrophysiological recordings: CR cells were located using the fluorescence tdTomato tag with a 535 nm LED and long-pass mCherry filter set in an Olympus BX51 microscope (Olympus Corporation, Japanese). A recording pipette with resistance between 2-5 MΩ with positive pressure was inserted into the layer I of the Barrel cortex. Whole-cell recordings were performed with intracellular solutions containing the following (in mM): K-methyl sulfonate 135, KCl 5, EGTA-KOH 0.1, HEPES 10, NaCl 2, MgATP 5, Na2GTP 0.4, Na2-phosphocreatine 10 and biocytin (4 mg/mL). Series resistance was < 20 MΩ and was monitored throughout the recordings. Data was discarded if the series resistance changed more than 10% during the experiment. The bridge balance was measured every 20 seconds and compensated with internal circuitry and monitored throughout experiments. The liquid junction potential was not corrected. Data were obtained using a Multiclamp 700B amplifier and digitized using a Digidata 1440 ADDA board. Data were sampled at 10 kHz. Axon™ pCLAMP® 9 electrophysiology data acquisition & analysis software (Molecular Devices, USA) was used for data acquisition. Action potential firing properties were measured with a series of 1-second-long depolarizing current steps.

Immunochemistry and cell identification: Post-hoc confirmation of all cells was performed by labelling intracellular biocytin. Following overnight incubation in 4% paraformaldehyde in PBS, slices were permeabilized with 0.2 % triton in PBS and blocked for 48 hours with 3% goat serum (50062Z, by Thermo Fisher Scientific) in PBS with 0.2 % triton. Streptavidin, Alexa Fluor™ 546 conjugate (S11225, by Thermo Fisher Scientific,1:300) incubation was carried out in block solution for 4 hours at room temperature. Slices were mounted in ProLong™ Diamond Antifade Mountant (P36970, Invitrogen by Thermo Fisher

Scientific), resulting in a partial clarification of tissue following incubation at room temperature for 24 hrs. Images were acquired.

Data analysis: Electrophysiological recordings were analyzed using custom-written macros with IGORpro (WaveMetrics Inc, USA) and Axograph software (Axograph Inc, USA). Action potentials (APs) were detected automatically by threshold crossing with Axograph (Axograph Inc, USA) followed by visual inspection. R_M measurements were calculated from linear fits of the voltage responses to current step injections of 10 pA. Action potential firing properties were measured on a positive current step series starting at 20 pA with increasing 10 pA current steps. The threshold was measured at the first AP at rheobase. The AP full-width at half-maximal amplitude (AP width) and after-hyperpolarizing potential (AHP) amplitude were measured for the first AP at threshold. The latency of the first AP and number of APs was measured with increasing current steps over rheobase. The instantaneous firing frequency and amplitude of the first 5 APs were measured at current injection steps 1.5 times over rheobase. Sag potentials were measured with a protocol injecting current as necessary to maintain a VM of -70 mV with a 1-second-long negative current step resulting in a membrane hyperpolarization of -100 mV. The sag was calculated as the difference between the peak and steady-state voltage during the 1 second hyperpolarization.

Multi-electrode array (MEA) recordings

All experiments were performed on adult (P75) mice. Mice were sacrificed and the brain removed. Coronal slices (400 µm) of S1 cortex were cut at low speed (0.04 mm/s) and at a vibration frequency of 70 Hz in ice cold oxygenated artificial cerebrospinal fluid (ACSF) supplemented with sucrose (in mM: 87 NaCl, 2.5 KCl, 2.5 $CaCl_2$, 7 $MgCl_2$, 1 NaH_2PO_4, 25 $NaHCO_3$ and 10 glucose, saturated with 95% O_2 and 5% CO_2). Slices were maintained at 32°C in a storage chamber containing standard ACSF (in mM: 119 NaCl, 2.5 KCl, 2.5 $CaCl_2$, 1.3 $MgSO_4$, 1 NaH_2PO_4, 26.2 $NaHCO_3$ and 11 glucose, saturated with 95% O_2 and 5% CO_2) for 20 min, and then stored for at least one hour before recording in a pro-epileptic (0 mM Mg^{2+}, 6 mM K^+; 0Mg6K) ACSF. S1 cortical slices were transferred on planar MEA petri dishes (200-30 ITO electrodes organized in a 12x12 matrix, with internal reference, 30 µm diameter and 200 µm inter-electrode distance; Multichannel Systems, Germany), and kept in place using

a small platinum anchor. The slices were continuously perfused at a rate of 2 ml/min with 0Mg6K ACSF during recordings. Image of S1 cortical slices on MEAs were acquired with a video microscope table (MEA-VMT1; Multichannel Systems, Germany) through MEA Monitor software (Multichannel Systems, Germany) to identify the location of the electrodes on the cortex and to select electrodes of interest. Data were sampled at 10 kHz and network activity was recorded at 32°C by MEA2100-120 system (bandwidth 1-3000 Hz, gain 5x, Multichannel Systems, Germany) through the MC Rack 4.5.1 software (Multichannel Systems, Germany).

Multi-electrode (MEA) data analysis: Bursting raw data were analyzed with MC Rack (Multichannel Systems, Germany). Detection of bursts was performed using the "Spike Sorter" algorithm, which sets a threshold based on multiples of standard deviation of the noise (5-fold) calculated over the first 500 ms of recording free of electrical activity. A 5-fold standard deviation threshold was used to automatically detect each event, which could be modified in real-time by the operator on visual check if needed. Bursts were arbitrarily defined as discharges shorter than 5 s in duration. Typically, bursts were characterized by fast voltage oscillations followed by slow oscillations or negative shifts. To analyze seizure activity, data were exported to Neuroexplorer (Nex Technologies, USA). Paroxysmal events were identified as discharges lasting more than 5 s; successive paroxysmal discharges were considered separate events based on their waveform and on the presence of a minimum (>10 s) interval of silent or bursting activity between them (Boido et al., 2010).

Behavior

Three independent cohorts were generated to produce a total of 15 to 20 mice per genotype (control and *Pten* model) and per sex (males and females). Due to deltaNp73 expression in the epidermal and hair follicle stem cells (Beeler et al., 2019), Pten models start to develop skin accumulation under paws and curly fur after 12 weeks that preclude later investigations for ethical considerations. Each cohort was submitted successively to an adapted SHIRPA test to evaluate clinically each animal at 8 weeks old, followed by the rearing activity (at 9 weeks-old) the open field (at 10 weeks-old) and the Y-Maze tests (at 11 weeks-old) according to the International Mouse Phenotyping Resource of Standardised Screens (IMPReSS) recommendations (https://www.mousephenotype.org/impress/index). Finally, 12 weeks-old mice were processed for kainate injection to test the sensitivity to epilepsy before euthanasia.

Horizontal activity: Spontaneous horizontal locomotor activity was assessed using the open field test (OFT). To do so, unacclimated mice were moved to the monitor area and immediately placed individually in the center of motor activity boxes (40 cm L, 40 cm W, 40 cm H) placed on an infrared floor under ~50 lux of light measured in the center of the arena, for a 120-min period. Total distance traveled by animal (horizontal activity), and time spent in the center (25 cm X 25 cm) of the arena were recorded by an infrared camera system connected to the Videotrack v2.6 Automated Behavioural Analysis (ViewPoint, France). The results are indicated as distance traveled in centimeters.

Vertical activity: Spontaneous locomotor activity was also evaluated with an infrared beam system fitted to rectangular cages (50cmx25cm) (ActiMot, TSE Systems GmbH, Germany version V5.1.9). Movement of the mice resulted in interruption of the infrared beams. Each interruption was automatically counted and the coordinates of the animal can be determined in three dimensions (X-Y-Z axis). Each unacclimated animal was placed in the center of the cage and the number of beam breaks recorded during a 1-h period. We examined and analyzed the vertical (Z beam breaks) and horizontal (X+Y beam breaks) activities directly from the data collected by the system software.

Y-maze: Short-term memory was assessed by spontaneous alternation behavior in the Y-maze task. Experiments were carried out in a standard Y-maze apparatus made of three

identical black plastic arms (60 cm arms; walls 10 cm) set at 120° angles from each other. Different visual cues (geometrical forms) were placed on the wall of 2 arms of the maze and were kept constant during the experiments. Mice were placed at the end of one arm of the Y-maze and the sequence of arm entries were recorded during 10 min. The introduction arm was randomly assigned for each animal. An arm visit was recorded when a rat moved all 4 paws into the arm. An alternation was defined as consecutive entries into all three arms (e.g. A,B,C or A,C,B) and was automatically recorded using Videotrack v2.6 Automated Behavioural Analysis (ViewPoint, France). The number of maximum alternations was the total number of arm entries minus two and the percentage of alternations was calculated as the ratio of actual to maximum alternations multiplied by 100: (actual alternations/maximum alternations) 9 100. Persevering behavior was defined as subjects making significantly fewer alternations than would be expected by chance (50%).

Kainate injection and sensitivity to epilepsy

Animals at 12 weeks old were injected with a single intraperitoneal dose of Kainate (#0222/10, 10mg Biotechne) at 15mg/kg and recorded for 2 h by a Videotrack v2.6 Automated Behavioural Analysis (ViewPoint, Lyon, France) software. The latency, duration, and the number of crises were recorded by a user blind to the animals.

Statistics:

Histological analysis: All data were expressed as mean±SD. According to the data structure, experiments involving two groups were assessed by using a two-tailed unpaired Student T test or Mann-Whitney U Test. Statistical significance of more than two groups and treatments were tested by one-way or two-way ANOVA tests followed by Sidak multiple comparisons as post-hoc test. Density curves were compared using the non-parametric Kolmogorov-Smirnov test. Statistics were performed using GraphPad Prism 8.00 (GraphPad Software Inc., USA) and plotting was performed using GraphPad Prism 9.00 and R program (R program version 4.0.3, Austria).

Patch-Cell and MEA recordings: Results are reported as mean ±SEM. Statistical significance of linear variables was assessed using paired or unpaired Student's T test,

repeated-measures ANOVA where appropriate. Normality was tested with the Jarque-Bera test.

In all cases: $P<0.05$ was considered significant. $*p < 0.05$, $**p < 0.01$, $***p < 0.001$

References

Arganda-Carreras, Ignacio, Verena Kaynig, Curtis Rueden, Kevin W. Eliceiri, Johannes Schindelin, Albert Cardona, and H. Sebastian Seung. 2017. "Trainable Weka Segmentation: A Machine Learning Tool for Microscopy Pixel Classification" edited by R. Murphy. *Bioinformatics* 33(15):2424–26. doi: 10.1093/bioinformatics/btx180.

Beeler, J. Scott, Clayton B. Marshall, Paula I. Gonzalez-Ericsson, Timothy M. Shaver, Gabriela L. Santos Guasch, Spencer T. Lea, Kimberly N. Johnson, Hailing Jin, Bryan J. Venters, Melinda E. Sanders, and Jennifer A. Pietenpol. 2019. "P73 Regulates Epidermal Wound Healing and Induced Keratinocyte Programming" edited by R. Mantovani. *PLOS ONE* 14(6):e0218458. doi: 10.1371/journal.pone.0218458.

Bermúdez Brito, Miriam. 2015. "Focus on PTEN Regulation." *Frontiers in Oncology* 5. doi: 10.3389/fonc.2015.00166.

Bielle, Franck, Amélie Griveau, Nicolas Narboux-Nême, Sébastien Vigneau, Markus Sigrist, Silvia Arber, Marion Wassef, and Alessandra Pierani. 2005. "Multiple Origins of Cajal-Retzius Cells at the Borders of the Developing Pallium." *Nature Neuroscience* 8(8):1002–12. doi: 10.1038/nn1511.

Blanquie, Oriane, Lutz Liebmann, Christian A. Hübner, Heiko J. Luhmann, and Anne Sinning. 2016. "NKCC1-Mediated GABAergic Signaling Promotes Postnatal Cell Death in Neocortical Cajal–Retzius Cells." *Cerebral Cortex* bhw004. doi: 10.1093/cercor/bhw004.

Bockaert, Joël, and Philippe Marin. 2015. "MTOR in Brain Physiology and Pathologies." *Physiological Reviews* 95(4):1157–87. doi: 10.1152/physrev.00038.2014.

Boido, D., P. Farisello, F. Cesca, E. Ferrea, F. Valtorta, F. Benfenati, and P. Baldelli. 2010. "Cortico-Hippocampal Hyperexcitability in Synapsin I/II/III Knockout Mice: Age-Dependency and Response to the Antiepileptic Drug Levetiracetam." *Neuroscience* 171(1):268–83. doi: 10.1016/j.neuroscience.2010.08.046.

Causeret, Frédéric, Eva Coppola, and Alessandra Pierani. 2018. "Cortical Developmental Death: Selected to Survive or Fated to Die." *Current Opinion in Neurobiology* 53:35–42. doi: 10.1016/j.conb.2018.04.022.

Causeret, Frédéric, Matthieu X. Moreau, Alessandra Pierani, and Oriane Blanquie. 2021. "The Multiple Facets of Cajal-Retzius Neurons." *Development* 148(11):dev199409. doi: 10.1242/dev.199409.

D'Gama, Alissa M., Mollie B. Woodworth, Amer A. Hossain, Sara Bizzotto, Nicole E. Hatem, Christopher M. LaCoursiere, Imad Najm, Zhong Ying, Edward Yang, A. James Barkovich, David J. Kwiatkowski, Harry V. Vinters, Joseph R. Madsen, Gary W. Mathern, Ingmar Blümcke, Annapurna Poduri, and Christopher A. Walsh. 2017. "Somatic Mutations Activating the MTOR Pathway in Dorsal Telencephalic Progenitors Cause a Continuum of Cortical Dysplasias." *Cell Reports* 21(13):3754–66. doi: 10.1016/j.celrep.2017.11.106.

Fulda, Simone. 2012. “Shifting the Balance of Mitochondrial Apoptosis: Therapeutic Perspectives.” *Frontiers in Oncology* 2:121. doi: 10.3389/fonc.2012.00121.

Garcia-Junco-Clemente, Pablo, and Peyman Golshani. 2014. “PTEN: A Master Regulator of Neuronal Structure, Function, and Plasticity.” *Communicative & Integrative Biology* 7(2):e28358. doi: 10.4161/cib.28358.

Griveau, Amélie, Ugo Borello, Frédéric Causeret, Fadel Tissir, Nicole Boggetto, Sonia Karaz, and Alessandra Pierani. 2010. “A Novel Role for Dbx1-Derived Cajal-Retzius Cells in Early Regionalization of the Cerebral Cortical Neuroepithelium.” *PLoS Biology* 8(7):e1000440. doi: 10.1371/journal.pbio.1000440.

Groszer, Matthias, Rebecca Erickson, Deirdre D. Scripture-Adams, Ralf Lesche, Andreas Trumpp, Jerome A. Zack, Harley I. Kornblum, Xin Liu, and Hong Wu. 2001. “Negative Regulation of Neural Stem/Progenitor Cell Proliferation by the *Pten* Tumor Suppressor Gene in Vivo.” *Science* 294(5549):2186–89. doi: 10.1126/science.1065518.

Jansen, Laura A., Ghayda M. Mirzaa, Gisele E. Ishak, Brian J. O’Roak, Joseph B. Hiatt, William H. Roden, Sonya A. Gunter, Susan L. Christian, Sarah Collins, Carissa Adams, Jean-Baptiste Rivière, Judith St-Onge, Jeffrey G. Ojemann, Jay Shendure, Robert F. Hevner, and William B. Dobyns. 2015. “PI3K/AKT Pathway Mutations Cause a Spectrum of Brain Malformations from Megalencephaly to Focal Cortical Dysplasia.” *Brain* 138(6):1613–28. doi: 10.1093/brain/awv045.

Jaworski, J. 2005. “Control of Dendritic Arborization by the Phosphoinositide-3’-Kinase-Akt-Mammalian Target of Rapamycin Pathway.” *Journal of Neuroscience* 25(49):11300–312. doi: 10.1523/JNEUROSCI.2270-05.2005.

Jossin, Yves, and André M. Goffinet. 2007. “Reelin Signals through Phosphatidylinositol 3-Kinase and Akt To Control Cortical Development and through MTor To Regulate Dendritic Growth.” *Molecular and Cellular Biology* 27(20):7113–24. doi: 10.1128/MCB.00928-07.

Kazdoba, Tatiana M., C. Nicole Sunnen, Beth Crowell, Gum Hwa Lee, Anne E. Anderson, and Gabriella D’Arcangelo. 2012. “Development and Characterization of NEX-***Pten,*** a Novel Forebrain Excitatory Neuron-Specific Knockout Mouse.” *Developmental Neuroscience* 34(2–3):198–209. doi: 10.1159/000337229.

Kwiatkowski, D. J. 2002a. “A Mouse Model of TSC1 Reveals Sex-Dependent Lethality from Liver Hemangiomas, and up-Regulation of P70S6 Kinase Activity in Tsc1 Null Cells.” *Human Molecular Genetics* 11(5):525–34. doi: 10.1093/hmg/11.5.525.

Kwiatkowski, D. J. 2002b. “A Mouse Model of TSC1 Reveals Sex-Dependent Lethality from Liver Hemangiomas, and up-Regulation of P70S6 Kinase Activity in Tsc1 Null Cells.” *Human Molecular Genetics* 11(5):525–34. doi: 10.1093/hmg/11.5.525.

Kwon, Chang-Hyuk, Bryan W. Luikart, Craig M. Powell, Jing Zhou, Sharon A. Matheny, Wei Zhang, Yanjiao Li, Suzanne J. Baker, and Luis F. Parada. 2006. “Pten Regulates Neuronal Arborization and Social Interaction in Mice.” *Neuron* 50(3):377–88. doi: 10.1016/j.neuron.2006.03.023.

Kwon, Chang-Hyuk, Xiaoyan Zhu, Junyuan Zhang, Lori L. Knoop, Ruby Tharp, Richard J. Smeyne, Charles G. Eberhart, Peter C. Burger, and Suzanne J. Baker. 2001. "Pten Regulates Neuronal Soma Size: A Mouse Model of Lhermitte-Duclos Disease." *Nature Genetics* 29(4):404–11. doi: 10.1038/ng781.

Ledonne, Fanny, David Orduz, Judith Mercier, Lisa Vigier, Elisabeth A. Grove, Fadel Tissir, Maria Cecilia Angulo, Alessandra Pierani, and Eva Coppola. 2016. "Targeted Inactivation of Bax Reveals a Subtype-Specific Mechanism of Cajal-Retzius Neuron Death in the Postnatal Cerebral Cortex." *Cell Reports* 17(12):3133–41. doi: 10.1016/j.celrep.2016.11.074.

Madisen, Linda, Theresa A. Zwingman, Susan M. Sunkin, Seung Wook Oh, Hatim A. Zariwala, Hong Gu, Lydia L. Ng, Richard D. Palmiter, Michael J. Hawrylycz, Allan R. Jones, Ed S. Lein, and Hongkui Zeng. 2010. "A Robust and High-Throughput Cre Reporting and Characterization System for the Whole Mouse Brain." *Nature Neuroscience* 13(1):133–40. doi: 10.1038/nn.2467.

Meng, Xiang-Fei, Jin-Tai Yu, Jing-Hui Song, Song Chi, and Lan Tan. 2013. "Role of the MTOR Signaling Pathway in Epilepsy." *Journal of the Neurological Sciences* 332(1–2):4–15. doi: 10.1016/j.jns.2013.05.029.

Ollion, Jean, Julien Cochennec, François Loll, Christophe Escudé, and Thomas Boudier. 2013. "TANGO: A Generic Tool for High-Throughput 3D Image Analysis for Studying Nuclear Organization." *Bioinformatics* 29(14):1840–41. doi: 10.1093/bioinformatics/btt276.

Riva, Martina, Ioana Genescu, Chloé Habermacher, David Orduz, Fanny Ledonne, Filippo M. Rijli, Guillermina López-Bendito, Eva Coppola, Sonia Garel, Maria Cecilia Angulo, and Alessandra Pierani. 2019. "Activity-Dependent Death of Transient Cajal-Retzius Neurons Is Required for Functional Cortical Wiring." *ELife* 8:e50503. doi: 10.7554/eLife.50503.

Rogers, Derek C., Jo Peters, Joanne E. Martin, Simon Ball, Sharon J. Nicholson, Abi S. Witherden, Majid Hafezparast, Judy Latcham, Tracey L. Robinson, Charlotte A. Quilter, and Elizabeth M. C. Fisher. 2001. "SHIRPA, a Protocol for Behavioral Assessment: Validation for Longitudinal Study of Neurological Dysfunction in Mice." *Neuroscience Letters* 306(1–2):89–92. doi: 10.1016/S0304-3940(01)01885-7.

Srinivasan, Lakshmi, Yoshiteru Sasaki, Dinis Pedro Calado, Baochun Zhang, Ji Hye Paik, Ronald A. DePinho, Jeffrey L. Kutok, John F. Kearney, Kevin L. Otipoby, and Klaus Rajewsky. 2009. "PI3 Kinase Signals BCR-Dependent Mature B Cell Survival." *Cell* 139(3):573–86. doi: 10.1016/j.cell.2009.08.041.

Suzuki, Akira, Manae Tsukio Yamaguchi, Toshiaki Ohteki, Takehiko Sasaki, Tsuneyasu Kaisho, Yuki Kimura, Ritsuko Yoshida, Andrew Wakeham, Tetsuya Higuchi, Manabu Fukumoto, Takeshi Tsubata, Pamela S. Ohashi, Shigeo Koyasu, Josef M. Penninger, Toru Nakano, and Tak W. Mak. 2001. "T Cell-Specific Loss of Pten Leads to Defects in Central and Peripheral Tolerance." *Immunity* 14(5):523–34. doi: 10.1016/S1074-7613(01)00134-0.

Teixeira, Cátia M., Eduardo D. Martín, Ignasi Sahún, Nuria Masachs, Lluís Pujadas, André Corvelo, Carles Bosch, Daniela Rossi, Albert Martinez, Rafael Maldonado, Mara Dierssen, and Eduardo Soriano. 2011. "Overexpression of Reelin Prevents the Manifestation of Behavioral Phenotypes Related to Schizophrenia and Bipolar Disorder." *Neuropsychopharmacology* 36(12):2395–2405. doi: 10.1038/npp.2011.153.

Tissir, Fadel, Aurélia Ravni, Younès Achouri, Dieter Riethmacher, Gundela Meyer, and Andre M. Goffinet. 2009. "DeltaNp73 Regulates Neuronal Survival in Vivo." *Proceedings of the National Academy of Sciences of the United States of America* 106(39):16871–76. doi: 10.1073/pnas.0903191106.

Venot, Quitterie, Thomas Blanc, Smail Hadj Rabia, Laureline Berteloot, Sophia Ladraa, Jean-Paul Duong, Estelle Blanc, Simon C. Johnson, Clément Hoguin, Olivia Boccara, Sabine Sarnacki, Nathalie Boddaert, Stephanie Pannier, Frank Martinez, Sato Magassa, Junna Yamaguchi, Bertrand Knebelmann, Pierre Merville, Nicolas Grenier, Dominique Joly, Valérie Cormier-Daire, Caroline Michot, Christine Bole-Feysot, Arnaud Picard, Véronique Soupre, Stanislas Lyonnet, Jeremy Sadoine, Lotfi Slimani, Catherine Chaussain, Cécile Laroche-Raynaud, Laurent Guibaud, Christine Broissand, Jeanne Amiel, Christophe Legendre, Fabiola Terzi, and Guillaume Canaud. 2018. "Targeted Therapy in Patients with PIK3CA-Related Overgrowth Syndrome." *Nature* 558(7711):540–46. doi: 10.1038/s41586-018-0217-9.

Wong, Fong Kuan, Kinga Bercsenyi, Varun Sreenivasan, Adrián Portalés, Marian Fernández-Otero, and Oscar Marín. 2018. "Pyramidal Cell Regulation of Interneuron Survival Sculpts Cortical Networks." *Nature* 557(7707):668–73. doi: 10.1038/s41586-018-0139-6.

Yao, Ryoji, and Geoffrey M. Cooper. 1995. "Requirement for Phosphatidylinositol-3 Kinase in the Prevention of Apoptosis by Nerve Growth Factor." *Science* 267(5206):2003–6. doi: 10.1126/science.7701324.

Zluhan, Eric, Joshua Enck, Russell T. Matthews, and Eric C. Olson. 2020. "Reelin Counteracts Chondroitin Sulfate Proteoglycan-Mediated Cortical Dendrite Growth Inhibition." *Eneuro* 7(4):ENEURO.0168-20.2020. doi: 10.1523/ENEURO.0168-20.2020.

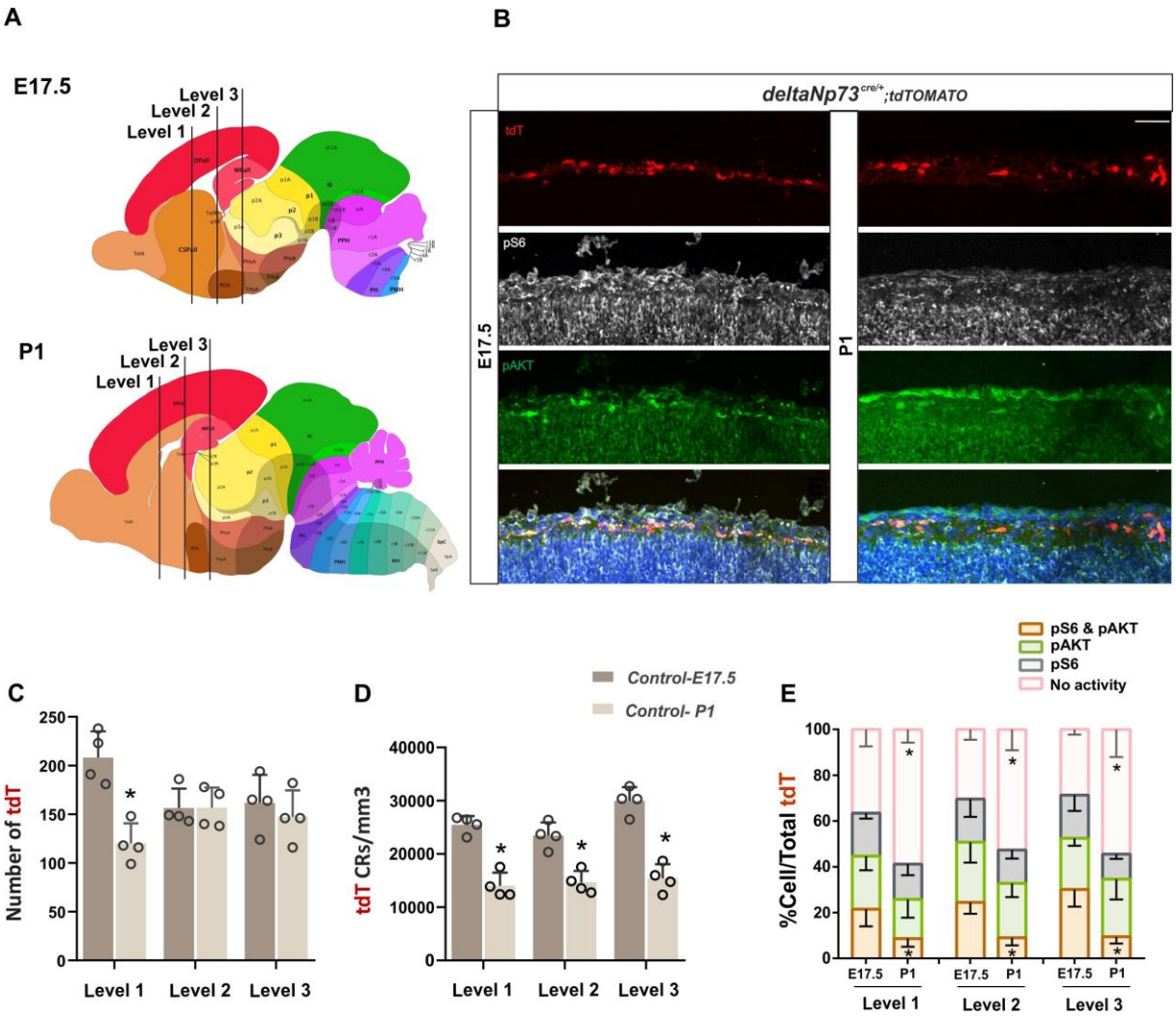

Figure 1 – Reduction of PI3K/AKT/mTOR pathway activity from P1 to E17.5 stages. (A) Sagittal representation of brains at E17.5 and P1 (adopted from Allen brain), black lines highlight three different level, which were analyzed along the Rostro-caudal axis. (B) Merged and single channel confocal images of E17.5 and P1 control brains stained for pS6 Ser 240/244 (gray), pAKT Ser 473 (green) and Dapi (blue). tdTOMATO (red) traces deltaNP73 derived CRs. (C) Number of the tdT positive cells at the neocortex levels 1, 2, and 3 (n=4 for E17.5 and P1). (D) CR density (CRs/mm3) at the neocortex levels 1, 2, and 3 (n=4 for E17.5 and P1). (E) Proportion of CRs positive for one or two marker or negative over total tdT cells (n=4 for E17.5 and P1). Mann-Whitney U test (C, D, E); Data are represented as mean ± SD; *p<0.05; **p<0.001; ***p<0.0001. Scale bars: 50 µm.

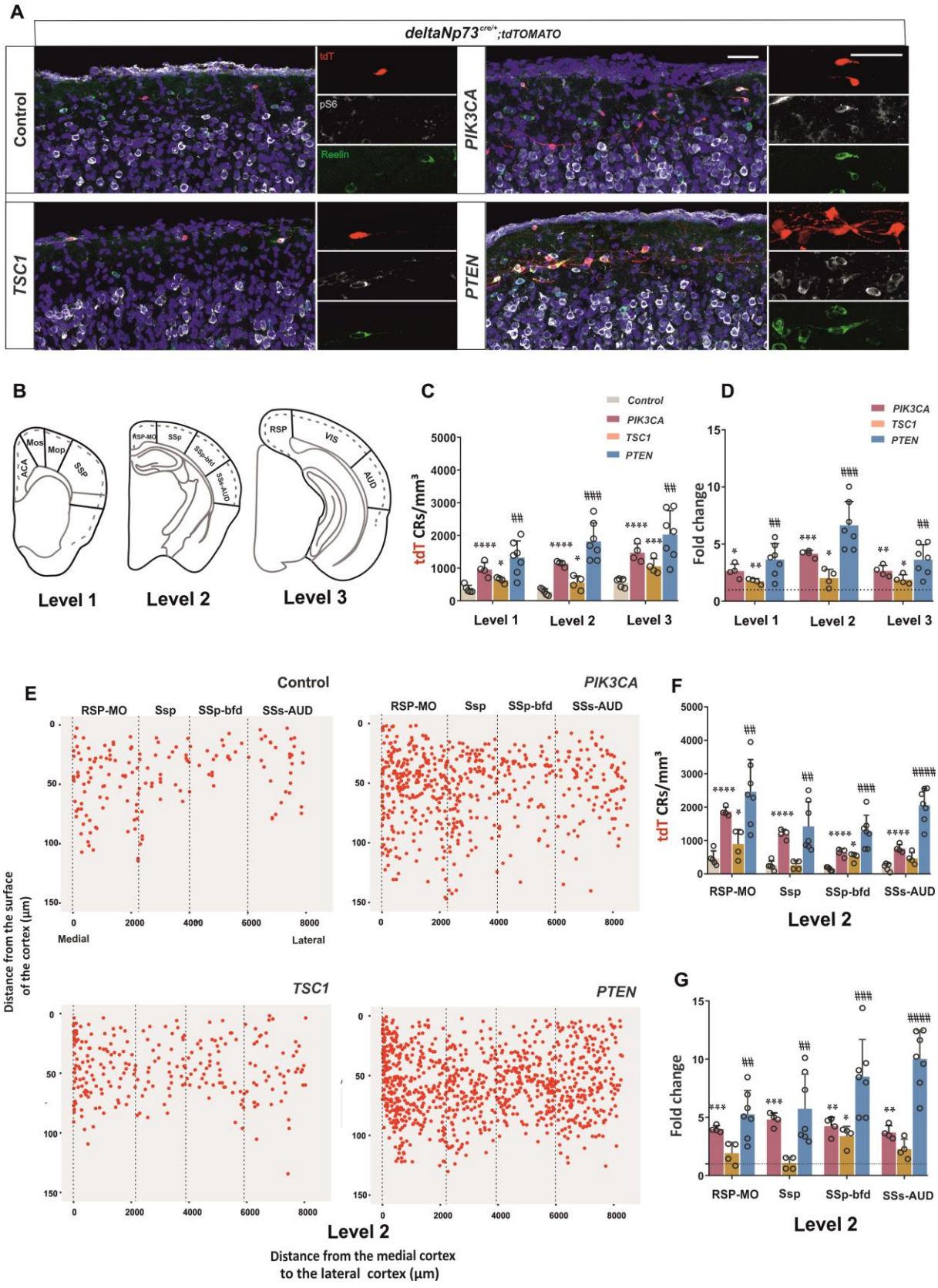
A
deltaNp73cre/+;tdTOMATO
Control
PIK3CA
TSC1
PTEN
tdT
pS6
Reelin
B
Level 1
Level 2
Level 3
C
Control
PIK3CA
TSC1
PTEN
tdT CRs/mm³
D
Fold change
E
RSP-MO
Ssp
SSp-bfd
SSs-AUD
Medial
Lateral
Distance from the surface of the cortex (µm)
Distance from the medial cortex to the lateral cortex (µm)
F
G

Figure 2 –Sustained postnatal activation of the PI3K/ AKT/ mTOR pathway leads to the persistence of CRs at later stages. (A) Merged and single channel confocal images of P24 control and mutants cortices in S1 barrel field stained for pS6 Ser 240/244 (gray), Reelin (green) and Dapi (blue). DeltaNP73 derived CRs in tdTOMATO (red). The 3 single channels images on right are zoom in from left merged images (B) Schematic representation of the analyzed Medio-lateral axes along the three rostro-caudal levels . (C) CR density (CRs/mm3) in the Rostro-caudal axis of the neocortex levels 1, 2, and 3 (n=4 for control and mutants) (D) Fold changes in CR densities in the three levels (n=4 for control and mutants) (E) scatter plot of CRs positions along the Medio-lateral axis in level 2. (F) CR density (CRs/mm3) in the medio-lateral axis of the neocortex levels 2 (G) Fold changes in CR densities in the medio axis of the neocortex levels 2. Two way Anova followed by a Sidak's multiple comparisons test for Control vs PI3K and TSC1; Multiple t-test control vs PTEN (C, F) One sample t test (D,G) . Data are represented as mean ± SD; *or # $p<0.05$; **or ## $p<0.001$; *** or ### $p<0.0001$. Scale bar 50 µm.

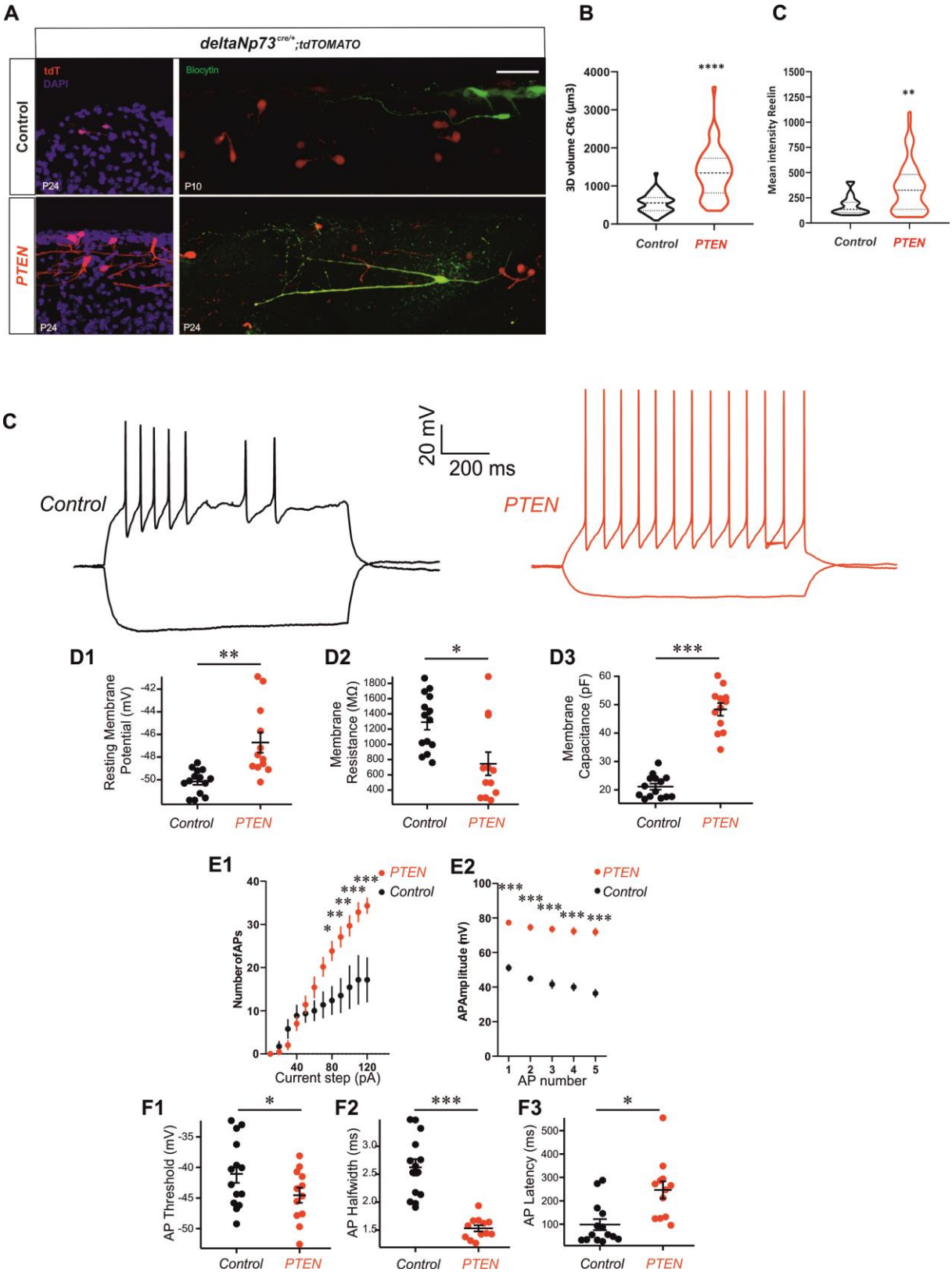
A
deltaNp73cre/+;tdTOMATO
Control
PTEN
tdT
DAPI
Biocytin
P24
P10
P24
P24
B
3D volume CRs (µm3)
****
Control
PTEN
C
Mean intensity Reelin
**
Control
PTEN
C
Control
20 mV
200 ms
PTEN
D1
Resting Membrane Potential (mV)
**
Control
PTEN
D2
Membrane Resistance (MΩ)
*
Control
PTEN
D3
Membrane Capacitance (pF)
***
Control
PTEN
E1
PTEN
Control
Number of APs
Current step (pA)
E2
PTEN
Control
APAmplitude (mV)
AP number
F1
AP Threshold (mV)
*
Control
PTEN
F2
AP Halfwidth (ms)
***
Control
PTEN
F3
AP Latency (ms)
*
Control
PTEN

Figure 3- Inactivation of PTEN in deltaNP73 derived CRs alters their morphology, their electrophysiological intrinsic properties and increases Reelin expression and AP amplitudes. (A) left: Merged channel confocal images of P24 control and PTEN brains Dapi (blue) and tdTOMATO (DeltaNP73 derived CRs). (A) right Merged channel confocal images of control (P10) and PTEN (P24) brains after Biocytin injection (green), tdTOMATO (DeltaNP73 derived CRs) (B) 3D-Volume of tdTOMATO positive CRs (µm3). (C) Mean fluorescent intensity of Reelin staining within CRs positive for tdTOMATO; Quantification from images Fig 2A at P24 (Control and Pten), Mann-Whitney U test (B,C); Data are represented as mean ± SD (**C**) Example trances of current clamp recordings of CR cells recorded from control (black) and Pten model mice. Cells were held at -75 mV and shown are a hyperpolarizing and depolarizing current steps. (**D**) Intrinsic properties of CR cells from control and Pten mice, D1, resting membrane potential, D2, Membrane resistance and D3, Membrane capacitance. (**E**) Action-potential firing properties of CR cells from control and Pten mice. E1, number of action potentials in one-second long depolarization as a function of injection current. E2, Action potential amplitude for the first 5 action potentials. (**F**) Action potential firing properties, F1, Action potential threshold, F2, Action potential halfwidth, F3, Action potential latency. D-F show average with error bars denoting SEM. *p<0.05; **p<0.001; ***p<0.0001. Scale bars: 50 µm.

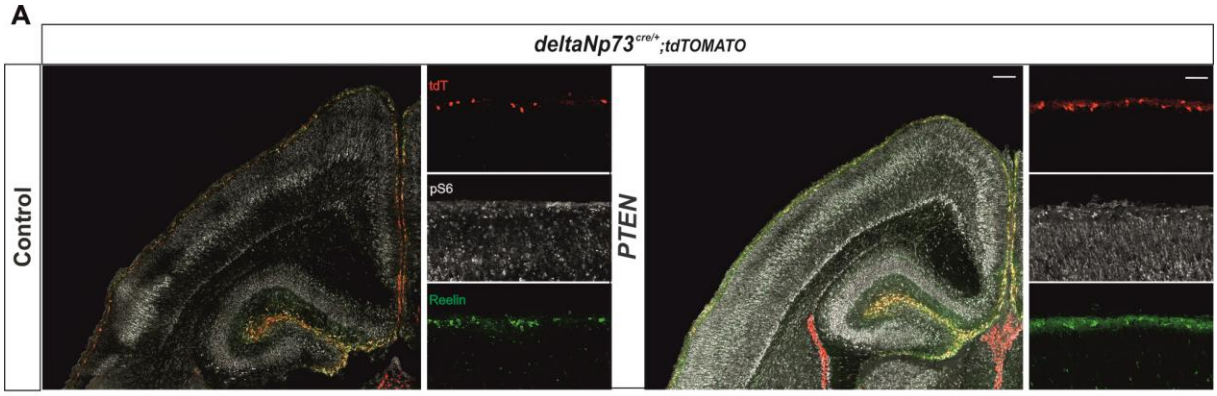
A
deltaNp73cre/+;tdTOMATO
Control
tdT
pS6
Reelin
PTEN

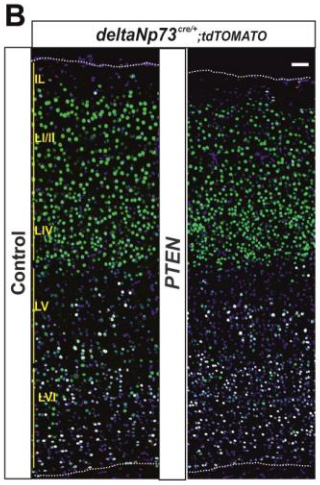
B
deltaNp73cre/+;tdTOMATO
Control
PTEN
IL
LI/II
LIV
LV
LVI

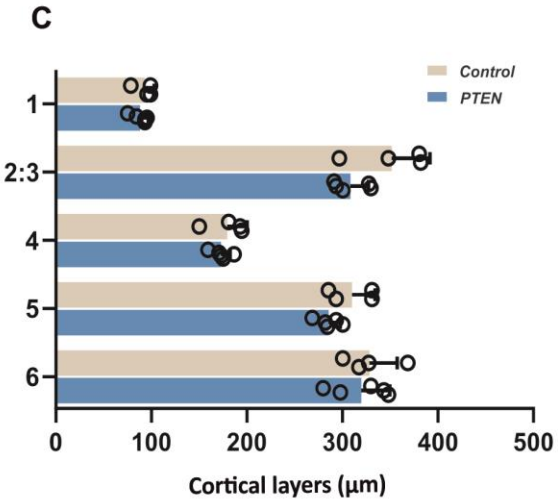
C
Control
PTEN
1
2:3
4
5
6
0
100
200
300
400
500
Cortical layers (µm)

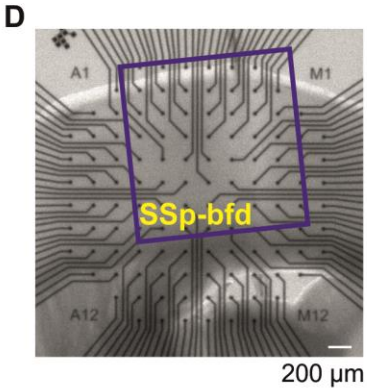
D
A1
M1
SSp-bfd
A12
M12
200 µm

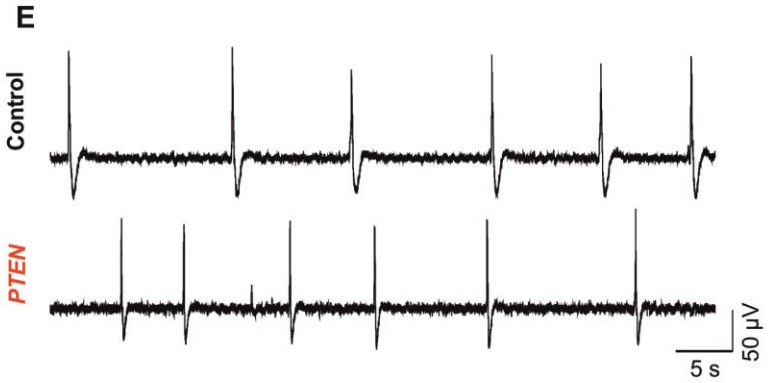
E
Control
PTEN
50 µV
5 s

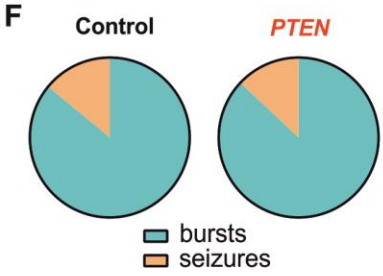
F
Control
PTEN
bursts
seizures

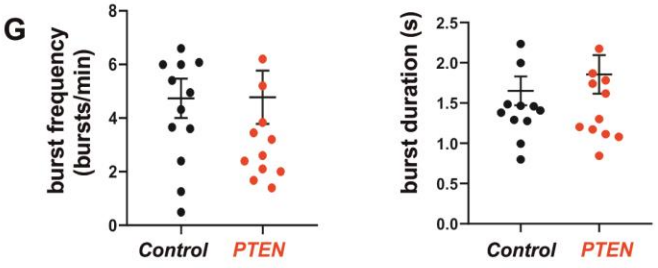
G
burst frequency (bursts/min)
Control
PTEN
burst duration (s)
Control
PTEN

Figure 4- Inactivation of PTEN in deltaNP73 derived CRs increases reelin secretion and activates mTOR in cortex without altering cortical layering nor neuronal network activity in S1 cortex. (**A**) Merged and single channel confocal images of control and Pten mutants brains at P1 stage stained for pS6 Ser 240/244 (gray), Reelin (green) and Dapi (blue). DeltaNP73 derived CRs in tdTOMATO (red). The 3 single channels images on right are zoom in from left merged images. (B) Merged and single channel confocal images of control and Pten mutants S1 barrel cortex at P24 stage stained for Cux1(green), Ctip2 (white) and dapi (blue) (C) Thickness of different layers in pten mutant and control; Data are represented as mean ± SD (D) Image of a cortical mouse slice placed in a multi-electrode array (MEA) dish. The S1B cortex is highlighted by the red square. Scale bar: Big images 200 µm, small images 50 µm. (E) Representative MEA recordings of bursting activity in 0Mg-6K ACSF in control (top) and PTEN mutant (bottom) mice. Scale bars: 50 µV, 5 s. (F) Percentage of slices with bursting (blue) or seizures (orange) activity in control and PTEN mutant mice (n = 14 and 15 slices for control and PTEN mutant mice, respectively, from 4 mice for both genotypes). (G) Quantification of burst frequency and duration in control (n = 13 slices) and PTEN mutant (n = 14 slices) mice. Data are represented as mean ±SEM.

Activation of the PI3K/ AKT/ mTOR pathway in Cajal-Retzius cells leads to their survival and increases Reelin secretion in the cortex.

Nasim Ramezanidoraki[1,2,5], Margaux Le[1,2,5], Mahboubeh Ahmadi[1,5], Stéphanie Moriceau[3], Dossi Elena[4], Danae Rolland[1], Philippe Bun[1], Lepen Gwenaelle[1,5], Mario Pende[3], Guillaume Canaud[3], Nadia Bahi-Buisson[1,2], Nathalie Rouach[4], Rebecca Piskorowski[1,5], Alessandra Pierani[1,2,5], Pierre Billuart §[1,2,5]

SUPPLEMENTAL INFORMATION

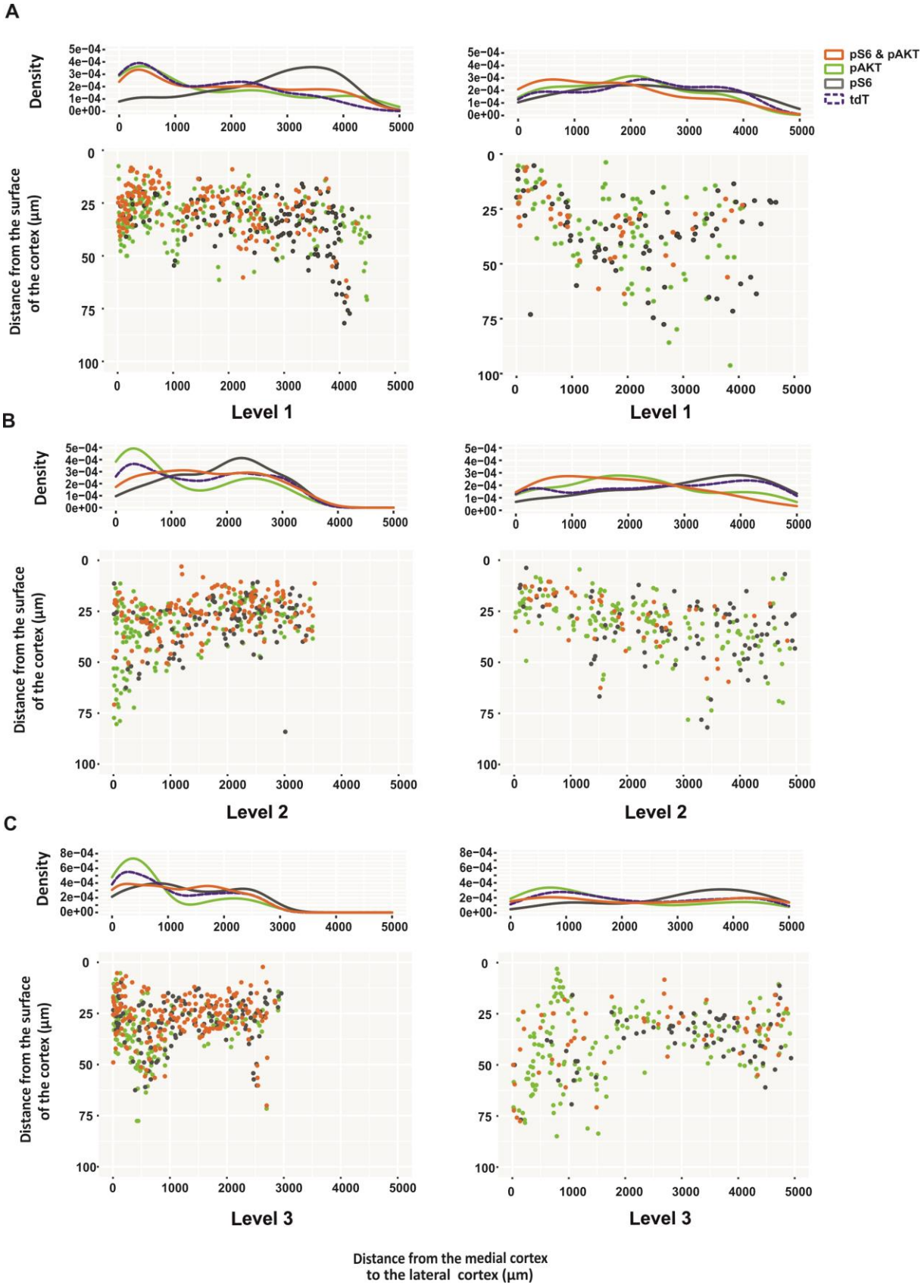
A
B
C
Density
Distance from the surface of the cortex (µm)
pS6 & pAKT
pAKT
pS6
tdT
Level 1
Level 2
Level 3
Distance from the medial cortex to the lateral cortex (µm)

Figure S1 – Differential activity of the PI3K/AKT/mTOR pathway along the medio-lateral axis in 3 neocortex levels between E17.5 and P1 stages. Kernel density (top) and scatter plots (bottom) of pS6 or pAKT positive CRs for levels 1 (A), 2 (B) and 3 (C) at E17.5 (left 6 panels) and P1 (right 6 panels) stages (n=4 for E17.5 and P1). Kolmogorov-Smirnov test (A, B, C).

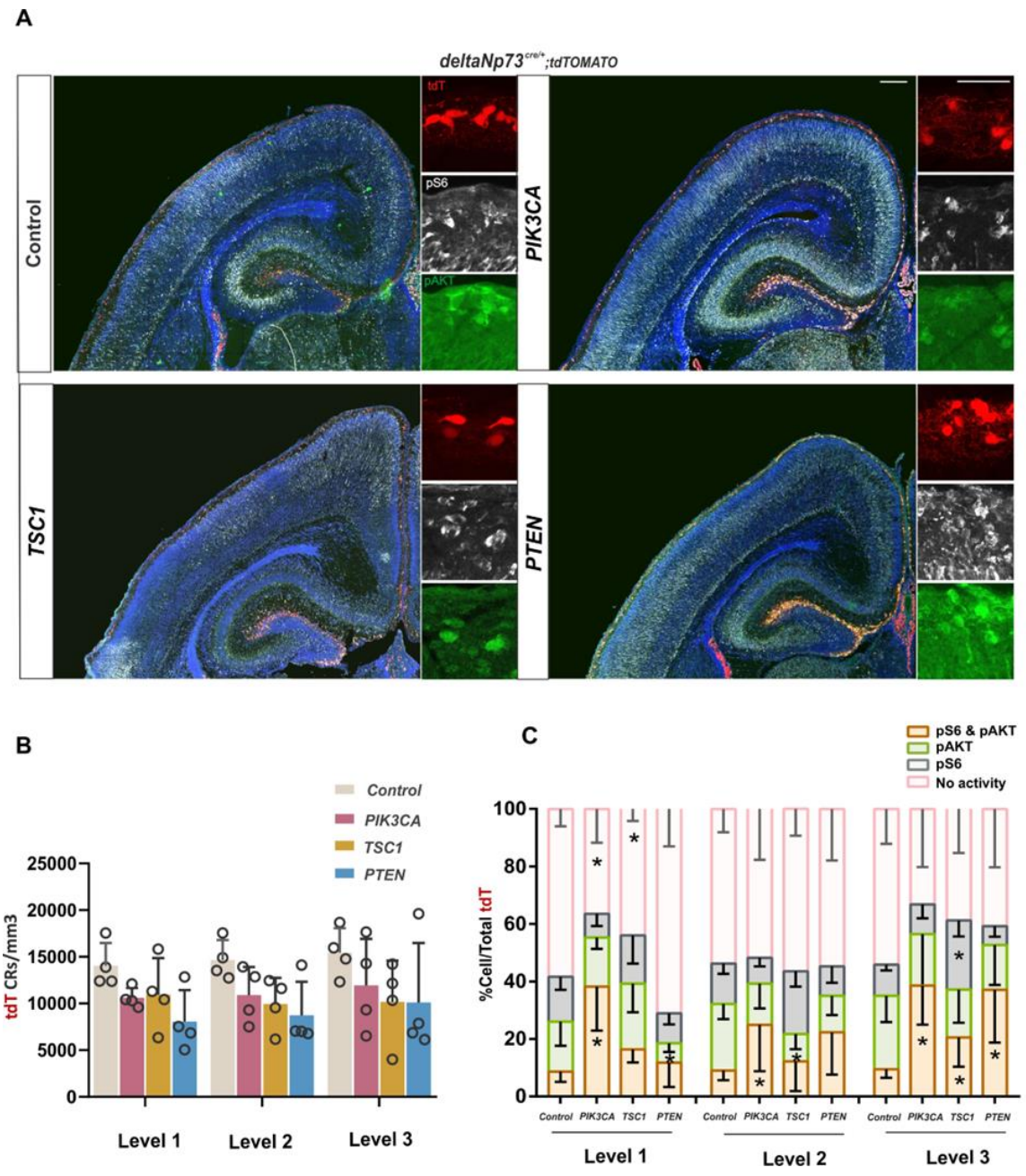

Figure S2 – Differential activation of the PI3K/ AKT/ mTOR pathway at P1 stage does not alter CR development nor cortex and hippocampus formations. (A) Merged and single channel confocal images of P1 control brains (level 2) stained for pS6 Ser 240/244 (gray), pAKT Ser 473 (green) and Dapi (blue). tdTOMATO (red) traces DeltaNP73 derived CRs. (B) CR density (CRs/mm3) at the neocortex levels 1, 2, and 3 (n=4 for controls and mutants). (C) Proportion of CRs positive for one or two marker or negative over total tdT cells (n=4 for controls and mutants) at the 3 levels. Two way anova test followed by Sidak post-hoc test (B); Mann-Whitney U test (C); Data are represented as mean ± SD; *p<0.05. Scale bars: big images 200 µm, small images 50 µm.

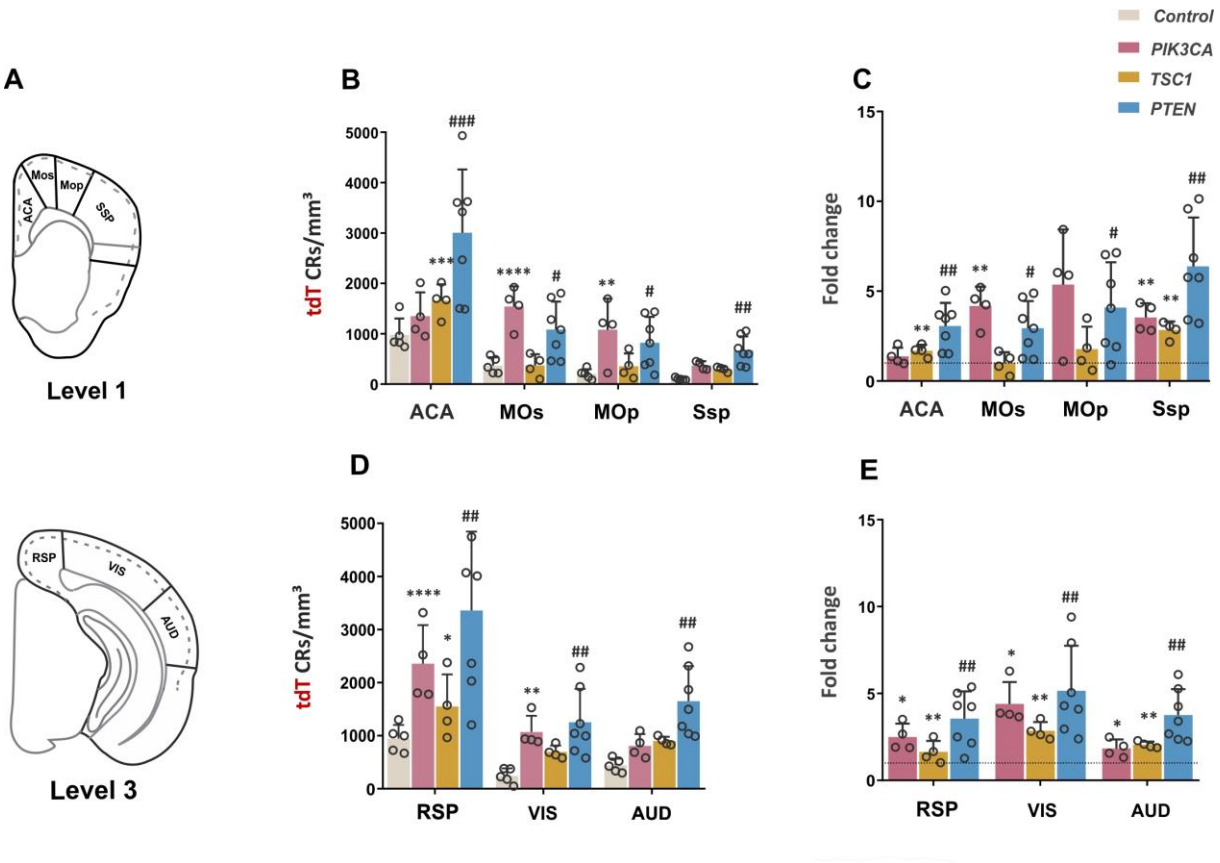

Figure S3 -Sustained postnatal activation of the PI3K/ AKT/ mTOR pathway leads to the persistence of CRs at later stages along medio-lateral axes in levels 1 and 3. (A) Schematic representation of the two other rostro-caudal levels 1 and 3 together with the analyzed Medio-lateral axes (B, D) CR density (CRs/mm3) in the medio-lateral axis of the neocortex levels 1 and 3 (C, E) Fold changes in CR densities in the medio axis of the neocortex levels 1 and 3. Two way Anova followed by a Sidak's multiple comparisons test for Control vs PI3K and TSC1; Multiple t-test control vs PTEN (B, D) One sample t test (C,E) . Data are represented as mean ± SD; *or # p<0.05; **or ## p<0.001; *** or ### p<0.0001.

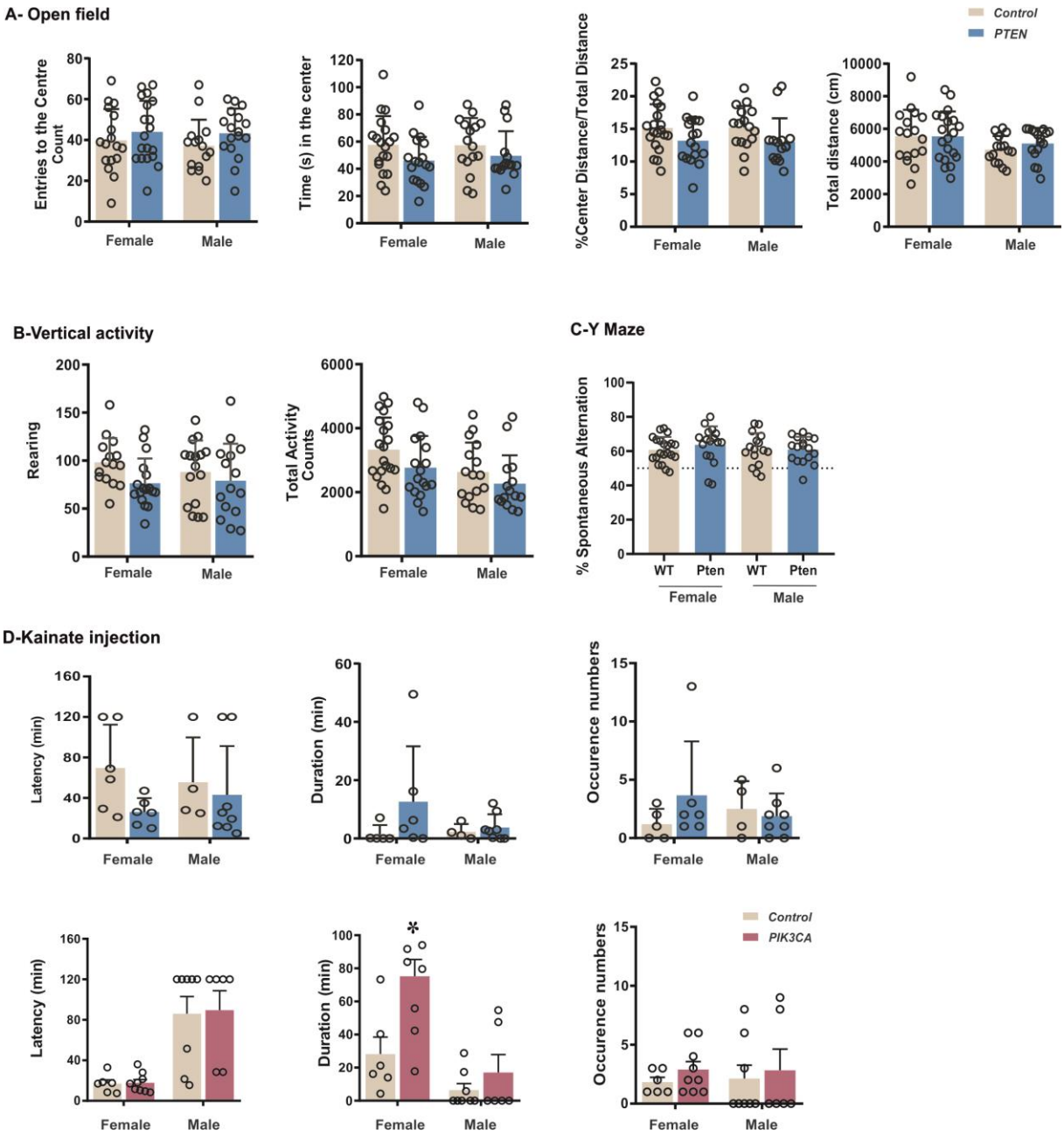

Figure S4_ Inactivation of PTEN in deltaNP73 derived CRs does not alter general animal behavior nor sensitivity to epilepsy induced by kainite. Anxiety in open-field (A), horizontal and vertical activities (A, B), spontaneous alternation in Y maze (C) were measured in control (grey) and Pten (blue) mutants males and females at 2 months and half stage. (D) Sensitivity to epilepsy after kainate injection was measured at 3 months by the latency, the duration and the number of crises developed in the genetic context of Pik3/AKT/mTOR pathway activation by either the Pten inactivation or the Pik3CA (red) expression.*p<0.05.

Supplemental Material and Methods

Reagent type (species) or resource	Designation	Source or reference	Identifiers	Additional information
Strain Mus musculus (males and female)	C57BL6J	Janvier		
Mus musculus (males and female)	deltaNp73^{CreIRESGFP}	(Tissir et al., 2009)	deltaNp73^{Cre}	
Mus musculus (males and female)	*ROSA26$^{loxP\text{-}stop\text{-}loxP\text{-}Tomato}$*	(Madisen et al., 2010)	R26^{mT}	
Mus musculus (males and female)	*R26StopFlp110**	(Srinivasan et al., 2009)	PIK3CA^{p110*}	
Mus musculus (males and female)	*Pten^{loxP}*	(Suzuki et al., 2001)	PTEN$^{lox/lox}$	
Mus musculus (males and female)	*TSC1^{loxP}*	(Kwiatkowski, 2002b)	TSC1$^{del/lox}$	
Sequence-based reagent	deltaNp73$^{Cre/+}$ genotyping delta1 delta2	This paper	PCR primers	delta1: GAA-TGC-CAA-CTC-TCA-GTC-CG

	83RC			delta2: GTC-TCT-CTG-AAC-CCC-AAC-CA 83RC: GGT-GTA-CGG-GCA-GTA-AAT-TGG-AC
Sequence-based reagent	$R26^{mT}$ genotyping RCE-1 RCE-2 RCE-3	This paper	PCR primers	RCE-1: CCC-AAA-GTC-GCT-CTG-AGT-TGT-TAT-C RCE-2: GAA-GGA-GCG-GGA-GAA-ATG-GAT-ATG RCE-3: CCA-GGC-GGG-CCA-TTT-ACC-GTA-AG
Sequence-based reagent	Rosap110* genotyping RCE-1 RCE-2 NeoR1	This paper	PCR primers	RCE-1: CCC-AAA-GTC-GCT-CTG-AGT-TGT-TAT-C RCE-2: GAA-GGA-GCG-GGA-GAA-ATG-GAT-ATG

				NeoR1: GAC-ATC-ATC-AAG-GAA-ACC-CTG-GAC
Sequence-based reagent	PTEN genotyping New_Sens Del_AS i5_S	(Suzuki et al., 2001)	PCR primers	New_Sens: AGA-TTG-TAT-GTG-ATC-ATC-TGT-CAG-G Del_AS: AGC-AGG-TGA-AAG-AGA-AGT-ACA-G i5_S: ATT-AAA-TTT-GGA-CTT-GTG-CCC-CA
Sequence-based reagent	TSC1 genotyping F4536 R4830 R6548	(Kwiatkowski, 2002a)	PCR primers	F4536: AGG-AGG-CCT-CTT-CTG-CTA-CC R4830: CAG-CTC-CGA-CCA-TGA-AGT-G R6548: TGG-GTC-CTG-ACC-TAT-CTC-CTA

Antibody	goat polyclonal IgG anti-reelin antibody	R&D Systems, USA	Cat# AF3820, RRID:AB_2253745	IF(1:500)
Antibody	rabbit monoclonal anti-phospho-AKT Serine 473 antibody (D9E)	Cell signaling Technology, USA	Cat# 4060, RRID:AB_2315049	IF(1:200)
Antibody	rabbit monoclonal anti-phospho-S6 antibody (Ser 240/244) (D68F8)	Cell signaling Technology, USA	Cat# 5364, RRID:AB_10694233	IF(1:1000)
Antibody	rat monoclonal anti-ctip2 antibody	Abcam, USA	Cat# ab18465, RRID:AB_2064130	IF(1:250)
Antibody	rabbit polyclonal anti-cux1,2 antibody	Santa Cruz Biotechnology, USA	Cat# sc13024, RRID:AB_2261231	IF(1:250)
Antibody	donkey anti-rabbit Alexa-488	Jackson ImmunoResearch Laboratories, USA	Cat# 711-545-152, RRID: AB_2313584	IF(1:500)
Antibody	donkey anti-goat Alexa-488	Molecular Probes, USA	Cat# A11055, RRID:AB_2534102	IF(1:500)
Antibody	donkey anti-goat Cy5	Jackson ImmunoResearch Laboratories, USA	Cat# 705-175-147, RRID: AB_2340415	IF(1:250)

Antibody	donkey anti-rat Alexa-Cy5	Jackson ImmunoResearch Laboratories, USA	Cat# 712-175-153, RRID: AB_2340672	IF(1:250)
Antibody	Zenon® Alexa Fluor® 488 Rabbit IgG Labeling Kit	Thermo Fisher Scientific, USA	Cat# Z25302, RRID:AB_2572214	
Antibody	DAPI (4',6-Diamidino-2-Phenylindole, Dihydrochloride)	ThermoFisher Scientific, USA	Cat# D1306, RRID:AB_2629482	IF(1:1000)
Antibody	Biocytin	ThermoFisher Scientific, USA	Cat#B1592	
Antibody	Streptavidin, Alexa Fluor™ 546 conjugate	Life Technologies, by Thermo Fisher Scientific, USA	Cat#S11225 RRID:AB_2532130	
Chemical compound, drug	Vectashield	Vector Laboratories, USA	Cat# H1000, RRID:AB_2336789	
Chemical compound, drug	Normal Goat Serum (10%)	Life Technologies, by Thermo Fisher Scientific, USA	cat # 50062Z	
Chemical compound, drug	ProLong™ Diamond Antifade Mountant	Invitrogen by Thermo Fisher Scientific, USA	cat # P36970	
Chemical compound, drug	Triton 100X	Eurobio, France	Cat# GAUTTR00-07	

Chemical compound, drug	Paraformaldehyde	Sigma-Aldrich, USA	Cat# P6148	
Chemical compound, drug	Tissue Tek * OCT compound	Sakura Finetek, USA	Cat# NC1862249	
Chemical compound, drug	Gelatin from porcine skin	Sigma-Aldrich, USA	Cat# G2500	
Chemical compound, drug	Ketamine (Imalgen 1000)	Centravet, Dinan, France	GTIN: 03661103003199	180mg/kg
Chemical compound, drug	Xylasine (Rompun 2%)	Centravet, Dinan, France	GTIN: 04007221032311	10mg/kg
Chemical compound, drug	Kainate	Bio-Techne, USA	Cat#0222/10	15mg/Kg
Software, algorithm	ImageJ/FIJI	National Institutes of Health (NIH), USA	RRID:SCR_002285	
Software, algorithm	Adobe Photoshop CS6	Adobe Inc., USA	RRID:SCR_014199	
Software, algorithm	GraphPad Prism 8.0	GraphPad Software, USA	RRID:SCR_000306	
Software, algorithm	CorelDraw Graphics Suite	Corel Corporation, Canada	RRID:SCR_014235	
Software, algorithm	Axon™ pCLAMP® 9 Software	Molecular Devices, USA	RRID:SCR_011323	

Software, algorithm	IGORpro	WaveMetrics Inc, USA	RRID:SCR_000325	
Software, algorithm	TaroTools	Jikei University School of Medicine, Japan	?	
Software, algorithm	Axograph software	Axograph Inc, USA	RRID:SCR_014284	
Software, algorithm	MEA Monitor software	Multichannel Systems, Germany	?	
Software, algorithm	MC Rack 4.5.1 software	Multichannel Systems, Germany	RRID:SCR_014955	
Software, algorithm	Videotrack v2.6 Automated Behavioural Analysis	ViewPoint, France		
Software, algorithm	R program version 4.0.3	R Core Team, Austria	RRID:SCR_001905	

Supplementary Table 1

ROSTRO-CAUDAL AXE

Quantification of total number of CR in three neocortex levels (Table 1.1)

Mann-Whitney U test	Two-tailed p value	U	N	E17.5) Mean (10) ± SD (1	(P1) Mean (10) ± SD (10)	Significant (alpha=0.05)?	P value summary
Level1- E17.5 vs P1	0.0286	0	4	20.8 ± 2.67	12.0 ± 2.04	Yes	*
Level2- E17.5 vs P1	0.6857	6	4	15.7 ± 1.98	15.7 ± 2.07	No	ns
Level3- E17.5 vs P1	0.4571	5	4	16.2 ± 2.88	14.8 ± 2.70	No	ns

Quantification of CR density (CRs/mm3) in three neocortex levels (Table 1.2)

Mann-Whitney U test	Two-tailed p value	U	N	(E17.5) Mean ± SD (10^3)	(P1) Mean ± SD (10^3)	Significant (alpha=0.05)?	P value summary
Level1- E17.5 vs P1	0.0286	0	4	25.5 ± 1.65	14.1 ± 2.43	Yes	*
Level2- E17.5 vs P1	0.0286	0	4	23.4 ± 2.47	14.7 ± 2.12	Yes	*
Level3- E17.5 vs P1	0.0286	0	4	30.0 ± 2.58	15.4 ± 2.64	Yes	*

Quantification of the proportion of CRs for the PI3K/AKT/mTOR activity over total tdTOMATO cells in three neocortex levels (Table 1.3)

Mann-Whitney U test	Two-tailed p value	U	N	(E17.5) Mean ± SD	(P1) Mean ± SD	Significant (alpha=0.05)?	P value summary
CRs positive only for pS6 over total tdTOMATO cells							
Level1- E17.5 vs P1	0.4857	5	4	18.7 ± 2.43	15.3 ± 4.86	No	ns
Level2- E17.5 vs P1	0.4857	5	4	18.8 ± 7.80	14.5 ± 3.69	No	ns
Level3- E17.5 vs P1	0.0571	1	4	18.8 ± 6.90	10.8 ± 2.04	No	ns
CRs positive only for pAKT over total tdTOMATO cells							
Level1- E17.5 vs P1	0.3429	4	4	23.2 ± 6.20	17.2 ± 8.04	No	ns
Level2- E17.5 vs P1	0.6857	6	4	26.2 ± 8.95	23.7 ± 6.00	No	ns
Level3- E17.5 vs P1	0.8857	7	4	22.3 ± 3.23	25.2 ± 8.93	No	ns
CRs positive for both pS6 & pAKT over total tdTOMATO cells							
Level1- E17.5 vs P1	0.0286	0	4	21.4 ± 7.45	8.6 ± 3.55	Yes	*
Level2- E17.5 vs P1	0.0286	0	4	24.4 ± 4.98	9.0 ± 3.37	Yes	*
Level3- E17.5 vs P1	0.0286	0	4	30.0 ± 7.46	9.4 ± 2.94	Yes	*
CRs negative for any activity over total tdTOMATO cells							
Level1- E17.5 vs P1	0.0286	0	4	36.5 ± 7.4	58.8 ± 5.7	Yes	*
Level2- E17.5 vs P1	0.0286	0	4	30.3 ± 4.50	52.6 ± 9.06	Yes	*
Level3- E17.5 vs P1	0.0286	0	4	28.6 ± 2.24	54.4 ± 12.07	Yes	*

MEDIO-LATERAL AXE in three neocortex levels

Analysis of the PI3K/AKT/mTOR Pathway activity distribution along the medio-lateral axis in three neocortex levels at P1 (Table 1.4 and Table 1.5)

	E17.5 (Table 1.4)				P1 (Table 1.5)			
Kolmogorov-Smirnov test	p value	Distance	N	Significant (alpha=0.05)?	p value	Distance	N	Significant (alpha=0.05)?	P value summary
pS6 vs tdT									
Level1	<0.0001	0.2943	4	Yes	0.7833	0.0828	4	No	ns
Level2	0.0006	0.2043	4	Yes	0.1294	0.1312	4	No	ns
Level3	0.0047	0.1707	4	Yes	<0.0001	0.294	4	Yes	****
pAKT vs tdT									
Level1	0.0094	0.1308	4	Yes	0.0577	0.1583	4	No	ns
Level2	0.0001	0.1911	4	Yes	<0.0001	0.2105	4	Yes	****
Level3	<0.0001	0.2086	4	Yes	0.0018	0.1696	4	Yes	**
pS6 & pAKT vs tdT									
Level1	0.0069	0.1401	4	Yes	0.003	0.2967	4	Yes	**
Level2	0.226	0.09316	4	No	0.0174	0.2148	4	Yes	*
Level3	0.0401	0.1154	4	Yes	0.4064	0.1225	4	No	ns

Supplementary Table 2

Table 2.1 Quantification of CR density (CRs/mm3) at P1 stage in three neocortex levels

	Control	PIK3CA	TSC1	PTEN
	Mean(10^3) ± SD (10^3)	Mean(10^3) ± SD (10^3)	Mean(10^3) ± SD (10^3)	Mean(10^3) ± SD (10^3)
Level 1	14.1 ± 2.43	10.6 ± 1.06	11.0 ± 3.89	8.1 ± 3.35
Level 2	14.7 ± 2.12	10.9 ± 3.00	9.9 ± 2.79	8.7 ± 3.59
Level 3	15.4 ± 2.64	11.9 ± 4.98	10.2 ± 4.41	10.1 ± 6.37

Table 2.2

Two way ANOVA table

	SS	DF	MS	F (DFn, DFd)	P value	Summary	Significant?
control vs PIK3CA							
Interaction	135.9E+3	2.0E+0	67.9E+3	F (2, 12) = 0.0.1026	989.8E-3	ns	No
levels	7.7E+6	2.0E+0	3.8E+6	F (2, 12) = 0.5810	574.3E-3	ns	No
Genotype	76.7E+6	1.0E+0	76.7E+6	F (1, 6) = 5.945	50.6E-3	ns	No
Subject	77.4E+6	6.0E+0	12.9E+6	F (6, 12) = 1.949	153.2E-3	ns	No
Residual	79.5E+6	12.0E+0	6.6E+6				
control vs TSC1							
Interaction	5.2E+6	2.0E+0	2.6E+6	F (2, 12) = 0.5317	600.8E-3	ns	No
levels	996.9E+3	2.0E+0	498.5E+3	F (2, 12) = 0.1026	903.3E-3	ns	No
Genotype	114.1E+6	1.0E+0	114.1E+6	F (1, 6) = 5.653	55.0E-3	ns	No
Subject	121.1E+6	6.0E+0	20.2E+6	F (6, 12) = 4.155	172E-3	*	Yes
Residual	58.3E+6	12.0E+0	4.9E+6				
control vs PTEN							
Interaction	555.2E+3	2.0E+0	277.6E+3	F (2, 12) = 0.04847	952.9E-3	ns	No
levels	12.0E+6	2.0E+0	6.0E+6	F (2, 12) = 1.047	380.9E-3	ns	No
Genotype	198.6E+6	1.0E+0	198.6E+6	F (1, 6) = 6.711	412E-3	*	Yes
Subject	177.5E+6	6.0E+0	29.6E+6	F (6, 12) = 5.167	7.7E-3	**	Yes
Residual	68.7E+6	12.0E+0	5.7E+6				

Sidak's multiple comparisons test	Mean 1 (Control)	Mean 2 (Mutant)	Mean Diff.	SE of diff.	95.00% CI of diff.	N1	N2	t	DF	Justed P Va	Summary	Significant?
Level 1												
Control vs. PIK3CA	14055	10606	3449	2577	-4805 to 11704	4	4	1.338	36	0.9771	ns	No
Control vs. TSC1	14055	10972	3083	2577	-5172 to 11337	4	4	1.196	36	0.9928	ns	No
Control vs. PTEN	14055	8072	5983	2577	-2272 to 14238	4	4	2.321	36	0.3781	ns	No
Level 2												
Control vs. PIK3CA	14685	10898	3787	2577	-4467 to 12042	4	4	1.469	36	0.9468	ns	No
Control vs. TSC1	14685	9944	4742	2577	-3513 to 12997	4	4	1.84	36	0.7496	ns	No
Control vs. PTEN	14685	8733	5953	2577	-2302 to 14207	4	4	2.31	36	0.3862	ns	No
Level 3												
Control vs. PIK3CA	15439	11948	3491	2577	-4764 to 11746	4	4	1.355	36	0.9743	ns	No
Control vs. TSC1	15439	10182	5257	2577	-2997 to 13512	4	4	2.04	36	0.5933	ns	No
Control vs. PTEN	15439	10116	5323	2577	-2932 to 13578	4	4	2.065	36	0.5728	ns	No

Supplementary Table 2

Table 2.3

Quantification of the proportion of CRs for the PI3K/AKT/mTOR activity over total tdTOMATO cells in three neocortex levels at P1 stage

Mann-Whitney U test	Two-tailed p value	U	N (Control and Mutants)	Mean ± SD Control	Mean ± SD Mutant	Significant (alpha=0.05)?	P value summary
CRs positive only for pS6 over total tdTOMATO cells P1 stage							
Level1							
Control vs. PIK3CA	0.1143	2	4	15.5 ± 4.57	8.2±4.21	No	ns
Control vs. TSC1	0.6857	6	4	15.5 ± 4.57	16.7± 9.78	No	ns
Control vs. PTEN	0.3429	4	4	15.5± 4.57	10.3±3.84	No	ns
Level2							
Control vs. PIK3CA	0.1143	2	4	14.0 ± 3.58	9.0±3.01	No	ns
Control vs. TSC1	0.1143	2	4	14.0 ± 3.58	21.8±5.33	No	ns
Control vs. PTEN	0.4571	5	4	14.0 ± 3.58	10.2±5.75	No	ns
Level3							
Control vs. PIK3CA	0.6857	6	4	10.8 ± 2.04	10.2±4.84	No	ns
Control vs. TSC1	0.0286	0	4	10.8 ± 2.04	24.0± 5.52	Yes	*
Control vs. PTEN	0.2	3	4	10.8 ± 2.04	6.5±3.63	No	ns
CRs positive only for pAKT over total tdTOMATO cells P1 stage							
Level1							
Control vs. PIK3CA	0.8857	7	4	17.4 ± 8.4	17.0±3.94	No	ns
Control vs. TSC1	0.4857	5	4	17.4 ± 8.4	22.9± 9.95	No	ns
Control vs. PTEN	0.0286	0	4	17.4 ± 8.4	6.7±3.05	Yes	*
Level2							
Control vs. PIK3CA	0.2	3	4	23.1 ± 5.26	14.3±8.62	No	ns
Control vs. TSC1	0.0286	0	4	23.1 ± 5.26	9.5±5.26	Yes	*
Control vs. PTEN	0.0571	1	4	23.1 ± 5.26	12.7±6.67	No	ns
Level3							
Control vs. PIK3CA	0.4857	5	4	25.5 ± 9.08	17.9±18.7	No	ns
Control vs. TSC1	0.4857	5	4	25.5 ± 9.08	16.6± 11.4	No	ns
Control vs. PTEN	0.3429	4	4	25.5 ± 9.08	15.6±13.90	No	ns
CRs positive for both pS6 & pAKT over total tdTOMATO cells P1 stage							
Level1							
Control vs. PIK3CA	0.0286	0	4	8.6 ± 3.55	38.1±15.3	Yes	*
Control vs. TSC1	0.0571	1	4	8.6 ± 3.55	16.3± 4.53	No	ns
Control vs. PTEN	0.8857	7	4	8.6 ± 3.55	11.7±8.49	No	ns
Level2							
Control vs. PIK3CA	0.0286	0	4	9.04 ± 3.37	24.8±16.09	Yes	*
Control vs. TSC1	0.8857	7	4	9.04 ± 3.37	12.2±10.27	No	ns
Control vs. PTEN	0.2	3	4	9.04 ± 3.37	22.2±14.67	No	ns
Level3							
Control vs. PIK3CA	0.0286	0	4	9.4 ± 2.94	38.5±13.58	Yes	*
Control vs. TSC1	0.0286	0	4	9.4 ± 2.94	20.5± 10.15	Yes	*
Control vs. PTEN	0.0286	0	4	9.4 ± 2.94	37.0±18.29	Yes	*
CRs negative for any activity over total tdTOMATO cells P1 stage							
Level1							
Control vs. PIK3CA	0.0286	0	4	58.3 ± 6.07	36.4±11.73	Yes	*
Control vs. TSC1	0.0286	0	4	58.3 ± 6.07	43.9± 4.21	Yes	*
Control vs. PTEN	0.2	3	4	58.3 ± 6.07	71.0±13.01	No	ns
Level2							
Control vs. PIK3CA	0.6857	6	4	53.7 ± 8.11	51.7±17.71	No	ns
Control vs. TSC1	0.6857	6	4	53.7 ± 8.11	56.4±9.30	No	ns
Control vs. PTEN	0.8857	7	4	53.7 ± 8.11	54.7±17.9	No	ns
Level3							
Control vs. PIK3CA	0.1143	2	4	54.1 ± 12.13	33.22±20.25	No	ns
Control vs. TSC1	0.3429	4	4	54.1 ± 12.13	38.8± 15.32	No	ns
Control vs. PTEN	0.4857	5	4	54.1 ± 12.13	40.7±20.3	No	ns

Supplementary Table 3

ROSTRO-CAUDAL AXE

Quantification of CR density (CRs/mm3) at P24 stage in three neocortex levels (Table 3.1)

	Control	PIK3CA	TSC1	PTEN
	Mean ±SD	Mean ±SD	Mean ±SD	Mean ±SD
Level 1	362.7 ± 111.4	957.0 ± 220.2	633.8 ± 84.5	1322.0 ± 508.9
Level 2	273.0 ± 97.1	1134.3 ± 82.0	553.4 ± 207.2	1816.4 ± 566.7
Level 3	556.7 ± 138.5	1472.2 ± 271.8	1054.3 ± 233.8	2022.5 ± 733.7

control vs PIK3CA

Two Way ANOVA table	SS	DF	MS	F (DFn, DFd)	P value	Summary	Significant?
Interaction	131369	2	65684	F (2, 14) = 4.074	0.0403	*	Yes
level	664455	2	332228	F (2, 14) = 20.61	<0.0001	****	Yes
Genotype	4164352	1	4164352	F (1, 7) = 89.42	<0.0001	****	Yes
Subjects (matching)	325989	7	46570	F (7, 14) = 2.888	0.0433	*	Yes
Residual	225730	14	16124				

Sidak's multiple comparisons test	Mean 1 (control)	Mean 2 (PIK3CA)	Mean Diff.	SE of diff.	95.00% CI of diff	N1 (control)	N2 (PIK3CA)	t	DF	Adjusted P Value	Summary	Significant?
Delta Np73^{Cre} - Delta Np73 ^{Cre}> R26 ^{p110*kd}	362.8	957.1	-594.3	108.7	-876.3 to -312.3	5	4	5.466	21	<0.0001	***	Yes
Level1 (control vs PIK3CA)	273.1	1134	-861.3	108.7	-1143 to -579.3	5	4	7.921	21	<0.0001	****	Yes
Level2 (control vs PIK3CA)	556.8	1472	-915.5	108.7	-1197 to -633.5	5	4	8.42	21	<0.0001	****	Yes
Level3 (control vs PIK3CA)												

control vs TSC1

Two Way ANOVA table	SS	DF	MS	F (DFn, DFd)	P value	Summary	Significant?
Interaction	73024	2	36512	F (2, 14) = 4.533	0.0304	*	Yes
Level	757233	2	378617	F (2, 14) = 47	<0.0001	****	Yes
Genotype	815284	1	815284	F (1, 7) = 15.6	0.0055	**	Yes
Subjects (matching)	365758	7	52251	F (7, 14) = 6.487	0.0015	**	Yes
Residual	112774	14	8055				

Sidak's multiple comparisons test	Mean 1 (control)	Mean 2 (TSC1)	Mean Diff.	SE of diff.	95.00% CI of diff	N1 (control)	N2 (TSC1)	t	DF	Adjusted P Value	Summary	Significant?
Delta Np73^{Cre} - Delta Np73Cre/+>TSC1lox/ del	362.8	633.9	-271.1	101.3	-533.8 to -8.492	5	4	2.677	21	0.0417	*	Yes
Level1 (control vs TSC1)	273.1	553.4	-280.4	101.3	-543 to -17.73	5	4	2.769	21	0.0341	*	Yes
Level2 (control vs TSC1)	556.8	1054	-497.6	101.3	-760.3 to -235	5	4	4.914	21	0.0002	***	Yes
Level3 (control vs TSC1)												

control vs PTEN*

Multiple t-test	Mean1 (control)	Mean2 (PTEN)	Difference	SE of difference	t ratio	df	N1 (control)	N2 (PTEN)	P value	Summary	Significant?
Level1 (control vs PTEN)	362.8	1322	959.3	234.5	4.091	10	5	7	0.0022	**	Yes
Level2 (control vs PTEN)	273.1	1816	1543	259.6	5.946	10	5	7	0.0001	***	Yes
Level3 (control vs PTEN)	556.8	2023	1466	336.7	4.353	10	5	7	0.0014	**	Yes

TSC1 vs PTEN*

Multiple t-test	Mean1 PTEN	Mean2 TSC1	Difference	SE of difference	t ratio	df	N1 (PTEN)	N2 (TSC1)	P value	Summary	Significant?
Level1 (PTEN vs TSC1)	1322	633.9	688.2	262.3	2.624	9	7	4	0.0276	*	Yes
Level2 (PTEN vs TSC1)	1816	553.4	1263	299.6	4.215	9	7	4	0.0022	**	Yes
Level3 (PTEN vs TSC1)	2023	1054	968.2	384.9	2.515	9	7	4	0.033	*	Yes

* Due to inequal variance (larger variation in pten mutants) we used multiple-t-test to compare Pten data to either control or Tsc1

Supplementary Table 3

MEDIO-LATERAL AXE in three neocortex levels

Quantification of CR density (CRs/mm3) at P24 along medio-lateral and rostro-caudal axes (Table 3.2)

control vs PIK3CA

Two ways ANOVA table	SS	DF	MS	F (DFn, DFd)	P value	Summary	Significant?
Level 1							
Interaction	1221622	3	407207	F (3, 21) = 5.353	0.0068	**	Yes
Lateral axe	4351360	3	1450453	F (3, 21) = 19.07	<0.0001	****	Yes
Genotype	4002641	1	4002641	F (1, 7) = 22.05	0.0022	**	Yes
Subjects (matching)	1270643	7	181520	F (7, 21) = 2.386	0.0581	ns	No
Residual	1597545	21	76074				
Level 2							
Interaction	1175038	3	391679	F (3, 21) = 29.31	<0.0001	****	Yes
Lateral Axe	3190997	3	1063666	F (3, 21) = 79.6	<0.0001	****	Yes
Genotype	6357467	1	6357467	F (1, 7) = 178.3	<0.0001	****	Yes
Subjects (matching)	249613	7	35659	F (7, 21) = 2.669	0.0384	*	Yes
Residual	280613	21	13363				
Level 3							
Interaction	1212739	2	606369	F (2, 14) = 6.746	0.0089	**	No
Lateral Axe	6063707	2	3031854	F (2, 14) = 33.73	<0.0001	****	Yes
Genotype	5026709	1	5026709	F (1, 7) = 30.13	0.0009	***	Yes
Subjects (matching)	1167724	7	166818	F (7, 14) = 1.856	0.1538	ns	No
Residual	1258330	14	89881				

Sidak's multiple comparisons test	Mean 1 (control)	Mean 2 (PIK3CA)	Mean Diff.	SE of diff.	95.00% CI of diff	N1 (control)	N2 (PIK3CA)	t	DF	Adjusted P Value	Summary	Significant?
Level 1												
ACA (control vs PIK3CA)	980	1349	-369.4	214.7	-940.8 to 202	5	4	1.721	28	0.3332	ns	No
MOs (control vs PIK3CA)	369	1541	-1172	214.7	-1743 to -600.3	5	4	5.457	28	<0.0001	****	Yes
MOp (control vs PIK3CA)	201.2	1080	-878.4	214.7	-1450 to -307	5	4	4.091	28	0.0013	**	Yes
SSp (control vs PIK3CA)	104.3	369	-264.7	214.7	-836.1 to 306.7	5	4	1.233	28	0.6445	ns	No
Level 2												
RSP-MO (control vs PIK3CA)	467.5	1866	-1398	92.31	-1644 to -1152	5	4	15.15	28	<0.0001	****	Yes
SSp (control vs PIK3CA)	247.9	1192	-943.9	92.31	-1190 to -698.2	5	4	10.22	28	<0.0001	****	Yes
SSp-bfd(control vs PIK3CA)	150.1	636.6	-486.4	92.31	-732.1 to -240.8	5	4	5.27	28	<0.0001	***	Yes
SSs-AUD (control vs PIK3CA)	205.5	759.8	-554.4	92.31	-800.1 to -308.7	5	4	6.005	28	<0.0001	***	Yes
Level 3												
RSP(control vs PIK3CA)	945.7	2356	-1410	228	-2002 to -819	5	4	6.186	21	<0.0001	****	Yes
VIS (control vs PIK3CA)	242.9	1069	-826.6	228	-1418 to -235.2	5	4	3.625	21	0.0048	**	Yes
AUD (control vs PIK3CA)	439.3	807.4	-368.1	228	-959.5 to 223.2	5	4	1.614	21	0.3217	ns	No

Supplementary Table 3

control vs TSC1

Two ways ANOVA table

	SS	DF	MS	F (DFn, DFd)	P value	Summary	Significant?
Level 1							
Interaction	565981	3	188660	F (3, 21) = 5.459	0.0062	***	Yes
Lateral axe	7267043	3	2422348	F (3, 21) = 70.09	<0.0001	****	Yes
Genotype	583725	1	583725	F (1, 7) = 8.285	0.0237	*	Yes
Subjects (matching)	493194	7	70456	F (7, 21) = 2.039	0.0977	ns	No
Residual	725786	21	34561				
Level 2							
Interaction	217565	3	72522	F (3, 21) = 3.332	0.0391	*	Yes
Lateral axe	971351	3	323784	F (3, 21) = 14.88	<0.0001	****	Yes
Genotype	628213	1	628213	F (1, 7) = 6.887	0.0342	*	Yes
Subjects (matching)	638661	7	91223	F (7, 21) = 4.191	0.0049	**	Yes
Residual	457044	21	21764				
Level 3							
Interaction	32517	2	16258	F (2, 14) = 0.2499	0.7823	ns	No
Lateral Axe	2910455	2	1455227	F (2, 14) = 22.37	<0.0001	****	Yes
Genotype	1694583	1	1694583	F (1, 7) = 17.97	0.0038	**	Yes
Subjects (matching)	660285	7	94326	F (7, 14) = 1.45	0.262	ns	No
Residual	910860	14	65061				

Sidak's multiple comparisons test

	Mean 1 (control)	Mean 2 (TSC1)	Mean Diff.	SE of diff.	95.00% CI of diff	N1 (control)	N2 (TSC1)	t	DF	Adjusted P Value	Summary	Significant?
Delta Np73+/+ - Delta Np73Cre/+TSC1lox/del												
Level 1												
ACA (control vs TSC1)	980	1656	-675.6	140	-1048 to -303.1	5	4	4.827	28	0.0002	***	Yes
MOs (control vs TSC1)	369	3714	-2,356	140	-374.9 to 370.1	5	4	0.01683	28	>0.9999	ns	No
MOp(control vs TSC1)	201.2	356.3	-155.1	140	-527.6 to 217.4	5	4	1.108	28	0.7271	ns	No
SSp (control vs TSC1)	104.3	296.2	-192	140	-564.5 to 180.5	5	4	1.371	28	0.5504	ns	No
Level 2												
RSP-MO (control vs TSC1)	467.5	895.7	-428.2	132.7	-781.4 to -75.1	5	4	3.227	28	0.0126	*	Yes
SSp (control vs TSC1)	247.9	262.7	-14.81	132.7	-368 to 338.3	5	4	0.1116	28	>0.9999	ns	No
SSp-bfd(control vs TSC1)	150.1	508.2	-358	132.7	-711.2 to -4.874	5	4	2.698	28	0.0459	*	Yes
SSs-AUD (control vs TSC1)	205.5	467.8	-262.3	132.7	-615.5 to 90.85	5	4	1.977	28	0.2126	ns	No
Level 3												
RSP (control vs TSC1)	945.7	1548	-602.7	183.5	-1079 to -126.8	5	4	3.285	21	0.0106	*	Yes
VIS (control vs TSC1)	2429	2919	-449	183.5	-924.9 to 26.88	5	4	2.447	21	0.0682	ns	No
AUD (control vs TSC1)	439.3	900.1	-460.8	183.5	-936.7 to 15.09	5	4	2.511	21	0.0596	ns	No

Supplementary Table 3

control vs PTEN*

Multiple t-test	Mean 1 (control)	Mean 2 (PTEN)	Difference	SE of difference	t ratio	df	P value	Summary	Significant?
Level 1									
ACA (control vs PTEN)	980	3005	2025	582.4	3.476	10	0.0059	**	Yes
MOs (control vs PTEN)	369	1084	714.5	258.8	2.761	10	0.0201	*	Yes
MOp (control vs PTEN)	201.2	821.9	620.7	233.8	2.655	10	0.0241	*	Yes
SSp (control vs PTEN)	104.3	666.1	561.8	128.8	4.361	10	0.0014	**	Yes
Level 2									
RSP-MO (control vs PTEN)	205.5	2057	1851	234.1	7.909	10	<0.0001	****	Yes
SSp (control vs PTEN)	150.1	1276	1126	219.1	5.137	10	0.0004	***	Yes
SSp-bfd (control vs PTEN)	467.5	2459	1991	444.6	4.479	10	0.0011	**	Yes
SSs-AUD (control vs PTEN)	247.9	1421	1173	339.4	3.457	10	0.0061	**	Yes
Level 2									
RSP (control vs PTEN)	945.7	3358	2412	680.6	3.544	10	0.0053	**	Yes
VIS (control vs PTEN)	242.9	1253	1010	289.3	3.491	10	0.0058	**	Yes
AUD (control vs PTEN)	439.3	1651	1211	302.4	4.005	10	0.0024	**	Yes

PTEN vs TSC1*

Multiple t-test	Mean 1 (PTEN)	Mean 2 (TSC1)	Difference	SE of difference	t ratio	df	P value	Summary	Significant?
Level 1									
ACA (TSC1 vs PTEN)	3005	1656	1349	653.8	2.063	9	0.0691	*	Yes
MOs (TSC1 vs PTEN)	1084	371.4	712.2	295	2.414	9	0.0389	*	Yes
MOp (TSC1 vs PTEN)	821.9	356.3	465.6	276.3	1.685	9	0.1261	ns	No
SSp (TSC1 vs PTEN)	666.1	296.2	369.9	146.2	2.53	9	0.0322	*	Yes
Level 2									
RSP-MO (TSC1 vs PTEN)	2459	895.7	1563	517.6	3.02	9	0.0144	*	Yes
SSp (TSC1 vs PTEN)	1421	262.7	1159	381.6	3.036	9	0.0141	*	Yes
SSp-bfd (TSC1 vs PTEN)	1276	508.2	767.6	250.5	3.064	9	0.0134	*	Yes
SSs-AUD (TSC1 vs PTEN)	2057	467.8	1589	267.6	5.938	9	0.0002	***	Yes
Level 3									
RSP (TSC1 vs PTEN)	3358	1548	1809	791.4	2.286	9	0.048	*	Yes
VIS (TSC1 vs PTEN)	1253	691.9	561	324.2	1.731	9	0.1175	ns	No
AUD (TSC1 vs PTEN)	1651	900.1	750.5	338.1	2.22	9	0.0535	*	Yes

* Due to inequal variance (larger variation in pten mutants) we used multiple-t-test to compare Pten data to either control ot Tsc1

Supplementary Table 4

ROSTRO-CAUDAL AXE

Quantification of CR fold changes in three neocortex levels : Control vs Mutants (Table 4.1)

	PIK3CA	TSC1	PTEN
	Mean ± SD	Mean ± SD	Mean ± SD
Level 1	2.6 ± 6.07	1.7 ± 2.33	3.64 ± 1.40
Level 2	4.1 ± 3.01	2.03 ± 7.59	6.65 ± 2.08
Level 3	2.6 ± 4.88	1.89 ± 4.20	3.63 ± 1.32

One sample t test	Theoretical mean	Actual mean	Discrepancy	95% CI of discrepancy	t, df	Std. Deviation	Std. Error of Mea	Lower 95% CI of mean	Upper 95% CI of mean	Sum	mber of val	alue (two tail	Significant
Level 1													
PIK3CA	1	2.638	1.638	0.6722 to 2.605	t=5.396 df=3	0.8072	0.3036	1.672	3.605	10.55	4	0.0125	Yes
TSC1	1	1.747	0.7474	0.3764 to 1.118	t=6.412 df=3	0.2331	0.1166	1.376	2.118	6.99	4	0.0077	Yes
PTEN	1	3.645	2.645	1.347 to 3.942	t=4.986 df=6	1.403	0.5303	2.347	4.942	25.51	7	0.0025	Yes
Level 2													
PIK3CA	1	4.154	3.154	2.676 to 3.632	t=20.99 df=3	0.3006	0.1503	3.676	4.632	16.62	4	0.0002	Yes
TSC1	1	2.027	1.027	-0.1807 to 2.234	t=2.706 df=3	0.7588	0.3794	0.8193	3.234	8.107	4	0.0734	No
PTEN	1	6.652	5.652	3.732 to 7.571	t=7.204 df=6	2.076	0.7845	4.732	8.571	46.56	7	0.0004	Yes
Level 3													
PIK3CA	1	2.644	1.644	0.8672 to 2.421	t=6.734 df=3	0.4883	0.2442	1.867	3.421	10.58	4	0.0067	Yes
TSC1	1	1.894	0.8938	0.2254 to 1.562	t=4.255 df=3	0.42	0.21	1.225	2.562	7.575	4	0.0238	Yes
PTEN	1	3.633	2.633	1.414 to 3.852	t=5.285 df=6	1.318	0.4981	2.414	4.852	25.43	7	0.0019	Yes

Quantification of CR fold changes between levels in mutants

RM one way ANOVA table	SS	DF	MS	F (DFn, DFd)	P value	P value summary	ificant (alpha=0.05)?
PIK3CA							
Level	6.102	2	3.051	F (1.174, 3.521) = 21.24	0.0127	*	Yes
Matching	1.231	3	0.4103	F (3, 6) = 2.857	0.1268	ns	No
Residual (random)	0.8617	6	0.1436				
Total	8.195	11					
TSC1							
Level	0.1561	2	0.07806	F (1.643, 4.929) = 0.702	0.5121	ns	No
Matching	1.753	3	0.5844	F (3, 6) = 5.26	0.0407	*	Yes
Residual (random)	0.6666	6	0.1111				
Total	2.576	11					
PTEN							
Level	42.37	2	21.18	F (1.229, 7.371) = 39.1	0.0002	***	Yes
Matching	41.58	6	6.931	F (6, 12) = 12.79	0.0001	***	Yes
Residual (random)	6.501	12	0.5418				
Total	90.45	20					

Supplementary Table 4

MEDIO-LATERAL AXE in three neocortex levels

Quantification of CR fold changes P24 _ Control vs Mutants (Table 4.2)

	PIK3CA	TSC1	PTEN
	Mean ± SD	Mean ± SD	Mean ± SD
Level 1			
ACA	1.3±0.4	1.6 ± 0.30	3.0 ± 1.28
Mos	4.1 ± 1.08	1.0 ± 0.60	2.9 ± 1.50
Mop	5.3 ± 3.07	1.7 ± 1.26	4.0 ± 2.53
SSp	3.5 ± 0.79	2.84 ± 0.48	6.3 ± 2.72
Level 2			
RSP-MO	3.9± 0.29	1.9 ± 0.93	5.2 ± 2.06
SSp	4.8 ± 0.58	1.0 ± 0.53	5.8 ± 3.0
SSp-bfd	4.2 ± 0.78	3.3 ± 0.84	8.5 ± 3.20
SSs-AUD	3.6 ± 0.58	2.2 ± 0.85	10.0± 2.47
Level 3			
RSP	2.5 ± 0.76	1.6± 0.60	3.5 ± 1.57
VIS	4.4 ± 1.26	2.9 ± 0.50	5.1 ± 2.56
AUD	1.9 ± 0.5	2.0 ± 0.18	3.8 ± 1.50

Quantification of CR fold changes in the different areas of the level 1_P24 _ Control vs Mutants

One sample t test														
ACA	Theoretical mean	Actual mean	Discrepancy	95% CI of discrepancy	t, df	Std. Deviation	Std. Error of Mea	Lower 95% CI of mean	Upper 95% CI of mean	Sum	mber of va	lue (two tai	ficant (alpha=	value summa
PIK3CA	1	1.377	0.3769	-0.3876 to 1.141	t=1.569, df=3	0.4805	0.2402	0.6124	2.141	5.508	4	0.2147	No	ns
TSC1	1	1.689	0.6894	0.1644 to 1.214	t=4.179, df=3	0.3293	0.1649	1.164	2.214	6.758	4	0.025	Yes	*
PTEN	1	3.066	2.066	0.8796 to 3.252	t=4.261, df=6	1.283	0.4848	1.88	4.252	21.46	7	0.0053	Yes	**
Mos														
PIK3CA	1	4.175	3.175	1.455 to 4.896	t=5.874, df=3	1.081	0.5405	2.455	5.896	16.7	4	0.0098	Yes	**
TSC1	1	1.006	0.006385	-0.9446 to 0.9574	t=0.02137, df=3	0.5977	0.2988	0.05539	1.957	4.026	4	0.9843	No	ns
PTEN	1	2.936	1.936	0.5454 to 3.327	t=3.406, df=6	1.504	0.5685	1.545	4.327	20.55	7	0.0144	Yes	*
Mop														
PIK3CA	1	5.366	4.366	-0.5213 to 9.254	t=2.843, df=3	3.071	1.536	0.4787	10.25	21.46	4	0.0655	No	ns
TSC1	1	1.771	0.771	-1.232 to 2.774	t=1.225, df=3	1.259	0.6295	-0.2324	3.774	7.084	4	0.3081	No	ns
PTEN	1	4.085	3.085	0.7445 to 5.427	t=3.225, df=6	2.531	0.9567	1.744	6.427	28.6	7	0.018	Yes	*
SSp														
PIK3CA	1	3.538	2.538	1.278 to 3.799	t=6.407, df=3	0.7924	0.3962	2.278	4.799	14.15	4	0.0017	Yes	**
TSC1	1	2.841	1.841	1.084 to 2.597	t=7.744, df=3	0.4754	0.2377	2.084	3.597	11.36	4	0.0045	Yes	**
PTEN	1	6.388	5.388	2.873 to 7.902	t=5.243, df=6	2.719	1.028	3.873	8.902	44.71	7	0.0019	Yes	**

Quantification of CR fold changes between areas of of level 1 in mutants

R.M one way ANOVA table	SS	DF	MS	F (DFn, DFd)	P value	P value summary	ificant (alpha=0.05)?
PIK3CA							
Area	33.58	3	11.19	F (1.121, 3.364) = 5.416	0.0924	ns	No
Matching	15.78	3	5.261	F (3, 9) = 2.546	0.1213	ns	No
Residual (random)	18.6	9	2.067				
Total	67.96	15					
TSC1							
Area	6.893	3	2.298	F (1.257, 3.770) = 4.086	0.1169	ns	No
Matching	1.771	3	0.5903	F (3, 9) = 1.050	0.4169	ns	No
Residual (random)	5.061	9	0.5623				
Total	13.72	15					
PTEN							
Area	53.59	3	17.86	F (1.719, 10.31) = 5.743	0.0242	*	Yes
Matching	50.24	6	8.374	F (6, 18) = 2.692	0.0481	*	Yes
Residual (random)	55.99	18	3.11				
Total	159.8	27					

Supplementary Table 4

Quantification of CR fold changes in the different areas of the level 2_P24_ Control vs Mutants

One sample t test	Theoretical mean	Actual mean	Discrepancy	95% CI of discrepancy	t, df	Std. Deviation	Std. Error of Mea	Lower 95% CI of mean	Upper 95% CI of mean	Sum	mber of val	alue (two tail	ificant (alpha=0	value summa
RSP-MO														
PIK3CA	1	4.807	3.807	2.896 to 4.718	t=13.30, df=3	0.2832	0.1416	3.54	4.441	15.96	4	0.0009	Yes	***
TSC1	1	1.06	0.05973	-0.7939 to 0.9134	t=0.2227, df=3	0.9306	0.4653	0.4353	3.397	7.864	4	0.8381	No	ns
PTEN	1	5.734	4.734	1.974 to 7.493	t=4.197, df=6	2.061	0.7789	3.354	7.166	36.82	7	0.0057	Yes	**
SSp														
PIK3CA	1	4.807	3.807	2.896 to 4.718	t=13.30, df=3	0.5725	0.2862	3.896	5.718	19.23	4	0.0009	Yes	***
TSC1	1	1.06	0.05973	-0.7939 to 0.9134	t=0.2227, df=3	0.5365	0.2682	0.2061	1.913	4.239	4	0.8381	No	ns
PTEN	1	5.734	4.734	1.974 to 7.493	t=4.197, df=6	2.984	1.128	2.974	8.493	40.14	7	0.0057	Yes	**
SSp-bfd														
PIK3CA	1	4.24	3.24	2.010 to 4.470	t=8.383, df=3	0.773	0.3865	3.01	5.47	16.96	4	0.0036	Yes	**
TSC1	1	3.385	2.385	1.033 to 3.736	t=5.617, df=3	0.8491	0.4245	2.033	4.736	13.54	4	0.0112	Yes	*
PTEN	1	8.497	7.497	4.533 to 10.46	t=6.190, df=6	3.204	1.211	5.533	11.46	59.48	7	0.0008	Yes	***
SSs-AUD														
PIK3CA	1	3.698	2.698	1.777 to 3.619	t=9.322, df=3	0.5789	0.2895	2.777	4.619	14.79	4	0.0026	Yes	**
TSC1	1	2.277	1.277	-0.07697 to 2.630	t=3.001, df=3	0.8507	0.4254	0.923	3.63	9.107	4	0.0576	No	ns
PTEN	1	10.01	9.01	6.723 to 11.30	t=9.640, df=6	2.473	0.9346	7.723	12.3	70.07	7	<0.0001	Yes	****

Quantification of CR fold changes between areas of of level 2 in mutants

RM one way ANOVA table	SS	DF	MS	F (DFn, DFd)	P value	P value summary	ificant (alpha=0.05)?
PIK3CA							
Area	2.66	3	0.8866	F (1.837, 5.511) = 3.410	0.1102	ns	No
Matching	1.682	3	0.5605	F (3, 9) = 2.156	0.1632	ns	No
Residual (random)	2.34	9	0.26				
Total	6.682	15					
TSC1							
Area	11.13	3	3.711	F (2.361, 7.084) = 16.28	0.0019	**	Yes
Matching	5.743	3	1.914	F (3, 9) = 8.398	0.0056	**	Yes
Residual (random)	2.052	9	0.228				
Total	18.93	15					
PTEN							
Area	107.6	3	35.87	F (2.004, 12.03) = 10.34	0.0024	**	Yes
Matching	114.7	6	19.12	F (6, 18) = 5.512	0.0022	**	Yes
Residual (random)	62.46	18	3.47				
Total	284.8	27					

Supplementary Table 4

Quantification of CR fold changes in the different areas of the level 3_P24_Control vs Mutants

One sample t test	Theoretical mean	Actual mean	Discrepancy	95% CI of discrepancy	t, df	Std. Deviation	Std. Error of Mean	Lower 95% CI of mean	Upper 95% CI of mean	Sum	mber of values	P value (two tail	ificant (alpha=0.05)?	P value summa
RSP														
PIK3CA	1	4.403	3.403	1.398 to 5.408	t=5.402, df=3	0.7687	0.3844	1.268	3.714	9.965	4	0.0124	Yes	*
TSC1	1	2.849	1.849	1.045 to 2.653	t=7.318, df=3	0.64	0.32	0.6189	2.656	6.549	4	0.0053	Yes	**
PTEN	1	5.158	4.158	1.769 to 6.548	t=4.259, df=6	1.571	0.5939	2.097	5.003	24.85	7	0.0053	Yes	**
VIS														
PIK3CA	1	4.403	3.403	1.398 to 5.408	t=5.402, df=3	1.26	0.63	2.398	6.408	17.61	4	0.0124	Yes	*
TSC1	1	2.849	1.849	1.045 to 2.653	t=7.318, df=3	0.5052	0.2526	2.045	3.653	11.39	4	0.0053	Yes	**
PTEN	1	5.158	4.158	1.769 to 6.548	t=4.259, df=6	2.583	0.9764	2.769	7.548	36.11	7	0.0053	Yes	**
AUD														
PIK3CA	1	1.838	0.838	0.02454 to 1.651	t=3.278, df=3	0.5112	0.2556	1.025	2.651	7.352	4	0.0465	Yes	*
TSC1	1	2.049	1.049	0.7625 to 1.335	t=11.65, df=3	0.18	0.09001	1.763	2.335	8.196	4	0.0014	Yes	**
PTEN	1	3.757	2.757	1.371 to 4.143	t=4.868, df=6	1.498	0.5664	2.371	5.143	26.3	7	0.0028	Yes	**

Quantification of CR fold changes between areas of of level 3 in mutants

RM one way ANOVA table	SS	DF	MS	F (DFn, DFd)	P value	P value summary	ificant (alpha=0.05)?
PIK3CA							
Area	14.22	2	7.108	F (1.167, 3.501) = 11.33	0.0333	*	Yes
Matching	3.554	3	1.185	F (3, 6) = 1.888	0.2326	ns	No
Residual (random)	3.765	6	0.6276				
Total	21.54	11					
TSC1							
Area	3.035	2	1.518	F (1.124, 3.373) = 8.073	0.0563	ns	No
Matching	0.9639	3	0.3213	F (3, 6) = 1.709	0.2637	ns	No
Residual (random)	1.128	6	0.188				
Total	5.127	11					
PTEN							
Area	10.71	2	5.357	F (1.447, 8.679) = 2.973	0.1127	ns	No
Matching	46.7	6	7.784	F (6, 12) = 4.320	0.0150	*	Yes
Residual (random)	21.62	12	1.802				
Total	79.04	20					

Supplementary Table 5

Quantification of volume (Table 5)		
	Control	PTEN
	Mean ± SD	Mean ± SD
volume (control vs PTEN)	382.5± 221.5	1144.5±644.4

Mann-Whitney U test	*Two-tailed p* value	U	Significant (alpha=0.05)?	P value summary
volume (control vs PTEN)	<0.0001	128	Yes	****

Quantification of Reelin intensity (Table 5)		
	Control	PTEN
	Mean ± SD	Mean ± SD
RLEN intensity (control vs PTEN)	176± 93.87	348.8 ±246.3

Mann-Whitney U test	*Two-tailed p* value	U	Significant (alpha=0.05)?	P value summary
RLEN intensity (control vs PTEN)	0.0026	442	Yes	**

Quantification of layers in the SSp-bfd (µm) (Table 5)		
	Control	PTEN
	Mean ± SD	Mean ± SD
Layer 1	92.9± 9.8	88.2 ±8.5
Layer 2/3	351.9± 39.9	308.4± 18.8
Layer 4	179.5± 20.5	172.8 ±9.7
Layer 5	310.2± 24.1	285.7 ±12.1
Layer 6	328.4± 29.0	319.8 ±29.7

Mann-Whitney U test	*Two-tailed p* value	U	N Control	N PTEN	Significant (alpha=0.05)?	P value summary
Layer 1	0.2302	4.5	4	5	No	ns
Layer 2/3	0.1111	3	4	5	No	ns
Layer 4	0.4127	6	4	5	No	ns
Layer 5	0.127	3.5	4	5	No	ns
Layer 6	0.9048	9	4	5	No	ns

Supplementary Table 6 and 7

Patch-Cell recording (Table 6)

	Mean ± SEM		
Intrinsic Properties	Control (n=14)	PTEN (n=12)	paired t -test (p value)
Vm (mV)	-50.3 ± 0.43	-46.7 ± 0.88	0.0095
Rm (MOhms)	1290.7 ± 98.8	745.65 ± 152.5	0.0379
Cm (pF)	21.15 ± 1.06	48.34 ± 2.23	< 0.0001

Action Potentials (AP)			
Frequency	Control (n=14)	PTEN (n=12)	anova 2 ways
10	0 ± 0	0 ± 0	>0.9999
20	1.7± 1.28	0.42 ± 0.42	>0.9999
30	5.8 ± 2.30	2 ± 1.17	0.9788
40	8.9 ± 2.53	7 ± 1.70	>0.9999
50	9.36 ± 2.15	11.4 ± 2.11	>0.9999
60	10 ± 2.41	15.4 ± 2.51	0.9105
70	11.4 ± 3.13	20.2 ± 2.32	0.2774
80	12.4 ± 3.37	23.3 ± 2.35	0.0427
90	13.5 ± 4.08	27.1 ± 2.46	0.0069
100	15.4 ± 5.07	29.7 ± 2.49	0.0039
110	15.2± 5.74	32.8 ± 2.31	0.001
120	17.1 ± 5.24	34.3 ± 1.91	0.0002

Amplitude (mV)	Control (n=14)	PTEN (n=12)	anova 2 ways
1	1.2 ± 2.22	77.3 ± 1.73	P < 0.0001
2	44.9 ± 1.84	74.6 ± 2.03	P < 0.0001
3	41.7 ± 2.79	73.5 ± 2.08	P < 0.0001
4	40.0 ± 2.45	72.4 ± 2.38	P < 0.0001
5	36.5 ± 2.56	71.9 ± 2.47	P < 0.0001

	Control (n=14)	PTEN (n=12)	paired t -test (p value)
Threshold (mV)	-41.05 ± 5.47	-44.505 ± 1.2	0.0434
Halfwidth (ms)	2.65 ± 0.11	1.53 ± 0.05	0.0001
Latency (ms)	98.138 ± 23.6	246.2 ± 36.3	0.0128

MEA (Table 7)

Type of activity				
Fisher's exact test	*p* value	odds ratio	cant (alpha=	value summary
two-sided	1	0.9231	No	ns

Burst properties							
unpaired t-test	*wo-tailed p* val	N (CTR)	N (PTEN)	R) Mean ± S	N) Mean ± S	cant (alpha=	value summa
burst frequency	0.9739	13	14	.735 ± 0.733	.776 ± 0.993	No	ns
burst duration	0.5072	13	14	.651 ± 0.179	.854 ± 0.239	No	ns

Supplementary Table 8

Behavior analysis (Tab.8)

Y-Maze Spontaneous Alternation

D'Agostino & Pearson normality te	K2	P value	Passed normality test (alpha=	P value summary
Control Female	0.8746	0.6458	Yes	ns
PTEN Female	3.64	0.162	Yes	ns
Control Male	0.3284	0.8486	Yes	ns
PTEN Male	1.706	0.426	Yes	ns

One sample t test	Theoretical mean	Actual mean	Discrepancy	95% CI of discrepan	t, df	P value (two tailed)	Significant (alpha=0.05)?
Control Female	50	60.8	10.8	7.398 to 14.19	t=6.628, df=20	<0.0001	Yes
PTEN Female	50	63.69	13.69	8.162 to 19.22	t=5.251, df=16	<0.0001	Yes
Control Male	50	61.13	11.13	6.126 to 16.13	t=4.742, df=15	0.0003	Yes
PTEN Male	50	60.84	10.84	6.972 to 14.72	t=5.937, df=16	<0.0001	Yes

Vertical activity

Two ways ANOVA table	SS (Type III)	DF	MS	F (DFn, DFd)	P value	P value summary	Significant?
Rearing 10 minutes							
Interaction	636	1	636	F (1, 59) = 0.6630	0.4188	ns	No
sex	216.9	1	216.9	F (1, 59) = 0.2261	0.6362	ns	No
genotype	3798	1	3798	F (1, 59) = 3.960	0.0512	ns	No
Residual	56595	59	959.2				
Rearing 50 minutes							
Interaction	4029	1	4029	F (1, 59) = 0.1807	0.6723	ns	No
sex	7668	1	7668	F (1, 59) = 0.3439	0.5598	ns	No
genotype	110553	1	110553	F (1, 59) = 4.958	0.0298	*	Yes
Residual	1315485	59	22296				

Sidak's multiple comparisons test	Mean 1 (Control)	Mean 2 (PTEN)	Mean Diff.	SE of diff.	95.00% CI of diff.	N1 (Control)	N2 (PTEN)	t	DF	justed P Va	Summary	Significant?
Rearing 10 minutes												
Female Control vs PTEN	98.27	76.35	21.91	10.97	-3.264 to 47.09	15	17	1.997	59	0.0983	ns	No
Male Control vs PTEN	88.19	79	9.188	11.13	-16.36 to 34.73	16	15	0.8254	59	0.6548	ns	No
Rearing 50 minutes												
Female Control vs PTEN	399.7	299.8	99.91	52.9	-21.47 to 221.3	15	17	1.889	59	0.1236	ns	No
Male Control vs PTEN	405.8	337.9	67.88	53.67	-55.27 to 191	16	15	1.265	59	0.3773	ns	No

Horizontal Activity

Multiple t-test	Mean 1 (Control)	Mean 2 (PTEN)	Difference	SE of difference	t ratio	df	P value	Summary	Significant?
Rearing Total Activity 10 minutes									
Female	3334	2768	566.4	327.6	1.729	35	0.0926	ns	No
Male	2632	2266	366	324.5	1.128	29	0.2685	ns	No

Rearing Total Activity 50 minutes

Two way anova ANOVA table	SS (Type III)	DF	MS	F (DFn, DFd)	P value	P value summary	Significant?
Interaction	16947	1	16947	F (1, 64) = 0.00214	0.9632	ns	No
Sex	14897559	1	14897559	F (1, 64) = 1.884	0.1747	ns	No
genotype	26471199	1	26471199	F (1, 64) = 3.347	0.0720	ns	No
Residual	506177882	64	7909029				

Supplementary Table 8

Open field (OF)

OF Entry center

Two way anova ANOVA table	SS (Type III)	DF	MS	F (DFn, DFd)	P value	P value summary	Significant?
Entry center 10min							
Interaction	16.49	1	16.49	F (1, 64) = 0.0843	0.7725	ns	No
Gender	48.45	1	48.45	F (1, 64) = 0.2478	0.6203	ns	No
Genotype	440.1	1	440.1	F (1, 64) = 2.251	0.1385	ns	No
Residual	12514	64	195.5				
Entry center 30 min							
Interaction	46.78	1	46.78	F (1, 64) = 0.0576	0.8111	ns	No
Gender	1593	1	1593	F (1, 64) = 1.962	0.1661	ns	No
Genotype	671.2	1	671.2	F (1, 64) = 0.8267	0.3666	ns	No
Residual	51957	64	811.8				
Entry center 1 h							
Interaction	916.2	1	916.2	F (1, 64) = 0.3509	0.5557	ns	No
Gender	2793	1	2793	F (1, 64) = 1.070	0.3048	ns	No
Genotype	8166	1	8166	F (1, 64) = 3.128	0.0817	ns	No
Residual	167075	64	2611				

OF Total distance

Two way anova ANOVA table	SS (Type III)	DF	MS	F (DFn, DFd)	P value	P value summary	Significant?
OF Total distance 10min							
Interaction	618196	1	618196	F (1, 65) = 0.3654	0.5476	ns	No
Gender	6834416	1	6834416	F (1, 65) = 4.040	0.0486	*	Yes
Genotype	566385	1	566385	F (1, 65) = 0.3348	0.5648	ns	No
Residual	109960040	65	1691693				
OF Total distance 30 min							
Interaction	3908881	1	3908881	F (1, 65) = 0.613	0.4365	ns	No
Gender	6979313	1	6979313	F (1, 65) = 1.094	0.2994	ns	No
Genotype	527564	1	527564	F (1, 65) = 0.08273	0.7745	ns	No
Residual	414506258	65	6377019				
OF Total distance 1 h							
Interaction	17653	1	17653	F (1, 64) = 0.00116	0.9728	ns	No
Gender	4229173	1	4229173	F (1, 64) = 0.2800	0.5985	ns	No
Genotype	4182524O	1	4182524O	F (1, 64) = 2.769	0.1010	ns	No
Residual	966690114	64	15104533				

OF Time in the center

Two way anova ANOVA table	SS (Type III)	DF	MS	F (DFn, DFd)	P value	P value summary	Significant?
OF Time center 10 min							
Interaction	63.08	1	63.08	F (1, 63) = 0.1705	0.6811	ns	No
Gender	40.62	1	40.62	F (1, 63) = 0.1098	0.7415	ns	No
Genotype	1556	1	1556	F (1, 63) = 4.205	0.0445	*	Yes
Residual	23310	63	370				
OF Time center 30 min							
Interaction	395.3	1	395.3	F (1, 65) = 0.08740	0.7685	ns	No
Gender	3738	1	3738	F (1, 65) = 0.8263	0.3667	ns	No
Genotype	3772	1	3772	F (1, 65) = 0.8339	0.3645	ns	No
Residual	293999	65	4523				
OF Time center 1h min							
Interaction	4576	1	4576	F (1, 64) = 0.3073	0.5813	ns	No
Gender	26821	1	26821	F (1, 64) = 1.801	0.1843	ns	No
Genotype	10887	1	10887	F (1, 64) = 0.7311	0.3957	ns	No
Residual	953003	64	14891				

Sidak's multiple comparisons test	Mean 1 F	Mean 2 M	Mean Diff.	SE of diff.	95.00% CI of diff.	N1	N2	t	DF	Adjusted P Val	Summary	Significant?
Behavior OF Time center 10 min												
PTEN	46.11	49.62	-3.511	6.814	-19.12 to 12.10	17	15	0.5153	63	0.8465	ns	No
Control	57.73	57.35	0.3847	6.527	-14.57 to 15.34	19	16	0.05895	63	0.9978	ns	No

Supplementary Table 8

OF ratio Center to total distance

Two way anova ANOVA table	SS (Type III)	DF	MS	F (DFn, DFd)	P value	P value summary	Significant?
OF ratio 10 min							
Interaction	0.00003316	1	0.00003316	F (1, 64) = 0.02689	0.8703	ns	No
Gender	0.000005945	1	0.000005945	F (1, 64) = 0.004821	0.9449	ns	No
Genotype	0.007357	1	0.007357	F (1, 64) = 5.966	0.0174	*	Yes
Residual	0.07892	64	0.001233				
OF ratio 30 min							
Interaction	0.00001148	1	0.00001148	F (1, 65) = 0.01041	0.9191	ns	No
Gender	0.001375	1	0.001375	F (1, 65) = 1.247	0.2682	ns	No
Genotype	0.001847	1	0.001847	F (1, 65) = 1.675	0.2001	ns	No
Residual	0.07168	65	0.001103				
OF ratio 1h min							
Interaction	0.00001209	1	0.00001209	F (1, 65) = 0.01495	0.9030	ns	No
Gender	0.0005724	1	0.0005724	F (1, 65) = 0.7078	0.4033	ns	No
Genotype	0.003107	1	0.003107	F (1, 65) = 3.843	0.0543	ns	No
Residual	0.05257	65	0.00080887				

Sidak's multiple comparisons test	Mean 1 F	Mean 2 M	Mean Diff.	SE of diff.	95.00% CI of diff.	N1	N2	t	DF	Adjusted P Value	Summary	Significant?
Behavior OF ratio 10 min												
PTEN	0.132	0.13	0.001999	0.01244	-0.02649 to 0.03049	17	15	0.1607	64	0.9838	ns	No
Control	0.1515	0.1523	-0.00081	0.01178	-0.02778 to 0.02616	20	16	0.06877	64	0.997	ns	No

kainate injection

PTEN								
Mann-Whitney U test	Two-tailed p value	U	(Control) Mean ± SD	N (Control)	(PTEN) Mean ± SD	N (PTEN)	Significant (alpha=0.05)?	P value summary
latency								
Females	0.0628	6	69.6 ± 4.28 (10)	5	26.2 ± 1.37 (10)	6	No	ns
Males	0.3636	10	55.5 ± 4.43 (10)	4	43.1 ± 4.8(10)	8	No	ns
Duration								
Females	0.1732	7	1.4 ± 3.15	5	12.6 ± 1.9 (10)	6	No	ns
Males	0.6848	13	2.3 ± 2.63	4	3.7 ± 4.5	8	No	ns
Number of occurance								
Females	0.2706	8.5	1.2 ± 1.30	5	3.6 ± 4.63	6	No	ns
Males	0.7818	14	2.5 ± 2.38	4	1.8 ± 1.95	8	No	ns

PIK3CA								
Mann-Whitney U test	Two-tailed p value	U	(Control) Mean ± SD	N (Control)	(PIK3CA) Mean ± SD	N (PIK3CA)	Significant (alpha=0.05)?	P value summary
latency								
Females	0.753	24	17 ± 9.17	6	17.8 ± 9.34	9	No	ns
Males	0.7902	22	86.0 ± 4.80 (10)	8	89.5 ± 4.73(10)	6	No	ns
Duration								
Females	0.0076	5	28.2± 2.51(10)	6	75.2 ± 3.04 (10)	9	Yes	**
Males	0.7902	22	6.5 ± 1.09 (10)	8	17.05 ± 2.65 (10)	6	No	ns
Number of occurance								
Females	0.3794	19.5	1.8 ± 0.98	6	2.8 ± 2.02	9	No	ns
Males	0.8741	22.5	2.1 ± 3.22	8	2.8 ± 4.40	6	No	ns

DISCUSSION

During my PhD, I investigated the Role of PI3K/AKT/mTOR pathway in programmed cell death of deltaNp73 derived CRs.Moreover, I explored the contribution of CRs persistence in the formation or malformation of cortical circuits and the system's susceptibility to seizure development.

1. The spatiotemporal activity of PI3K/AKR/mTOR pathway as possible mechanisms explaining the disappearance of deltaNP73 derived CRs

In the developing cortex, CRs are among the very first generated transient neurons (Hevner et al., 2003; Radnikow et al., 2002a; Zecevic & Rakic, 2001). According to their origin, CRs are divided into 4 subpopulations(Ruiz-Reig et al., 2017; Tissir et al., 2009) , which based on that preferentially populate distinct cortical territories: SE-CRs is located in the rostro-medial, PSB mainly in the rostro-lateral cortex, CH in the medio-caudal, and ET the entorhinal and piriform cortex laterally (Barber & Pierani, 2016; Bielle et al., 2005; Griveau et al., 2010; Meyer, 2010; Tissir et al., 2009). Despite their common morphology, CRs subpopulations are not a uniform population and the dynamic of their disappearance differs temporally and spatially (Barber & Pierani, 2016; Bielle et al., 2005; Griveau et al., 2010; Meyer, 2010; Tissir et al., 2009). persistence of CR-like cells has been described in some pathological conditions associated with epilepsy (Eriksson et al. 2001; Blumcke et al. 1999; Garbelli et al. 2001), because of these observations, it is necessary to investigate the persistence of CRs as a potential cause or effect of these diseases. In this study, we investigated the role of the PI3K/Akt/mTOR pathway as one of the potential cell survival signals in the modulation of PCD in CRs.

Spatial analysis of the PI3K/AKT/mTOR pathway in the medio-lateral axis in CRs confirmed that this pathway does not behave in a linear manner, which means upon the activity of PI3K/AKT we do not necessarily observe the activity of mTOR. CRs which are located in the medial part of the cortex show more PI3K/AKT pathway activation whereas lateral CR has more activation of the mTOR pathway. This suggests that the position of the cell in the cortex can affect its molecular properties. This has nicely shown that hippocampal CRs are derived from the CH, die way later than neocortical CRs drive from the same origin

suggesting the significance of the environment for the survival of CRs of the same lineage (Bielle et al., 2005a).

In addition, investigation of the PI3K/Akt/mTOR pathway as one of the potential survival signals in a temporal manner in CRs revealed that overall activity of this pathway significantly decreases after birth and at P1 which is about the same time that the expression of deltaNp73 (P0) begins to decrease (Tissir et al., 2009). According to a temporal sequence of PCD, the most significant change in the number of cortical cells occurs in mice between the first and second postnatal weeks (Causeret et al., 2018, 2021; Verney et al., 2000; Wong & Marín, 2019; Y. Yamaguchi & Miura, 2015). The first two weeks of postnatal development in rodents' cerebral cortex are characterized by the formation of mature activity patterns and the modification of embryonic connections and structures (Blanquie, Liebmann, et al., 2017; Blanquie, Yang, et al., 2017; Butt et al., 2017), as well as the establishment of mature patterns of activity (Allene & Cossart, 2010; Khazipov & Luhmann, 2006; Luhmann & Khazipov, 2018). Nevertheless, it is now known that different populations of cortical cells are being unevenly affected by PCD, leading to the complete eradication of entire populations of transitory cells (Causeret et al., 2018, 2021). In line with that, it has been demonstrated from our lab by Riva et al. that the formation of this early electrical activity plays an important role in the elimination of CRs (Riva et al., 2019). A decrease in the expression of NKCC1 and a strong expression of the co-transporter K+/Cl- co-transporter (KCC2) are observed in mice during the first week after birth, which extrude Cl- together with a Na+ ion resulting in low concentration of Cl- inside the cells. Following the fixation of its ligand, the opening of the GABAA receptor will allow the chlorine to enter via an osmotic gradient, resulting in neuron hyperpolarization (Ben-Ari, 2002). The exception is the CRs, which, according to Menville, continue to be depolarized by GABA until at least P13 in the rat. The fact that CRs do not express KCC2 at P11, whereas interneurons and pyramidal neurons express this co-transporter strongly at this stage (J.-M. Mienville, 1998; Pozas et al., 2008). This can lead to the excitotoxicity in CRs. The following scenario may be the cause of CR cell death in this context. It has been shown that excitotoxicity can induce c-Jun N-terminal kinase activation, which triggers the neuronal death (Centeno et al., 2007). On the other hand, it has been demonstrated that deltaNp73 which serves as anti-apoptotic factor

and plays a critical role in CRs survival, is degraded in a c-Jun-dependent manner upon stress through proteasome-dependent mechanism (Dulloo et al., 2010). Eventually, upon degradation of deltaNp73, PTEN can be free from antagonize activity of deltaNp73 and resume its function as a negative regulator of the PI3K/AKT/mTOR pathway (Vella et al., 2009b). In addition, pro-apototic form of p73, TAp73, also will get free from inhibiting the activity of deltaNp73 and can induce cell death. Altogether, the chain of these events can speed up CRs death.

2. Maintenance of the PI3K/AKT/mTOR activity mediates persistence of CRs after birth

In this study via genetic tools, we generated 3 different mouse models associated with PI3K/AKT and mTOR pathways by targeting positive (PIK3CA) and negative regulators of this large pathway (PTEN and TSC1). In all 3 models, the development of the cortex and CRs occurred as normal situation, suggesting that this over-activation of this pathway in CRs does not interfere with the correct development of the cortex. Overall in all models, we observed the persistence of CRs after the time point of cell death suggesting the critical role of this pathway as a protective signal against cell death in CRs. Interestingly the portion of the persistent cell was different in each model highlighting the distinct role of each of these molecules in cell survival despite their close collaboration. The observed difference can be explained through a more detailed view of possible downstream factors of each molecule. Through activating PIK3CA, we mainly targeted activation of Akt as an anti-apoptotic factor that prevents cell death triggered by both extrinsic and intrinsic signals from happening either directly or indirectly (Shaw & Cantley, 2006). It has been demonstrated that Akt interferes with cell death pathways by phosphorylating key apoptosis-regulatory proteins and shifts the ratio of pro- and anti-apoptotic proteins toward the inhibition of cell death. One procedure in that Akt directly interferes with intrinsic cell death mechanism is through phosphorylating pro-apoptotic proteins, which reduces their activity, for instance: Ser184 in BAX (Gardai et al., 2004; H. Yamaguchi & Wang, 2001) , Ser 87 of Bim (Qi et al., 2006), also Bad, HtrA2 and Caspase 9 (Parcellier et al., 2008). In addition to phosphorylating important signal transduction molecules, which directly interfere with cell death signaling pathways,

Akt has also been observed to indirectly interfere with cell death programs by phosphorylating TFs or molecules involve in their control.

Some of the well-known transcription factors involved in tumor suppressing are p53 and p73 which are crucial for controlling the cell cycle and the initiation of apoptosis. AKT modulates the activity of p53 and p73 mainly through MDM2, which significantly controls p53 and p73 activity via different approaches. AKT- mediated phosphorylation of MDM2's Ser 183 is a key step involved in the protein stability of MDM2 as we as its nuclear translocation (Bálint et al., 1999; Boyd et al., 2000; Chibaya et al., 2021; Honda et al., 1997; Killick et al., 2011; Stad et al., 2000; Zeng et al., 1999).

It has been demonstrated that deltaNp73 is degraded in a c-Jun-dependent manner upon toxic stress (Dulloo et al., 2010). Akt can inhibit the JNK activation that is induced by stress and cytokines through antagonizing and the formation of the JIP1-JNK module as well as the activities of upstream kinases such as ASK1, MKK4/7 (H.-F. Zhao et al., 2015). Besides that, AKT mediates phosphorylation of transcription factors such as FOXO1, FOXO3a, FOXO4, and FOXO6 as well as the NF-kB (Fulda, 2012). When forkhead TFs become phosphorylated by AKT, their transcriptional activity is stopped by cytosolic sequestration. In turn, this leads to a decrease in the production of pro-apoptotic proteins, such as Bim, Noxa, tumor necrosis factor TRAIL, and FAS ligand, which are known to be controlled by forkhead TFs (Van Der Heide et al., 2004). As a result of transcription factor NF-KB phosphorylation it transactivates IAPs proteins, Bcl-XL, and Bcl-2 (Ozes et al., 1999; Romashkova & Makarov, 1999).

Upon activation of PIk3CA in our model, persisted CRs maintained their typical morphology but showed an increase in their soma size which was expected from activation of the mTOR pathway, downstream of PI3K. Besides that, they demonstrated a slight increase in RELN expression in a not homogenous manner.

However, conditional inactivation of PTEN, resulted in a higher number of persisted CRs in the neocortex in comparison to PIK3CA. this can be explained through PTEN's role in the control of cell death independent from the PI3K pathway. For instance: it can, directly and indirectly, regulate the activity of p53. Directly via antagonizes the p53-MDM2 interaction and also promotes p300/CBP-mediated acetylation of p53 for stabilizing the protein (Ito et

al., 2001, p. 2; Nakanishi et al., 2014). Indirectly through downregulation of PI3K which eventually leads to a lack of MDM2 phosphorylation by AKT as well as a decrease in expression of MDM2 (Chibaya et al., 2021).

It has been demonstrated that p73α and PTEN proteins can directly bind to one another after DNA damage and form a p73/PTEN complex in the nucleus. The formation of this complex has been associated with the induction of PUMA/Bax. This mechanism initiates apoptosis independently from p53 (Lehman et al., 2011). Besides that, PTEN is a crucial mediator of mitochondria-dependent apoptosis. Dephosphorylates NKAP which leads to suppression of NF-κB (Chatterjee et al., 2019; Vasudevan et al., 2004)

Besides the difference in the number of observed CRs in the PTEN model, the morphology of cells was drastically changed, cells get significantly bigger with more dendritic branches and in some cases, they completely changed their bipolar morphology to a dysmorphic neuron. This can be associated with PTEN interaction with the structural, accessory, or regulatory proteins of the actin cytoskeleton. Although the direct effects of PTEN activity or actin cytoskeleton function are typically unknown (Kim et al., 2011). In addition, CRs were expressing significantly higher amounts of reelin both at the P1 and P24 stages with the track of the reelin expression in the extracellular matrix at P1. It seems that an increase in the reelin expression by CRs into extracellular matrix consequently activated PI3K/AKT/mTOR through the DAB-1 mechanism (Jossin & Goffinet, 2007a) in the neighboring pyramidal neurons.

It has been demonstrated that the mTOR pathway (downstream of AKT) is involved in the control of autophagy. Autophagy is happening to maintain the homeostasis inside the cell through the elimination of damaged organelles, aged proteins, misfolded proteins, or cytoplasmic cargo in a lysosome-mediated degradation (Noguchi et al., 2020). However, autophagic cell death, on the other hand, will take place under unfavourable circumstances like infection, oxidative stress, or a lack of nutrients (Denton & Kumar, 2019; S. Jung et al., 2020). It has been demonstrated that there is a cross-talk between apoptosis and autophagy more likely through Atgs. Calpain-mediated cleavage of Atg5, for instance, which is known to initiate autophagy, transforms autophagy into apoptosis (Rubinstein et al., 2011). Atg12 regulates the apoptotic pathway by binding to and inactivating two anti-apoptotic members

of Bcl-2 family, MCL-1 and BCL-2 (Rubinstein et al., 2011). To test whether autophagy contributes to CRs cell death we targeted activation of mTORC1 via deletion of TSC1. Despite the increase in the number of CRs from the medial to the caudal part of the brain, CRs could not get even close to the number of cells observed in PTEN or PIK3CA models. Suggesting that activation of the mTOR pathway does not contribute much to the persistence of CRs. In addition, cells were showing normal morphology of CRs with and slightly increase in their size and reelin expression.

3. The outcome of CR persistence is associated with the mechanism which mediated their survival

Further investigation on persisted CRs mediated by the inactivation of PTEN, showed that these cells are perfectly active. However, we could not find any trace associated with dysfunction of neuronal circuit or increase in the susceptibility to develop seizures. This was quite surprising to us as, in theory, PTEN and Bax inactivation should have similar secondary phenotypes linked to CR persistence. They have similar increases in cell densities, about 5 times. However, the Bax model presents with an increase of dendrites and dendritic spine in upper pyramidal neurons which lead to an alteration of the excitatory/inhibitory balance and hyperexcitability together with an increase in sensitivity to kainate-induced epilepsy. Although we did not investigate the morphological changes of these pyramidal cells in the Pten model, neuronal network activity is unaffected in the S1 barrel cortex and Pten animals do not present sensitivity to epilepsy. The mechanism by which rescued CRs in bax model induces morphological and functional changes in pyramidal neurons remains unresolved. Reelin has been shown to counteract the inhibitory effects of chondroitin sulfate proteoglycan (CSPG) on dendritic growth in the MZ by activating the AKT pathway in pyramidal neurons (Zluhan et al., 2020). Recently in several studies increase of the reelin in the system has been possibly associated with the prevention of certain behavioural phenotypes related to schizophrenia, bipolar disorder (Teixeira et al., 2011b), and even epilepsy (Kiroski et al., 2020).

Therefore, one hypothesis to explain the discrepancies between Bax and Pten models would be the different levels of Reelin secretion. However, we found in our study that the

Reelin secretion is increased in the Pten model together with an increase of pS6 staining in the cortex, suggesting the PI3K/AKT/mTOR pathway is activated in pyramidal cells after reelin binding to its receptor. Thus this hypothesis is unlikely but we need to compare it with Reelin secretion in the Bax model to conclude. Alternatively, Pten inactivation also leads to morphological changes in CRs which are not observed in the Bax model. They have more dendrites linked to AKT activation and bigger soma size due to mTOR activation. These changes alter the intrinsic properties of CRs which also respond with larger depolarization to the current application. Differences in the intrinsic properties and in neuronal activity may explain the different outcomes between Bax and Pten models similar to the Kir1.3 model in which induced hyperpolarization of CRs increased the CR densities without altering the morphology nor the excitability of underneath pyramidals neurons (Riva et al., 2019).
Our results suggest that the outcome of CR persistence is associated with the mechanism which mediates their survival, as it can strongly alter the internal molecular profile of persisted cells and in the case of CRs which are well known for their secretion properties, other neighbouring cells.

4. Conclusion and Perspectives

The result from my PhD project revealed the existence of spatiotemporal regulation of the PI3K/AKT/mTOR pathway in the deltaNp7-derived CRs. Considering the fact that this Cre line targets two main sub-populations of CRs Hem and Septum it would be interesting to investigate whether this regulation is applicable for both sub-populations by repeating the same experiment with Wnt3a Cre which is only supposed to target hem-derived CRs

In this study through the generation of 3 mouse models for conditional activation of the pathway, I showed a differential pattern of CRs rescue not only between models but also between brain areas within each model through analysis of the medio-lateral. For example, the secondary somatosensory auditory cortex presents with a 10-fold increase in CR at P24 in the Pten model, it would be interesting in the future to challenge the animal behavioral response to various tests involving auditory stimulation (ie: pre-pulse inhibition or fear conditioning test).

It would be also interesting to investigate the contribution of each subpopulation of CRs by repeating the same experiment and analysis with Wnt3a Cre.

During this PhD project, we showed that despite a significant increase in the number of persisted CRs in the PTEN mutant and drastic change in terms of its morphology and intrinsic properties PTEN model did not show any sign of increasing the susceptibility to develop seizure. The obtained result was not expected as Bax mutant with almost the same number of persisted cells led to an increase in the susceptibility to develop seizure. Further investigation between these two mutants point strongly to the differential expression and secretion of reelin by persisted CRs in the Pten model compared to Bax. To investigate whether overexpression of reelin is the main reason for the observed difference, it is necessary first to analyze morphology, intrinsic properties, and synaptic changes of the surrounding neurons and compare with models of reelin overexpression. It is also interesting to remove reelin from the PTEN model by crossing these animals to the Reelin flox model that already exist in the lab and see if generated animals are susceptible to developing seizure via kainate injection.

Last but not the least, it would be intriguing to extend such investigations already done in this PhD project to hippocampal CRs, which despite originating from the same source the Hem as deltaNp73 cortical CRs manifest a completely different timeline of cell death.

RÉSUMÉ LONG EN FRANÇAIS

Les cellules Cajal-Retzius (CRs) appartiennent à une classe particuliére de neurones excitateurs transitoires, générés à partir de différents domaines situés aux bords du pallium dans le télencéphale des jours embryonnaires (E) 9,5 à E12.5 : le septum pallial (SE), la frontière palliale-sous-palliale (PSB), l'heme cortical (CH) et l'éminence thalamique (ET)(Figure 10, page 39). À partir de ces sources, elles migrent tangentiellement pour couvrir toute la surface du cortex au cours de son développement. Environ 80 % de la population totale de CR dans le néocortex, exprimant le facteur de transcription DeltaNP73, est issu des régions SE, CH et ET. Les CRs jouent un rôle de régulateur clé dans plusieurs étapes du développement cortical via la sécrétion de plusieurs protéines dont la glycoprotéine de la matrice extracellulaire Reelin : le contrôle de la migration des neurones (Figure 9, page 37), la formation de couches et la structuration des zones corticales dans le télencéphale en développement (Figure 11, page 42).

Bien qu'elles aient une forme similaire, les sous-populations de CR diffèrent les unes des autres de plusieurs manières, notamment par leur signature moléculaire, leur propension à coloniser des régions particulières du cortex en croissance et la dynamique de leur disparition, qui varient à la fois dans l'espace et dans le temps.

Des études de traçage génétique chez la souris ont montré que les CRs ne disparaissent pas par migration, transformation ou dilution dans un cortex en croissance mais par mort cellulaire programmée (MCP) très probablement par apoptose dans les premières semaines après la naissance. Certains états pathologiques liés à l'épilepsie ont été associés à une persistance des CRs dans le cortex et dans l’héme.

Bien que les études citées suggèrent un lien entre la malformation des développements corticaux associés à l'épilepsie et la survie de la CR, il n'est pas clair si cette persistance anormale est la cause ou simplement la conséquence des différentes maladies. Cependant, la maturation adéquate des circuits corticaux pourrait être affectée par la persistance des CR. Afin de répondre à cette question, mon laboratoire s'est concentré sur l'identification et la régulation du mécanisme potentiel de mort cellulaire des CR, ainsi que sur l'étude des conséquences de leur persistance. Une étude récente de notre laboratoire sur l'inactivation conditionnelle de Bax, l'une des protéines pro-apoptotiques impliquées dans la voie mitochondriale intrinsèque, a démontré que les sous-types de CR meurent selon plusieurs

mécanismes de mort cellulaire, ceux du SE partiellement par apoptose et ceux de l'hème par une autre voie. Ce résultat est en accord avec la littérature récente, démontrant l'existence de nombreux mécanismes de mort cellulaire, déclenchés par des signaux à la fois intrinsèques et extrinsèques, qui par une interaction complexe collaborent entre eux pour provoquer la mort d'un neurone. Pour cette raison, déterminer le mécanisme précis par lequel une population cellulaire particulière meurt est rendu difficile. Cela nous a incité à aborder le sujet d'un autre point de vue : au lieu d'étudier de nombreux mécanismes de mort cellulaire, qui peuvent éventuellement se compenser, nous nous sommes concentrés sur la recherche de signaux qui protègent les CR de la mort jusqu'aux premières semaines après la naissance.

Il a été démontré que l'élimination complète du facteur de transcription deltaNp73 en utilisant des mutants deltaNp73cre/cre, provoque la mort précoce des CR à E12.5. Par conséquent, deltaNp73 est essentiel pour la survie de CH et SH-CR jusqu'à P0, lorsque son expression commence à diminuer. Ce facteur de transcription protège probablement les CR tout au long du développement, mais sa baisse d'expression après la naissance rend ces neurones plus sensibles aux signaux nocifs, qu'ils soient intrinsèques ou externes. Il a été démontré que deltaNp73 et peut antagoniser l'activité de p73, un facteur de transcription impliqué dans l'initiation de la mort cellulaire. En effet, deltaNp73 et p73 entrent en compétition pour la régulation génique de diverses cibles dont PTEN, un gène suppresseurs de tumeurs dont la protéine régule la voie PI3K/AKT/mTOR (Figure 23, page 71). Il a été démontré que l'élimination des facteurs neurotrophiques, qui sont essentiels à la survie des neurones, provoque l'apoptose. Il a été établi que les molécules de signalisation du facteur de croissance PI3K et la protéine kinase activée par les mitogènes (MAPK) sont nécessaires à la survie neuronale. Des preuves récentes indiquent qu'Akt, l'une des cibles en aval de PI3K, est la principale cause de ces défenses contre diverses voies de mort cellulaire. De plus, il a été déterminé que la dérégulation de ce système est la cause sous-jacente d'un certain nombre de troubles neurodéveloppementaux et neuropsychiatriques.

Au cours de ma thèse je me suis concentré sur les mécanismes de la mort cellulaire programmée (MCP) de la population de CRs dérivés des regions SE, CH et ET et en particulier sur le rôle de la voie PI3K/AKT/mTOR dans la survie des CRs.

J'ai tout d'abord étudié l'activité spatio-temporelle de cette voie de manière à couvrir toutes les sous-population de CRs ainsi que leur chronologie de mort. Pour cela nous avons profité du traçage génétique permanent en utilisant des lignées deltaNp73Cre/+> R26mT/+ à deux stades : E17.5 et P1, avant la mort cellulaire donc le pic est entre P4 et P10. J'ai étudié par immunofluorescence sur des coupes de cerveau la phosphorylation de deux protéines AKT et S6 de la voie de signalisation.

L'analyse spatiale de la voie PI3K/AKT/mTOR dans l'axe médio-latéral des CR a confirmé que cette voie ne se comporte pas de manière linéaire. Les CR situés dans la partie médiale du cortex montrent plus d'activation de la voie PI3K/AKT alors que les CR latéraux ont plus d'activation de la voie mTOR. Cela suggère que la position de la cellule dans le cortex peut affecter ses propriétés moléculaires (Figure S1, page 126). De plus, l'étude temporelle de cette voie comme l'un des signaux de survie potentiels dans les CR a révélé que l'activité globale de cette voie diminue significativement après la naissance et à P1, soit à peu près au même moment où l'expression de l'isoforme deltaNp73 (P0) commence à diminuer (Figure 1, page 117).

Ensuite, nous avons étudié si le maintien de l'activité de la voie PI3K/Akt/mTOR module la MCP dans les CRs. Trois modèles de souris conditionnelles ont été générés par des approches génétiques pour cibler l'activation de la voie dans les CRs dérivés de deltaNp73 : le premier permet l'activation de la kinase PI3K (R26p110*) et les 2 autres inactivent des régulateurs négatifs (PTEN et TSC1). Cibler différents membres de la voie PI3K/AKT/mTOR nous a donné l'avantage de disséquer l'implication des différents mécanismes (apoptose, autophagie…) dans la MCP des CRs. De plus, PTEN possède des fonctions indépendantes de son activité phosphatase du PIP3 et la comparaison des modèles PIK3 et PTEN nous a permis d' inhiber le(s) mécanisme(s) connu(s) et inconnu(s) probablement impliqué(s) dans la MCP de CR.

Dans les trois modèles, deltaNp73$^{Cre/+}$> R26 $^{mT/+;}$Pten$^{lox/lox}$, deltaNp73$^{Cre/+}$> R26$^{mT/+}$;Tsc1$^{-/lox}$ et deltaNp73$^{Cre/+}$> R26p110*$^{lox/mT}$, le développement du cortex et des CRs ne sont pas altérés, suggérant que la suractivation de cette voie dans les CR n'interfère pas avec le bon développement du cortex (Figure S2, page 128). Dans l'ensemble, nous avons observé la persistance de CRs dans tous les modèles après P10, ce qui suggère le rôle critique de cette voie dans la survie des CRs (Figure 2, page 118). Fait intéressant, la proportion de cellules persistantes était différente dans chaque modèle, soulignant le rôle distinct de chacune de ces molécules dans la survie cellulaire malgré leur étroite collaboration. La différence observée peut être expliquée par l'implication possible de divers facteurs en aval de chaque molécule. En

activant PI3K, nous avons principalement ciblé l'activation d'Akt en tant que facteur anti-apoptotique interférant avec les voies de la mort cellulaire en phosphorylant les principales protéines régulatrices de l'apoptose et en déplaçant le rapport des protéines pro- et anti-apoptotique vers l'inhibition de la mort cellulaire.

Cependant, l'inactivation conditionnelle de PTEN a entraîné un nombre plus élevé de CR persistants dans le néocortex par rapport à PIK3CA. Cela peut s'expliquer par le rôle de PTEN dans le contrôle de la mort cellulaire indépendamment de la voie PI3K. Outre la différence dans le nombre de CR observés dans le modèle PTEN, la morphologie des cellules a été radicalement modifiée, les cellules grossissent considérablement avec davantage de branches dendritiques et, dans certains cas, elles ont complètement changé leur morphologie bipolaire en un neurone dysmorphique. Cela peut être associé à l'interaction de PTEN avec les protéines structurelles, accessoires ou régulatrices du cytosquelette d'actine bien que les effets directs ne soient pas encore connus.

Il a été démontré que la voie mTOR (en aval de l'AKT) est impliquée dans le contrôle de la mort cellulaire autophagique. Pour tester si l'autophagie contribue à la mort cellulaire des CR, nous avons ciblé l'activation de mTORC1 via la suppression de TSC1. Malgré l'augmentation du nombre de CR dans les parties intermédiaires et caudale du cerveau, le phénotype est moindre que dans les modèles PTEN ou PIK3CA suggérant que l'activation de la voie mTOR ne contribue pas beaucoup à la persistance des CR.

De plus, les CR exprimaient des quantités significativement plus élevées de reelin aux stades P1 et P24 avec le suivi de l'expression de la reelin dans la matrice extracellulaire à P1 (Figure 4, page 122). Pour étudier les conséquences de la persistance des CR dans la maturation des circuits corticaux et également tester l'hypothèse selon laquelle la persistance des CR est responsable de certaines affections neurologiques mentionnées ci-dessus, nous avons mené diverses expériences, principalement axées sur les mutants PTEN. L'enregistrement par patch-clamp des CR a révélé des altérations de leurs propriétés électrophysiologiques intrinsèques et de leurs réponses aux courants injectés (Figure 3, page 120). Cependant, le cortex des animaux mutés pour PTEN ne montre pas d'altération majeure dans les couches de neurones pyramidaux mais une augmentation de l'activité de la voie mTOR plus probablement due à une augmentation de la sécrétion de la reelin par les CRs (Figure 4, page 122). Les analyses comportementales de l'activité locomotrice, de l'anxiété ou de la mémoire de travail n'ont montré aucune différence par rapport aux témoins (Figure 4, page 130). De manière

surprenante, l'augmentation de la signalisation mTOR dans le cortex n'a pas entraîné d'hypersensibilité au développement de crises induites par l'injection de kaïnate (Figure S4, page 130), un résultat négatif confirmé par les enregistrements multiélectrodes (MEA) du potentiel de champ des neurones dans le cortex somatosensoriel S1 (Figure 4, page 122).

Au total, le résultat de ce projet de thèse a montré que la réduction de l'activité de la voie PI3K/AKT/mTOR dans les CRs sensibilise ces cellules à la mort cellulaire probablement en inhibant un mécanisme anti-apoptotique et que la branche mTOR de cette voie contribue peu à cette survie. De plus, nous avons montré que la persistance des CR par l'inactivation de PTEN n'augmente pas la susceptibilité à développer des crises plus probablement en raison d'une augmentation de l'expression de la reelin dans le système, comme récemment montré dans plusieurs études dans lesquelles l'augmentation de la reelin dans le système prévient l'apparition de certains phénotypes comportementaux liés à la schizophrénie, au trouble bipolaire et même à l'épilepsie.

Mots-clés : Développement, programme de mort cellulaire, cellules de Cajal-Retzius, survie neuronale, voie PI3K/AKT/mTOR

REFERENCES

REFERENCES

REFERENCE

Achilles, K., Okabe, A., Ikeda, M., Shimizu-Okabe, C., Yamada, J., Fukuda, A., Luhmann, H. J., & Kilb, W. (2007). Kinetic Properties of Cl− Uptake Mediated by Na+-Dependent K+-2Cl− Cotransport in Immature Rat Neocortical Neurons. *Journal of Neuroscience*, *27*(32), 8616–8627. https://doi.org/10.1523/JNEUROSCI.5041-06.2007

Alcantara, D., Timms, A. E., Gripp, K., Baker, L., Park, K., Collins, S., Cheng, C., Stewart, F., Mehta, S. G., Saggar, A., Sztriha, L., Zombor, M., Caluseriu, O., Mesterman, R., Van Allen, M. I., Jacquinet, A., Ygberg, S., Bernstein, J. A., Wenger, A. M., … Mirzaa, G. M. (2017). Mutations of AKT3 are associated with a wide spectrum of developmental disorders including extreme megalencephaly. *Brain: A Journal of Neurology*, *140*(10), 2610–2622. https://doi.org/10.1093/brain/awx203

Alfano, C., & Studer, M. (2013). Neocortical arealization: Evolution, mechanisms, and open questions. *Developmental Neurobiology*, *73*(6), 411–447. https://doi.org/10.1002/dneu.22067

Al-Khouri, A. M., Ma, Y., Togo, S. H., Williams, S., & Mustelin, T. (2005). Cooperative phosphorylation of the tumor suppressor phosphatase and tensin homologue (PTEN) by casein kinases and glycogen synthase kinase 3beta. *The Journal of Biological Chemistry*, *280*(42), 35195–35202. https://doi.org/10.1074/jbc.M503045200

Allene, C., & Cossart, R. (2010). Early NMDA receptor-driven waves of activity in the developing neocortex: Physiological or pathological network oscillations? *The Journal of Physiology*, *588*(Pt 1), 83–91. https://doi.org/10.1113/jphysiol.2009.178798

Anderson, S. A., Marín, O., Horn, C., Jennings, K., & Rubenstein, J. L. (2001). Distinct cortical migrations from the medial and lateral ganglionic eminences. *Development (Cambridge, England)*, *128*(3), 353–363. https://doi.org/10.1242/dev.128.3.353

Angevine, J. B., & Sidman, R. L. (1961). Autoradiographic study of cell migration during histogenesis of cerebral cortex in the mouse. *Nature*, *192*, 766–768. https://doi.org/10.1038/192766b0

Anstötz, M., Cosgrove, K. E., Hack, I., Mugnaini, E., Maccaferri, G., & Lübke, J. H. R. (2014). Morphology, input-output relations and synaptic connectivity of Cajal-Retzius cells in layer 1 of the developing neocortex of CXCR4-EGFP mice. *Brain Structure & Function*, *219*(6), 2119–2139. https://doi.org/10.1007/s00429-013-0627-2

Arch, E. M., Goodman, B. K., Wesep, R. A. V., Liaw, D., Clarke, K., Parsons, R., McKusick, V. A., & Geraghty, M. T. (1997). Deletion of PTEN in a patient with Bannayan-Riley-Ruvalcaba syndrome suggests allelism with Cowden disease. *American Journal of Medical Genetics*, *71*(4), 489–493. https://doi.org/10.1002/(SICI)1096-8628(19970905)71:4<489::AID-AJMG24>3.0.CO;2-B

Arganda-Carreras, I., Kaynig, V., Rueden, C., Eliceiri, K. W., Schindelin, J., Cardona, A., & Sebastian Seung, H. (2017). Trainable Weka Segmentation: A machine learning tool for microscopy pixel classification. *Bioinformatics*, *33*(15), 2424–2426. https://doi.org/10.1093/bioinformatics/btx180

Assimacopoulos, S., Grove, E. A., & Ragsdale, C. W. (2003). Identification of a Pax6-dependent epidermal growth factor family signaling source at the lateral edge of the embryonic cerebral cortex. *The Journal of Neuroscience: The Official Journal of the Society for Neuroscience*, *23*(16), 6399–6403.

Bachler, M., & Neubüser, A. (2001). Expression of members of the Fgf family and their receptors during midfacial development. *Mechanisms of Development*, *100*(2), 313–316. https://doi.org/10.1016/s0925-4773(00)00518-9

Baffi, T. R., Lordén, G., Wozniak, J. M., Feichtner, A., Yeung, W., Kornev, A. P., King, C. C., Del Rio, J. C., Limaye, A. J., Bogomolovas, J., Gould, C. M., Chen, J., Kennedy, E. J., Kannan, N., Gonzalez, D. J., Stefan, E., Taylor, S. S., & Newton, A. C. (2021). MTORC2 controls the activity of PKC and Akt by phosphorylating a conserved TOR interaction motif. *Science Signaling*, *14*(678), eabe4509. https://doi.org/10.1126/scisignal.abe4509

Bai, L., Smith, D. C., & Wang, S. (2014). Small-molecule SMAC mimetics as new cancer therapeutics. *Pharmacology & Therapeutics*, *144*(1), 82–95. https://doi.org/10.1016/j.pharmthera.2014.05.007

Bálint, E., Bates, S., & Vousden, K. H. (1999). Mdm2 binds p73α without targeting degradation. *Oncogene*, *18*(27), Article 27. https://doi.org/10.1038/sj.onc.1202781

Barber, M., Arai, Y., Morishita, Y., Vigier, L., Causeret, F., Borello, U., Ledonne, F., Coppola, E., Contremoulins, V., Pfrieger, F. W., Tissir, F., Govindan, S., Jabaudon, D., Proux-Gillardeaux, V., Galli, T., & Pierani, A. (2015). Migration Speed of Cajal-Retzius Cells Modulated by Vesicular Trafficking Controls the Size of Higher-Order Cortical Areas. *Current Biology: CB*, *25*(19), 2466–2478. https://doi.org/10.1016/j.cub.2015.08.028

Barber, M., & Pierani, A. (2016). Tangential migration of glutamatergic neurons and cortical patterning during development: Lessons from Cajal-Retzius cells. *Developmental Neurobiology*, *76*(8), 847–881. https://doi.org/10.1002/dneu.22363

Bedoui, S., Herold, M. J., & Strasser, A. (2020). Emerging connectivity of programmed cell death pathways and its physiological implications. *Nature Reviews Molecular Cell Biology*, *21*(11), Article 11. https://doi.org/10.1038/s41580-020-0270-8

Beeler, J. S., Marshall, C. B., Gonzalez-Ericsson, P. I., Shaver, T. M., Santos Guasch, G. L., Lea, S. T., Johnson, K. N., Jin, H., Venters, B. J., Sanders, M. E., & Pietenpol, J. A. (2019). P73 regulates epidermal wound healing and induced keratinocyte programming. *PLOS ONE*, *14*(6), e0218458. https://doi.org/10.1371/journal.pone.0218458

Ben-Ari, Y. (2002). Excitatory actions of gaba during development: The nature of the nurture. *Nature Reviews. Neuroscience*, *3*(9), 728–739. https://doi.org/10.1038/nrn920

Bermúdez Brito, M., Goulielmaki, E., & Papakonstanti, E. A. (2015). Focus on PTEN Regulation. *Frontiers in Oncology*, *5*, 166. https://doi.org/10.3389/fonc.2015.00166

Bielle, F., Griveau, A., Narboux-Nême, N., Vigneau, S., Sigrist, M., Arber, S., Wassef, M., & Pierani, A. (2005b). Multiple origins of Cajal-Retzius cells at the borders of the developing pallium. *Nature Neuroscience*, *8*(8), 1002–1012. https://doi.org/10.1038/nn1511

Bishop, K. M., Rubenstein, J. L. R., & O'Leary, D. D. M. (2002). Distinct actions of Emx1, Emx2, and Pax6 in regulating the specification of areas in the developing neocortex. *The Journal of Neuroscience: The Official Journal of the Society for Neuroscience*, *22*(17), 7627–7638.

Blanquie, O., Liebmann, L., Hübner, C. A., Luhmann, H. J., & Sinning, A. (2017). NKCC1-Mediated GABAergic Signaling Promotes Postnatal Cell Death in Neocortical Cajal-Retzius Cells. *Cerebral Cortex (New York, N.Y.: 1991)*, *27*(2), 1644–1659. https://doi.org/10.1093/cercor/bhw004

Blanquie, O., Yang, J.-W., Kilb, W., Sharopov, S., Sinning, A., & Luhmann, H. J. (2017). Electrical activity controls area-specific expression of neuronal apoptosis in the mouse developing cerebral cortex. *ELife*, *6*, e27696. https://doi.org/10.7554/eLife.27696

Blom, H. J., Shaw, G. M., den Heijer, M., & Finnell, R. H. (2006). Neural tube defects and folate: Case far from closed. *Nature Reviews. Neuroscience*, *7*(9), 724–731. https://doi.org/10.1038/nrn1986

Blümcke, I., Thom, M., Aronica, E., Armstrong, D. D., Bartolomei, F., Bernasconi, A., Bernasconi, N., Bien, C. G., Cendes, F., Coras, R., Cross, J. H., Jacques, T. S., Kahane, P., Mathern, G. W., Miyata, H., Moshé, S. L., Oz, B., Özkara, Ç., Perucca, E., … Spreafico, R. (2013). International consensus classification of hippocampal sclerosis in temporal lobe epilepsy: A Task Force report from the ILAE Commission on Diagnostic Methods. *Epilepsia*, *54*(7), 1315–1329. https://doi.org/10.1111/epi.12220

Blümcke, I., Thom, M., & Wiestler, O. D. (2002). Ammon's horn sclerosis: A maldevelopmental disorder associated with temporal lobe epilepsy. *Brain Pathology (Zurich, Switzerland)*, *12*(2), 199–211.

Bockaert, J., & Marin, P. (2015). MTOR in Brain Physiology and Pathologies. *Physiological Reviews*, *95*(4), 1157–1187. https://doi.org/10.1152/physrev.00038.2014

Boido, D., Farisello, P., Cesca, F., Ferrea, E., Valtorta, F., Benfenati, F., & Baldelli, P. (2010). Cortico-hippocampal hyperexcitability in synapsin I/II/III knockout mice: Age-dependency and response to the antiepileptic drug levetiracetam. *Neuroscience*, *171*(1), 268–283. https://doi.org/10.1016/j.neuroscience.2010.08.046

Boland, E., Clayton-Smith, J., Woo, V. G., McKee, S., Manson, F. D. C., Medne, L., Zackai, E., Swanson, E. A., Fitzpatrick, D., Millen, K. J., Sherr, E. H., Dobyns, W. B., & Black, G. C. M. (2007). Mapping of deletion and translocation breakpoints in 1q44 implicates the serine/threonine kinase AKT3 in postnatal microcephaly and agenesis of the corpus callosum. *American Journal of Human Genetics*, *81*(2), 292–303. https://doi.org/10.1086/519999

Borello, U., Madhavan, M., Vilinsky, I., Faedo, A., Pierani, A., Rubenstein, J., & Campbell, K. (2014). Sp8 and COUP-TF1 reciprocally regulate patterning and Fgf signaling in cortical progenitors. *Cerebral Cortex (New York, N.Y.: 1991)*, *24*(6), 1409–1421. https://doi.org/10.1093/cercor/bhs412

Borello, U., & Pierani, A. (2010). Patterning the cerebral cortex: Traveling with morphogens. *Current Opinion in Genetics & Development*, *20*(4), 408–415. https://doi.org/10.1016/j.gde.2010.05.003

Boyd, S. D., Tsai, K. Y., & Jacks, T. (2000). An intact HDM2 RING-finger domain is required for nuclear exclusion of p53. *Nature Cell Biology*, *2*(9), 563–568. https://doi.org/10.1038/35023500

Boyle, M. P., Bernard, A., Thompson, C. L., Ng, L., Boe, A., Mortrud, M., Hawrylycz, M. J., Jones, A. R., Hevner, R. F., & Lein, E. S. (2011). Cell-type-specific consequences of Reelin deficiency in the mouse neocortex, hippocampus, and amygdala. *The Journal of Comparative Neurology*, *519*(11), 2061–2089. https://doi.org/10.1002/cne.22655

Bradley, J. (2008). TNF-mediated inflammatory disease. *The Journal of Pathology*, *214*(2), 149–160. https://doi.org/10.1002/path.2287

Briggs, F. (2010). Organizing principles of cortical layer 6. *Frontiers in Neural Circuits*, *4*, 3. https://doi.org/10.3389/neuro.04.003.2010

Butt, S. J., Stacey, J. A., Teramoto, Y., & Vagnoni, C. (2017). A role for GABAergic interneuron diversity in circuit development and plasticity of the neonatal cerebral cortex. *Current Opinion in Neurobiology*, *43*, 149–155. https://doi.org/10.1016/j.conb.2017.03.011

Buxbaum, J. D., Cai, G., Chaste, P., Nygren, G., Goldsmith, J., Reichert, J., Anckarsäter, H., Rastam, M., Smith, C. J., Silverman, J. M., Hollander, E., Leboyer, M., Gillberg, C., Verloes, A., & Betancur, C. (2007). Mutation screening of the PTEN gene in patients with autism spectrum disorders and macrocephaly. *American Journal of Medical Genetics. Part B, Neuropsychiatric Genetics: The Official Publication of the International Society of Psychiatric Genetics*, *144B*(4), 484–491. https://doi.org/10.1002/ajmg.b.30493

Camacho, J., Ejaz, E., Ariza, J., Noctor, S. C., & Martínez-Cerdeño, V. (2014). RELN-expressing neuron density in layer I of the superior temporal lobe is similar in human brains with autism and in age-matched controls. *Neuroscience Letters*, *579*, 163–167. https://doi.org/10.1016/j.neulet.2014.07.031

Carnero, A., Blanco-Aparicio, C., Renner, O., Link, W., & Leal, J. F. M. (2008). The PTEN/PI3K/AKT signalling pathway in cancer, therapeutic implications. *Current Cancer Drug Targets*, *8*(3), 187–198. https://doi.org/10.2174/156800908784293659

Caronia-Brown, G., & Grove, E. A. (2011). Timing of cortical interneuron migration is influenced by the cortical hem. *Cerebral Cortex (New York, N.Y.: 1991)*, *21*(4), 748–755. https://doi.org/10.1093/cercor/bhq142

Caulfield, A. J., & Lathem, W. W. (2014). Disruption of Fas-Fas Ligand Signaling, Apoptosis, and Innate Immunity by Bacterial Pathogens. *PLOS Pathogens*, *10*(8), e1004252. https://doi.org/10.1371/journal.ppat.1004252

Cauller, L. (1995). Layer I of primary sensory neocortex: Where top-down converges upon bottom-up. *Behavioural Brain Research*, *71*(1–2), 163–170. https://doi.org/10.1016/0166-4328(95)00032-1

Causeret, F., Coppola, E., & Pierani, A. (2018a). Cortical developmental death: Selected to survive or fated to die. *Current Opinion in Neurobiology*, *53*, 35–42. https://doi.org/10.1016/j.conb.2018.04.022

Causeret, F., Moreau, M. X., Pierani, A., & Blanquie, O. (2021). The multiple facets of Cajal-Retzius neurons. *Development*, *148*(11), dev199409. https://doi.org/10.1242/dev.199409

Cecconi, F., Alvarez-Bolado, G., Meyer, B. I., Roth, K. A., & Gruss, P. (1998). Apaf1 (CED-4 homolog) regulates programmed cell death in mammalian development. *Cell*, *94*(6), 727–737. https://doi.org/10.1016/s0092-8674(00)81732-8

Centeno, C., Repici, M., Chatton, J.-Y., Riederer, B. M., Bonny, C., Nicod, P., Price, M., Clarke, P. G. H., Papa, S., Franzoso, G., & Borsello, T. (2007). Role of the JNK pathway in NMDA-mediated excitotoxicity of cortical neurons. *Cell Death and Differentiation*, *14*(2), 240–253. https://doi.org/10.1038/sj.cdd.4401988

Chan, T. O., & Tsichlis, P. N. (2001). PDK2: A complex tail in one Akt. *Science's STKE: Signal Transduction Knowledge Environment*, *2001*(66), pe1. https://doi.org/10.1126/stke.2001.66.pe1

Chao, D. L., Ma, L., & Shen, K. (2009). Transient cell-cell interactions in neural circuit formation. *Nature Reviews. Neuroscience*, *10*(4), 262–271. https://doi.org/10.1038/nrn2594

Chatterjee, N., Pazarentzos, E., Mayekar, M. K., Gui, P., Allegakoen, D. V., Hrustanovic, G., Olivas, V., Lin, L., Verschueren, E., Johnson, J. R., Hofree, M., Yan, J. J., Newton, B. W., Dollen, J. V., Earnshaw, C. H., Flanagan, J., Chan, E., Asthana, S., Ideker, T., … Bivona, T. G. (2019). Synthetic Essentiality of Metabolic Regulator PDHK1 in PTEN-Deficient Cells and Cancers. *Cell Reports*, *28*(9), 2317-2330.e8. https://doi.org/10.1016/j.celrep.2019.07.063

Chen, H.-C., Kanai, M., Inoue-Yamauchi, A., Tu, H.-C., Huang, Y., Ren, D., Kim, H., Takeda, S., Reyna, D. E., Chan, P. M., Ganesan, Y. T., Liao, C.-P., Gavathiotis, E., Hsieh, J. J., & Cheng, E. H. (2015). An interconnected hierarchical model of cell death regulation by the BCL-2 family. *Nature Cell Biology*, *17*(10), 1270–1281. https://doi.org/10.1038/ncb3236

Chen, J., Tang, H., Hay, N., Xu, J., & Ye, R. D. (2010). Akt isoforms differentially regulate neutrophil functions. *Blood*, *115*(21), 4237–4246. https://doi.org/10.1182/blood-2009-11-255323

Chen, J.-F., Zhang, Y., Wilde, J., Hansen, K. C., Lai, F., & Niswander, L. (2014). Microcephaly disease gene Wdr62 regulates mitotic progression of embryonic neural stem cells and brain size. *Nature Communications*, *5*(1), Article 1. https://doi.org/10.1038/ncomms4885

Chen, S.-K., Chew, K. S., McNeill, D. S., Keeley, P. W., Ecker, J. L., Mao, B. Q., Pahlberg, J., Kim, B., Lee, S. C. S., Fox, M. A., Guido, W., Wong, K. Y., Sampath, A. P., Reese, B. E., Kuruvilla, R., & Hattar, S. (2013). Apoptosis regulates ipRGC spacing necessary for rods and cones to drive circadian photoentrainment. *Neuron*, *77*(3), 503–515. https://doi.org/10.1016/j.neuron.2012.11.028

Chen, W. S., Xu, P.-Z., Gottlob, K., Chen, M.-L., Sokol, K., Shiyanova, T., Roninson, I., Weng, W., Suzuki, R., Tobe, K., Kadowaki, T., & Hay, N. (2001). Growth retardation and increased apoptosis in mice with homozygous disruption of the akt1 gene. *Genes & Development*, *15*(17), 2203–2208. https://doi.org/10.1101/gad.913901

Chibaya, L., Karim, B., Zhang, H., & Jones, S. N. (2021). Mdm2 phosphorylation by Akt regulates the p53 response to oxidative stress to promote cell proliferation and tumorigenesis. *Proceedings of the National Academy of Sciences of the United States of America*, *118*(4), e2003193118. https://doi.org/10.1073/pnas.2003193118

Cho, H., Mu, J., Kim, J. K., Thorvaldsen, J. L., Chu, Q., Crenshaw, E. B., Kaestner, K. H., Bartolomei, M. S., Shulman, G. I., & Birnbaum, M. J. (2001). Insulin resistance and a diabetes mellitus-like syndrome in mice lacking the protein kinase Akt2 (PKB beta). *Science (New York, N.Y.)*, *292*(5522), 1728–1731. https://doi.org/10.1126/science.292.5522.1728

Cho, H., Thorvaldsen, J. L., Chu, Q., Feng, F., & Birnbaum, M. J. (2001). Akt1/PKBalpha is required for normal growth but dispensable for maintenance of glucose homeostasis in mice. *The Journal of Biological Chemistry*, *276*(42), 38349–38352. https://doi.org/10.1074/jbc.C100462200

Chong, Z. Z., Li, F., & Maiese, K. (2005). Activating Akt and the brain's resources to drive cellular survival and prevent inflammatory injury. *Histology and Histopathology*, *20*(1), 299–315.

Chowdhury, T. G., Jimenez, J. C., Bomar, J. M., Cruz-Martin, A., Cantle, J. P., & Portera-Cailliau, C. (2010). Fate of cajal-retzius neurons in the postnatal mouse neocortex. *Frontiers in Neuroanatomy*, *4*, 10. https://doi.org/10.3389/neuro.05.010.2010

Cosgrove, K. E., & Maccaferri, G. (2012). MGlu1α-dependent recruitment of excitatory GABAergic input to neocortical Cajal-Retzius cells. *Neuropharmacology*, *63*(3), 486–493. https://doi.org/10.1016/j.neuropharm.2012.04.025

Costa-Mattioli, M., & Monteggia, L. M. (2013). MTOR complexes in neurodevelopmental and neuropsychiatric disorders. *Nature Neuroscience*, *16*(11), 1537–1543. https://doi.org/10.1038/nn.3546

Crino, P. B. (2015). The enlarging spectrum of focal cortical dysplasias. *Brain*, *138*(6), 1446–1448. https://doi.org/10.1093/brain/awv098

Crossley, P. H., & Martin, G. R. (1995). The mouse Fgf8 gene encodes a family of polypeptides and is expressed in regions that direct outgrowth and patterning in the developing embryo. *Development (Cambridge, England)*, *121*(2), 439–451. https://doi.org/10.1242/dev.121.2.439

Crowley, J. C., & Katz, L. C. (1999). Development of ocular dominance columns in the absence of retinal input. *Nature Neuroscience*, *2*(12), 1125–1130. https://doi.org/10.1038/16051

Cuesto, G., Enriquez-Barreto, L., Caramés, C., Cantarero, M., Gasull, X., Sandi, C., Ferrús, A., Acebes, Á., & Morales, M. (2011). Phosphoinositide-3-kinase activation controls synaptogenesis and spinogenesis in hippocampal neurons. *The Journal of Neuroscience: The Official Journal of the Society for Neuroscience*, *31*(8), 2721–2733. https://doi.org/10.1523/JNEUROSCI.4477-10.2011

Czabotar, P. E., Lessene, G., Strasser, A., & Adams, J. M. (2014). Control of apoptosis by the BCL-2 protein family: Implications for physiology and therapy. *Nature Reviews. Molecular Cell Biology*, *15*(1), 49–63. https://doi.org/10.1038/nrm3722

da Costa, N. M., & Martin, K. A. C. (2010). Whose Cortical Column Would that Be? *Frontiers in Neuroanatomy*, *4*, 16. https://doi.org/10.3389/fnana.2010.00016

D'Amelio, M., Cavallucci, V., & Cecconi, F. (2010). Neuronal caspase-3 signaling: Not only cell death. *Cell Death and Differentiation*, *17*(7), 1104–1114. https://doi.org/10.1038/cdd.2009.180

Dangelmaier, C., Manne, B. K., Liverani, E., Jin, J., Bray, P., & Kunapuli, S. P. (2014). PDK1 selectively phosphorylates Thr(308) on Akt and contributes to human platelet functional responses. *Thrombosis and Haemostasis*, *111*(3), 508–517. https://doi.org/10.1160/TH13-06-0484

D'Arcangelo, G., Miao, G. G., Chen, S. C., Soares, H. D., Morgan, J. I., & Curran, T. (1995a). A protein related to extracellular matrix proteins deleted in the mouse mutant reeler. *Nature*, *374*(6524), 719–723. https://doi.org/10.1038/374719a0

Duve, C. (2005). The lysosome turns fifty. *Nature Cell Biology*, *7*(9), 847–849. https://doi.org/10.1038/ncb0905-847

de Keizer, P. L. J., Burgering, B. M. T., & Dansen, T. B. (2011). Forkhead box o as a sensor, mediator, and regulator of redox signaling. *Antioxidants & Redox Signaling*, *14*(6), 1093–1106. https://doi.org/10.1089/ars.2010.3403

DeFelipe, J., Alonso-Nanclares, L., & Arellano, J. I. (2002). Microstructure of the neocortex: Comparative aspects. *Journal of Neurocytology*, *31*(3–5), 299–316. https://doi.org/10.1023/a:1024130211265

Degterev, A., & Yuan, J. (2008). Expansion and evolution of cell death programmes. *Nature Reviews. Molecular Cell Biology*, *9*(5), 378–390. https://doi.org/10.1038/nrm2393

Del Río, J. A., Heimrich, B., Borrell, V., Förster, E., Drakew, A., Alcántara, S., Nakajima, K., Miyata, T., Ogawa, M., Mikoshiba, K., Derer, P., Frotscher, M., & Soriano, E. (1997). A role for Cajal-Retzius cells and reelin in the development of hippocampal connections. *Nature*, *385*(6611), 70–74. https://doi.org/10.1038/385070a0

Denton, D., & Kumar, S. (2019). Autophagy-dependent cell death. *Cell Death & Differentiation*, *26*(4), Article 4. https://doi.org/10.1038/s41418-018-0252-y

Derer, P., & Derer, M. (1990). Cajal-Retzius cell ontogenesis and death in mouse brain visualized with horseradish peroxidase and electron microscopy. *Neuroscience*, *36*(3), 839–856. https://doi.org/10.1016/0306-4522(90)90027-2

D'Gama, A. M., Pochareddy, S., Li, M., Jamuar, S. S., Reiff, R. E., Lam, A.-T. N., Sestan, N., & Walsh, C. A. (2015). Targeted DNA Sequencing from Autism Spectrum Disorder Brains Implicates Multiple Genetic Mechanisms. *Neuron*, *88*(5), 910–917. https://doi.org/10.1016/j.neuron.2015.11.009

D'Gama, A. M., Woodworth, M. B., Hossain, A. A., Bizzotto, S., Hatem, N. E., LaCoursiere, C. M., Najm, I., Ying, Z., Yang, E., Barkovich, A. J., Kwiatkowski, D. J., Vinters, H. V., Madsen, J. R., Mathern, G. W., Blümcke, I., Poduri, A., & Walsh, C. A. (2017). Somatic mutations activating the mTOR pathway in dorsal telencephalic progenitors cause a continuum of cortical dysplasias. *Cell Reports*, *21*(13), 3754–3766. https://doi.org/10.1016/j.celrep.2017.11.106

Dhumale, P., Menon, S., Chiang, J., & Püschel, A. W. (2018). The loss of the kinases SadA and SadB results in early neuronal apoptosis and a reduced number of progenitors. *PloS One*, *13*(4), e0196698. https://doi.org/10.1371/journal.pone.0196698

Du, K., & Tsichlis, P. N. (2005). Regulation of the Akt kinase by interacting proteins. *Oncogene*, *24*(50), 7401–7409. https://doi.org/10.1038/sj.onc.1209099

Dulloo, I., Gopalan, G., Melino, G., & Sabapathy, K. (2010). The antiapoptotic DeltaNp73 is degraded in a c-Jun-dependent manner upon genotoxic stress through the antizyme-mediated pathway. *Proceedings of the National Academy of Sciences of the United States of America*, *107*(11), 4902–4907. https://doi.org/10.1073/pnas.0906782107

Easton, R. M., Cho, H., Roovers, K., Shineman, D. W., Mizrahi, M., Forman, M. S., Lee, V. M.-Y., Szabolcs, M., de Jong, R., Oltersdorf, T., Ludwig, T., Efstratiadis, A., & Birnbaum, M. J. (2005). Role for Akt3/protein kinase Bgamma in attainment of normal brain size. *Molecular and Cellular Biology*, *25*(5), 1869–1878. https://doi.org/10.1128/MCB.25.5.1869-1878.2005

Elmore, S. (2007). Apoptosis: A Review of Programmed Cell Death. *Toxicologic Pathology*, *35*(4), 495–516. https://doi.org/10.1080/01926230701320337

Englund, C., Fink, A., Lau, C., Pham, D., Daza, R. A. M., Bulfone, A., Kowalczyk, T., & Hevner, R. F. (2005). Pax6, Tbr2, and Tbr1 are expressed sequentially by radial glia, intermediate progenitor cells, and postmitotic neurons in developing neocortex. *The Journal of Neuroscience: The Official Journal of the Society for Neuroscience*, *25*(1), 247–251. https://doi.org/10.1523/JNEUROSCI.2899-04.2005

Enriquez-Barreto, L., & Morales, M. (2016). The PI3K signaling pathway as a pharmacological target in Autism related disorders and Schizophrenia. *Molecular and Cellular Therapies*, *4*, 2. https://doi.org/10.1186/s40591-016-0047-9

Eriksson, S. H., Thom, M., Heffernan, J., Lin, W. R., Harding, B. N., Squier, M. V., & Sisodiya, S. M. (2001). Persistent reelin-expressing Cajal-Retzius cells in polymicrogyria. *Brain: A Journal of Neurology*, *124*(Pt 7), 1350–1361. https://doi.org/10.1093/brain/124.7.1350

European Chromosome 16 Tuberous Sclerosis Consortium. (1993). Identification and characterization of the tuberous sclerosis gene on chromosome 16. *Cell*, *75*(7), 1305–1315. https://doi.org/10.1016/0092-8674(93)90618-z

Falconer, D. S. (1951). Two new mutants, “trembler” and “reeler”, with neurological actions in the house mouse (Mus musculus L.). *Journal of Genetics*, *50*(2), 192–201. https://doi.org/10.1007/BF02996215

Fang, L., Lee, S. W., & Aaronson, S. A. (1999). Comparative Analysis of P73 and P53 Regulation and Effector Functions. *The Journal of Cell Biology*, *147*(4), 823–830.

Fatemi, S. H., Kroll, J. L., & Stary, J. M. (2001). Altered levels of Reelin and its isoforms in schizophrenia and mood disorders. *Neuroreport*, *12*(15), 3209–3215. https://doi.org/10.1097/00001756-200110290-00014

Feldmeyer, D. (2012). Excitatory neuronal connectivity in the barrel cortex. *Frontiers in Neuroanatomy*, *6*, 24. https://doi.org/10.3389/fnana.2012.00024

Fiacco, T. A., & McCarthy, K. D. (2006). Astrocyte calcium elevations: Properties, propagation, and effects on brain signaling. *Glia*, *54*(7), 676–690. https://doi.org/10.1002/glia.20396

Flames, N., Pla, R., Gelman, D. M., Rubenstein, J. L. R., Puelles, L., & Marín, O. (2007). Delineation of multiple subpallial progenitor domains by the combinatorial expression of transcriptional codes. *The Journal of Neuroscience: The Official Journal of the Society for Neuroscience*, *27*(36), 9682–9695. https://doi.org/10.1523/JNEUROSCI.2750-07.2007

Flores-Sarnat, L. (2002). Hemimegalencephaly: Part 1. Genetic, clinical, and imaging aspects. *Journal of Child Neurology*, *17*(5), 373–384; discussion 384. https://doi.org/10.1177/088307380201700512

Flores-Sarnat, L., Sarnat, H. B., Dávila-Gutiérrez, G., & Álvarez, A. (2003). Hemimegalencephaly: Part 2. Neuropathology Suggests a Disorder of Cellular Lineage. *Journal of Child Neurology*, *18*(11), 776–785. https://doi.org/10.1177/08830738030180111101

Fraser, M. M., Zhu, X., Kwon, C.-H., Uhlmann, E. J., Gutmann, D. H., & Baker, S. J. (2004). Pten loss causes hypertrophy and increased proliferation of astrocytes in vivo. *Cancer Research*, *64*(21), 7773–7779. https://doi.org/10.1158/0008-5472.CAN-04-2487

Fresno Vara, J. A., Casado, E., de Castro, J., Cejas, P., Belda-Iniesta, C., & González-Barón, M. (2004). PI3K/Akt signalling pathway and cancer. *Cancer Treatment Reviews*, *30*(2), 193–204. https://doi.org/10.1016/j.ctrv.2003.07.007

Fricker, M., Tolkovsky, A. M., Borutaite, V., Coleman, M., & Brown, G. C. (2018). Neuronal Cell Death. *Physiological Reviews*, *98*(2), 813–880. https://doi.org/10.1152/physrev.00011.2017

Frotscher, M., Seress, L., Abraham, H., & Heimrich, B. (2001). Early generated Cajal-Retzius cells have different functions in cortical development. *Symposia of the Society for Experimental Biology*, *53*, 43–49.

Fruman, D. A., Meyers, R. E., & Cantley, L. C. (1998). Phosphoinositide kinases. *Annual Review of Biochemistry*, *67*, 481–507. https://doi.org/10.1146/annurev.biochem.67.1.481

Fukuchi-Shimogori, T., & Grove, E. A. (2003). Emx2 patterns the neocortex by regulating FGF positional signaling. *Nature Neuroscience*, *6*(8), 825–831. https://doi.org/10.1038/nn1093

Fulda, S. (2012). Shifting the balance of mitochondrial apoptosis: Therapeutic perspectives. *Frontiers in Oncology*, *2*, 121. https://doi.org/10.3389/fonc.2012.00121

Galluzzi, L., Vitale, I., Aaronson, S. A., Abrams, J. M., Adam, D., Agostinis, P., Alnemri, E. S., Altucci, L., Amelio, I., Andrews, D. W., Annicchiarico-Petruzzelli, M., Antonov, A. V., Arama, E., Baehrecke, E. H., Barlev, N. A., Bazan, N. G., Bernassola, F., Bertrand, M. J. M., Bianchi, K., … Kroemer, G. (2018). Molecular mechanisms of cell death: Recommendations of the Nomenclature Committee on Cell Death 2018. *Cell Death and Differentiation*, *25*(3), 486–541. https://doi.org/10.1038/s41418-017-0012-4

Garbelli, R., Frassoni, C., Ferrario, A., Tassi, L., Bramerio, M., & Spreafico, R. (2001). Cajal-Retzius cell density as marker of type of focal cortical dysplasia. *Neuroreport*, *12*(12), 2767–2771. https://doi.org/10.1097/00001756-200108280-00034

Garcia-Junco-Clemente, P., & Golshani, P. (2014). PTEN: A master regulator of neuronal structure, function, and plasticity. *Communicative & Integrative Biology*, *7*(2), e28358. https://doi.org/10.4161/cib.28358

Gardai, S. J., Hildeman, D. A., Frankel, S. K., Whitlock, B. B., Frasch, S. C., Borregaard, N., Marrack, P., Bratton, D. L., & Henson, P. M. (2004). Phosphorylation of Bax Ser184 by Akt regulates its activity and apoptosis in neutrophils. *The Journal of Biological Chemistry*, *279*(20), 21085–21095. https://doi.org/10.1074/jbc.M400063200

Ghosh, A., Antonini, A., McConnell, S. K., & Shatz, C. J. (1990). Requirement for subplate neurons in the formation of thalamocortical connections. *Nature*, *347*(6289), 179–181. https://doi.org/10.1038/347179a0

Granholm, A. C., Reyland, M., Albeck, D., Sanders, L., Gerhardt, G., Hoernig, G., Shen, L., Westphal, H., & Hoffer, B. (2000). Glial cell line-derived neurotrophic factor is essential for postnatal survival of midbrain dopamine neurons. *The Journal of Neuroscience: The Official Journal of the Society for Neuroscience*, *20*(9), 3182–3190.

Green, D. R. (2019). The Coming Decade of Cell Death Research: Five Riddles. *Cell*, *177*(5), 1094–1107. https://doi.org/10.1016/j.cell.2019.04.024

Green, D. R., Galluzzi, L., & Kroemer, G. (2011). Mitochondria and the autophagy-inflammation-cell death axis in organismal aging. *Science (New York, N.Y.)*, *333*(6046), 1109–1112. https://doi.org/10.1126/science.1201940

Greig, L. C., Woodworth, M. B., Galazo, M. J., Padmanabhan, H., & Macklis, J. D. (2013a). Molecular logic of neocortical projection neuron specification, development and diversity. *Nature Reviews. Neuroscience*, *14*(11), 755–769. https://doi.org/10.1038/nrn3586

Griffith, T. S., Brunner, T., Fletcher, S. M., Green, D. R., & Ferguson, T. A. (1995). Fas ligand-induced apoptosis as a mechanism of immune privilege. *Science (New York, N.Y.)*, *270*(5239), 1189–1192. https://doi.org/10.1126/science.270.5239.1189

Griveau, A., Borello, U., Causeret, F., Tissir, F., Boggetto, N., Karaz, S., & Pierani, A. (2010). A novel role for Dbx1-derived Cajal-Retzius cells in early regionalization of the cerebral cortical neuroepithelium. *PLoS Biology*, *8*(7), e1000440. https://doi.org/10.1371/journal.pbio.1000440

Gross, C., & Bassell, G. (2014). Neuron-specific regulation of class I PI3K catalytic subunits and their dysfunction in brain disorders. *Frontiers in Molecular Neuroscience*, *7*. https://www.frontiersin.org/articles/10.3389/fnmol.2014.00012

Groszer, M., Erickson, R., Scripture-Adams, D. D., Lesche, R., Trumpp, A., Zack, J. A., Kornblum, H. I., Liu, X., & Wu, H. (2001). Negative regulation of neural stem/progenitor cell proliferation by the Pten tumor suppressor gene in vivo. *Science (New York, N.Y.)*, *294*(5549), 2186–2189. https://doi.org/10.1126/science.1065518

Gulisano, M., Broccoli, V., Pardini, C., & Boncinelli, E. (1996). Emx1 and Emx2 show different patterns of expression during proliferation and differentiation of the developing cerebral cortex in the mouse. *The European Journal of Neuroscience*, *8*(5), 1037–1050. https://doi.org/10.1111/j.1460-9568.1996.tb01590.x

Guo, J., & Anton, E. S. (2014). Decision making during interneuron migration in the developing cerebral cortex. *Trends in Cell Biology*, *24*(6), 342–351. https://doi.org/10.1016/j.tcb.2013.12.001

Gyori, D., Chessa, T., Hawkins, P. T., & Stephens, L. R. (2017). Class (I) Phosphoinositide 3-Kinases in the Tumor Microenvironment. *Cancers*, *9*(3), E24. https://doi.org/10.3390/cancers9030024

Haas, C. A., Dudeck, O., Kirsch, M., Huszka, C., Kann, G., Pollak, S., Zentner, J., & Frotscher, M. (2002). Role for reelin in the development of granule cell dispersion in temporal lobe epilepsy. *The Journal of Neuroscience: The Official Journal of the Society for Neuroscience*, *22*(14), 5797–5802. https://doi.org/20026621

Hakem, R., Hakem, A., Duncan, G. S., Henderson, J. T., Woo, M., Soengas, M. S., Elia, A., de la Pompa, J. L., Kagi, D., Khoo, W., Potter, J., Yoshida, R., Kaufman, S. A., Lowe, S. W., Penninger, J. M., & Mak, T. W. (1998). Differential requirement for caspase 9 in apoptotic pathways in vivo. *Cell*, *94*(3), 339–352. https://doi.org/10.1016/s0092-8674(00)81477-4

Hansen, D. V., Lui, J. H., Parker, P. R. L., & Kriegstein, A. R. (2010). Neurogenic radial glia in the outer subventricular zone of human neocortex. *Nature*, *464*(7288), 554–561. https://doi.org/10.1038/nature08845

Happo, L., Strasser, A., & Cory, S. (2012). BH3-only proteins in apoptosis at a glance. *Journal of Cell Science*, *125*(5), 1081–1087. https://doi.org/10.1242/jcs.090514

Harris, K. D., & Shepherd, G. M. G. (2015). The neocortical circuit: Themes and variations. *Nature Neuroscience*, *18*(2), 170–181. https://doi.org/10.1038/nn.3917

Hauptman, J. S., & Mathern, G. W. (2012). Surgical treatment of epilepsy associated with cortical dysplasia: 2012 update. *Epilepsia*, *53 Suppl 4*, 98–104. https://doi.org/10.1111/j.1528-1167.2012.03619.x

He, L., Ingram, A., Rybak, A. P., & Tang, D. (2010). Shank-interacting protein-like 1 promotes tumorigenesis via PTEN inhibition in human tumor cells. *The Journal of Clinical Investigation*, *120*(6), 2094–2108. https://doi.org/10.1172/JCI40778

Hendrickson, W. A., & Ward, K. B. (1975). Atomic models for the polypeptide backbones of myohemerythrin and hemerythrin. *Biochemical and Biophysical Research Communications*, *66*(4), 1349–1356. https://doi.org/10.1016/0006-291x(75)90508-2

Hevner, R. F., Neogi, T., Englund, C., Daza, R. A. M., & Fink, A. (2003). Cajal-Retzius cells in the mouse: Transcription factors, neurotransmitters, and birthdays suggest a pallial origin. *Brain Research. Developmental Brain Research*, *141*(1–2), 39–53. https://doi.org/10.1016/s0165-3806(02)00641-7

Hoch, R. V., Rubenstein, J. L. R., & Pleasure, S. (2009). Genes and signaling events that establish regional patterning of the mammalian forebrain. *Seminars in Cell & Developmental Biology*, *20*(4), 378–386. https://doi.org/10.1016/j.semcdb.2009.02.005

Hoeffer, C. A., & Klann, E. (2010). mTOR signaling: At the crossroads of plasticity, memory and disease. *Trends in Neurosciences*, *33*(2), 67–75. https://doi.org/10.1016/j.tins.2009.11.003

Honda, R., Tanaka, H., & Yasuda, H. (1997). Oncoprotein MDM2 is a ubiquitin ligase E3 for tumor suppressor p53. *FEBS Letters*, *420*(1), 25–27. https://doi.org/10.1016/s0014-5793(97)01480-4

Horton, J. C., & Adams, D. L. (2005). The cortical column: A structure without a function. *Philosophical Transactions of the Royal Society of London. Series B, Biological Sciences*, *360*(1456), 837–862. https://doi.org/10.1098/rstb.2005.1623

Houart, C., Westerfield, M., & Wilson, S. W. (1998). A small population of anterior cells patterns the forebrain during zebrafish gastrulation. *Nature*, *391*(6669), 788–792. https://doi.org/10.1038/35853

Huang, R., Dai, Q., Yang, R., Duan, Y., Zhao, Q., Haybaeck, J., & Yang, Z. (2022). A Review: PI3K/AKT/mTOR Signaling Pathway and Its Regulated Eukaryotic Translation Initiation Factors May Be a Potential Therapeutic Target in Esophageal Squamous Cell Carcinoma. *Frontiers in Oncology*, *12*, 817916. https://doi.org/10.3389/fonc.2022.817916

Huber, K. M., Klann, E., Costa-Mattioli, M., & Zukin, R. S. (2015). Dysregulation of Mammalian Target of Rapamycin Signaling in Mouse Models of Autism. *The Journal of Neuroscience: The Official Journal of the Society for Neuroscience*, *35*(41), 13836–13842. https://doi.org/10.1523/JNEUROSCI.2656-15.2015

Huttenlocher, P. R., & Wollmann, R. L. (1991). Cellular Neuropathology of Tuberous Sclerosisa. *Annals of the New York Academy of Sciences*, *615*(1), 140–148. https://doi.org/10.1111/j.1749-6632.1991.tb37756.x

Ibrahim, L. A., Schuman, B., Bandler, R., Rudy, B., & Fishell, G. (2020). Mining the jewels of the cortex's crowning mystery. *Current Opinion in Neurobiology*, *63*, 154–161. https://doi.org/10.1016/j.conb.2020.04.005

Impagnatiello, F., Guidotti, A. R., Pesold, C., Dwivedi, Y., Caruncho, H., Pisu, M. G., Uzunov, D. P., Smalheiser, N. R., Davis, J. M., Pandey, G. N., Pappas, G. D., Tueting, P., Sharma, R. P., & Costa, E. (1998). A decrease of reelin expression as a putative vulnerability factor in schizophrenia. *Proceedings of the National Academy of Sciences of the United States of America*, *95*(26), 15718–15723. https://doi.org/10.1073/pnas.95.26.15718

Ito, A., Lai, C. H., Zhao, X., Saito, S., Hamilton, M. H., Appella, E., & Yao, T. P. (2001). P300/CBP-mediated p53 acetylation is commonly induced by p53-activating agents and inhibited by MDM2. *The EMBO Journal*, *20*(6), 1331–1340. https://doi.org/10.1093/emboj/20.6.1331

Izzo, E., Martin-Fardon, R., Koob, G. F., Weiss, F., & Sanna, P. P. (2002). Neural plasticity and addiction: PI3-kinase and cocaine behavioral sensitization. *Nature Neuroscience*, *5*(12), 1263–1264. https://doi.org/10.1038/nn977

J, M., Xh, Y., Y, F., & Yc, Y. (2014). Development of layer 1 neurons in the mouse neocortex. *Cerebral Cortex (New York, N.Y. : 1991)*, *24*(10). https://doi.org/10.1093/cercor/bht114

Jabaudon, D. (2017). Fate and freedom in developing neocortical circuits. *Nature Communications*, *8*, 16042. https://doi.org/10.1038/ncomms16042

Jabaudon, D., & López Bendito, G. (2012). Development and plasticity of thalamocortical systems. *The European Journal of Neuroscience*, *35*(10), 1522–1523. https://doi.org/10.1111/j.1460-9568.2012.08117.x

Jansen, L. A., Mirzaa, G. M., Ishak, G. E., O'Roak, B. J., Hiatt, J. B., Roden, W. H., Gunter, S. A., Christian, S. L., Collins, S., Adams, C., Rivière, J.-B., St-Onge, J., Ojemann, J. G., Shendure, J., Hevner, R. F., & Dobyns, W. B. (2015a). PI3K/AKT pathway mutations cause a spectrum of brain malformations from megalencephaly to focal cortical dysplasia. *Brain: A Journal of Neurology*, *138*(Pt 6), 1613–1628. https://doi.org/10.1093/brain/awv045

Jansen, L. A., Mirzaa, G. M., Ishak, G. E., O'Roak, B. J., Hiatt, J. B., Roden, W. H., Gunter, S. A., Christian, S. L., Collins, S., Adams, C., Rivière, J.-B., St-Onge, J., Ojemann, J. G., Shendure, J., Hevner, R. F., & Dobyns, W. B. (2015b). PI3K/AKT pathway mutations cause a spectrum of brain malformations from megalencephaly to focal cortical dysplasia. *Brain*, *138*(6), 1613–1628. https://doi.org/10.1093/brain/awv045

Janušonis, S., Gluncic, V., & Rakic, P. (2004). Early Serotonergic Projections to Cajal-Retzius Cells: Relevance for Cortical Development. *Journal of Neuroscience*, *24*(7), 1652–1659. https://doi.org/10.1523/JNEUROSCI.4651-03.2004

Jaworski, J. (2005). Control of Dendritic Arborization by the Phosphoinositide-3'-Kinase-Akt-Mammalian Target of Rapamycin Pathway. *Journal of Neuroscience*, *25*(49), 11300–11312. https://doi.org/10.1523/JNEUROSCI.2270-05.2005

Jaworski, J., Spangler, S., Seeburg, D. P., Hoogenraad, C. C., & Sheng, M. (2005). Control of dendritic arborization by the phosphoinositide-3'-kinase-Akt-mammalian target of

rapamycin pathway. *The Journal of Neuroscience: The Official Journal of the Society for Neuroscience*, *25*(49), 11300–11312. https://doi.org/10.1523/JNEUROSCI.2270-05.2005

Jean, S., & Kiger, A. A. (2014). Classes of phosphoinositide 3-kinases at a glance. *Journal of Cell Science*, *127*(5), 923–928. https://doi.org/10.1242/jcs.093773

Jossin, Y., & Goffinet, A. M. (2007a). Reelin Signals through Phosphatidylinositol 3-Kinase and Akt To Control Cortical Development and through mTor To Regulate Dendritic Growth. *Molecular and Cellular Biology*, *27*(20), 7113–7124. https://doi.org/10.1128/MCB.00928-07

Jossin, Y., & Goffinet, A. M. (2007b). Reelin Signals through Phosphatidylinositol 3-Kinase and Akt To Control Cortical Development and through mTor To Regulate Dendritic Growth. *Molecular and Cellular Biology*, *27*(20), 7113–7124. https://doi.org/10.1128/MCB.00928-07

Jung, C. H., Ro, S.-H., Cao, J., Otto, N. M., & Kim, D.-H. (2010). MTOR regulation of autophagy. *FEBS Letters*, *584*(7), 1287–1295. https://doi.org/10.1016/j.febslet.2010.01.017

Jung, S., Jeong, H., & Yu, S.-W. (2020). Autophagy as a decisive process for cell death. *Experimental & Molecular Medicine*, *52*(6), Article 6. https://doi.org/10.1038/s12276-020-0455-4

Ka, M., Condorelli, G., Woodgett, J. R., & Kim, W.-Y. (2014). MTOR regulates brain morphogenesis by mediating GSK3 signaling. *Development (Cambridge, England)*, *141*(21), 4076–4086. https://doi.org/10.1242/dev.108282

Kalkman, H. O. (2006). The role of the phosphatidylinositide 3-kinase-protein kinase B pathway in schizophrenia. *Pharmacology & Therapeutics*, *110*(1), 117–134. https://doi.org/10.1016/j.pharmthera.2005.10.014

Kanatani, S., Tabata, H., & Nakajima, K. (2005). Neuronal migration in cortical development. *Journal of Child Neurology*, *20*(4), 274–279. https://doi.org/10.1177/08830738050200040201

Kandel, E. R. (2013). *Principles of neural science* (5th ed). McGraw-Hill. http://lib.myilibrary.com/browse/open.asp?id=396874&entityid=https://idp.brunel.ac.uk/entity

Karam, C. S., Ballon, J. S., Bivens, N. M., Freyberg, Z., Girgis, R. R., Lizardi-Ortiz, J. E., Markx, S., Lieberman, J. A., & Javitch, J. A. (2010). Signaling Pathways in Schizophrenia: Emerging targets and therapeutic strategies. *Trends in Pharmacological Sciences*, *31*(8), 381–390. https://doi.org/10.1016/j.tips.2010.05.004

Kato, M., & Dobyns, W. B. (2003). Lissencephaly and the molecular basis of neuronal migration. *Human Molecular Genetics*, *12 Spec No 1*, R89-96. https://doi.org/10.1093/hmg/ddg086

Keller, G. B., & Mrsic-Flogel, T. D. (2018). Predictive Processing: A Canonical Cortical Computation. *Neuron*, *100*(2), 424–435. https://doi.org/10.1016/j.neuron.2018.10.003

Kerr, J. F., Wyllie, A. H., & Currie, A. R. (1972). Apoptosis: A basic biological phenomenon with wide-ranging implications in tissue kinetics. *British Journal of Cancer*, *26*(4), 239–257. https://doi.org/10.1038/bjc.1972.33

Khazipov, R., & Luhmann, H. J. (2006). Early patterns of electrical activity in the developing cerebral cortex of humans and rodents. *Trends in Neurosciences*, *29*(7), 414–418. https://doi.org/10.1016/j.tins.2006.05.007

Kilb, W., & Frotscher, M. (2016). Cajal-Retzius cells: Organizers of cortical development. *E-Neuroforum*, *7*(4), 82–88. https://doi.org/10.1007/s13295-016-0031-5

Kilb, W., & Luhmann, H. J. (2001). Spontaneous GABAergic postsynaptic currents in Cajal–Retzius cells in neonatal rat cerebral cortex. *European Journal of Neuroscience*, *13*(7), 1387–1390. https://doi.org/10.1046/j.0953-816x.2001.01514.x

Killick, R., Niklison-Chirou, M., Tomasini, R., Bano, D., Rufini, A., Grespi, F., Velletri, T., Tucci, P., Sayan, B. S., Conforti, F., Gallagher, E., Nicotera, P., Mak, T. W., Melino, G., Knight, R. A., & Agostini, M. (2011). p73: A multifunctional protein in neurobiology. *Molecular Neurobiology*, *43*(2), 139–146. https://doi.org/10.1007/s12035-011-8172-6

Kim, J. K., Cho, J., Kim, S. H., Kang, H.-C., Kim, D.-S., Kim, V. N., & Lee, J. H. (2019). Brain somatic mutations in *MTOR* reveal translational dysregulations underlying intractable focal epilepsy. *The Journal of Clinical Investigation*, *129*(10), 4207–4223. https://doi.org/10.1172/JCI127032

Kim, J.-S., Xu, X., Li, H., Solomon, D., Lane, W. S., Jin, T., & Waldman, T. (2011). Mechanistic analysis of a DNA damage-induced, PTEN-dependent size checkpoint in human cells. *Molecular and Cellular Biology*, *31*(13), 2756–2771. https://doi.org/10.1128/MCB.01323-10

Kirischuk, S., Luhmann, H. J., & Kilb, W. (2014). Cajal-Retzius cells: Update on structural and functional properties of these mystic neurons that bridged the 20th century. *Neuroscience*, *275*, 33–46. https://doi.org/10.1016/j.neuroscience.2014.06.009

Kiroski, I., Jiang, Y., Gavrilovici, C., Gao, F., Lee, S., Scantlebury, M. H., Vandal, M., Park, S. K., Tsai, L.-H., Teskey, G. C., Rho, J. M., & Nguyen, M. D. (2020). Reelin Improves Cognition and Extends the Lifespan of Mutant Ndel1 Mice with Postnatal CA1 Hippocampus Deterioration. *Cerebral Cortex (New York, N.Y.: 1991)*, *30*(9), 4964–4978. https://doi.org/10.1093/cercor/bhaa088

Klingler, E. (2017). Development and Organization of the Evolutionarily Conserved Three-Layered Olfactory Cortex. *ENeuro*, *4*(1), ENEURO.0193-16.2016. https://doi.org/10.1523/ENEURO.0193-16.2016

Klingler, E., De la Rossa, A., Fièvre, S., Devaraju, K., Abe, P., & Jabaudon, D. (2019). A Translaminar Genetic Logic for the Circuit Identity of Intracortically Projecting Neurons. *Current Biology: CB*, *29*(2), 332-339.e5. https://doi.org/10.1016/j.cub.2018.11.071

Koboldt, D. C., Miller, K. E., Miller, A. R., Bush, J. M., McGrath, S., Leraas, K., Crist, E., Fair, S., Schwind, W., Wijeratne, S., Fitch, J., Leonard, J., Shaikhouni, A., Hester, M. E., Magrini, V., Ho, M.-L., Pierson, C. R., Wilson, R. K., Ostendorf, A. P., … Bedrosian, T. A. (2021). PTEN

somatic mutations contribute to spectrum of cerebral overgrowth. *Brain*, *144*(10), 2971–2978. https://doi.org/10.1093/brain/awab173

Krahe, T. E., Medina, A. E., Lantz, C. L., & Filgueiras, C. C. (2015). Hyperactivity and depression-like traits in Bax KO mice. *Brain Research*, *1625*, 246–254. https://doi.org/10.1016/j.brainres.2015.09.002

Kreis, P., Leondaritis, G., Lieberam, I., & Eickholt, B. (2014). Subcellular targeting and dynamic regulation of PTEN: Implications for neuronal cells and neurological disorders. *Frontiers in Molecular Neuroscience*, *7*. https://www.frontiersin.org/articles/10.3389/fnmol.2014.00023

Kuida, K., Haydar, T. F., Kuan, C.-Y., Gu, Y., Taya, C., Karasuyama, H., Su, M. S.-S., Rakic, P., & Flavell, R. A. (1998). Reduced Apoptosis and Cytochrome c–Mediated Caspase Activation in Mice Lacking Caspase 9. *Cell*, *94*(3), 325–337. https://doi.org/10.1016/S0092-8674(00)81476-2

Kwan, K. Y., Sestan, N., & Anton, E. S. (2012). Transcriptional co-regulation of neuronal migration and laminar identity in the neocortex. *Development (Cambridge, England)*, *139*(9), 1535–1546. https://doi.org/10.1242/dev.069963

Kwiatkowski, D. J. (2002a). A mouse model of TSC1 reveals sex-dependent lethality from liver hemangiomas, and up-regulation of p70S6 kinase activity in Tsc1 null cells. *Human Molecular Genetics*, *11*(5), 525–534. https://doi.org/10.1093/hmg/11.5.525

Kwon, C.-H., Luikart, B. W., Powell, C. M., Zhou, J., Matheny, S. A., Zhang, W., Li, Y., Baker, S. J., & Parada, L. F. (2006). Pten Regulates Neuronal Arborization and Social Interaction in Mice. *Neuron*, *50*(3), 377–388. https://doi.org/10.1016/j.neuron.2006.03.023

Kwon, C.-H., Zhu, X., Zhang, J., Knoop, L. L., Tharp, R., Smeyne, R. J., Eberhart, C. G., Burger, P. C., & Baker, S. J. (2001). Pten regulates neuronal soma size: A mouse model of Lhermitte-Duclos disease. *Nature Genetics*, *29*(4), 404–411. https://doi.org/10.1038/ng781

Lachyankar, M. B., Sultana, N., Schonhoff, C. M., Mitra, P., Poluha, W., Lambert, S., Quesenberry, P. J., Litofsky, N. S., Recht, L. D., Nabi, R., Miller, S. J., Ohta, S., Neel, B. G., & Ross, A. H. (2000). A Role for Nuclear PTEN in Neuronal Differentiation. *The Journal of Neuroscience*, *20*(4), 1404–1413. https://doi.org/10.1523/JNEUROSCI.20-04-01404.2000

Ledonne, F., Orduz, D., Mercier, J., Vigier, L., Grove, E. A., Tissir, F., Angulo, M. C., Pierani, A., & Coppola, E. (2016). Targeted Inactivation of Bax Reveals a Subtype-Specific Mechanism of Cajal-Retzius Neuron Death in the Postnatal Cerebral Cortex. *Cell Reports*, *17*(12), 3133–3141. https://doi.org/10.1016/j.celrep.2016.11.074

Lee, E. F., Czabotar, P. E., van Delft, M. F., Michalak, E. M., Boyle, M. J., Willis, S. N., Puthalakath, H., Bouillet, P., Colman, P. M., Huang, D. C. S., & Fairlie, W. D. (2008). A novel BH3 ligand that selectively targets Mcl-1 reveals that apoptosis can proceed without Mcl-1 degradation. *The Journal of Cell Biology*, *180*(2), 341–355. https://doi.org/10.1083/jcb.200708096

Lee, E. F., Harris, T. J., Tran, S., Evangelista, M., Arulananda, S., John, T., Ramnac, C., Hobbs, C., Zhu, H., Gunasingh, G., Segal, D., Behren, A., Cebon, J., Dobrovic, A., Mariadason, J. M.,

Strasser, A., Rohrbeck, L., Haass, N. K., Herold, M. J., & Fairlie, W. D. (2019). BCL-XL and MCL-1 are the key BCL-2 family proteins in melanoma cell survival. *Cell Death & Disease*, *10*(5), Article 5. https://doi.org/10.1038/s41419-019-1568-3

Lee, J. O., Yang, H., Georgescu, M. M., Di Cristofano, A., Maehama, T., Shi, Y., Dixon, J. E., Pandolfi, P., & Pavletich, N. P. (1999). Crystal structure of the PTEN tumor suppressor: Implications for its phosphoinositide phosphatase activity and membrane association. *Cell*, *99*(3), 323–334. https://doi.org/10.1016/s0092-8674(00)81663-3

Lee, Y.-K., & Lee, J.-A. (2016). Role of the mammalian ATG8/LC3 family in autophagy: Differential and compensatory roles in the spatiotemporal regulation of autophagy. *BMB Reports*, *49*(8), 424–430. https://doi.org/10.5483/BMBRep.2016.49.8.081

Lehman, J. A., Waning, D. L., Batuello, C. N., Cipriano, R., Kadakia, M. P., & Mayo, L. D. (2011). Induction of Apoptotic Genes by a p73-Phosphatase and Tensin Homolog (p73-PTEN) Protein Complex in Response to Genotoxic Stress. *The Journal of Biological Chemistry*, *286*(42), 36631–36640. https://doi.org/10.1074/jbc.M110.217620

Leonard, J. R., Klocke, B. J., D'Sa, C., Flavell, R. A., & Roth, K. A. (2002). Strain-dependent neurodevelopmental abnormalities in caspase-3-deficient mice. *Journal of Neuropathology and Experimental Neurology*, *61*(8), 673–677. https://doi.org/10.1093/jnen/61.8.673

Li, L., Liu, F., Salmonsen, R. A., Turner, T. K., Litofsky, N. S., Di Cristofano, A., Pandolfi, P. P., Jones, S. N., Recht, L. D., & Ross, A. H. (2002). PTEN in neural precursor cells: Regulation of migration, apoptosis, and proliferation. *Molecular and Cellular Neurosciences*, *20*(1), 21–29. https://doi.org/10.1006/mcne.2002.1115

Li, P., Nijhawan, D., Budihardjo, I., Srinivasula, S. M., Ahmad, M., Alnemri, E. S., & Wang, X. (1997). Cytochrome c and dATP-dependent formation of Apaf-1/caspase-9 complex initiates an apoptotic protease cascade. *Cell*, *91*(4), 479–489. https://doi.org/10.1016/s0092-8674(00)80434-1

Lim, J. S., Gopalappa, R., Kim, S. H., Ramakrishna, S., Lee, M., Kim, W.-I., Kim, J., Park, S. M., Lee, J., Oh, J.-H., Kim, H. D., Park, C.-H., Lee, J. S., Kim, S., Kim, D. S., Han, J. M., Kang, H.-C., Kim, H. H., & Lee, J. H. (2017). Somatic Mutations in TSC1 and TSC2 Cause Focal Cortical Dysplasia. *American Journal of Human Genetics*, *100*(3), 454–472. https://doi.org/10.1016/j.ajhg.2017.01.030

Lin, C. S., Nicolelis, M. A., Schneider, J. S., & Chapin, J. K. (1991). GABAergic pathway from zona incerta to neocortex: Clarification. *Science (New York, N.Y.)*, *251*(4998), 1162.

Liu, Q., Dwyer, N. D., & O'Leary, D. D. (2000). Differential expression of COUP-TFI, CHL1, and two novel genes in developing neocortex identified by differential display PCR. *The Journal of Neuroscience: The Official Journal of the Society for Neuroscience*, *20*(20), 7682–7690.

Liu, R., Chen, Y., Liu, G., Li, C., Song, Y., Cao, Z., Li, W., Hu, J., Lu, C., & Liu, Y. (2020). PI3K/AKT pathway as a key link modulates the multidrug resistance of cancers. *Cell Death & Disease*, *11*(9), Article 9. https://doi.org/10.1038/s41419-020-02998-6

Llambi, F., & Green, D. R. (2011). Apoptosis and oncogenesis: Give and take in the BCL-2 family. *Current Opinion in Genetics & Development*, *21*(1), 12–20. https://doi.org/10.1016/j.gde.2010.12.001

Lodato, S., & Arlotta, P. (2015). Generating neuronal diversity in the mammalian cerebral cortex. *Annual Review of Cell and Developmental Biology*, *31*, 699–720. https://doi.org/10.1146/annurev-cellbio-100814-125353

Lodato, S., Shetty, A. S., & Arlotta, P. (2015). Cerebral cortex assembly: Generating and reprogramming projection neuron diversity. *Trends in Neurosciences*, *38*(2), 117–125. https://doi.org/10.1016/j.tins.2014.11.003

Lopes, F., Torres, F., Soares, G., van Karnebeek, C. D., Martins, C., Antunes, D., Silva, J., Muttucomaroe, L., Botelho, L. F., Sousa, S., Rendeiro, P., Tavares, P., Van Esch, H., Rajcan-Separovic, E., & Maciel, P. (2019). The Role of AKT3 Copy Number Changes in Brain Abnormalities and Neurodevelopmental Disorders: Four New Cases and Literature Review. *Frontiers in Genetics*, *10*. https://www.frontiersin.org/articles/10.3389/fgene.2019.00058

Louvi, A., Yoshida, M., & Grove, E. A. (2007). The derivatives of the Wnt3a lineage in the central nervous system. *Journal of Comparative Neurology*, *504*(5), 550–569. https://doi.org/10.1002/cne.21461

Luhmann, H. J., & Khazipov, R. (2018). Neuronal activity patterns in the developing barrel cortex. *Neuroscience*, *368*, 256–267. https://doi.org/10.1016/j.neuroscience.2017.05.025

Luo, H. R., Hattori, H., Hossain, M. A., Hester, L., Huang, Y., Lee-Kwon, W., Donowitz, M., Nagata, E., & Snyder, S. H. (2003). Akt as a mediator of cell death. *Proceedings of the National Academy of Sciences*, *100*(20), 11712–11717. https://doi.org/10.1073/pnas.1634990100

Luzzati, F. (2015). A hypothesis for the evolution of the upper layers of the neocortex through co-option of the olfactory cortex developmental program. *Frontiers in Neuroscience*, *9*, 162. https://doi.org/10.3389/fnins.2015.00162

Madisen, L., Zwingman, T. A., Sunkin, S. M., Oh, S. W., Zariwala, H. A., Gu, H., Ng, L. L., Palmiter, R. D., Hawrylycz, M. J., Jones, A. R., Lein, E. S., & Zeng, H. (2010). A robust and high-throughput Cre reporting and characterization system for the whole mouse brain. *Nature Neuroscience*, *13*(1), 133–140. https://doi.org/10.1038/nn.2467

Marin-Padilla, M. (1978). Dual origin of the mammalian neocortex and evolution of the cortical plate. *Anatomy and Embryology*, *152*(2), 109–126. https://doi.org/10.1007/BF00315920

Marín-Padilla, M. (1998). Cajal-Retzius cells and the development of the neocortex. *Trends in Neurosciences*, *21*(2), 64–71. https://doi.org/10.1016/s0166-2236(97)01164-8

Martínez-Cerdeño, V., & Noctor, S. C. (2014). Cajal, Retzius, and Cajal-Retzius cells. *Frontiers in Neuroanatomy*, *8*, 48. https://doi.org/10.3389/fnana.2014.00048

Matsuura, K., Canfield, K., Feng, W., & Kurokawa, M. (2016). Metabolic Regulation of Apoptosis in Cancer. *International Review of Cell and Molecular Biology*, *327*, 43–87. https://doi.org/10.1016/bs.ircmb.2016.06.006

McIlwain, D. R., Berger, T., & Mak, T. W. (2013). Caspase functions in cell death and disease. *Cold Spring Harbor Perspectives in Biology*, *5*(4), a008656. https://doi.org/10.1101/cshperspect.a008656

Medina, L., & Abellán, A. (2009). Development and evolution of the pallium. *Seminars in Cell & Developmental Biology*, *20*(6), 698–711. https://doi.org/10.1016/j.semcdb.2009.04.008

Meng, X.-F., Yu, J.-T., Song, J.-H., Chi, S., & Tan, L. (2013). Role of the mTOR signaling pathway in epilepsy. *Journal of the Neurological Sciences*, *332*(1–2), 4–15. https://doi.org/10.1016/j.jns.2013.05.029

Meyer, G. (2010). Building a human cortex: The evolutionary differentiation of Cajal-Retzius cells and the cortical hem. *Journal of Anatomy*, *217*(4), 334–343. https://doi.org/10.1111/j.1469-7580.2010.01266.x

Mienville, J. M., & Pesold, C. (1999). Low resting potential and postnatal upregulation of NMDA receptors may cause Cajal-Retzius cell death. *The Journal of Neuroscience: The Official Journal of the Society for Neuroscience*, *19*(5), 1636–1646.

Mienville, J.-M. (1998). Persistent depolarizing action of GABA in rat Cajal-Retzius cells. *The Journal of Physiology*, *512*(3), 809–817. https://doi.org/10.1111/j.1469-7793.1998.809bd.x

Mihalas, A. B., & Hevner, R. F. (2018). Clonal analysis reveals laminar fate multipotency and daughter cell apoptosis of mouse cortical intermediate progenitors. *Development (Cambridge, England)*, *145*(17), dev164335. https://doi.org/10.1242/dev.164335

Moloney, P. B., Cavalleri, G. L., & Delanty, N. (2021). Epilepsy in the mTORopathies: Opportunities for precision medicine. *Brain Communications*, *3*(4), fcab222. https://doi.org/10.1093/braincomms/fcab222

Muntané, J. (2011). Harnessing tumor necrosis factor receptors to enhance antitumor activities of drugs. *Chemical Research in Toxicology*, *24*(10), 1610–1616. https://doi.org/10.1021/tx2002349

Myakhar, O., Unichenko, P., & Kirischuk, S. (2011). GABAergic projections from the subplate to Cajal-Retzius cells in the neocortex. *Neuroreport*, *22*(11), 525–529. https://doi.org/10.1097/WNR.0b013e32834888a4

Na, E. J., Nam, H. Y., Park, J., Chung, M. A., Woo, H. A., & Kim, H.-J. (2017). PI3K-mTOR-S6K Signaling Mediates Neuronal Viability via Collapsin Response Mediator Protein-2 Expression. *Frontiers in Molecular Neuroscience*, *10*, 288. https://doi.org/10.3389/fnmol.2017.00288

Najm, I. M., Sarnat, H. B., & Blümcke, I. (2018). Review: The international consensus classification of Focal Cortical Dysplasia - a critical update 2018. *Neuropathology and Applied Neurobiology*, *44*(1), 18–31. https://doi.org/10.1111/nan.12462

Nakamura, T., Okamoto, I., Sasaki, K., Yabuta, Y., Iwatani, C., Tsuchiya, H., Seita, Y., Nakamura, S., Yamamoto, T., & Saitou, M. (2016). A developmental coordinate of pluripotency among

mice, monkeys and humans. *Nature*, *537*(7618), 57–62. https://doi.org/10.1038/nature19096

Nakanishi, A., Kitagishi, Y., Ogura, Y., & Matsuda, S. (2014). The tumor suppressor PTEN interacts with p53 in hereditary cancer (Review). *International Journal of Oncology*, *44*(6), 1813–1819. https://doi.org/10.3892/ijo.2014.2377

Noctor, S. C., Flint, A. C., Weissman, T. A., Dammerman, R. S., & Kriegstein, A. R. (2001). Neurons derived from radial glial cells establish radial units in neocortex. *Nature*, *409*(6821), 714–720. https://doi.org/10.1038/35055553

Noctor, S. C., Martínez-Cerdeño, V., Ivic, L., & Kriegstein, A. R. (2004). Cortical neurons arise in symmetric and asymmetric division zones and migrate through specific phases. *Nature Neuroscience*, *7*(2), 136–144. https://doi.org/10.1038/nn1172

Noda, T. (2017). Regulation of Autophagy through TORC1 and mTORC1. *Biomolecules*, *7*(3), 52. https://doi.org/10.3390/biom7030052

Noguchi, M., Hirata, N., Tanaka, T., Suizu, F., Nakajima, H., & Chiorini, J. A. (2020). Autophagy as a modulator of cell death machinery. *Cell Death & Disease*, *11*(7), Article 7. https://doi.org/10.1038/s41419-020-2724-5

Oegema, R., Barakat, T. S., Wilke, M., Stouffs, K., Amrom, D., Aronica, E., Bahi-Buisson, N., Conti, V., Fry, A. E., Geis, T., Andres, D. G., Parrini, E., Pogledic, I., Said, E., Soler, D., Valor, L. M., Zaki, M. S., Mirzaa, G., Dobyns, W. B., … Di Donato, N. (2020). International consensus recommendations on the diagnostic work-up for malformations of cortical development. *Nature Reviews. Neurology*, *16*(11), 618–635. https://doi.org/10.1038/s41582-020-0395-6

Ogawa, M., Miyata, T., Nakajima, K., Yagyu, K., Seike, M., Ikenaka, K., Yamamoto, H., & Mikoshiba, K. (1995). The reeler gene-associated antigen on Cajal-Retzius neurons is a crucial molecule for laminar organization of cortical neurons. *Neuron*, *14*(5), 899–912. https://doi.org/10.1016/0896-6273(95)90329-1

Ohashi, A., Ohori, M., Iwai, K., Nakayama, Y., Nambu, T., Morishita, D., Kawamoto, T., Miyamoto, M., Hirayama, T., Okaniwa, M., Banno, H., Ishikawa, T., Kandori, H., & Iwata, K. (2015). Aneuploidy generates proteotoxic stress and DNA damage concurrently with p53-mediated post-mitotic apoptosis in SAC-impaired cells. *Nature Communications*, *6*, 7668. https://doi.org/10.1038/ncomms8668

Ohshima, K., Karube, K., Hamasaki, M., Makimoto, Y., Fujii, A., Kawano, R., Tutiya, T., Yamaguchi, T., Suzumiya, J., & Kikuchi, M. (2004). Apoptosis- and cell cycle-associated gene expression profiling of histiocytic necrotising lymphadenitis. *European Journal of Haematology*, *72*(5), 322–329. https://doi.org/10.1111/j.1600-0609.2004.00226.x

Ohtaka-Maruyama, C., Okamoto, M., Endo, K., Oshima, M., Kaneko, N., Yura, K., Okado, H., Miyata, T., & Maeda, N. (2018). Synaptic transmission from subplate neurons controls radial migration of neocortical neurons. *Science (New York, N.Y.)*, *360*(6386), 313–317. https://doi.org/10.1126/science.aar2866

O'Leary, D. D. M., Chou, S.-J., & Sahara, S. (2007). Area patterning of the mammalian cortex. *Neuron*, *56*(2), 252–269. https://doi.org/10.1016/j.neuron.2007.10.010

Ollion, J., Cochennec, J., Loll, F., Escudé, C., & Boudier, T. (2013). TANGO: A generic tool for high-throughput 3D image analysis for studying nuclear organization. *Bioinformatics*, *29*(14), 1840–1841. https://doi.org/10.1093/bioinformatics/btt276

Oo, T. F., Kholodilov, N., & Burke, R. E. (2003). Regulation of natural cell death in dopaminergic neurons of the substantia nigra by striatal glial cell line-derived neurotrophic factor in vivo. *The Journal of Neuroscience: The Official Journal of the Society for Neuroscience*, *23*(12), 5141–5148.

Ozes, O. N., Mayo, L. D., Gustin, J. A., Pfeffer, S. R., Pfeffer, L. M., & Donner, D. B. (1999). NF-kappaB activation by tumour necrosis factor requires the Akt serine-threonine kinase. *Nature*, *401*(6748), 82–85. https://doi.org/10.1038/43466

Parcellier, A., Tintignac, L. A., Zhuravleva, E., & Hemmings, B. A. (2008). PKB and the mitochondria: AKTing on apoptosis. *Cellular Signalling*, *20*(1), 21–30. https://doi.org/10.1016/j.cellsig.2007.07.010

Parenti, I., Rabaneda, L. G., Schoen, H., & Novarino, G. (2020). Neurodevelopmental Disorders: From Genetics to Functional Pathways. *Trends in Neurosciences*, *43*(8), 608–621. https://doi.org/10.1016/j.tins.2020.05.004

Paridaen, J. T. M. L., & Huttner, W. B. (2014). Neurogenesis during development of the vertebrate central nervous system. *EMBO Reports*, *15*(4), 351–364. https://doi.org/10.1002/embr.201438447

Park, E., Kim, Y., Noh, H., Lee, H., Yoo, S., & Park, S. (2013). EphA/ephrin-A signaling is critically involved in region-specific apoptosis during early brain development. *Cell Death & Differentiation*, *20*(1), Article 1. https://doi.org/10.1038/cdd.2012.121

Patrylo, P. R., Browning, R. A., & Cranick, S. (2006). Reeler homozygous mice exhibit enhanced susceptibility to epileptiform activity. *Epilepsia*, *47*(2), 257–266. https://doi.org/10.1111/j.1528-1167.2006.00417.x

Peterson, S. E., Yang, A. H., Bushman, D. M., Westra, J. W., Yung, Y. C., Barral, S., Mutoh, T., Rehen, S. K., & Chun, J. (2012). Aneuploid Cells Are Differentially Susceptible to Caspase-Mediated Death during Embryonic Cerebral Cortical Development. *The Journal of Neuroscience*, *32*(46), 16213–16222. https://doi.org/10.1523/JNEUROSCI.3706-12.2012

Pettmann, B., & Henderson, C. E. (1998). Neuronal cell death. *Neuron*, *20*(4), 633–647. https://doi.org/10.1016/s0896-6273(00)81004-1

Pilarski, R., Burt, R., Kohlman, W., Pho, L., Shannon, K. M., & Swisher, E. (2013). Cowden syndrome and the PTEN hamartoma tumor syndrome: Systematic review and revised diagnostic criteria. *Journal of the National Cancer Institute*, *105*(21), 1607–1616. https://doi.org/10.1093/jnci/djt277

Pilaz, L.-J., McMahon, J. J., Miller, E. E., Lennox, A. L., Suzuki, A., Salmon, E., & Silver, D. L. (2016). Prolonged Mitosis of Neural Progenitors Alters Cell Fate in the Developing Brain. *Neuron*, *89*(1), 83–99. https://doi.org/10.1016/j.neuron.2015.12.007

Porta, C., Paglino, C., & Mosca, A. (2014). Targeting PI3K/Akt/mTOR Signaling in Cancer. *Frontiers in Oncology*, *4*, 64. https://doi.org/10.3389/fonc.2014.00064

Pouchelon, G., Gambino, F., Bellone, C., Telley, L., Vitali, I., Lüscher, C., Holtmaat, A., & Jabaudon, D. (2014). Modality-specific thalamocortical inputs instruct the identity of postsynaptic L4 neurons. *Nature*, *511*(7510), 471–474. https://doi.org/10.1038/nature13390

Pozas, E., Paco, S., Soriano, E., & Aguado, F. (2008). Cajal-Retzius cells fail to trigger the developmental expression of the Cl- extruding co-transporter KCC2. *Brain Research*, *1239*, 85–91. https://doi.org/10.1016/j.brainres.2008.08.058

Pozniak, C. D., Radinovic, S., Yang, A., McKeon, F., Kaplan, D. R., & Miller, F. D. (2000). An anti-apoptotic role for the p53 family member, p73, during developmental neuron death. *Science (New York, N.Y.)*, *289*(5477), 304–306. https://doi.org/10.1126/science.289.5477.304

Price, D. J., Aslam, S., Tasker, L., & Gillies, K. (1997). Fates of the earliest generated cells in the developing murine neocortex. *The Journal of Comparative Neurology*, *377*(3), 414–422.

Puelles, L., & Rubenstein, J. L. R. (2003). Forebrain gene expression domains and the evolving prosomeric model. *Trends in Neurosciences*, *26*(9), 469–476. https://doi.org/10.1016/S0166-2236(03)00234-0

Qi, X.-J., Wildey, G. M., & Howe, P. H. (2006). Evidence That Ser87 of BimEL Is Phosphorylated by Akt and Regulates BimEL Apoptotic Function *. *Journal of Biological Chemistry*, *281*(2), 813–823. https://doi.org/10.1074/jbc.M505546200

Quattrocolo, G., & Maccaferri, G. (2014). Optogenetic activation of cajal-retzius cells reveals their glutamatergic output and a novel feedforward circuit in the developing mouse hippocampus. *The Journal of Neuroscience: The Official Journal of the Society for Neuroscience*, *34*(39), 13018–13032. https://doi.org/10.1523/JNEUROSCI.1407-14.2014

Radnikow, G., Feldmeyer, D., & Lübke, J. (2002a). Axonal projection, input and output synapses, and synaptic physiology of Cajal-Retzius cells in the developing rat neocortex. *The Journal of Neuroscience: The Official Journal of the Society for Neuroscience*, *22*(16), 6908–6919. https://doi.org/20026725

Rahdar, M., Inoue, T., Meyer, T., Zhang, J., Vazquez, F., & Devreotes, P. N. (2009). A phosphorylation-dependent intramolecular interaction regulates the membrane association and activity of the tumor suppressor PTEN. *Proceedings of the National Academy of Sciences of the United States of America*, *106*(2), 480–485. https://doi.org/10.1073/pnas.0811212106

Rakic, P. (1971). Guidance of neurons migrating to the fetal monkey neocortex. *Brain Research*, *33*(2), 471–476. https://doi.org/10.1016/0006-8993(71)90119-3

Rallu, M., Machold, R., Gaiano, N., Corbin, J. G., McMahon, A. P., & Fishell, G. (2002). Dorsoventral patterning is established in the telencephalon of mutants lacking both Gli3 and Hedgehog signaling. *Development (Cambridge, England)*, *129*(21), 4963–4974. https://doi.org/10.1242/dev.129.21.4963

Ramon y Cajal, S. (1890). Sobre la existencia de células nerviosas especiales en la primera capa de la scircumvoluciones cerebrales. *Gaceta Medica Catalana*, 13, 23.

Retzius, G. (1893). Die Cajal'schen Zellender Grosshirnrin de beim Menschenund bei Säiugerthieren. *BiologischesUntersuchungen*, 5:1.

Riva, M., Genescu, I., Habermacher, C., Orduz, D., Ledonne, F., Rijli, F. M., López-Bendito, G., Coppola, E., Garel, S., Angulo, M. C., & Pierani, A. (2019a). Activity-dependent death of transient Cajal-Retzius neurons is required for functional cortical wiring. *ELife*, *8*, e50503. https://doi.org/10.7554/eLife.50503

Rogers, D. C., Peters, J., Martin, J. E., Ball, S., Nicholson, S. J., Witherden, A. S., Hafezparast, M., Latcham, J., Robinson, T. L., Quilter, C. A., & Fisher, E. M. C. (2001). SHIRPA, a protocol for behavioral assessment: Validation for longitudinal study of neurological dysfunction in mice. *Neuroscience Letters*, *306*(1–2), 89–92. https://doi.org/10.1016/S0304-3940(01)01885-7

Romashkova, J. A., & Makarov, S. S. (1999). NF-kappaB is a target of AKT in anti-apoptotic PDGF signalling. *Nature*, *401*(6748), 86–90. https://doi.org/10.1038/43474

Roth, K. A., Kuan, C.-Y., Haydar, T. F., D'Sa-Eipper, C., Shindler, K. S., Zheng, T. S., Kuida, K., Flavell, R. A., & Rakic, P. (2000). Epistatic and independent functions of Caspase-3 and Bcl-XL in developmental programmed cell death. *Proceedings of the National Academy of Sciences of the United States of America*, *97*(1), 466–471.

Rubenstein, J. L., & Beachy, P. A. (1998). Patterning of the embryonic forebrain. *Current Opinion in Neurobiology*, *8*(1), 18–26. https://doi.org/10.1016/s0959-4388(98)80004-4

Rubinstein, A. D., Eisenstein, M., Ber, Y., Bialik, S., & Kimchi, A. (2011). The autophagy protein Atg12 associates with antiapoptotic Bcl-2 family members to promote mitochondrial apoptosis. *Molecular Cell*, *44*(5), 698–709. https://doi.org/10.1016/j.molcel.2011.10.014

Rubio-Garrido, P., Pérez-de-Manzo, F., Porrero, C., Galazo, M. J., & Clascá, F. (2009). Thalamic input to distal apical dendrites in neocortical layer 1 is massive and highly convergent. *Cerebral Cortex (New York, N.Y.: 1991)*, *19*(10), 2380–2395. https://doi.org/10.1093/cercor/bhn259

Ruiz-Reig, N., Andrés, B., Huilgol, D., Grove, E. A., Tissir, F., Tole, S., Theil, T., Herrera, E., & Fairén, A. (2017). Lateral Thalamic Eminence: A Novel Origin for mGluR1/Lot Cells. *Cerebral Cortex (New York, N.Y.: 1991)*, *27*(5), 2841–2856. https://doi.org/10.1093/cercor/bhw126

Sakayori, N., Kimura, R., & Osumi, N. (2013). Impact of lipid nutrition on neural stem/progenitor cells. *Stem Cells International*, *2013*, 973508. https://doi.org/10.1155/2013/973508

Satterstrom, F. K., Kosmicki, J. A., Wang, J., Breen, M. S., De Rubeis, S., An, J.-Y., Peng, M., Collins, R., Grove, J., Klei, L., Stevens, C., Reichert, J., Mulhern, M. S., Artomov, M., Gerges, S., Sheppard, B., Xu, X., Bhaduri, A., Norman, U., … Buxbaum, J. D. (2020). Large-Scale Exome Sequencing Study Implicates Both Developmental and Functional Changes in the Neurobiology of Autism. *Cell*, *180*(3), 568-584.e23. https://doi.org/10.1016/j.cell.2019.12.036

Sava, B. A., Dávid, C. S., Teissier, A., Pierani, A., Staiger, J. F., Luhmann, H. J., & Kilb, W. (2010). Electrophysiological and morphological properties of Cajal-Retzius cells with different ontogenetic origins. *Neuroscience*, *167*(3), 724–734. https://doi.org/10.1016/j.neuroscience.2010.02.043

Saxton, R. A., & Sabatini, D. M. (2017). MTOR Signaling in Growth, Metabolism, and Disease. *Cell*, *168*(6), 960–976. https://doi.org/10.1016/j.cell.2017.02.004

Settembre, C., Fraldi, A., Medina, D. L., & Ballabio, A. (2013). Signals from the lysosome: A control centre for cellular clearance and energy metabolism. *Nature Reviews. Molecular Cell Biology*, *14*(5), 283–296. https://doi.org/10.1038/nrm3565

Shao, D. D., Achkar, C. M., Lai, A., Srivastava, S., Doan, R. N., Rodan, L. H., Chen, A. Y., Brain Development Study Group, Poduri, A., Yang, E., & Walsh, C. A. (2020). Polymicrogyria is Associated With Pathogenic Variants in PTEN. *Annals of Neurology*, *88*(6), 1153–1164. https://doi.org/10.1002/ana.25904

Shaw, R. J., & Cantley, L. C. (2006). Ras, PI(3)K and mTOR signalling controls tumour cell growth. *Nature*, *441*(7092), 424–430. https://doi.org/10.1038/nature04869

Shi, Y., Paluch, B. E., Wang, X., & Jiang, X. (2012). PTEN at a glance. *Journal of Cell Science*, *125*(20), 4687–4692. https://doi.org/10.1242/jcs.093765

Sidira, C., Vargiami, E., Dragoumi, P., & Zafeiriou, D. I. (2021). Hemimegalencephaly and tuberous sclerosis complex: A rare yet challenging association. *European Journal of Paediatric Neurology: EJPN: Official Journal of the European Paediatric Neurology Society*, *30*, 58–65. https://doi.org/10.1016/j.ejpn.2020.12.007

Simões-Wüst, A. P., Sigrist, B., Belyanskaya, L., Hopkins Donaldson, S., Stahel, R. A., & Zangemeister-Wittke, U. (2005). ΔNp73 antisense activates PUMA and induces apoptosis in neuroblastoma cells. *Journal of Neuro-Oncology*, *72*(1), 29–34. https://doi.org/10.1007/s11060-004-3118-8

Sisodiya, S. M., Fauser, S., Cross, J. H., & Thom, M. (2009). Focal cortical dysplasia type II: Biological features and clinical perspectives. *The Lancet. Neurology*, *8*(9), 830–843. https://doi.org/10.1016/S1474-4422(09)70201-7

Skelton, P. D., Frazel, P. W., Lee, D., Suh, H., & Luikart, B. W. (2019). Pten loss results in inappropriate excitatory connectivity. *Molecular Psychiatry*, *24*(11), 1627–1640. https://doi.org/10.1038/s41380-019-0412-6

Song, G., Ouyang, G., & Bao, S. (2005). The activation of Akt/PKB signaling pathway and cell survival. *Journal of Cellular and Molecular Medicine*, *9*(1), 59–71. https://doi.org/10.1111/j.1582-4934.2005.tb00337.x

Song, M. S., Carracedo, A., Salmena, L., Song, S. J., Egia, A., Malumbres, M., & Pandolfi, P. P. (2011). Nuclear PTEN regulates the APC-CDH1 tumor-suppressive complex in a phosphatase-independent manner. *Cell*, *144*(2), 187–199. https://doi.org/10.1016/j.cell.2010.12.020

Srinivasan, L., Sasaki, Y., Calado, D. P., Zhang, B., Paik, J. H., DePinho, R. A., Kutok, J. L., Kearney, J. F., Otipoby, K. L., & Rajewsky, K. (2009). PI3 Kinase Signals BCR-Dependent Mature B Cell Survival. *Cell*, *139*(3), 573–586. https://doi.org/10.1016/j.cell.2009.08.041

Stad, R., Ramos, Y. F., Little, N., Grivell, S., Attema, J., van Der Eb, A. J., & Jochemsen, A. G. (2000). Hdmx stabilizes Mdm2 and p53. *The Journal of Biological Chemistry*, *275*(36), 28039–28044. https://doi.org/10.1074/jbc.M003496200

Striano, P., & Zara, F. (2012). Genetics: Mutations in mTOR pathway linked to megalencephaly syndromes. *Nature Reviews. Neurology*, *8*(10), 542–544. https://doi.org/10.1038/nrneurol.2012.178

Sui, L., Wang, J., & Li, B.-M. (2008). Role of the phosphoinositide 3-kinase-Akt-mammalian target of the rapamycin signaling pathway in long-term potentiation and trace fear conditioning memory in rat medial prefrontal cortex. *Learning & Memory (Cold Spring Harbor, N.Y.)*, *15*(10), 762–776. https://doi.org/10.1101/lm.1067808

Supèr, H., Martínez, A., Del Río, J. A., & Soriano, E. (1998). Involvement of Distinct Pioneer Neurons in the Formation of Layer-Specific Connections in the Hippocampus. *The Journal of Neuroscience*, *18*(12), 4616–4626. https://doi.org/10.1523/JNEUROSCI.18-12-04616.1998

Suzuki, A., Yamaguchi, M. T., Ohteki, T., Sasaki, T., Kaisho, T., Kimura, Y., Yoshida, R., Wakeham, A., Higuchi, T., Fukumoto, M., Tsubata, T., Ohashi, P. S., Koyasu, S., Penninger, J. M., Nakano, T., & Mak, T. W. (2001). T Cell-Specific Loss of Pten Leads to Defects in Central and Peripheral Tolerance. *Immunity*, *14*(5), 523–534. https://doi.org/10.1016/S1074-7613(01)00134-0

Takiguchi-Hayashi, K., Sekiguchi, M., Ashigaki, S., Takamatsu, M., Hasegawa, H., Suzuki-Migishima, R., Yokoyama, M., Nakanishi, S., & Tanabe, Y. (2004). Generation of reelin-positive marginal zone cells from the caudomedial wall of telencephalic vesicles. *The Journal of Neuroscience: The Official Journal of the Society for Neuroscience*, *24*(9), 2286–2295. https://doi.org/10.1523/JNEUROSCI.4671-03.2004

Tariq, K., Cullen, E., Getz, S. A., Conching, A. K. S., Goyette, A. R., Prina, M. L., Wang, W., Li, M., Weston, M. C., & Luikart, B. W. (2022). Disruption of mTORC1 rescues neuronal overgrowth and synapse function dysregulated by Pten loss. *Cell Reports*, *41*(5), 111574. https://doi.org/10.1016/j.celrep.2022.111574

Teixeira, C. M., Martín, E. D., Sahún, I., Masachs, N., Pujadas, L., Corvelo, A., Bosch, C., Rossi, D., Martinez, A., Maldonado, R., Dierssen, M., & Soriano, E. (2011a). Overexpression of Reelin Prevents the Manifestation of Behavioral Phenotypes Related to Schizophrenia and Bipolar

Disorder. *Neuropsychopharmacology*, *36*(12), 2395–2405. https://doi.org/10.1038/npp.2011.153

Teixeira, C. M., Martín, E. D., Sahún, I., Masachs, N., Pujadas, L., Corvelo, A., Bosch, C., Rossi, D., Martinez, A., Maldonado, R., Dierssen, M., & Soriano, E. (2011b). Overexpression of Reelin prevents the manifestation of behavioral phenotypes related to schizophrenia and bipolar disorder. *Neuropsychopharmacology: Official Publication of the American College of Neuropsychopharmacology*, *36*(12), 2395–2405. https://doi.org/10.1038/npp.2011.153

Thorpe, L. M., Yuzugullu, H., & Zhao, J. J. (2015). PI3K in cancer: Divergent roles of isoforms, modes of activation and therapeutic targeting. *Nature Reviews. Cancer*, *15*(1), 7–24. https://doi.org/10.1038/nrc3860

Tissir, F., & Goffinet, A. M. (2003). Reelin and brain development. *Nature Reviews. Neuroscience*, *4*(6), 496–505. https://doi.org/10.1038/nrn1113

Tissir, F., Ravni, A., Achouri, Y., Riethmacher, D., Meyer, G., & Goffinet, A. M. (2009). DeltaNp73 regulates neuronal survival in vivo. *Proceedings of the National Academy of Sciences of the United States of America*, *106*(39), 16871–16876. https://doi.org/10.1073/pnas.0903191106

Tokuda, S., Mahaffey, C. L., Monks, B., Faulkner, C. R., Birnbaum, M. J., Danzer, S. C., & Frankel, W. N. (2011). A novel Akt3 mutation associated with enhanced kinase activity and seizure susceptibility in mice. *Human Molecular Genetics*, *20*(5), 988–999. https://doi.org/10.1093/hmg/ddq544

Tokunaga, E., Oki, E., Egashira, A., Sadanaga, N., Morita, M., Kakeji, Y., & Maehara, Y. (2008). Deregulation of the Akt pathway in human cancer. *Current Cancer Drug Targets*, *8*(1), 27–36. https://doi.org/10.2174/156800908783497140

Torres, J., & Pulido, R. (2001). The tumor suppressor PTEN is phosphorylated by the protein kinase CK2 at its C terminus. Implications for PTEN stability to proteasome-mediated degradation. *The Journal of Biological Chemistry*, *276*(2), 993–998. https://doi.org/10.1074/jbc.M009134200

Tremblay, R., Lee, S., & Rudy, B. (2016). GABAergic Interneurons in the Neocortex: From Cellular Properties to Circuits. *Neuron*, *91*(2), 260–292. https://doi.org/10.1016/j.neuron.2016.06.033

Trotman, L. C., Wang, X., Alimonti, A., Chen, Z., Teruya-Feldstein, J., Yang, H., Pavletich, N. P., Carver, B. S., Cordon-Cardo, C., Erdjument-Bromage, H., Tempst, P., Chi, S.-G., Kim, H.-J., Misteli, T., Jiang, X., & Pandolfi, P. P. (2007). Ubiquitination regulates PTEN nuclear import and tumor suppression. *Cell*, *128*(1), 141–156. https://doi.org/10.1016/j.cell.2006.11.040

Tschopp, O., Yang, Z.-Z., Brodbeck, D., Dummler, B. A., Hemmings-Mieszczak, M., Watanabe, T., Michaelis, T., Frahm, J., & Hemmings, B. A. (2005). Essential role of protein kinase B gamma (PKB gamma/Akt3) in postnatal brain development but not in glucose homeostasis. *Development (Cambridge, England)*, *132*(13), 2943–2954. https://doi.org/10.1242/dev.01864

Vadas, O., Burke, J. E., Zhang, X., Berndt, A., & Williams, R. L. (2011). Structural basis for activation and inhibition of class I phosphoinositide 3-kinases. *Science Signaling*, *4*(195), re2. https://doi.org/10.1126/scisignal.2002165

Vahidnezhad, H., Youssefian, L., & Uitto, J. (2016). Molecular Genetics of the PI3K-AKT-mTOR Pathway in Genodermatoses: Diagnostic Implications and Treatment Opportunities. *Journal of Investigative Dermatology*, *136*(1), 15–23. https://doi.org/10.1038/JID.2015.331

Van Der Heide, L. P., Hoekman, M. F. M., & Smidt, M. P. (2004). The ins and outs of FoxO shuttling: Mechanisms of FoxO translocation and transcriptional regulation. *Biochemical Journal*, *380*(Pt 2), 297–309. https://doi.org/10.1042/BJ20040167

Vanhaesebroeck, B., Guillermet-Guibert, J., Graupera, M., & Bilanges, B. (2010). The emerging mechanisms of isoform-specific PI3K signalling. *Nature Reviews. Molecular Cell Biology*, *11*(5), 329–341. https://doi.org/10.1038/nrm2882

Vasudevan, K. M., Gurumurthy, S., & Rangnekar, V. M. (2004). Suppression of PTEN expression by NF-kappa B prevents apoptosis. *Molecular and Cellular Biology*, *24*(3), 1007–1021. https://doi.org/10.1128/MCB.24.3.1007-1021.2004

Vella, V., Puppin, C., Damante, G., Vigneri, R., Sanfilippo, M., Vigneri, P., Tell, G., & Frasca, F. (2009a). ΔNp73α inhibits PTEN expression in thyroid cancer cells. *International Journal of Cancer*, *124*(11), 2539–2548. https://doi.org/10.1002/ijc.24221

Vella, V., Puppin, C., Damante, G., Vigneri, R., Sanfilippo, M., Vigneri, P., Tell, G., & Frasca, F. (2009b). DeltaNp73alpha inhibits PTEN expression in thyroid cancer cells. *International Journal of Cancer*, *124*(11), 2539–2548. https://doi.org/10.1002/ijc.24221

Venot, Q., Blanc, T., Rabia, S. H., Berteloot, L., Ladraa, S., Duong, J.-P., Blanc, E., Johnson, S. C., Hoguin, C., Boccara, O., Sarnacki, S., Boddaert, N., Pannier, S., Martinez, F., Magassa, S., Yamaguchi, J., Knebelmann, B., Merville, P., Grenier, N., … Canaud, G. (2018). Targeted therapy in patients with PIK3CA-related overgrowth syndrome. *Nature*, *558*(7711), 540–546. https://doi.org/10.1038/s41586-018-0217-9

Verney, C., Takahashi, T., Bhide, P. G., Nowakowski, R. S., & Caviness, V. S. (2000). Independent controls for neocortical neuron production and histogenetic cell death. *Developmental Neuroscience*, *22*(1–2), 125–138. https://doi.org/10.1159/000017434

Volpe, E., Sambucci, M., Battistini, L., & Borsellino, G. (2016). Fas-Fas Ligand: Checkpoint of T Cell Functions in Multiple Sclerosis. *Frontiers in Immunology*, *7*, 382. https://doi.org/10.3389/fimmu.2016.00382

Vucic, D., Deshayes, K., Ackerly, H., Pisabarro, M. T., Kadkhodayan, S., Fairbrother, W. J., & Dixit, V. M. (2002). SMAC negatively regulates the anti-apoptotic activity of melanoma inhibitor of apoptosis (ML-IAP). *The Journal of Biological Chemistry*, *277*(14), 12275–12279. https://doi.org/10.1074/jbc.M112045200

Waite, K., & Eickholt, B. J. (2010). The neurodevelopmental implications of PI3K signaling. *Current Topics in Microbiology and Immunology*, *346*, 245–265. https://doi.org/10.1007/82_2010_82

Wajant, H. (2003). Death receptors. *Essays in Biochemistry*, *39*, 53–71. https://doi.org/10.1042/bse0390053

Walther, C., & Gruss, P. (1991). Pax-6, a murine paired box gene, is expressed in the developing CNS. *Development (Cambridge, England)*, *113*(4), 1435–1449. https://doi.org/10.1242/dev.113.4.1435

Wang, D., Zeesman, S., Tarnopolsky, M. A., & Nowaczyk, M. J. M. (2013). Duplication of AKT3 as a cause of macrocephaly in duplication 1q43q44. *American Journal of Medical Genetics. Part A*, *161A*(8), 2016–2019. https://doi.org/10.1002/ajmg.a.35999

Wang, L., Zhou, K., Fu, Z., Yu, D., Huang, H., Zang, X., & Mo, X. (2017). Brain Development and Akt Signaling: The Crossroads of Signaling Pathway and Neurodevelopmental Diseases. *Journal of Molecular Neuroscience: MN*, *61*(3), 379–384. https://doi.org/10.1007/s12031-016-0872-y

Wen, W., Li, H., & Luo, J. (2022). Potential Role of MANF, an ER Stress Responsive Neurotrophic Factor, in Protecting Against Alcohol Neurotoxicity. *Molecular Neurobiology*, *59*(5), 2992–3015. https://doi.org/10.1007/s12035-022-02786-7

White, F. A., Keller-Peck, C. R., Knudson, C. M., Korsmeyer, S. J., & Snider, W. D. (1998). Widespread Elimination of Naturally Occurring Neuronal Death inBax-Deficient Mice. *The Journal of Neuroscience*, *18*(4), 1428–1439. https://doi.org/10.1523/JNEUROSCI.18-04-01428.1998

Willis, S. N., Fletcher, J. I., Kaufmann, T., van Delft, M. F., Chen, L., Czabotar, P. E., Ierino, H., Lee, E. F., Fairlie, W. D., Bouillet, P., Strasser, A., Kluck, R. M., Adams, J. M., & Huang, D. C. S. (2007). Apoptosis initiated when BH3 ligands engage multiple Bcl-2 homologs, not Bax or Bak. *Science (New York, N.Y.)*, *315*(5813), 856–859. https://doi.org/10.1126/science.1133289

Wong, F. K., Bercsenyi, K., Sreenivasan, V., Portalés, A., Fernández-Otero, M., & Marín, O. (2018a). Pyramidal cell regulation of interneuron survival sculpts cortical networks. *Nature*, *557*(7707), Article 7707. https://doi.org/10.1038/s41586-018-0139-6

Wong, F. K., & Marín, O. (2019). Developmental Cell Death in the Cerebral Cortex. *Annual Review of Cell and Developmental Biology*, *35*, 523–542. https://doi.org/10.1146/annurev-cellbio-100818-125204

Woodgett, J. R. (2005). Recent advances in the protein kinase B signaling pathway. *Current Opinion in Cell Biology*, *17*(2), 150–157. https://doi.org/10.1016/j.ceb.2005.02.010

Xie, X., Hu, H., Tong, X., Li, L., Liu, X., Chen, M., Yuan, H., Xie, X., Li, Q., Zhang, Y., Ouyang, H., Wei, M., Huang, J., Liu, P., Gan, W., Liu, Y., Xie, A., Kuai, X., Chirn, G.-W., … Gao, D. (2018). The mTOR-S6K Pathway Links Growth Signaling to DNA Damage Response by Targeting RNF168. *Nature Cell Biology*, *20*(3), 320–331. https://doi.org/10.1038/s41556-017-0033-8

Xie, Y., Shi, X., Sheng, K., Han, G., Li, W., Zhao, Q., Jiang, B., Feng, J., Li, J., & Gu, Y. (2019). PI3K/Akt signaling transduction pathway, erythropoiesis and glycolysis in hypoxia (Review). *Molecular Medicine Reports*, *19*(2), 783–791. https://doi.org/10.3892/mmr.2018.9713

Xu, D., Yao, Y., Jiang, X., Lu, L., & Dai, W. (2010). Regulation of PTEN stability and activity by Plk3. *The Journal of Biological Chemistry*, *285*(51), 39935–39942. https://doi.org/10.1074/jbc.M110.166462

Xu, Q., Cobos, I., De La Cruz, E., Rubenstein, J. L., & Anderson, S. A. (2004). Origins of cortical interneuron subtypes. *The Journal of Neuroscience: The Official Journal of the Society for Neuroscience*, *24*(11), 2612–2622. https://doi.org/10.1523/JNEUROSCI.5667-03.2004

Yamaguchi, H., & Wang, H. G. (2001). The protein kinase PKB/Akt regulates cell survival and apoptosis by inhibiting Bax conformational change. *Oncogene*, *20*(53), 7779–7786. https://doi.org/10.1038/sj.onc.1204984

Yamaguchi, Y., & Miura, M. (2015). Programmed cell death in neurodevelopment. *Developmental Cell*, *32*(4), 478–490. https://doi.org/10.1016/j.devcel.2015.01.019

Yang, A. H., Kaushal, D., Rehen, S. K., Kriedt, K., Kingsbury, M. A., McConnell, M. J., & Chun, J. (2003). Chromosome Segregation Defects Contribute to Aneuploidy in Normal Neural Progenitor Cells. *The Journal of Neuroscience*, *23*(32), 10454–10462. https://doi.org/10.1523/JNEUROSCI.23-32-10454.2003

Yang, X., Klein, R., Tian, X., Cheng, H.-T., Kopan, R., & Shen, J. (2004). Notch activation induces apoptosis in neural progenitor cells through a p53-dependent pathway. *Developmental Biology*, *269*(1), 81–94. https://doi.org/10.1016/j.ydbio.2004.01.014

Yeo, W., & Gautier, J. (2004). Early neural cell death: Dying to become neurons. *Developmental Biology*, *274*(2), 233–244. https://doi.org/10.1016/j.ydbio.2004.07.026

Yoon, M.-K., Ha, J.-H., Lee, M.-S., & Chi, S.-W. (2015). Structure and apoptotic function of p73. *BMB Reports*, *48*(2), 81–90. https://doi.org/10.5483/BMBRep.2015.48.2.255

Yoshida, M., Assimacopoulos, S., Jones, K. R., & Grove, E. A. (2006). Massive loss of Cajal-Retzius cells does not disrupt neocortical layer order. *Development (Cambridge, England)*, *133*(3), 537–545. https://doi.org/10.1242/dev.02209

Yudushkin, I. (2019). Getting the Akt Together: Guiding Intracellular Akt Activity by PI3K. *Biomolecules*, *9*(2), E67. https://doi.org/10.3390/biom9020067

Zecevic, N., & Rakic, P. (2001). Development of layer I neurons in the primate cerebral cortex. *The Journal of Neuroscience: The Official Journal of the Society for Neuroscience*, *21*(15), 5607–5619.

Zeng, X., Chen, L., Jost, C. A., Maya, R., Keller, D., Wang, X., Kaelin, W. G., Oren, M., Chen, J., & Lu, H. (1999). MDM2 suppresses p73 function without promoting p73 degradation. *Molecular and Cellular Biology*, *19*(5), 3257–3266. https://doi.org/10.1128/MCB.19.5.3257

Zhang, T., Shi, Z., Wang, Y., Wang, L., Zhang, B., Chen, G., Wan, Q., & Chen, L. (2019). Akt3 deletion in mice impairs spatial cognition and hippocampal CA1 long long-term potentiation through downregulation of mTOR. *Acta Physiologica (Oxford, England)*, *225*(1), e13167. https://doi.org/10.1111/apha.13167

Zhang, Y., Zhang, Y., & Yu, Y. (2017). Global Phosphoproteomic Analysis of Insulin/Akt/mTORC1/S6K Signaling in Rat Hepatocytes. *Journal of Proteome Research*, *16*(8), 2825–2835. https://doi.org/10.1021/acs.jproteome.7b00140

Zhao, H.-F., Wang, J., & Tony To, S.-S. (2015). The phosphatidylinositol 3-kinase/Akt and c-Jun N-terminal kinase signaling in cancer: Alliance or contradiction? (Review). *International Journal of Oncology*, *47*(2), 429–436. https://doi.org/10.3892/ijo.2015.3052

Zhao, L., & Vogt, P. K. (2008). Class I PI3K in oncogenic cellular transformation. *Oncogene*, *27*(41), 5486–5496. https://doi.org/10.1038/onc.2008.244

Zhou, J., & Parada, L. F. (2012). PTEN signaling in autism spectrum disorders. *Current Opinion in Neurobiology*, *22*(5), 873–879. https://doi.org/10.1016/j.conb.2012.05.004

Zhou, X., Zeng, W., Li, H., Chen, H., Wei, G., Yang, X., Zhang, T., & Wang, H. (2018). Rare mutations in apoptosis related genes APAF1, CASP9, and CASP3 contribute to human neural tube defects. *Cell Death & Disease*, *9*(2), 43. https://doi.org/10.1038/s41419-017-0096-2

Zhu, J., Tsai, H.-J., Gordon, M. R., & Li, R. (2018). Cellular Stress Associated with Aneuploidy. *Developmental Cell*, *44*(4), 420–431. https://doi.org/10.1016/j.devcel.2018.02.002

Zhu, Y., Hoell, P., Ahlemeyer, B., & Krieglstein, J. (2006). PTEN: A crucial mediator of mitochondria-dependent apoptosis. *Apoptosis: An International Journal on Programmed Cell Death*, *11*(2), 197–207. https://doi.org/10.1007/s10495-006-3714-5

Zluhan, E., Enck, J., Matthews, R. T., & Olson, E. C. (2020). Reelin Counteracts Chondroitin Sulfate Proteoglycan-Mediated Cortical Dendrite Growth Inhibition. *Eneuro*, *7*(4), ENEURO.0168-20.2020. https://doi.org/10.1523/ENEURO.0168-20.2020

Zou, Z., Tao, T., Li, H., & Zhu, X. (2020). mTOR signaling pathway and mTOR inhibitors in cancer: Progress and challenges. *Cell & Bioscience*, *10*(1), 31. https://doi.org/10.1186/s13578-020-00396-1

Zu, L., Zheng, X., Wang, B., Parajuli, N., Steenbergen, C., Becker, L. C., & Cai, Z. P. (2011). Ischemic preconditioning attenuates mitochondrial localization of PTEN induced by ischemia-reperfusion. *American Journal of Physiology. Heart and Circulatory Physiology*, *300*(6), H2177-2186. https://doi.org/10.1152/ajpheart.01138.2010